NCHRP Project No. 22-22(2) COPY No._____
TTI Project No. 479330-001

Placement of Traffic Barriers on Roadside and Median Slopes

DRAFT FINAL REPORT

Prepared for
National Cooperative Highway Research Program
Transportation Research Board
of The National Academies

Roger P. Bligh, Ph.D, P.E.
Akram Y. Abu-Odeh, Ph.D.
Nauman M. Sheikh, P.E.
Ryan Allcorn
Kimberly Rau
Daniel Pearson

Texas A&M Transportation Institute
College Station, TX

TTI Project No. 479330-001

May 2016

ACKNOWLEDGMENT OF SPONSORSHIP

This work was sponsored by the American Association of State Highway and Transportation Officials, in cooperation with the Federal Highway Administration, and was conducted in the National Cooperative Highway Research Program, which is administered by the Transportation Research Board of the National Research Council.

AKNOWLEDGMENTS

The researchers would like to acknowledge the computational resources and support provided by Texas A&M High Performance Research Computing (http://hprc.tamu.edu/). Additionally, the authors acknowledge Livermore Software Technology Corporation (LSTC) for providing the explicit finite element code LS-DYNA. The researchers would also like to thank Michael Bychkowski, Zach Rohl, and Katherine McCaskey for their contributions to this report.

ABSTRACT

Placement guidelines for implementation of selected guardrail and median barrier systems on slopes and ditches were developed using barrier impact performance limits derived from finite element impact simulations and vehicle trajectory encroachment data. The finite element barrier models were validated against available MASH crash test data, and the vehicle models used in the vehicle dynamics simulations were validated against available ditch encroachment tests. The barrier performance limits were defined in terms of interaction heights that resulted in vehicle override and underride. The vehicle trajectory data was defined in terms of vehicle bumper trajectory profiles as the vehicles encroached across selected ditch configurations.

Various commonly used guardrail and median barrier systems were included in the analyses. The ditch configurations included in the analyses included both V-shaped and trapezoidal ditches with 1V:6H and 1V:8H slopes and widths ranging from 32 ft to 62 ft.

The placement guideline development process involved identifying locations (lateral offsets) along the ditch profile where the bumper heights associated with vehicle encroachments of the same ditch profile were contained within the override and underride

limits for the barrier system. Placement guidelines for the median barrier systems considered impacts from both directions in the ditch. Explicit finite element impact simulations of the barrier placed in the ditch were performed to further validate the placement guidelines and revise them as warranted.

The resulting placement guidelines were presented in both tabulated and graphical form. The tubular format provides a very concise presentation, while the graphical format can be more readily visualized and applied to a range of ditch widths.

TABLE OF CONTENTS

LIST OF FIGURES

LIST OF TABLES

1. INTRODUCTION

1.1. RESEARCH PROBLEM STATEMENT

In the 1970s, an analysis of barriers placed on slopes indicated that most guardrails do not perform well when placed on slopes that are 1V:6H or steeper. Since that time, the vehicle fleet has changed dramatically, with an increase in the popularity of light trucks and sport utility vehicles. Further, there has been a significant change in the design of roadside barriers in recent decades, including changes to traditional W-beam barriers. It is unclear how these changes affect the behavior of longitudinal barriers placed on slopes. Information from the National Highway Traffic Safety Administration (NHTSA) Fatality Analysis Reporting System (FARS) database indicates that some cross-median crashes have occurred where median barriers were in place. With the dramatic increase in use of barriers in depressed medians, a more detailed study of the performance of barriers in depressed medians is needed to develop guidance related to acceptable barrier performance and placement.

1.2. RESEARCH OBJECTIVE

The objective of this project was to produce recommendations for placement of barriers on roadside and median slopes. The guidelines address most common types of barriers used in the United States. The barriers considered in this project include: modified thrie beam guardrail, Midwest Guardrail System (MGS), modified weak post W-beam guardrail (modified G2), modified strong steel-post W-beam guardrail (modified G4(1S)), 31-inch strong steel post W-beam median barrier (MGS median), concrete single slope barrier, and weak-post W-beam median barrier (MB2). These barrier types were selected in consultation with the research panel after giving consideration to the barrier systems that have met American Association of State Highway and Transportation Officials (AASHTO) Manual for Assessing Safety Hardware (MASH) impact performance criteria on flat terrain, and other parallel or recent research studies that may have addressed placement of a specific barrier type on slopes, such as cable barrier systems.

1.3. SCOPE

Under National Cooperative Highway Research Project (NCHRP) Project 22-22, the performance of barriers on slopes were evaluated using NCHRP Report 350 criteria. Under this project, the selected barrier systems were evaluated on slopes using MASH criterias.

NCHRP Report 350 used two primary design test vehicles: an 1800-lb (820-kg) small passenger car and a 4400-lb (2000-kg), ¾ ton, standard cab pickup truck. In MASH, the design vehicles changed to a 5000-lb (2270-kg), ½ ton, four-door pickup truck and a heavier 2425-lb (1100-kg) passenger car. These changes were implemented to ensure that the design vehicles remain representative of the vehicle fleet on the nation roadway.

The impact speed for Test Level 3 (TL-3) did not change from NCHRP Report 350 to MASH and remains 62 mi/h (100 km/h). However, the impact angles did experience some

change. NCHRP Report 350 used a 25 degree impact angle for the pickup truck and a 20-degree impact angle for the small car. MASH retained a 25-degree impact angle for the pickup truck and increased the impact angle for the small car to a similar 25 degrees.

A comparison of NCHRP Report 350 and MASH TL-3 impact conditions is provided in Table 1.1. The two design test vehicles are considered to represent the practical worst case vehicles for evaluating highway safety features.

Table 1.1: Comparison of NCHRP Report 350 and MASH Test Matrices for Test Level 3 Evaluation of Longitudinal Barriers

	NCHRP Report 350		**MASH**	
Test Vehicle Type	Small Car	Pickup Truck	Small Car	Pickup Truck
Mass (kg)	820	2000	1100	2270
Impact Angle	20°	25°	25°	25°
Impact Speed (km/h)	100	100	100	100

This report provides details of the research performed under this project. The report presents the results of a literature review, describes typical or representative slope and ditch configurations defined in conjunction with NCHRP Project 22-21, and discusses various guardrail and median barrier types and the current state-of-the-knowledge in regard to their impact performance limits. The report also presents details of vehicle dynamics simulations that define vehicle kinematics during encroachments across slopes and ditches, the development and validation of finite element models of the selected barrier systems against full-scale crash tests, and results of finite element simulation analyses used to define the performance limits of the barrier systems on slopes. Finally, recommended guidelines derived from a combination of the vehicle dynamics trajectories and finite element simulation defined performance limits are developed and presented.

2. RESEARCH APPROACH

The research plan consisted of a simulation-based approach to develop guidelines for placement of guardrails and median barriers on sloped terrain. The barrier systems and terrain configurations of interest were selected in conjunction with the project panel. The placement guidance was developed based on MASH design test vehicles and a prescribed set of encroachment conditions that included the MASH Test Level 3 (TL-3) impact conditions.

First, finite element barrier models were developed for the selected barrier systems. The barrier models were then validated against available MASH crash test data. This involved performing simulations that replicating the impact conditions of the tests and comparing the results using various metrics that included MASH evaluation criteria, signal analysis, barrier damage, and barrier deflection. These simulations were performed using the LS-DYNA explicit finite element code.

The validated barrier models were then subjected to impacts at different interaction heights to determine the performance limits of each barrier system. The performance limits were defined in terms of both override and underride thresholds. The override threshold was defined as the interaction height of the pickup truck with the barrier above which barrier override or vehicle rollover would result. The underride threshold was defined as the interaction height of the small passenger car with the barrier below which barrier underride or unacceptable vehicle decelerations would result.

The next task in the guideline development included quantifying vehicle trajectory across the selected dich configurations for a set of prescribed encroachment conditions. Vehicle models were developed to represent the MASH 2270P pickup truck and 1100C passenger car design vehicles. These vehicles were validated against available, albeit limited, encroachment test data. The vehicle trajectory simulations were performed using the CarSim vehicle dynamics code. A program was written to extract bumper trajectory data for the various ditch encroachments.

The barrier placement guidelines were then developed through a combination of the barrier performance limits and bumper trajectory profiles. Acceptable placement regions were defined as locations for which the bumper trajectories for all encroachment conditions for both design vehicles were contained within the performance limit thresholds. The median barrier guidelines considered impacts from both directions across the ditch.

The initial placement guidelines were verified and revised as needed by performing finite element impact simulations of the barrier systems at or near the edge of the prescribed placement range on a given ditch profile. The placement range was expanded or contracted as appropriate based on the outcomes of the simulations.

The final placement guidelines resulting from this process were presented in tabular and graphical form for guardrails and slopes and median barriers in ditches. The guidelines are

considered suitable for incorporation into guidance documents to assist practitioners and designers with the proper placement of barriers on sloped terrain.

3. BACKGROUND

3.1. CURRENT CRASH TESTING GUIDELINES

Subsequent to its publication in 1993, the impact performance of longitudinal barriers (e.g., median barriers, guardrails) was evaluated following guidelines set forth in National Cooperative Highway Research Program (NCHRP*)* Report 350*, "Recommended Procedures for the Safety Performance Evaluation of Highway Features." NCHRP Report 350* represented a comprehensive update to crash test and evaluation procedures. It incorporated significant changes and additions to procedures for the safety-performance evaluation of roadside devices, and updates reflecting the changing character of the highway network and the vehicles using it. Subsequent to its publication, the Federal Highway Administration (FHWA) adopted *NCHRP Report 350* as policy through the federal rulemaking process to govern the testing and evaluation of traffic barriers.

NCHRP Report 350 used a 4400 lb (2000 kg) pickup truck as the standard design test vehicle. This reflected the fact that over one-half of new passenger vehicle sales in the U.S. were in the "light truck" category, which included pickup trucks, sport-utility vehicles (SUVs), and mini-vans. This change was made recognizing the differences in wheel bases, bumper heights, body stiffness and structure, front overhang, and other vehicular design factors associated with light trucks that could affect impact performance. *NCHRP Report 350* further defined other supplemental test vehicles including a 17,640 lb (8000 kg) single-unit cargo truck and 79,366 lb (36000 kg) tractor-trailer vehicles to provide the basis for optional testing to meet higher performance levels.

Six test levels were defined for longitudinal barriers that place an increasing level of demand on the structural capacity of a barrier system. The basic test level was Test Level 3 (TL-3). The structural adequacy test for this test level consisted of a 4400 lb (2000 kg) pickup truck (2000P) impacting a barrier at 62 mph (100 km/h) and 25 degrees. The severity test consists of an 1800 lb (820 kg) passenger car impacting the barrier at 62 mph (100 km/h) and 20 degrees.

At a minimum, all barriers on high-speed roadways on the National Highway System (NHS) were required to meet TL-3 requirements. Some state departments of transportation (DOTs) require that their bridge railings and/or median barriers meet TL-4, which requires accommodation of an 17,640 lb (8000 kg) single unit truck impacting the barrier at 50 mph (80 km/h) and 15 degrees. Higher containment barriers are sometimes used when conditions such as a high percentage of truck traffic warrant. Such barriers are necessarily taller, stronger, and more expensive to construct.

The forward of *NCHRP Report 350* states the following: "The evolution of the knowledge of roadside safety and performance evaluations is reflected in this document. Inevitably, parts of this document will need to be revised in the future…" It was recognized that periodic changes in crash testing and evaluation methodologies are necessary to keep pace with changes in vehicle fleet characteristics and operating conditions on U.S. highways, and to

address issues and data gleaned from ran-off-road crash data. NCHRP Project 22-14(2), "Improvement of Procedures for the Safety-Performance Evaluation of Roadside Features," was initiated to take the next step in the continued advancement and evolution of roadside safety testing and evaluation. The final product of Project 22-14(2) was a document published by the American Association of State Highway and Transportation Officials (AASHTO) in October 2009 known as the *Manual for Assessment of Safety Hardware (MASH)*. This document superseded *NCHRP Report 350* as the latest guidance for the impact performance evaluation of roadside safety devices.

The recommended guidelines in *MASH* reflect input received from researchers, hardware manufacturers, user agencies, and other professionals in the field of roadside safety design. They provide a basis upon which the impact performance of roadside safety features can be assessed and compared. *MASH* contains updated matrices for vehicular crash tests defined in terms of vehicle type, impact conditions (i.e., speed and angle), and impact location. It further prescribes how to evaluate impact performance of a safety feature in terms of occupant risk, structural adequacy, and post-impact behavior of the vehicle, and other factors.

The underlying philosophy behind the development of the *MASH* guidelines continues to be one of "worst practical conditions." When selecting test parameters such as test vehicle type and weight, impact speed and angle, and point of impact, effort was made to specify the worst, or most critical, conditions with consideration given to available technology, relevancy in terms of the incremental increase in the level of safety provided, and associated costs of new features compared to existing features. For example, the weights of the selected small passenger car and pickup truck test vehicles represent the 2^{nd} and 94^{th} percentiles, respectively, of passenger vehicles based on sales data available during the writing of the document. The selected impact speed and angle combination represents the 92.5^{th} percentile as determined from available real-world crash data. When the combined effects of all testing parameters are considered, the tests prescribed in *MASH* are believed to reasonably represent the range of impact conditions expected to be encountered in real-world crashes.

Major revisions incorporated into the *MASH* guidelines include new design test vehicles, revised test matrices and impact conditions, changes to the evaluation criteria, inclusion of tests for additional features, and increased emphasis on in-service performance evaluation. Some key changes and observations include:

- Evaluation of vehicle sales data indicates that vehicles in the fleet became larger and heavier since the publication of *NCHRP Report 350*. The efforts of automobile manufacturers to add additional comfort and safety amenities to their vehicles have added weight to even the smallest of passenger vehicles. This added weight can change the performance characteristics of these vehicles and place more demand on barrier systems. The center-of-gravity (C.G.) heights also increased, which may further aggravate vehicle stability with some existing barriers. Future increases in energy and fuel prices may ultimately reverse this trend. However, any reversal will likely be gradual in nature, and these heavier vehicles will remain part of the vehicle fleet for many years to come.

- The large design test vehicle was changed from a standard cab, ¾-ton pickup truck with a C.G. height of approximately 27 inches (686 mm) to a ½-ton, four-door crew-cab pickup truck with a minimum C.G. height of 28 inches (711 mm). Similar to *NCHRP Report 350*, it is still the intent to have this design test vehicle represent the light truck segment of the vehicle fleet. The weight of the test vehicle increased approximately 13 percent from 4400 lb to 5000 lb (2000 kg to 2270 kg), which represents the 94th percentile heaviest passenger vehicle in terms of sales (i.e., only 6 percent of new passenger-type vehicles sold weigh more than the specified test weight). The increase in weight places more structural demand (i.e., increased impact forces) on existing appurtenances, and the increase in C.G. height may result in stability issues with some barrier systems.

- The weight of the small car test vehicle increased 35 percent from 1800 lb to 2425 lb (820 kg to 1100 kg). This change reflects the fact that 1800 lb (820 kg) vehicles are virtually nonexistent in terms of new car sales. The weight specified for the newly recommended small passenger car represents the 2nd percentile lightest passenger vehicle in terms of sales (i.e., only 2 percent of new vehicles sold weigh less than the specified test weight).

- The impact angle for all redirection tests was adjusted to 25 degrees. This change means an increase from the 20 degree impact angle used under *NCHRP Report 350* for small car tests with longitudinal barriers. Considering both the increase in weight and impact angle, the impact severity of the small car redirection test (Test 3-10) increased by 106 percent. This can lead to increased vehicle snagging, which can exacerbate issues with occupant compartment deformation and occupant risk for some devices.

- The impact conditions for Test 4-12 were modified to make it a more discerning test. The weight of the TL-4 single-unit truck increased 25 percent from 17,640 lb to 22,050 lb (8000 kg to 10000 kg), and the impact speed increased 12 percent from 50 mph to 56 mph (80 km/h to 90 km/h). The resulting increase in impact severity is 57 percent. This change will affect the status of barriers currently classified as TL-4 barriers under *NCHRP Report 350*.

- Evaluation Criterion D of *NCHRP Report 350* states that "Deformations of, or intrusions into, the occupant compartment that could cause serious injuries should not be permitted." *MASH* adopts a quantitative approach that has correlation to injuries observed in real-world crashes. Up to 9 inches (229 mm) of deformation or intrusion is permitted in the wheel/foot well and toe pan areas, as well as the front side door area above the seat. As much as 12 inches (305 mm) of deformation or intrusion is permissible in the floor pan and transmission tunnel areas, the side front panel, and the front side door area below the seat.

3.1.1. Basic Summary of Crash Testing of Common Barriers

In the mid-1990s, TTI researchers conducted full-scale crash tests of many commonly used guardrail systems in accordance with *NCHRP Report 35*0 Test Level 3 impact conditions (Bullard et al., 1996; Mak et al., 1998a; Mak et al., 1998b). It was under this testing program

that performance issues with the strong steel-post W-beam guardrail (G4(1S)), weak-post W-beam guardrail (G2), and strong steel-post thrie beam guardrail (G9) were first identified.

Figure 3.1 below shows the vehicle after impacting the G4(1S) guardrail with steel blockouts. The truck rolled on its side as it exited the system. A summary of other tests is presented in Table 3.1. These tests helped define the performance limits of common barrier systems with light truck vehicles.

Figure 3.1: Vehicle after test 471470-27 with a G4(1S) guardrail system (Mak et al., 1998b)

NCHRP published a synthesis by Ray et al. (1997) on crashworthiness of existing guardrails and median barriers. It described the impact performance, typical applications, and the state of the practice for existing nonproprietary guardrail systems and median barriers used in the United States. State-of-the-practice information was collected to assist in the selection and effective placement of these systems.

The synthesis presented comparisons between barrier categories. These included weak post barrier systems, strong-post barrier systems, concrete median barriers, and aesthetic guardrails and median barriers. The synthesis also included design details for each system and some variations of these designs. Results from crash tests performed to evaluate different designs were summarized. The synthesis also presented the current usage of different types of barriers and their distribution across different states in the U.S. Advantages and disadvantages associated with the use of these systems were presented to provide guidance for selecting effective guardrail and median barrier systems.

Table 3.1: Summary of full-scale crash tests of barriers on a flat terrain conducted at TTI (Bullard et al, 1996 and Mak et al. 1998b)

Test Number	Barrier System	Result and Comments
405421-01	Modified (G4(1S)) with timber blockout	The rail system considered passed. However, it was considered marginally failed the preferable post impact vehicle trajectory.
471470-28	Cable (G1)	Successful containment & redirection. Impact speed was 95.1 km/h (lower than target impact speed of 100 km/h) but impact angle was 26.7 degrees which was higher than target of 25 degrees.
471470-21	W-Beam, Weak-Post (G2)	Vehicle overrode barrier.
471470-22	W-Beam, Weak-Post (G2)	Successful containment & redirection (TL-2)
471470-33	Box-Beam (G3)	Successful containment & redirection.
471470-26	W-Beam, Wood-Post (G4(2W))	Successful containment & redirection.
471470-27	W-Beam, Steel-Post (G4(1S)	Vehicle rolled over on its side.
471470-31	Thrie-Beam (G9)	Vehicle rolled over two and a quarter revolutions.
471470-30	Modified Thrie-Beam	Successful containment & redirection.

* All tests were conducted with 2000P pickup per *NCHRP Report 350* test designation 3-11 impact conditions, except for test # 471470-22 which was conducted per *NCHRP Report 350* test designation 2-11

3.2. CURRENT PLACEMENT GUIDELINES

The 2002 AASHTO *Roadside Design Guide (RDG)* recognizes that the impact performance of a roadside barrier is sensitive to the slope of the approach area in front of the barrier. Where possible, barriers should be installed on relatively flat (1V:10H or flatter) and unobstructed terrain. It recommends that any barrier installed on slopes as steep as 1V:6H be offset such that it is probable an errant vehicle will be in its normal position at time of impact with the barrier. This lateral offset distance will vary depending on the encroachment conditions and barrier type, but is generally recommended to be at least 12 ft (3.7 m) from the slope break point.

Chapter 6 of the AASHTO *RDG* provides current guidance on the use and placement of median barriers. It describes characteristics of common median barrier types and recommendations for their placement on sloped medians. These guidelines are based on the type of median cross section, which are broadly categorized into three types:

1- Depressed medians or medians with ditches (Section I)
2- Stepped medians (Section II)
3- Raised medians or medians berms (Section III)

Figure 3.2 depicts these medians types and some of their various sub-types. Pages 6-14 of Chapter 6 of the *RDG* provide the following guidance for barrier placement in these types of medians:

> "**Section I** – The slopes and the ditch section should first be checked by the criteria in Chapter 3 to determine if the guidelines suggest the installation of a roadside barrier. If both slopes require shielding (Illustration 1), a roadside barrier should be placed near the shoulder on each side of the median ("b" and "d"). If only one slope requires shielding, e.g., S_3, a median barrier should be placed at "d." In this situation, a rigid or semi-rigid barrier is suggested, and a rubrail should be installed on the ditch side of the barrier to prevent vehicles that have crossed the ditch from snagging on a post and beam railing system.
>
> If neither slope requires shielding but either one or both are steeper than 1V:10H (Illustration 2), a median barrier should be placed on the side with the steeper slope when warranted. For example, if
>
> S_2 = 1V:6H and S_3 = 1V:10H,
>
> the barrier would be placed at "b." A rigid or semi-rigid system is suggested in this situation. If both slopes are relatively flat (Illustration 3), a median barrier may be placed at or near the center of the median (at "c") if vehicle override is not likely. Any type of median barrier having an appropriate test level for the application can be used provided its dynamic deflection is not greater than one-half the median width.
>
> **Section II** - If the embankment slope is steeper than approximately 1V:10H (Illustration 4), a median barrier should be placed at "b." If the slope is not traversable (rough rock cut, etc.), a roadside barrier should be placed at both "b" and "d" (Illustration

5). It is not unusual for this section to have a retaining wall at "d." If so, it is suggested that the base of the wall be contoured to the exterior shape of a concrete median barrier. If the cross slope is flatter than approximately 1V:10H, a barrier could be placed at or near the center of the median (Illustration 6).

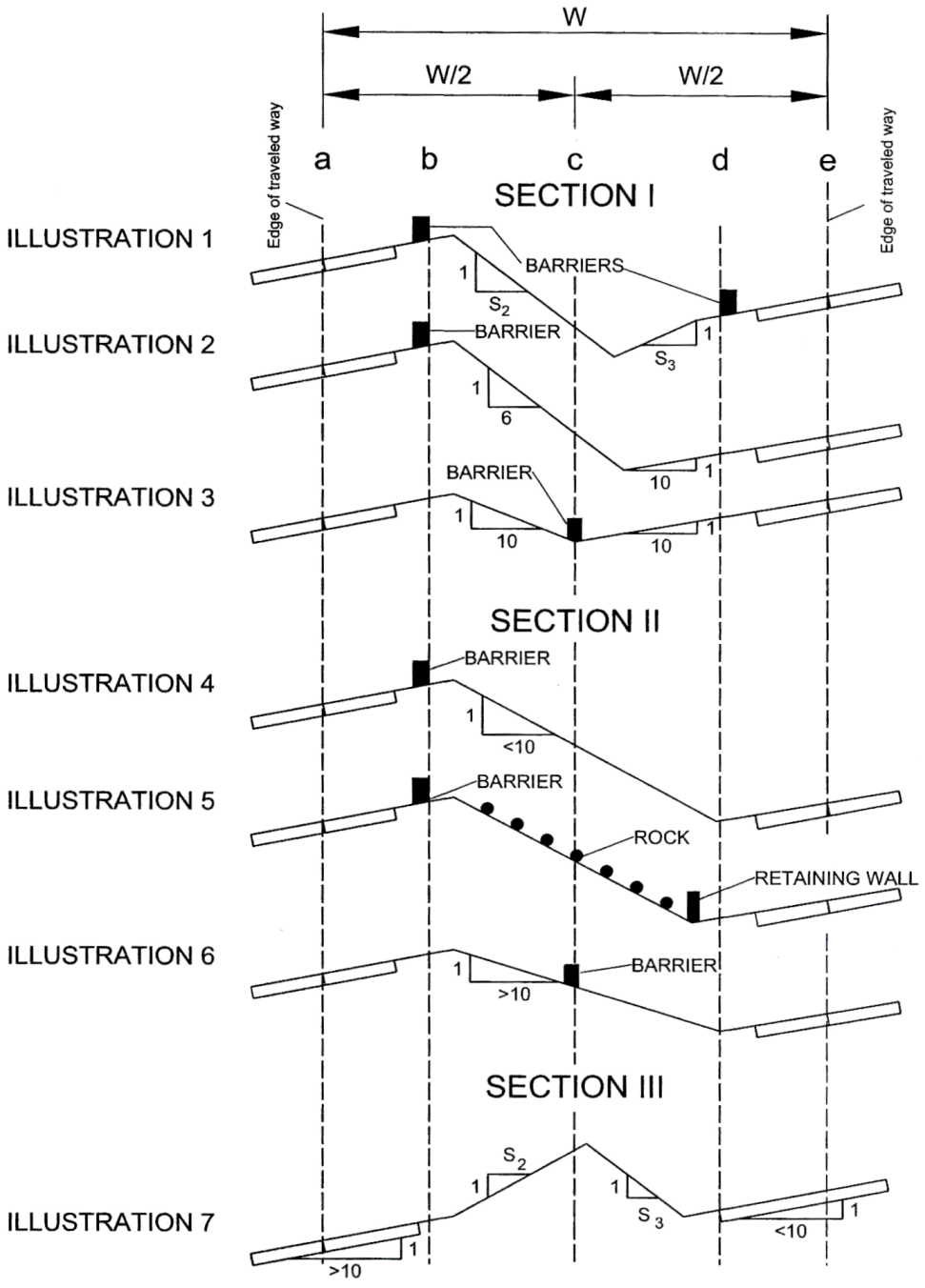

Figure 3.2: Recommend barrier placement in non-level medians

(2002 AASHTO Roadside Design Guide)

Section III—Placement criteria for median barriers on this cross section (Illustration 7) are not clearly defined. Research has shown that such a cross section, if high enough and wide enough, can redirect vehicles impacting at relatively shallow angles.

As a general rule, if the cross section itself is inadequate for redirecting errant vehicles (i.e., the slopes are relatively flat) a semi-rigid median barrier should be placed at the apex of the cross section.

If slopes are not traversable (rough rock cut, etc.), a roadside barrier should be placed at "b" and "d." If retaining walls are used at "b" and "d," it is recommended that the base of the wall be contoured to the exterior shape of a standard concrete barrier.

When the guidelines suggest installing a median barrier, it is desirable that the same barrier be used throughout the length of need, and that the barrier be placed in the middle of a flat median. However, it may be necessary to deviate from this policy in some cases. For example, the median in Section I of Figure 6.11 may require a barrier on both sides of the median. If a median barrier is warranted upstream and downstream from the section, it is suggested that the median barrier be "split" as illustrated in Figure 6.12. Most of the operational median barriers can be split this way, especially box beams, W-beam types, and the shaped concrete barrier."

An update to Chapter 6 of the AASHTO *Roadside Design Guide* included some changes that were made to reflect the results of recent research and crash tests. The amended median barrier placement guidance from the revised Chapter 6 is provided below for reference.

"**Section I** – The slopes and the ditch section should first be checked by the criteria in Chapter 3 to determine if the guidelines suggest the installation of a roadside barrier. If both slopes require shielding, i.e., the ditch is non-traversable (Illustration 1), a roadside barrier should be placed near the shoulder on each side of the median ("b" and "d"). If only one slope requires shielding, e.g., S2, a median barrier should be placed at "b." In this situation, a rigid or semi-rigid barrier is suggested, and a rubrail should be installed on the ditch side of the barrier to prevent vehicles that have crossed the ditch from snagging on a post-and-beam railing system. There has also been some anecdotal evidence that a vehicle traveling up a slope steeper than lV:6H before contacting the barrier may override it. Research is planned to quantify possible placement concerns when a rigid or semi-rigid barrier is located on one side of a traversable, sloped median. If neither slope requires shielding but either one or both are steeper than IV: 10H (Illustration 2), a median barrier should generally be placed on the side with the steeper slope. For example, if

S2 = 1V:6H and S3 = 1V:10H,

the barrier would be placed at "b." A rigid or semi-rigid system is suggested in this situation. If both slopes are relatively flat (Illustration 3), a median barrier may be placed at or near the center of the median (at "c") if vehicle override is not likely. Any type of median barrier having an appropriate test level for the application can be used provided its dynamic deflection is not greater than one-half the median width.

Although any median barrier is likely to perform best when it is installed on relatively flat terrain, cable barriers have been shown to perform effectively when placed on an IV: 6H sideslope when the vehicle travels down the slope prior to impact. However, based on recent crash reports, some vehicle types, when striking a cable barrier from behind after traveling across a ditch, can underride the barrier. Computer simulation and limited full-scale testing on 1V:6H slopes have shown that the barrier will redirect vehicles after traversing the ditch when it is placed within 0.3 m [1 ft] (either side) of the ditch line. However, when the current configuration of cable median barrier was placed 1.2 m [4 ft] from the ditch line, a test with a passenger sedan showed that after crossing the ditch the vehicle reached the cables with its suspension compressed; the bumper passed under the lowest cable, and the vehicle continued through the cable median barrier with no redirection. Computer simulation has predicted that when the barrier is placed eight feet from the ditch bottom, the vehicle will be contained. Based on this testing and more recent simulation studies, it appears that maximum redirection can be achieved with the current configuration if the area from 0.3 m [1 ft] to 2.4 m [8 ft] from the ditch line on 1V:6H slopes is avoided. Additional research is needed to further support the recommended offset distances for this and other slopes and to determine what practical modifications to the barrier can be developed to enhance its performance in locations that may be less than optimal. These placement guidelines apply to all cable barriers, including high-tension designs and four-cable systems.

Since most reported penetrations have involved passenger vehicles with relatively low front profiles impacting at high speeds and high angles, it is not considered cost-effective to reposition existing cable barrier that has been installed within this area unless a recurring crash problem is evident.

Section II – If the embankment slope is steeper than approximately 1V:10H (Illustration 4), a median barrier should be placed at "b." If the slope contains obstacles or consists of a rough rock cut (as discussed in Chapter 3) a roadside barrier should be placed at both "b" and "d" (Illustration 5). It is not unusual for this section to have a retaining wall at "d." If so, it is suggested that the base of the wall be contoured to the exterior shape of a concrete median barrier. If the cross slope is flatter than approximately 1V:10H, a barrier could be placed at or near the center of the median (Illustration 6).

Section III – Placement criteria for median barriers on this cross section (Illustration 7) are not clearly defined. Research has shown that such a cross section, if high enough and wide enough, can redirect vehicles impacting at relatively shallow angles. However, this type of median design should not generally be construed to be a barrier or to provide positive protection against crossover crashes.

If slopes are not traversable (rough rock cut, etc.), a roadside barrier should be placed at "b" and "d." If retaining walls are used at "b" and "d," it is recommended that the base of the wall be contoured to the exterior shape of a standard concrete barrier.

When the guidelines suggest installing a median barrier, it is desirable that the same barrier be used throughout the length of need, and that the barrier be placed in the middle of relatively flat medians that have slopes that are 1V:6H or flatter. However, it may be necessary to deviate from these guidelines in some cases. For example, the median in Section I of Figure 6.18, where the roadways are stepped (on significantly different elevations), may require a barrier on both sides of the median. If a single median barrier is installed upstream and downstream from the section, it may be necessary to "split" the median barrier as illustrated in Figure 6.19. Most of the operational median barriers can be split this way, especially box beams, W-beam types, and concrete barrier."

The change in language regarding the placement of barriers on the back slope of a ditch reflects a documented concern that a vehicle can underride a barrier if it is located in close proximity to the ditch bottom. The probability of underride depends on a number of factors including vehicle type, encroachment conditions, and ditch geometry. When a car travels across a ditch bottom, its suspension can compress and lower the height of the front end of the vehicle. This compression of the suspension in combination with the back slope geometry can leave the front bumper at or near ground level – a condition conducive to barrier underride. Hence, the recommendation in the revised Chapter 6 of the RDG to avoid barrier placement in the "*area from 0.3 m* [1 ft] *to 2.4 m* [8 ft] *from the ditch line on IV:6H slopes."*

It is this placement guidance that is being critically reviewed and updated under this project. The revised guidelines will consider the modern vehicle fleet, which contains a significant percentage of light trucks, and current barrier systems that have complied with *MASH* criteria when tested on flat, level ground.

3.3. KEY RESEARCH STUDIES RELATED TO TRAVERSAL OF SLOPES AND/OR PLACEMENT OF BARRIERS ON SLOPES

3.3.1. "Dynamic Behavior of an Automobile Traversing Selected Curbs and Medians" (Ross et al., 1983)

In 1975, Ross et al. performed a study to determine the dynamic behavior of a vehicle as it traversed sloped medians and different curb configurations. Texas Transportation Institute's version of the Highway-Vehicle-Object Simulation Model (HVOSM) computer simulation code was used as a tool to perform parametric simulations with a 4000 lb (1800 kg) passenger car. The objective of these simulations was to determine the potential for a vehicle to vault over a barrier that was placed behind a curb or on a sloped median.

Simulations were performed with 6 inch (152 mm) and 8 inch (203 mm) curbs and with medians that had slopes of 11H:1V, 8H:1V, and 2.5H:1V. Due to limitations in the computer

code, the contact between the vehicle and the barrier was not modeled. Simulations were thus terminated when the vehicle reached the barrier.

The performance of the vehicle while traversing existing curb and median configurations was compared to its performance on modified configurations. The comparison was based on vehicular accelerations and bumper height data collected from the HVOSM simulations. Bumper heights were calculated with respect to the local terrain. Simulations were performed assuming a "free-wheeling" mode in which no steering, braking or throttle inputs were applied to the vehicle as it encroached onto the roadside.

It was concluded that, in general, barriers should not be placed near curbs. Simulation results indicated that curbs destabilize the vehicle, causing it to vault the barrier, or in some cases impact the barrier at a lower than design impact position. It was suggested that a flat approach area to the barriers should be considered whenever possible.

3.3.2. "Development of Guidelines for Placement of Longitudinal Barriers on Slopes," (Ross and Sicking, 1983)

Historically, the barrier placement guidance in the AASHTO *Roadside Design Guide* (2002) emanated from research sponsored by the Federal Highway Administration (FHWA) and conducted by TTI in the early 1980s (Ross and Sicking, 1983). This research was undertaken specifically to investigate the impact performance of longitudinal barriers installed on non-level terrain.

A limited crash test program coupled with an extensive computer simulation effort using HVOSM was used to develop guidelines for placement of barriers on non-level terrain. The HVOSM vehicle handling code was used to establish the trajectory of a vehicle's bumper as the vehicle traversed various terrain configurations at various encroachment conditions. This data was combined with barrier containment criteria to establish regions of acceptable and unacceptable (e.g., override and underride) barrier performance. As an example, a bumper height profile plot for a 4500 lb (2040 kg) vehicle encroaching on a simulated 1V:4H slope at 60 mph (96.5 km/h) and 15 degrees is shown in Figure 3.3.

The barrier containment criteria were based on a limited number of crash tests and engineering judgment. The criterion used for W-beam guardrail is summarized in Figure 2.3. It assumes that vehicle override will result if the mid-height of the bumper impacts above the center of the W-beam's upper corrugation. Acceptable barrier behavior is expected if the mid-height of the bumper impacts between the centers of the W-beam's upper and lower corrugations. Vehicle underride is considered probable if the mid-height of the vehicle's bumper impacts below the center of the W-beam's lower corrugation. The two horizontal lines in Figure 2.2 correspond to the region of acceptable barrier behavior defined in Figure 3.4.

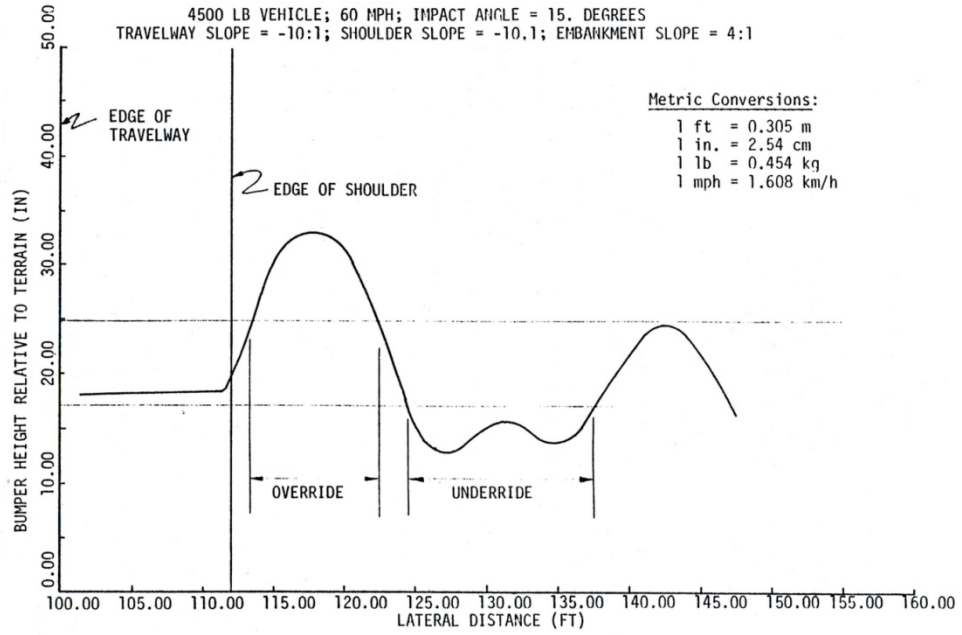

Figure 3.3: Plot of a 4500 lb vehicle right front bumper relative to terrain (Ross and Sicking, 1983)

Seven full-scale crash tests were conducted to evaluate the impact behavior of three widely used roadside barriers placed on a 1V:6H side slope. Four tests involved a standard W beam guardrail on metal posts (G4 (1S) system). Two tests involved a three-cable barrier attached to metal posts (G1 system), and one test involved a thrie beam rail on metal posts (G9 system). Barrier offsets of 6 ft (1.8 m) and 12 ft (3.7 m) from the edge of the shoulder were evaluated. Table 3.2 presents a summary of these tests.

Vehicle override of the barrier occurred in the 25 degree, 60 mph (96.5 km/h) tests of the W-beam and thrie beam systems offset 6 ft (1.8 m) from the break point of the 1V:6H slope. The unsatisfactory behavior of these strong post barriers was attributed to a higher than normal contact height caused by the vehicle launching across the slope and a tendency for the rail element to bend backward and create a ramp for the vehicle. In subsequent testing of a W-beam guardrail offset 12 ft (3.7 m) from the slope break, the rail ruptured and resulted in penetration when impacted at 60 mph (96.5 km/h) and 25 degrees. Successful containment and redirection was achieved under these same conditions when the impact angle was decreased to 15 degrees. In this same series of tests, a 4500 lb (1800 kg) passenger sedan was successfully contained and smoothly redirected by a cable barrier offset 6 ft (1.8 m) from the break point of the 1V:6H slope when impacted at a speed of 60 mph (96.5 km/h) and an angle of 25 degrees (a placement condition for which the impact performance of W-beam and thrie beam guardrail systems was found to be unsatisfactory).

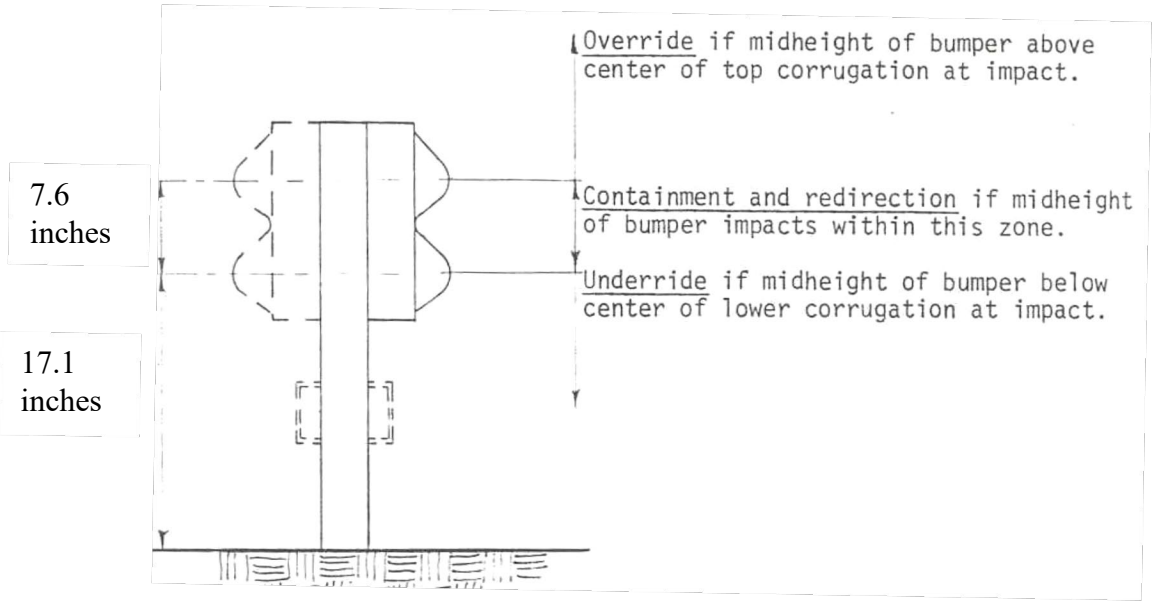

Figure 3.4: Containment criteria for W-beam barrier
(Ross and Sicking, 1983)

The resulting guidelines were presented in 75 figures based on five barrier categories and three different performance standards. For example, placement guidelines for a cable barrier (or box beam barrier) on terrains with slopes ranging from 1V:10H up to 1V:4H is shown in Figure 3.5. The chart indicates that the placement on a 1V:4H slope is more restrictive than placement on a 1V:10H slope as one would expect.

This study illustrated the sensitivity of strong-post guardrail systems to placement on slopes. The problems encountered during the testing with passenger cars will be further aggravated when the pickup truck test vehicle is considered. The higher C.G., higher bumper height, and shorter front overhang of the pickup truck give it an increased propensity to climb or rollover in barrier impacts. The shorter front overhang of the pickup truck also tends to result in more severe post snagging and higher impact loads on the rail, resulting in a greater probability of rail rupture compared to a test with a similar weight passenger sedan.

Table 3.2: Summary of full-scale crash tests of barriers on a 1V:6H sideslope (Ross and Sicking, 1983)

Test Number	Barrier System	Barrier Offset (ft)	Vehicle Weight (lb)	Impact Speed (mph)	Impact Angle (deg)	Result
1	G4(1S)	6.0	4500	62.8	25	Vehicle overrode barrier
2	G4(1S)	6.0	4500	63.3	14.75	Successful containment & redirection
3	G4(1S)	12.0	4500	62.9	26.25	Rail rupture; vehicle penetration
4	G4(1S)	12.0	2300	58.2	14.75	Successful containment & redirection
5	G1	6.0	4500	59.6	24.75	Successful containment & redirection
6	G1	6.0	2250	58.4	17.25	Successful containment & redirection
7	G9	6.0	4500	62.0	26.0	Vehicle overrode barrier

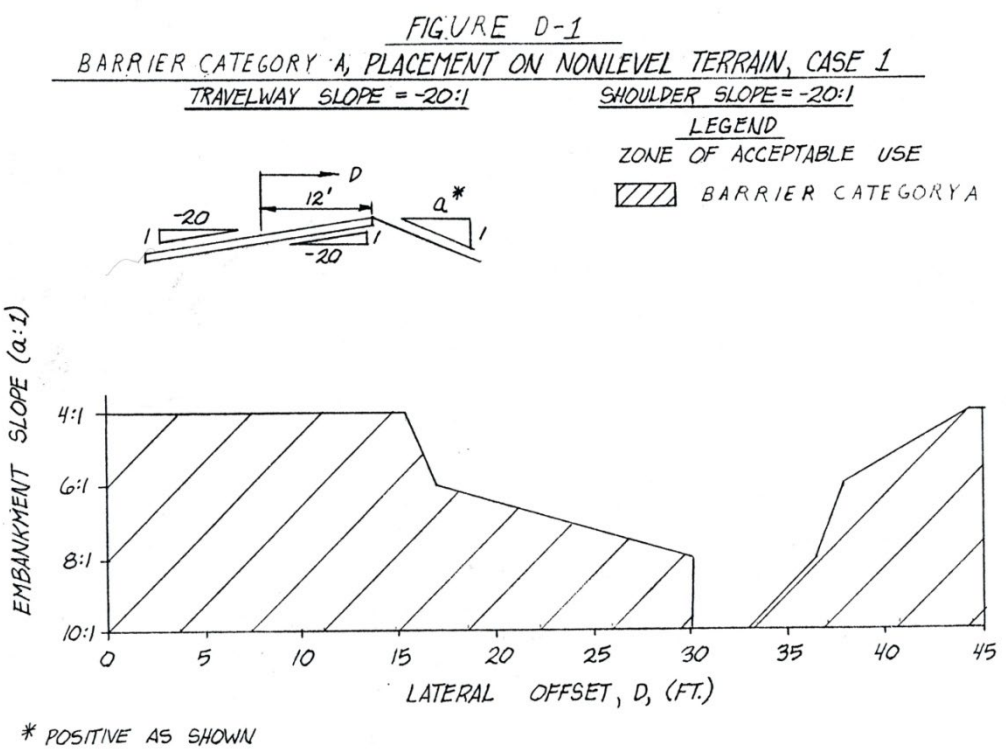

Figure 3.5: Guideline for the placement of cable barrier (or box-beam barrier) to contain and redirect passenger cars (Ross and Sicking, 1983)

While these voluminous guidelines were not implemented in their entirety, the results of this research form the basis of the guidance currently found in the AASHTO *Roadside Design Guide* (2002). There are two limitations to this work that will be addressed under the current project. First, due to the composition of the vehicle fleet and the design test vehicles used in the late 1970s and early 1980s, light trucks were not considered in the analysis and testing program. Second, the research did not include scenarios in which the barrier was impacted on the back slope of a depressed median.

3.3.3. "Evaluating the Benefits of Slope Rounding" (Ross et al., 1993)

In 1993, Ross et al. conducted research to investigate the benefits of rounding the "hinges" at the intersections of shoulders and side slopes. Analysis was performed to investigate the dynamics of a vehicle as it traversed different roadside shoulder and side slope configurations. HVOSM was used to perform this simulation analysis.

Some initial simulations were performed to identify the sensitivity of tire-terrain friction, vehicle type, and driver response to the dynamics of an encroaching vehicle. It was determined that a tire-terrain friction coefficient of 1.0 would be used because it represented the most critical condition evaluated and would serve as an appropriate value for a "soft" soil condition. Higher vehicular accelerations and roll angles were observed for the small car (Honda Civic) than for

the pickup truck (GMC). Initial investigation also revealed that a panic "return-to-the-road" type steering input was more critical compared to no steer input.

Once these critical parameters were identified, a more detailed parametric simulation analysis was performed. Vehicle encroachment speeds of 45 and 65 mph (72 and 105 km/h) were investigated at encroachment angles of 5, 15, 25, 35, and 45 degrees. Side slopes of 1V:6H, 1V:4H, and 1V:3H were investigated with a shoulder and roadway cross-slope of 1V:25H and 1V:50H, respectively. All simulations were performed with a Honda Civic vehicle model with a "return-to-the-road" steering input of 8 degrees at the wheels. It was determined that the body-to-terrain contact was an important factor for this analysis. Therefore, a TTI version of HVOSM (V-3) that permitted modeling of this type of contact was used. All roadsides ditches were assumed to have flat bottoms. Curved roadways and V-ditches were not considered in this research.

Vehicle overturn was predicted for rounded and unrounded side slopes for several combinations of encroachment speeds, angles, and ditch configurations. It was determined that high cornering forces due to panic steering, in combination with soft soil and body-to-terrain contact resulted in significant vehicular instability. For many cases, this instability lead to vehicle overturns.

Occupant risk was evaluated for each simulation and a severity index was assigned for use in a benefit/cost analysis. The benefit/cost analysis was used to develop guidelines for identifying scenarios when slope rounding is cost beneficial.

3.3.4. "Analysis of the Impact Performance of Concrete Median Barrier Placed on or Adjacent to Slopes," (Sheikh et al., 2006), and "Crash Testing and Evaluation of F-Shape Barriers on Slopes," (Sheikh et al., 2008)

In 2005, Sheikh et al. conducted a research study to evaluate the performance of concrete median barriers placed on or adjacent to medians with 1V:6H cross slopes using finite element analysis. According to existing guidelines, the maximum slope on which a concrete barrier could be placed was 1V:10H. The researchers performed vehicular impact simulations on an F-shape barrier installed at various offsets in a V-ditch with 1V:6H cross-slopes. The objective of the research was to determine if the concrete median barrier could be placed on steeper cross slopes, thus allowing placement of the barrier farther from the travel way.

To evaluate barrier performance, lateral offset positions of the barrier most likely to result in vehicle override or instability were determined. Initial simulations were performed to determine the encroachment trajectory of the vehicle as it freely traversed a 1V:6H slope in the absence of a barrier. The results of these simulations were used to trace the path of the vehicle's bumper with respect to the local ground elevation as a function of the vehicle's lateral movement down a 1V:6H slope in the absence of a back slope. Using these bumper height curves, critical barrier offset locations were identified and evaluated in full-scale finite element impact simulations.

Simulation results indicated that the F-shape concrete barrier had a reasonable probability of acceptable impact performance when placed on slopes as steep as 1V:6H. However, since the finite element pickup truck model used in the simulation analyses had not been thoroughly validated for encroachments across median slopes and ditches, it was recommended that full-scale crash tests be conducted to verify simulation results.

In a subsequent research project, the researchers performed full-scale crash tests to evaluate the performance of the F-shaped barrier on 1V:6H cross-slopes. Two full-scale crash tests were performed to evaluate the use of both permanent and free-standing barriers on 1V:6H cross-slopes. These tests were performed with a pickup truck because it was considered to be a more critical design vehicle than the small passenger car in terms of stability, potential for barrier override, and occupant compartment deformation.

TxDOT's permanent cast-in-place F-shape barrier was evaluated in the first crash test. The barrier performed acceptably for *NCHRP Report 350* test 3-11. However, the lateral offset of the barrier in the crash test was inadvertently 6 ft (1.8 m) more than the critical lateral offset. Consequently, the vehicle was losing height when it impacted the barrier and, therefore, the concern of vehicle instability may not have been fully evaluated. However, the researchers stated that the tested barrier location was considered more critical in terms of vehicle occupant compartment deformation (OCD) due increased impact forces imparted to the vehicle as it nosed down into the barrier.

Compared to a permanent barrier, a free-standing barrier generally results in greater vehicular instability as it deflects laterally and allows greater vehicle climb and roll during impact. The second test, which was conducted with a free-standing barrier was, therefore, considered to be a worse case evaluation of vehicular stability for both types of barriers when placed at the critical lateral offset from the slope breakpoint.

TxDOT's free-standing, precast F-shape barrier with X-bolt connection was evaluated at the critical lateral offset of 7.25 ft (2.2 m) from the slope breakpoint in the second crash test. The barrier successfully contained and redirected the vehicle in an upright manner, and met all relevant performance evaluation criteria for *NCHRP Report 350* test 3-11.

It was concluded that TxDOT's permanent and free-standing F-shape concrete barriers perform adequately on roadside and median cross-slopes of 1V:6H or flatter. Since their performance was successfully evaluated for the critical lateral offset, the barriers should perform adequately for any lateral offset of the barrier from the roadway edge; and for any width of depressed V-ditch median as long as the barrier is placed at its center. Similar or better performance would be expected for similar barrier placements on more gentle (e.g., 1V:8H) slopes.

3.3.5. Crash Testing Methods

Previous testing conducted by TTI has included live drivers, cable guided tests, and vehicles driven by remote control. TTI performed remote control vehicle tests to investigate the influence of side slope design on safety as early as 1973 under NCHRP Project 20-7 (Weaver et

al., 1974). They conducted tests in which vehicles traversed various roadside geometries. The objective of the research was to provide guidance in selecting and designing safe roadside configurations.

TTI researchers also conducted embankment traversal tests using remote control vehicles as part of FHWA Contract DTFH61-82-C-00051, "Performance Limits of Longitudinal Barrier Systems."(Buth et al., 1986) Thirteen full-scale crash tests were performed including five tests of a standard strong steel post W-beam guardrail (G4(1S)), two tests of a low-tension, three-cable guardrail (G1), one test with a strong wood post W-beam guardrail (G4(1W)), one using a thrie beam median barrier (MB9), and three tests using a 42 inch (1067 mm) high concrete median barrier. Table 3.3 provides a summary of the crash tests conducted under this study.

Table 3.3: Summary of crash tests conducted by Buth et al, 1986

Test No.	Barrier Type	Test Conditions lb/mph/degree	Vehicle type Test inertia weight (lb)	Height of Vehicle C.G. (in)	Results and Comment
4798-2	Modified G1 Cable guardrail	2220/59.3/14.5	Honda Civic 1888	20.4	Excessive accelerations on the vehicle. Vehicle rolled
4709-4	G4(1S)	2192/59.9/21.5	Honda Civic 1856	20.4	Wheel snagged post.
4798-5	G4(1S)	2100/59.5/15.0	Honda Civic 1764	20.4	Smooth redirection. Acceptable performance.
4798-6	G4(1S)	3260/60.0/22.0	Chevrolet S10 pickup 2923	25.0	Wheel snagged on post but with good vehicular stability and trajectory.
4798-7	G4(1S)	4324/59.2/24.0	Dodge B200 Van 3983	29.5	Vehicle rolled 270 degrees.
4798-8	G4(1S)	4179/56.9/23.5	Ford F150 Pickup 3834	26.1	Wheel snagged on post.
4798-11	Modified G1 Cable guardrail	4585/61.2/25/5	Plymouth Sedan 4249	N/A	Vehicle was contained and the barrier had extensive damage.

3.3.5.1. NCHRP Project 20-7 Vehicle Dynamics

Simulations were conducted for speeds from 40 to 80 mph (65 to 130 km/h) and encroachment angles of 7, 15, and 25 degrees. Freewheeling and "return-to-the-road" type steering inputs were applied to the vehicle. Terrain slopes were varied from 1V:3H to 1V:10H.

To account for the driver's reaction time, steering input was applied 1.5 seconds after the vehicle left the pavement. This was followed by a "return-to-the-road" steering input that was applied over a period of two seconds. The vehicle was then driven for an additional 4.5 seconds or until it returned to a position 3 m (10 ft) outside the edge of the pavement. Thus, the vehicle was allowed to travel for a maximum of eight seconds after leaving the pavement.

It was noted that in the absence of humps and depressions, a tire-terrain coefficient of friction of 0.6 was reasonable for soil embankments. The path of the vehicle during the return maneuver was found to depend greatly on the tire-terrain coefficient of friction. For a 0.2 friction coefficient, no return maneuvers could be performed successfully. It was noted that front slopes less than 1V:4H are desired to reduce bumper contact and penetration in the terrain as the vehicle traverses the ditch.

HVOSM was used as a tool to evaluate vehicle dynamics during roadside encroachments. Twenty-four full-scale vehicle tests were conducted and used for validation of the program. It was noted that HVOSM showed good correlation to test results. At 25-degree encroachment angles, bumper-to-terrain contact and rear overhang drag were observed in all tests above 40 mph. In the absence of a steering and braking input, very little redirection was observed in the vehicle as it traversed a ditch. It was observed that steering input applied while the vehicle is airborne greatly affects vehicle response once the vehicle lands. Sharply turned front wheels induce high side forces on landing and increase wheel digging in the terrain. This increase in the side forces increases the potential of the vehicle to rollover. It was also observed that as a free-wheeling vehicle crosses a slope hinge-point, it is in a state of instability for a short while. However, once all wheels have landed, the vehicle regains stability.

3.3.6. Testing of the Midwest Guardrail System on an 8:1 Slope

The Midwest Roadside Safety Facility (MwRSF) conducted two full-scale crash tests on the Midwest Guardrail System (MGS) placed on a 1V:8H slope. In the MGS system, the W-beam rail is mounted to 6-ft (1.8 m) long W6x8.5 steel posts at a height of 31 inches (787 mm) relative to the local terrain as shown in Figure 3.6. The guardrail splices are located midspan between posts, and the wooden offset blocks are 12 inches (305 mm) deep. The face of the guardrail was offset 5-ft (1.5 m) from the slope break, which was the critical offset distance for the 1V:8H slope as determined through computer simulation.

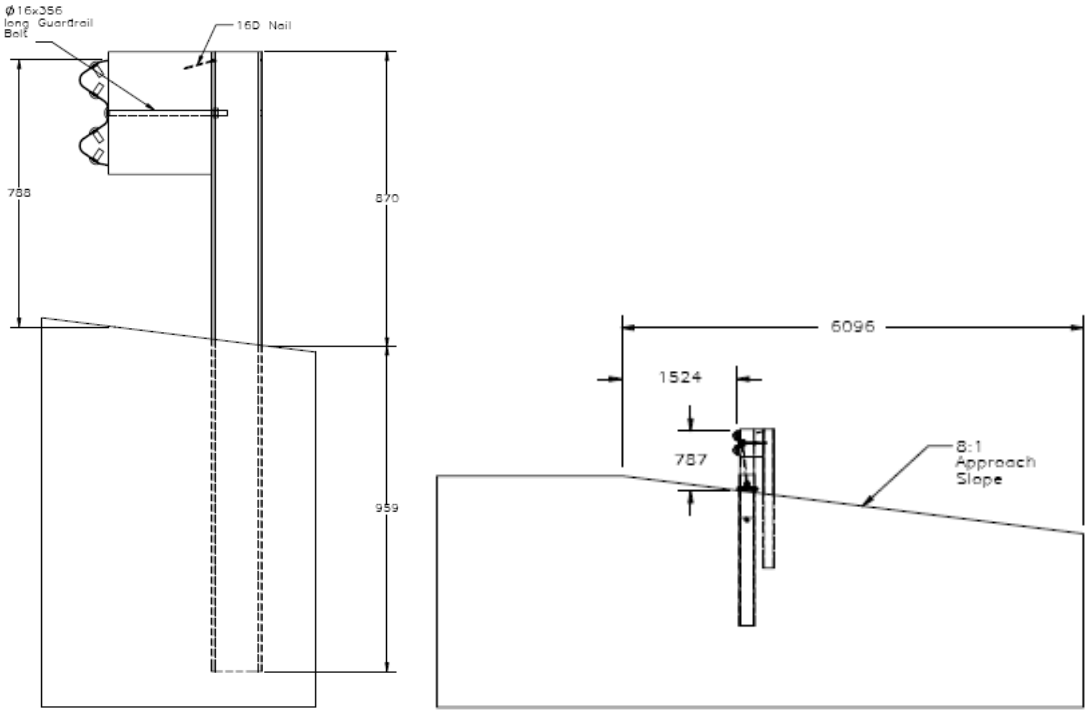

Figure 3.6: Post (left) and guardrail (right) placement of the MGS system on a 1V:8H slope

The rail was impacted with a 4400 lb (2000 kg) pickup truck and an 1800 lb (820 kg) small car per *NCHRP Report 350* TL-3 conditions (see Figure 3.7). Both tests were judged to have met *NCHRP Report 350* criteria. However, the pickup truck experienced significant roll and was only marginally stable when engaging the rail on the 1V:8H slope. This test clearly defined the performance limits of the taller 31 inches (787 mm) guardrail system and demonstrated the sensitivity of W-beam guardrail performance to vehicle dynamics on slopes.

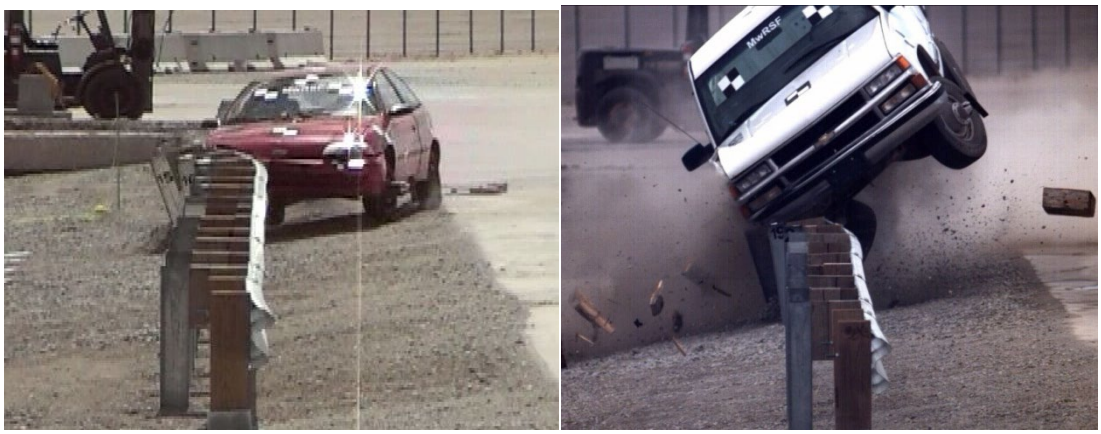

Figure 3.7: MGS system on 1V:8H slope as impacted by a small car (left) and a pickup truck (right)

3.3.7. Guardrail Height Tolerance Performance

In another study, computer simulation was used to study the effect of mounting height on impact performance (Marzougui et al., 2007). LS-DYNA was used to model steel post W-beam guardrail with tolerances of -3,-1.5,+1.5, and +3.0 inches (-76, -38, +38, and +76 mm) with respect to a standard W-beam rail height of 27 inches (686 mm). The simulation results agreed with established engineering knowledge that W-beam rail performance is compromised when its height is decreased below 27 inches (686 mm) to the top of the rail. Two full-scale crash tests were conducted per *NCHRP Report 350* Test Designation 3-11 using a 2000P test vehicle. In the first test with the rail mounted at standard height, the vehicle was successfully redirected. In the second test, the rail height was lowered 2.5 inches (64 mm) and the pickup truck overrode the barrier. These tests provide good validation points for establishing performance limits of barriers under the current project. A vehicle impacting a barrier at a lower barrier mounting height is analogous to a vehicle engaging a rail at a higher than normal height due to the effects of sloped geometry and/or suspension rebound.

4. TERRAIN CONFIGURATION AND BARRIER TYPES

4.1. TERRAIN CONFIGURATIONS

For the purposes of this project, the "median width" is defined to be the total horizontal width of the ditch from one slope break point (point A) to the opposite slope break point (point B) excluding inside shoulders (if any) as illustrated in Figure 4.1.

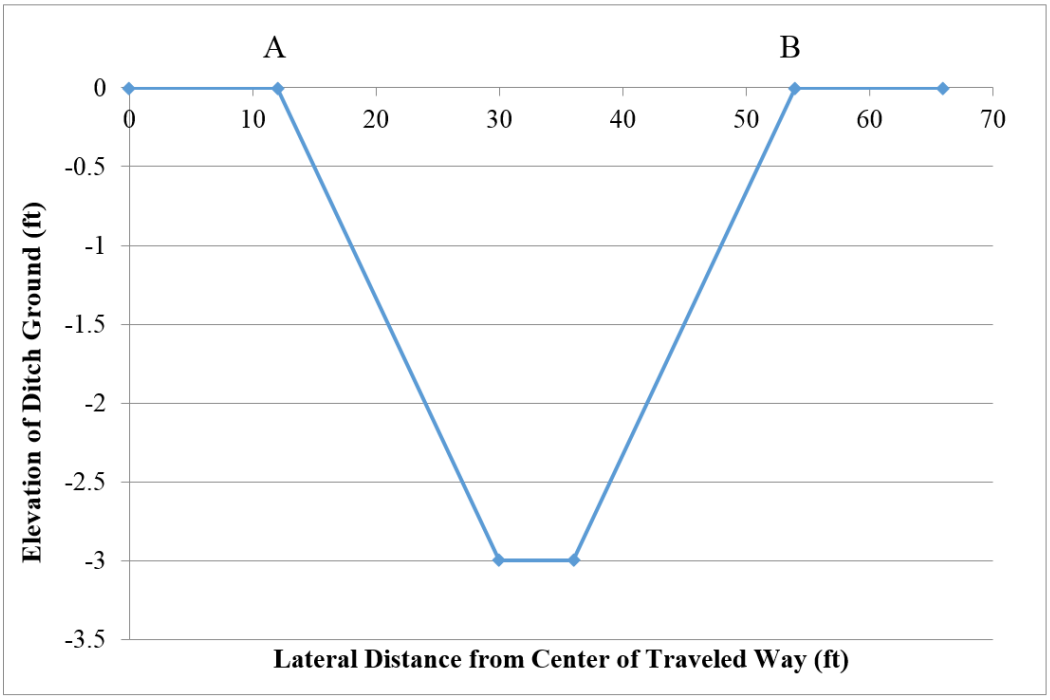

Figure 4.1: Median Width Definition from Point A to Point B

The initial designs for the "target median profiles" are summarized in Table 4.1 and Table 4.2. This project focuses on ditches with side slopes of 1V:6H and 1V:8H. For both slope cases, median profiles were selected with ditch widths of 32 feet, 42 feet, 52 feet, and 62 feet. Finally, each combination of specified slope and specified ditch width were considered for ditch depths of 3 feet, 4 feet, and 6 feet. This provided a total of 24 different possible median profiles.

Table 4.1: Dynamic Analysis Design Parameters (as Specified by Panel)

MASH Vehicle	5000 lb (2270 kg) Pickup Truck / 2425 lb (1100 kg) Small Passenger Car							
Design Speed	49.7 mph (80kph)				62.1 mph (100kph)			
Entrance Angle	15°		25°		15°		25°	
Ditch Slope (V:H)	1:6	1:8	1:6	1:8	1:6	1:8	1:6	1:8
Ditch Width	*Refer to Table 4.2, Target Median Profile Properties (as Defined by Panel)*							
Ditch Depth								

Table 4.2: Target Median Profile Dimensions (as Defined by Panel)

Ditch Slope (V:H)	1:6												1:8											
Ditch Width (ft)	32			42			52			62			32			42			52			62		
Ditch Depth (ft)	3	4	6	3	4	6	3	4	6	3	4	6	3	4	6	3	4	6	3	4	6	3	4	6

The defined median ditch parameters resulted in both V-shaped and trapezoidal ditches as depicted in Figure 4.2 and Figure 4.3, respectively. It was noted that defining ditch slope, width, and depth was over-prescriptive for some of ditch configurations. Several of the specified "target profiles" cannot be fully satisfied. For these over-defined V-shaped ditches, the depth is limited by the specified slope and median width.

For example, consider a median profile with a 1V:6H slope and a ditch width of 32 feet (Table 4.3). The slope and width create a V-shaped ditch with a depth of 2.67 feet. Therefore, the target ditch depths of 3 feet, 4 feet, and 6 feet cannot be achieved for this profile. In such cases, only the limiting ditch depth was used. Considering another profile with a 1V:6H slope and a ditch width of 42 feet, the limiting depth is 3.5 feet. In this case, the target depth of 3 feet can be obtained, but the target depths of 4 feet and 6 feet cannot be achieved. Therefore, for a 1V:6H slope and 42 foot width, two median ditch profiles were analyzed— one trapezoidal in shape with a depth of 3 feet, and the other a V-shaped ditch with a depth of 3.5 feet. This example is illustrated visually in Figure 4.4.

Based on this geometric assessment, the 24 possible ditch combinations were reduced to fifteen unique median profiles that were analyzed under the project. Table 4.3 summarizes the median profiles having a 1V:6H slope. Table 4.4 summarizes the median profiles having a 1V:8H slope. Note that the target ditch depths marked with an asterisk (*) were not physically attainable based on the defined slope and median width. For these cases, the actual limiting ditch depth is indicated and corresponds to what was used in the analyses.

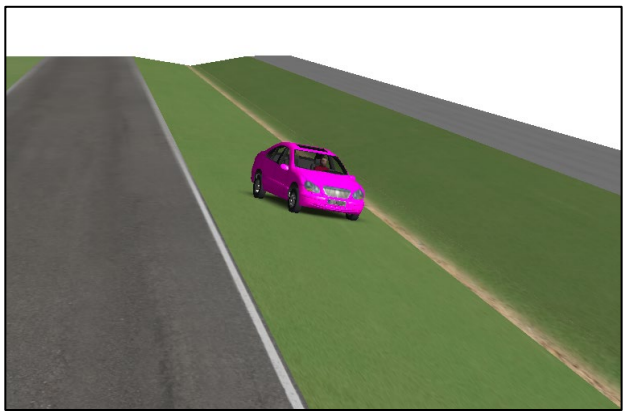

Figure 4.2: CarSim V-Shaped Profile

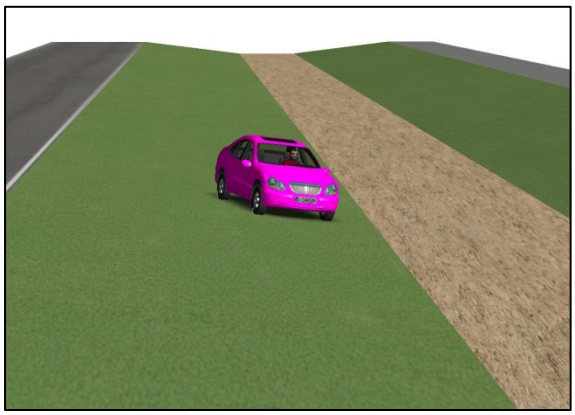

Figure 4.3: CarSim Trapezoidal Profile

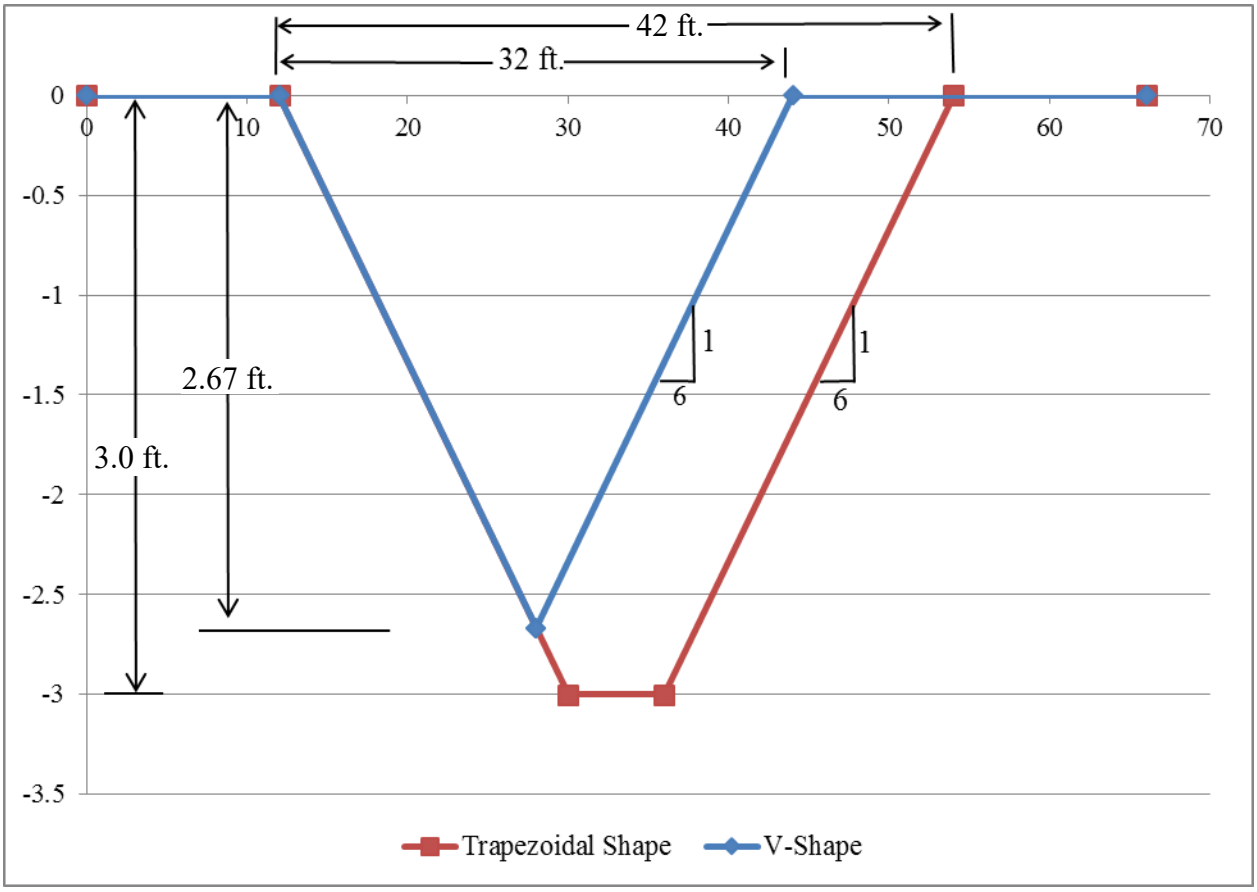

Figure 4.4: Median Profiles (V-shape and Trapezoidal)

Table 4.3: Feasible Median Profiles Analyzed for 1V:6H Slope

Ditch Slope (V:H)	1:6											
Ditch Width (ft)	32			42			52			62		
Target Ditch Depth (ft)	3*	4*	6*	3	4*	6*	3	4	6*	3	4	6*
Actual Ditch Depth (ft)	2.67			3	3.5		3	4	4.33	3	4	5.17
Ditch Shape (T=Trap, V=V-shaped)	V for depth≥2.67ft			T	V for depth≥3.5ft		T	T	V for depth≥4.33ft	T	T	V for depth ≥5.17ft

*Specifying ditch depth over-defines this median profile.

Table 4.4: Actual Median Profiles Analyzed for 1V:8H Slope

Ditch Slope (V:H)	1:8											
Ditch Width (ft)	32			42			52			62		
Target Ditch Depth (ft)	3*	4*	6*	3*	4*	6*	3	4*	6*	3	4*	6*
Actual Ditch Depth (ft)	2.0			2.63			3	3.25		3	3.88	
Ditch Shape (T=Trap, V=V-shaped)	V for depth≥ 2.0ft			V for depth≥2.63ft			T	V for depth≥3.25ft		T	V for depth≥3.88ft	

*Specifying ditch depth over-defines this median profile.

4.2. BARRIER SELECTION

While several different types of barriers are used on the national highway system, some types are used more frequently than the others. Table 4.5 documents common barrier types tested under *NCHRP Report 350* impact performance guidelines. Other median barrier systems such as strong post W-beam and strong post thrie beam were not tested under *NCHRP Report 350*, but were accepted for use based on testing of their counterpart guardrail systems.

Table 4.5: Common barrier types tested under NCHRP Report 350

Guardrail	Median Barriers	
Low-tension cable (G1)	High-tension cable	
Modified weak post W-beam (G2)	Weak-post W-beam (MB2)	
Box beam (G3)	Box beam (MB3)	
Modified strong steel-post W-beam (G4(1S))		
Strong wood-post W-beam (G4(2W))		New Jersey
Modified strong steel-post thrie beam (G9-S)	Concrete:	F-shape
Strong wood-post thrie beam (G9-W)		Single slope
Modified thrie beam		
Midwest Guardrail System (MGS)		

4.2.1. Guardrail Systems

Guardrails and median barriers can be generally classified into three categories: weak post systems, strong post systems, and rigid concrete barriers. Weak post systems are the most flexible and have the greatest dynamic deflection. The "weak" posts serve primarily to support the rail elements at their proper elevation for contact with an impacting vehicle. The posts are readily detached from the rail element(s) and dissipate little energy as they yield to the impacting vehicle and are pushed to the ground. Provided there is adequate space to accommodate the deflection, these barriers impart lower deceleration on an impacting vehicle and are, therefore, more forgiving and less likely to cause injury. Examples of weak-post barrier systems include cable, weak-post W-beam, and box beam, which are shown in Figure 4.5 (a), (b), and (c), respectively. S3x5.7 steel posts are common to all three of these generic guardrail systems. It is noteworthy to mention that both the modified weak post W-beam and box beam guardrail systems have successfully met *MASH* impact performance guidelines.

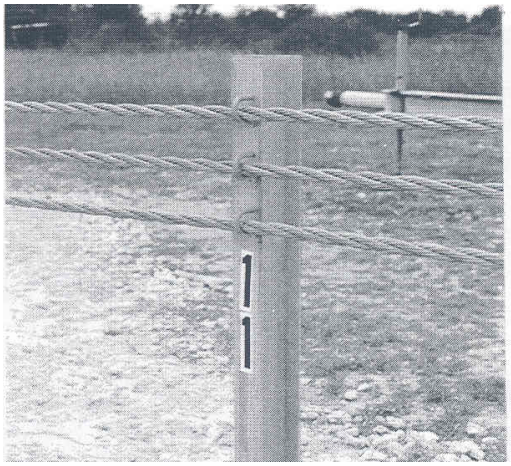

(a)

(b)

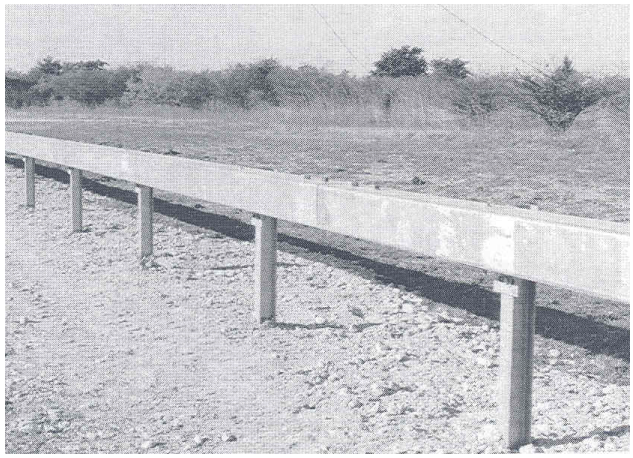

(c)

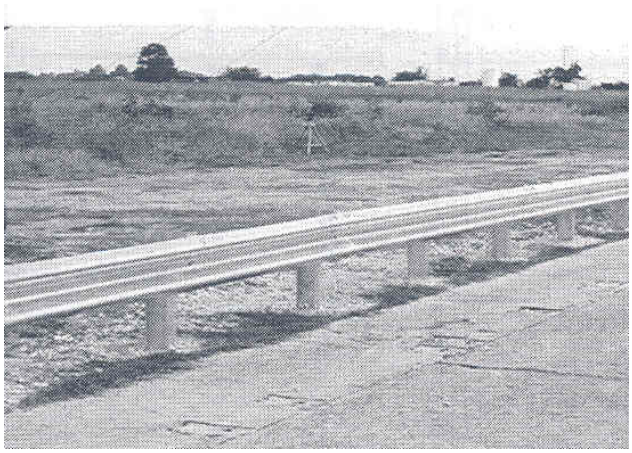

(d)

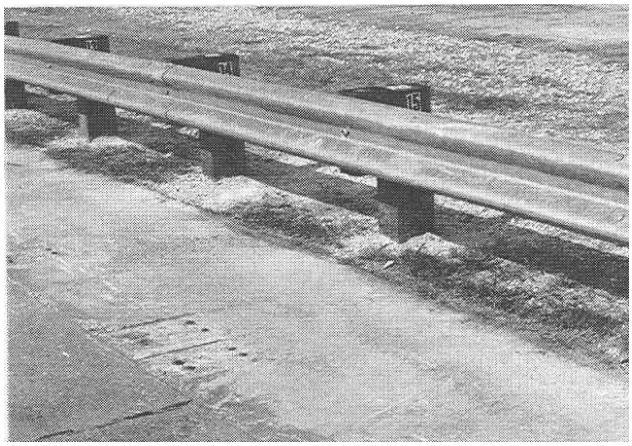

(e)

Figure 4.2: Types of guardrails: (a) Low tension cable (G1), (b) Weak post W-beam (G2), (c) Box beam (G3), (d) Strong steel post W-beam (G4(1S)), and (e) Strong wood post W-beam (G4(2W)) guardrail

In contrast, strong-post barriers incorporate larger, stronger posts that absorb significant energy as they rotate through the soil during an impact. The increased post stiffness results in reduced dynamic deflection and increased deceleration rates. Spacer blocks are used to offset the rail element from the posts to minimize vehicle snagging on the posts. Severe post snagging can impart high decelerations to the vehicle and lead to vehicle instability or significant occupant compartment deformation. Examples of strong post barriers include the strong post W-beam and thrie beam. Both of these barrier systems have wood (e.g. 6 inch x 8 inch (152 mm x 203 mm)) and steel (e.g., W6×9 (W150×14)) post variations. Strong-post W-beam is the most common barrier system in use in the U.S. Figure 4.5 (d) and (e) show strong steel post W-beam (modified G4(1S)) and strong wood post W-beam (G4(2W)) guardrails, respectively.

The strong steel post W-beam guardrail system, G4(1S), failed to meet *NCHRP Report 350* when tested with the ¾-ton, 2-door, pickup truck design vehicle (denoted 2000P). Collapse of the W6×9 (W150×14) steel offset blocks permitted the wheel of the pickup truck to snag and ride over the steel support posts. This behavior resulted in rollover of the truck as it exited the barrier. Subsequent testing demonstrated that a modified G4(1S) system with 8 inch (203 mm) deep wood or structural plastic offset blocks between the W-beam rail element and W6×9 (W150×14) steel posts could accommodate the 2000P pickup truck and comply with *NCHRP Report 350* guidelines (Mak et al., 1998a; Mak et al., 1998b; Bullard et al., 1996; and Polivka et al., 2006).

The strong wood post W-beam guardrail system, G4(2W), which utilizes 6 inch x 8 inch (152 mm x 203 mm) wood posts and offset blocks, successfully contained and redirected the 2000P pickup (Mak et al., 1998a and 1998b). However, instability of the pickup truck resulted in the test being classified as marginally acceptable.

Both of these strong-post W-beam guardrail systems have been widely used as national standards. Testing under *MASH* guidelines has demonstrated that these strong-post W-beam guardrail systems are at or near their performance limits. Under NCHRP Projects 22-14(02) and 22-14(03), a series of crash tests were performed to assess the impact performance of commonly used barrier systems when impacted by the ½-ton, four-door, pickup truck design vehicle (designated 2270P) under the AASHTO *MASH* guidelines. The increase in the weight of the new pickup truck from approximately 4400 lb to 5000 lb (2000 kg to 2270 kg) increases the impact severity of the structural adequacy test (Test 3-11) for longitudinal barriers by 13 percent. A summary of these barrier tests is shown in Table 4.6.

In a test of a modified G4 (1S) steel post W-beam guardrail, the pickup truck was contained and redirected (Polivka et al., 2006). However, the rail had a vertical tear through approximately half of its cross-section, indicating that the modified G4 (1S) guardrail is at its performance limits with no factor of safety. In a test of the G4 (2W) wood post W-beam guardrail, the rail ruptured and failed to contain the pickup truck.

Table 4.6: Summary of *MASH* crash tests performed on barriers under NCHRP Project 22-14

Agency Test No.	Test Designation	Test Article	Vehicle Make and Model	Vehicle Mass (lb)	Impact Speed (mph)	Impact Angle (deg)	PASS/ FAIL
2214WB-1	3-11	Modified G4(1S) Guardrail	2002 GMC 2500 ¾-ton Pickup	5000	61.1	25.6	PASS
2214WB-2	3-11	Modified G4(1S) Guardrail	2002 Dodge Ram 1500 Quad Cab Pickup	5000	62.4	26.0	PASS
2214MG-1	3-11	Midwest Guardrail System (MGS)	2002 GMC 2500 ¾-ton Pickup	5000	62.6	25.2	PASS
2214MG-2	3-11	MGS	2002 Dodge Ram 1500 Quad Cab Pickup	5000	62.8	25.5	PASS
2214MG-3	3-10	MGS (Max. Height)	2002 Kia Rio	2588	60.8	25.4	PASS
2214NJ-1	3-10	32-inch Permanent New Jersey Safety Shape Barrier	2002 Kia Rio	2579	60.8	26.1	PASS
476460-1-4	3-11	32-inch Permanent New Jersey Safety Shape Barrier	2007 Chevrolet Silverado Pickup	5049	62.6	25.2	PASS
476460-1-6	3-11	G3 Weak Post Box-Beam Guardrail	2007 Chevrolet Silverado Pickup	5011	63.2	25.4	PASS
476460-1-7	3-11	G2 Weak Post W-Beam Guardrail	2007 Chevrolet Silverado Pickup	5004	62.4	24.6	PASS
476460-1-10	3-10	MB4-S W-Beam Median Barrier	2002 Kia Rio	2584	61.4	26.0	PASS
476460-1-5	3-11	G4(2W) W-Beam Guardrail	2007 Chevrolet Silverado Pickup	5009	64.4	26.1	FAIL
476460-1-8	3-11	G9 Thrie Beam Guardrail	2007 Chevrolet Silverado Pickup	5019	63.3	26.4	FAIL
476460-1-9	3-11	G4(1S) W-Beam Median Barrier	2007 Chevrolet Silverado Pickup	5029	64.0	25.1	FAIL

As a result, many states have adopted alternate strong-post guardrail systems that offer enhanced capacity. As an example, a modified guardrail design known as the Midwest Guardrail System (MGS) (Polivka et al., 2006) successfully met the *MASH* guidelines and has been shown to have additional capacity or factor of safety beyond the design impact conditions. The MGS guardrail increases the W-beam rail height from 27 inches to 31 inches (686 mm to 787 mm), increases the depth of the offset blocks between the rail and posts from 8 inches to 12 inches (203 mm to 305 mm), and moves the rail splice locations from the posts to mid-span between posts.

Thrie beam guardrails were originally developed to extend the performance range of strong post guardrails. The concept is that the taller, stronger beam element will have expanded containment capacity and offer improved stability for a broader range of vehicles. However, full-scale crash testing performed under *NCHRP Report 350* and, more recently, *MASH,* indicates this assumption is not entirely accurate.

There are two basic types of thrie beams guardrails: standard strong steel and wood post thrie-beam (G9), and modified thrie-beam. The modified thrie-beam is the result of improvements made to the standard thrie-beam that were specifically designed to reduce rollover probability when impacted by larger vehicles such as school and intercity buses (Ivey et al., 1982). Figure 4.6 (a) and (b) show strong steel post thrie-beam (G9-S) and modified thrie-beam guardrail, respectively.

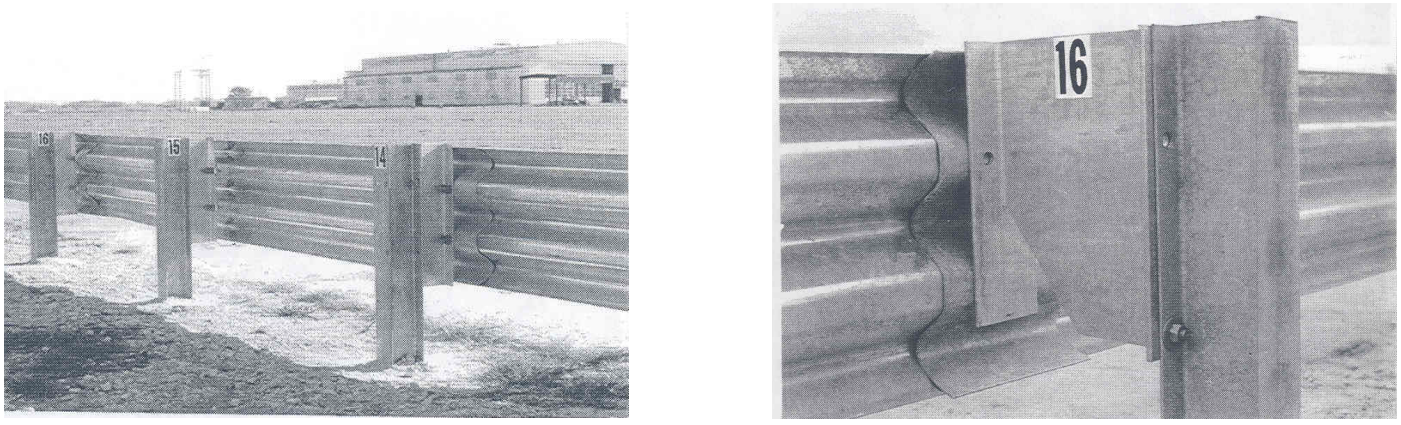

(a) (b)

Figure 4.3: (a) Strong steel post thrie-beam (G9-S),
and (b) Modified thrie-beam guardrail section

The strong steel post thrie-beam with steel offset blocks (G9-S) failed to meet *NCHRP Report 350* impact performance requirements (Mak et al., 1998a and Mak et al., 1998b). During the impact event, the left front wheel of the pickup severely snagged the flanges of two posts. This caused the pickup to pitch forward as it was redirecting. Consequently, the backslap contact between the vehicle and rail occurred at a higher point on the pickup, and induced a roll

moment. The vehicle instability was aggravated by the ramp-like deflected shape of the thrie beam rail. These events caused the pickup truck to rollover as it exited the barrier system.

Following the failure of the standard G9 thrie-beam guardrail system, a modified steel post thrie-beam guardrail system with routed wood offset blocks was tested and evaluated. The modified steel post thrie-beam guardrail system with routed wood blocks successfully contained and redirected the pickup and met all *NCHRP Report 350* evaluation criteria (Buth et al., 2000).

Under NCHRP Project 22-14(03), this same modified steel post thrie-beam guardrail system with routed wood offset blocks was tested in accordance with the new *MASH* guidelines. Somewhat unexpectedly, the pickup truck rolled over 360 degrees while exiting barrier. The behavior looked similar to the unsuccessful test of the original strong steel post thrie-beam with steel offset blocks that failed *NCHRP Report 350* Test 3-11. Additional research and testing will be required to arrive at a design modification that addresses this failure.

This raises the issue of whether or not this barrier system, and others that have failed to meet *MASH* impact performance guidelines, should be included in the present study. By nature of the vehicle behavior and interaction, the placement of barriers placed on slopes and in ditches tends to degrade impact performance. Therefore, it does not seem appropriate to consider developing guidelines for the placement of the modified steel post thrie beam guardrail system and other systems on slopes and in ditches if they have failed to meet the latest impact performance requirements on flat, level ground.

4.2.2. Median Barrier Systems

The guardrail systems described above are sometimes used in median applications. Because guardrails are "single-sided" rather than "dual-sided" in design, such instances typically require the use of two barriers – one on each side of the median. This practice may be followed if the median is not safely traversable, the user agency wants to avoid complications with drainage and erosion that can be associated with the placement of a barrier in a median ditch, or they have a disposition toward a particular barrier system and desire to use it on both roadside and median applications to reduce inventory and/or simplify maintenance and repair training and operations.

Other barrier systems are specifically designed for use in a median by configuring them to accommodate an impact on both sides of the barrier. As mentioned previously, high-tension cable, weak-post W-beam, and box beam median barriers were all successfully tested under *NCHRP Report 350*.

High-tension cable median barrier systems have been widely used across the country as a cost-effective alternative for shielding motorists from crossover crashes. Their relatively low cost makes cable median barrier systems appealing for treating long stretches of highway. Additionally, the flexibility of these systems results in lower decelerations to an impacting vehicle, which lowers the probability of injury to occupants. However, sufficient space must be available to accommodate the greater design deflections associated with these systems.

All of high-tension cable barriers in the market place are proprietary in design. Various issues associated with the use of high-tension cable barrier systems, including guidelines for their placement in median ditches is the subject of NCHRP Project 22-25. Therefore, cable barrier systems were excluded from the analyses performed under Project 22-20(02). This permitted project resources to be applied toward the development of placement guidelines for other guardrail and median barrier systems.

Although they may occasionally have roadside application, concrete barriers are much more commonly used as median barriers. The rigid nature of cast-in-place concrete barriers results in essentially no dynamic deflection. Thus, vehicle deceleration rates and probability of injury are greater for concrete barriers than for more flexible systems. However, although their installation cost is relatively high, concrete barriers require little maintenance or repair after an impact. Thus, exposure and risk to maintenance and repair personnel is dramatically reduced, as is the cost and congestion associated with temporary lane closures that would otherwise be required for maintenance and repair. This makes concrete barriers particularly appealing for use on high-speed, high-volume urban freeways with narrow medians.

Common concrete barrier profiles that met *NCHRP Report 350* impact performance criteria include the New Jersey safety shape, F-shape, constant or single slope, and vertical wall (Mak and Menges, 1996; Beason et al., 1989). While the New Jersey profile has a long history of widespread use, it has been falling out of favor in recent years based on the realization that it can impart significant climb and instability to impacting vehicles under certain impact conditions. The F-shape and constant slope barriers are generally considered to provide the same level of impact performance. Both permit considerable vehicle climb (which helps dissipate energy), but provide improved vehicle stability compared to the New Jersey profile. Figure 4.7 (a), (b), and (c) show New Jersey safety shape, F-shape, and single slope concrete barrier profiles, respectively.

The New Jersey safety shape barrier was tested and evaluated to *MASH* criteria under NCHRP Project 22-14(03). The 2270P pickup was successfully contained and redirected, and the New Jersey safety shape met all required performance criteria. It was noted that the stability of the vehicle was improved over the similar *NCHRP Report 350* test.

As mentioned above, previous testing has shown that the New Jersey profile will impart more climb and instability to an impacting vehicle than an F-shape or constant slope profile. This effect is primarily due to the taller "toe" of the New Jersey barrier. Therefore, given that the New Jersey profile has successfully met the *MASH* guidelines, it can be inferred that the F-shape and constant slope barriers will also satisfy *MASH*.

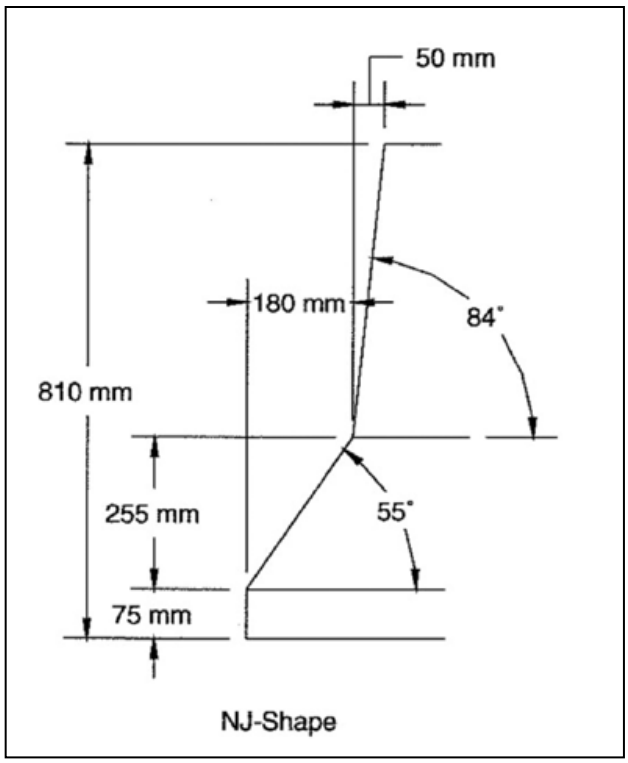

(a)

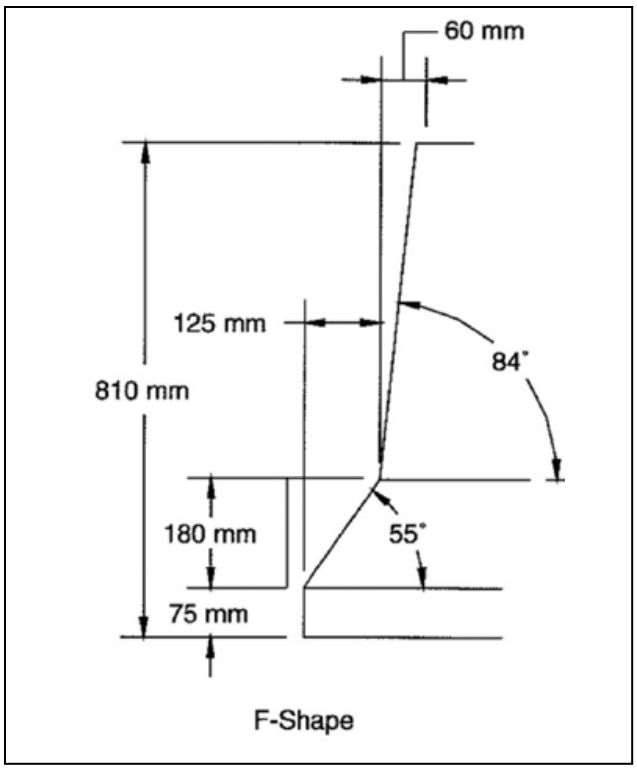

(b)

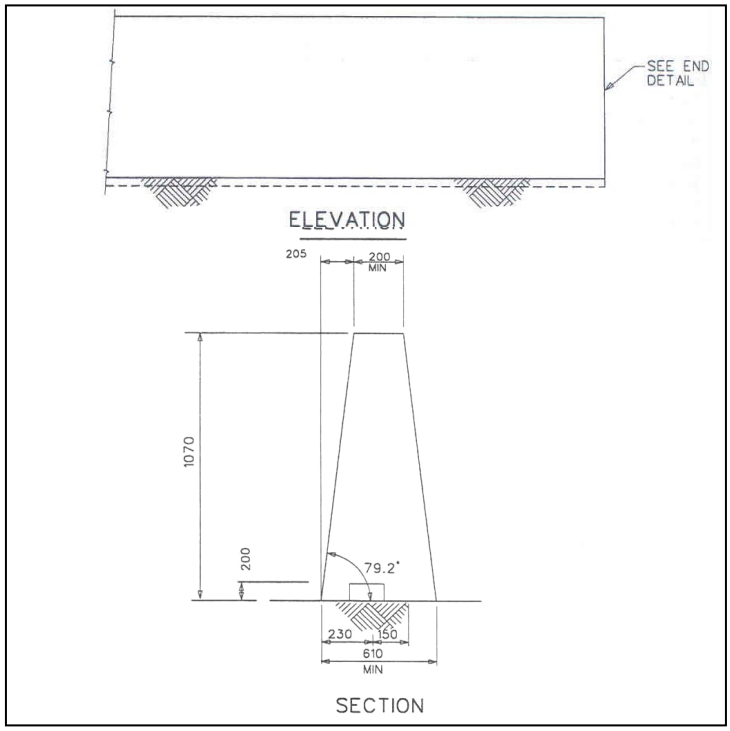

(c)

Figure 4.4: Concrete barriers; (a) New Jersey safety shape (b) F-shape, and, (c) Constant slope concrete barriers

Strong-post W-beam and thrie beam median barrier systems were never explicitly tested under *NCHRP Report 350*. However, they were accepted for use as *NCHRP Report 350* compliant barriers by FHWA based on the successful testing of their counterpart guardrail systems (FHWA, 2000). However, given the marginal performance of the modified G4(1S) guardrail system when tested under *MASH*, it was decided to test the median barrier version (MB4-S) as part of NCHRP Project 22-14(03).

In *MASH* Test 3-11, the 2270P pickup truck overrode the strong steel post W-beam median barrier. Typically, when a strong steel post guardrail system is impacted, the rail detaches from the support posts by means of the post bolt pulling through the rail slot as the guardrail deflects and the posts displace laterally. However, in the test of the median barrier system, the rear W-beam rail element restrained the lateral displacement of the posts, and the front W-beam rail was unable to detach from the posts. Thus, the front W-beam rail was pulled down in height and permitted the vehicle to climb and vault the barrier.

This failed test once again raised the issue of whether or not this median barrier system should be included for further evaluation under this project. The strong steel post median barrier failed when tested on flat, level ground. The vaulting behavior of the vehicle observed in this test will only be exacerbated by the placement of this median barrier on a slope.

There is another version of the strong steel post median barrier in the AASHTO *Roadside Design Guide (RDG)*. The height of the W-beam rail is increased from 27 inches to 30 inches (686 mm to 762 mm), and a channel rubrail is added between the ground and the bottom of the W-beam to reduce underride potential for small cars resulting from the increased clear opening. However, there is no consensus among roadside safety researchers regarding whether or not this version of the strong steel post median barrier will meet the *MASH* guidelines. While the added height should indeed be beneficial, it is not clear how the vehicle will interact with the rubrail and whether or not this barrier system will meet *MASH* criteria. Additional research and testing is needed to determine what configurations of strong-post W-beam median barrier will satisfy *MASH* impact performance requirements. Until this is accomplished, it was not considered appropriate to include this system for further evaluation under the current project.

Weak post W-beam and box beam median barriers were successfully tested to *NCHRP Report 350* (Abu-Odeh et al., 2003; Mak and Menges, 1999). Although it is not absolutely known if these systems will meet *MASH* guidelines, the successful testing of the guardrail systems under *NCHRP Report 350* and *MASH*, and the successful testing of the median barriers under *NCHRP Report 350* does provide a certain level of confidence that they will. These systems were, therefore, considered good candidates for further evaluation under this project.

4.2.3. Frequency of Use

In a survey conducted under NCHRP Project 22-21, which was designed with input from the Project 22-22(02) research team, state highway agencies were asked to estimate their percent usage of different median barriers types. The replies of the participating states are shown in Table 4.7. Among concrete barriers, the New Jersey profile and F-shaped barrier had the highest indicated usage. Strong post W-beam was also among the most commonly used median barrier types. Weak post W-beam and box beam median barriers had significant usage indicated by

some states. These systems have more frequent application in some northern states due to the increased clear opening beneath the rail which is desirable in areas with large amounts of snowfall. Some states also prefer to use these systems because they are more flexible and forgiving and, thus, less likely to impart injury to the occupants of impact vehicles. However, they do tend to be more maintenance and repair intensive than some other median barrier systems.

It should be noted that the results presented in Table 4.7 pertain only to median applications. The percentages for roadside applications will likely differ. Furthermore, the percent usage per state is not a comprehensive measure for determining the national frequency of usage for each barrier type. Determining a national percentage would depend on the current inventory of the miles installed of each barrier type. Thus the current usage percentages presented in Table 4.7 should only be taken as a partial indicator of the most commonly used median barrier types.

Under NCHRP Project 22-14(03), TTI researchers surveyed state departments of transportation (DOTs) to identify the type and frequency of use of non-proprietary roadside-safety features used in their respective state. Devices included in the survey were non-proprietary guardrails, median barriers, transitions, crash cushions, terminals, and breakaway hardware (i.e. sign and luminaire supports).

The survey included a comprehensive list of non-proprietary roadside safety features, grouped by category. Five check boxes were provided for each device to indicate associated percentages of use: [Never; Rarely (1-25 percent); Somewhat Frequently (26-50 percent); Frequently (51-75 percent); and Very Frequently (76-100 percent)]. Each device name listed on the survey was hyperlinked to the device's respective FHWA acceptance letter. This enabled the respondent to view the FHWA letter and any associated engineering drawings for clarification of system details. Responses were received from 44 states.

The researchers analyzed the survey information and determined those features which are most frequently used and would, therefore, potentially be a high priority for evaluation to *MASH* criteria. The results of the survey were weighted by individual hardware item and ranked among the hardware category. The rankings obtained for the guardrail and median barrier categories are presented in Table 4.8.

Table 4.7: Survey from participating states (from NCHRP Project 22-21 Interim Report)

Agency	Current agency usage (percent) of each of the approved barrier types									
	Weak-post W-beam guardrail	Box-beam barrier	Blocked-out W-beam guardrail (strong post)	Blocked-out thrie-beam guardrail (strong post)	Modified thrie-beam guardrail	New-Jersey-shaped concrete barrier	Single-slope concrete barrier	F-shaped concrete barrier	Three-strand cable (weak post)	High-tensioned cable barrier
Arkansas			Less than 5%			20%	30%	Less than 5%		Less than 5%
Delaware			100% where barriers are place in rural medians which is very seldom							
Idaho			~ 30%	~ 10%(mostly across structures that do not use a concrete barrier system)		~ 60%				
Indiana			19%		1%			80%		
Iowa			1%	0%				60%		40%
Kentucky	19%					80%				1%
Maryland			75%	5%		10%		10%		
Minnesota		5%	5%				5%	5%		80%
Nebraska										1%
New York	15%	25%	25%				25%	10%	0	
Oregon			5%		0% (to date)		5%	85%		5%
South Dakota				3%		92%	5%	0%		0%
Texas						50%	30%	5%		15%
Virginia	20%		20%					10%		
Wyoming		40%	40%	5%		5%		5%		5%

Table 4.8: Weighted prioritization by hardware category

Test Article	Tested to MASH	Prioritization from Survey
Guardrails		
Strong-Post (Steel) W-Beam	✓	1
Strong-Post (Wood) W-Beam	✓	2
Strong-Post (Steel) Thrie-Beam	✓	3
Strong-Post (Wood) Thrie-Beam		4
Low-Tension Cable (3-Strand)		5
Midwest Guardrail System (MGS)	✓	6
Weak-Post Box-Beam	✓	7
Strong-Post Modified Thrie-Beam		7
Weak-Post W-Beam	✓	9
Median Barriers		
Safety-Shape (New Jersey)	✓	1
Strong-Post (Steel) W-Beam	✓	2
F-Shape		3
Strong-Post (Wood) W-Beam		4
Constant Slope (Single-Slope) Barrier (TX & CA designs)		5
Strong-Post (Steel) Thrie-Beam		6
Strong-Post (Wood) Thrie-Beam		7
Low-Tension Cable (3-Strand)		8
Vertical Concrete Barrier		8
Strong-Post Modified Thrie-Beam		10
Weak-Post W-Beam		11
Weak-Post Box-Beam		11

Among guardrails, the strong post W-beam and thrie beam systems had the highest frequency of usage across the states responding. The low ranking for the MGS is reflective of the fact that it is a relatively new system and is just now beginning to see more widespread implementation. The weak post W-beam and box beam ranked relatively low in the survey when considered across all states responding, but it was noted that they are used very extensively by a few states.

In regard to median barriers, various profiles of concrete barriers occupied three of the top five spots in the rankings, including the New Jersey profile which had the highest overall ranking. However, as mentioned previously, the New Jersey profile is falling out of favor and it is anticipated that the F-shape and constant slope barriers will continue to rise in usage. The other two median barrier systems completing the top five were the strong steel post W-beam (rank #2) and the strong wood post W-beam (rank #4). Strong-post thrie beam followed at #6 and #7 for steel and wood post versions, respectively. The weak post systems were at the bottom of the rankings.

It should be noted that high-tension cable barriers are not present in the rankings of the Project 22-14(03) survey. This is by design. NCHRP Project 22-14(03) was limited in scope to non-proprietary roadside safety devices. All of the high-tension cable barrier systems currently on the market are proprietary in design and were thus excluded from the survey. High-tension cable barriers have seen widespread and frequent use across the country. However, as mentioned previously, these systems are specifically addressed under NCHRP Project 22-25 and, thus, do not require further study under the current project.

Both of the surveys indicated high usage for strong-post W-beam median barrier systems. However, the recent failure of this system when tested to *MASH* guidelines complicates consideration of these systems under the current project. A necessary condition for evaluating the performance of a barrier system on slopes is that the system has demonstrated crashworthiness on flat, level ground.

Table 4.9 contains the guardrail and median barriers that were analyzed for this project. These barrier types were selected in consultation with the research panel after giving consideration to the barrier systems that have met MASH testing criteria on flat terrain, and other parallel or recent research studies that may have addressed placement of a specific barrier type on slopes, such as the cable barrier systems.

Table 4.9: Selected Barrier Types

Roadside Barriers	**Median Barriers**
Modified Weak Post W-beam (G2)	Weak-Post W-beam (MB2)
Midwest Guardrail System (MGS)	Midwest Guardrail System Median Barrier
Modified Strong Steel-Post W-beam (G4 (1S))	Concrete: Single Slope (42-inch)
Modified Thrie Beam Guardrail	

5. MODEL DEVELOPMENT AND VALIDATION

To aid in the assessment of the performance limits of the selected barrier types, finite element models were developed for use in impact simulations. Each barrier system model was validated to the extent practical using available full-scale crash test data. This chapter describes the development and validation of these barrier system models.

5.1. VALIDATION PROCEDURE

To confirm the accuracy of the finite element models, each barrier system underwent a validation procedure presented in Figure 4.1. This validation procedure serves as a standard for each barrier system. The first step in the procedure is to visually compare the simulation and test snapshots. Then, the energy balance of the simulation is analyzed. These are preliminary steps in the validation procedure.

If the visual comparison and energy balance indicate the simulation and test could be in agreement, the simulation data is filtered by using an SAE 180 filter to match the processing of the crash test data. After the simulation data from LS-DYNA is filtered in LS-PrePost using the SAE 180 filter, the simulation data is processed through the Test Risk Assessment Program (TRAP), which computes MASH occupant risk criteria in the same manner used in the full-scale crash tests. Occupant risk results such as occupant impact velocity (OIV) and ridedown acceleration (RA) and other phenomenon such as angular displacements and dynamic deflection are evaluated through Roadside Safety Phenomena Importance Ranking Tables, which compare the simulation results to crash test data.

The SAE 180 filtered crash test data such as acceleration-time histories and angular displacements versus time is uploaded into the Roadside Safety Verification and Validation Program (RSVVP) along with the SAE 180 filtered simulation data. RSVVP then performs a signal analysis between the two sets of data and provides quantitative metrics to assess signal similarity.

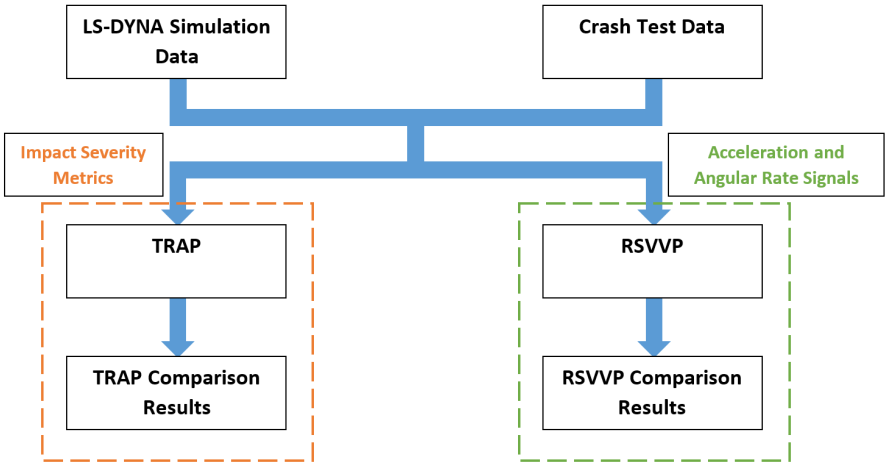

Figure 4.1: Signal Validation Procedure

5.2. MODIFIED G2 WEAK POST W-BEAM

During the *MASH* crash test of the Modified G2 Weak Post W-beam the truck stays in contact with the system for over one second. Phenomenon that define barrier performance limits such as barrier override and underride typically occur relatively early in the impact event. Consequently, the research team decided the validation of the Modified G2 weak post W-beam finite element model did not have to correspond to the entire impact event. A contact time of 0.5 seconds was chosen, which corresponds to the time of maximum dynamic barrier.

The first step in the validation process was a qualitative visual comparison of the simulation results to the modified G2 weak post W-beam guardrail crash test. Figure 5.2 and Figure 5.3 show a sequential comparison of the impact event at selected times from frontal and overhead perspectives, respectively.

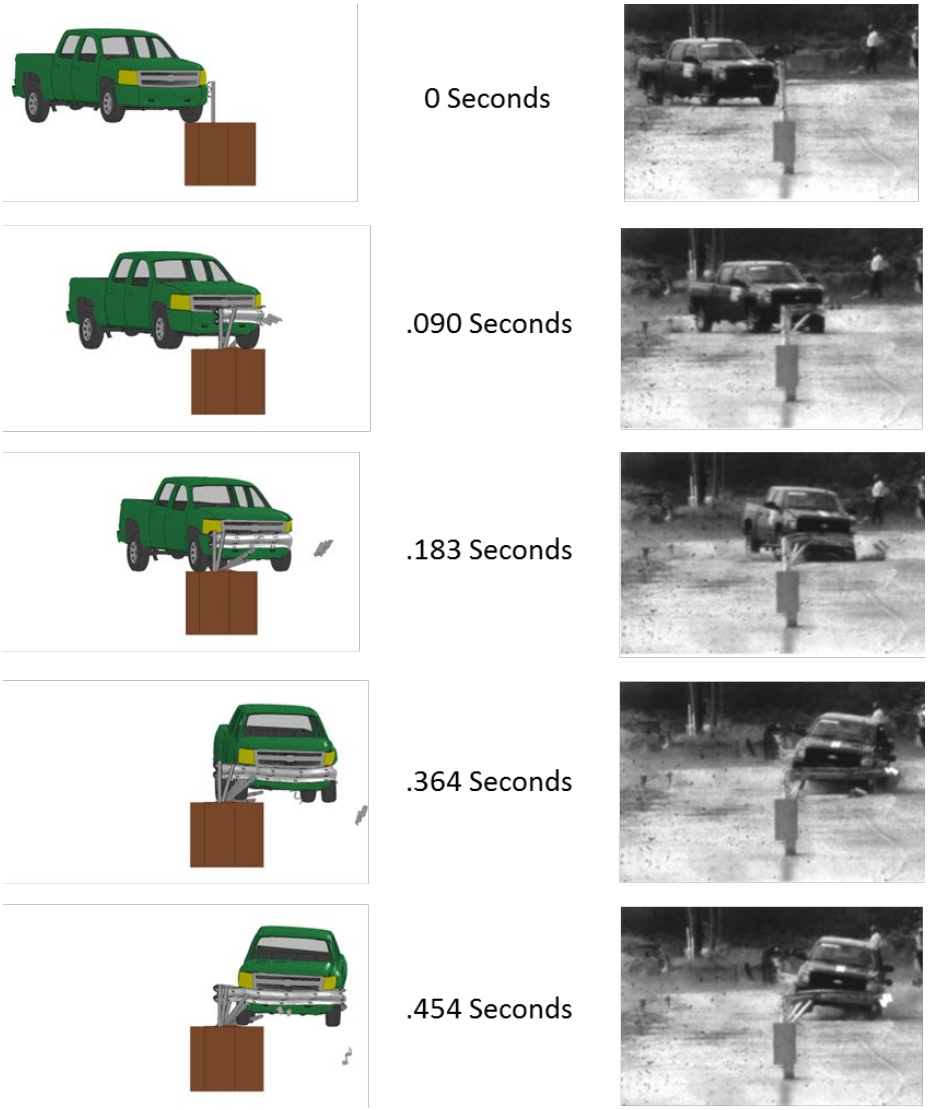

Figure 5.2: Comparison of Sequential Images for MASH Test 3-11 on Modified G2 (Front View)

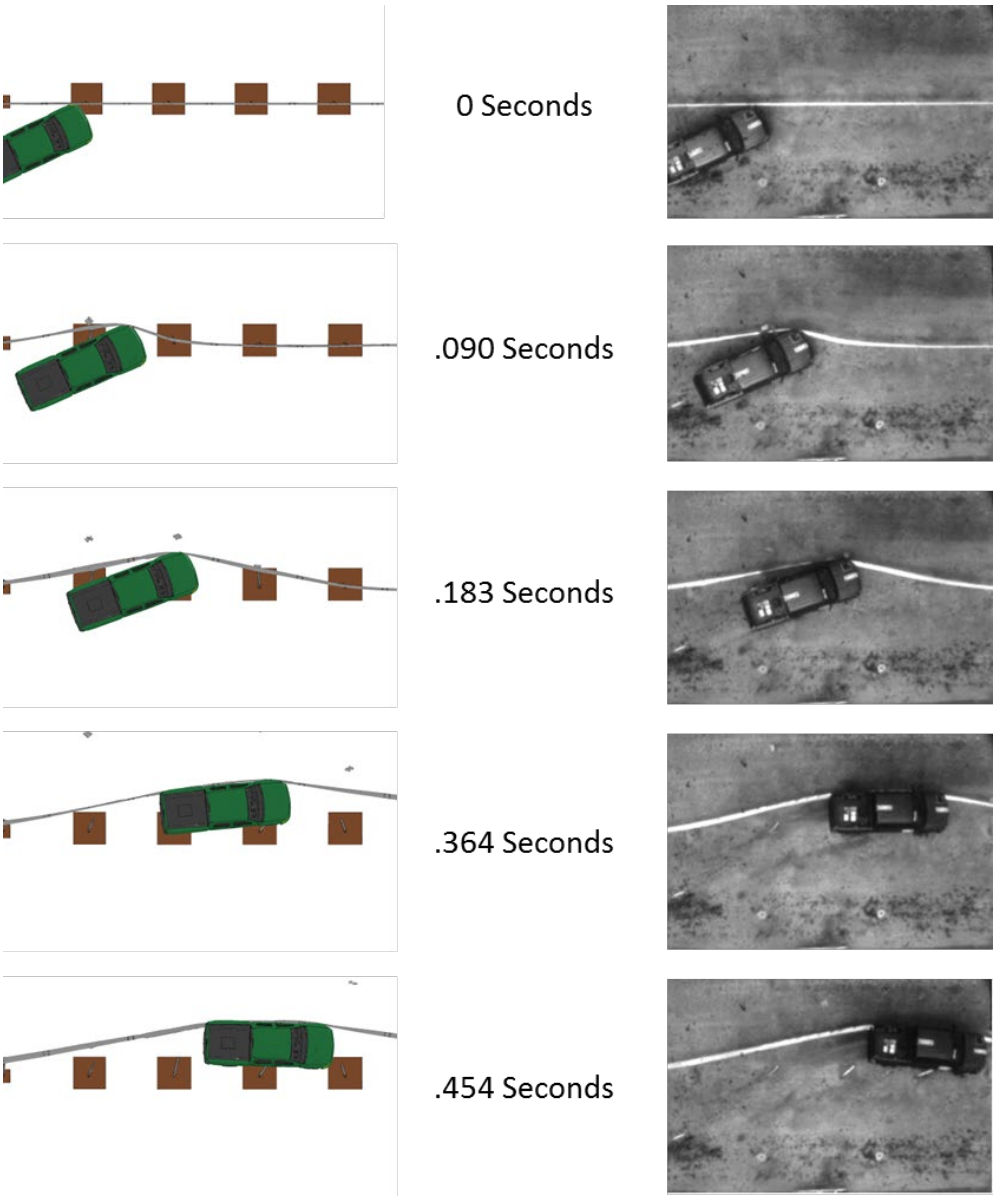

Figure 5.3: Comparison of Sequential Images for MASH Test 3-11 on Modified G2 (Top View)

The comparison of the simulation and test results in Figure 5.2 and Figure 5.3 shows good agreement in terms of both yaw angle, vehicle redirection, and dynamic barrier deflection. A comparison of angular displacements (roll, pitch, and yaw angles) versus time is shown in Figure 5.4. The yaw angle compares favorably, with the crash test reaching a maximum angle of 30 degrees and simulation reaching a maximum angle of 28 degrees. The roll angle varies in magnitude between the simulation and crash test by about 6 degrees but shows a similar trend. The crash test shows a positive pitch while the simulation shows a negative pitch. The pitch is not captured, but the magnitude is very small and is not consequential to the outcome of the test.

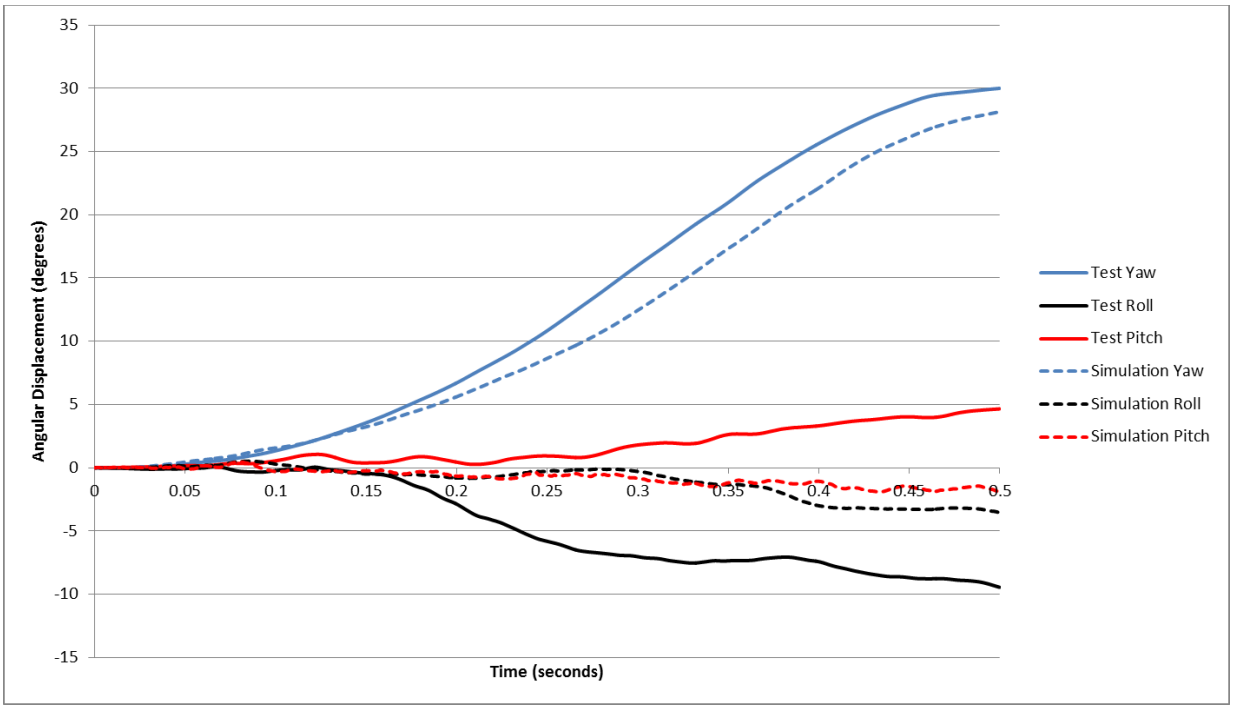

Figure 5.4: Comparison of Roll, Pitch and Yaw Angles for MASH Test 3-11 on Modified G2

Figure 5.5 shows a plot of the energy balance for the simulation of the modified G2 weak post W-beam guardrail. The plot shows the total energy stays relatively constant with only a small decrease beginning around 0.2 seconds. The small decrease can be attributed to hourglass energy developing. The magnitude of the hourglass energy is very small, on the order of 2% of the total energy, which is within the desired result. The plot also shows the kinetic energy decreasing as the truck decelerates and the internal energy going up as the barrier deflects and deforms. The sliding interface energy also increases as the truck slides along the barrier and work is done by friction. The energy balance shows that the simulation behaves as expected in terms of global energy characteristics.

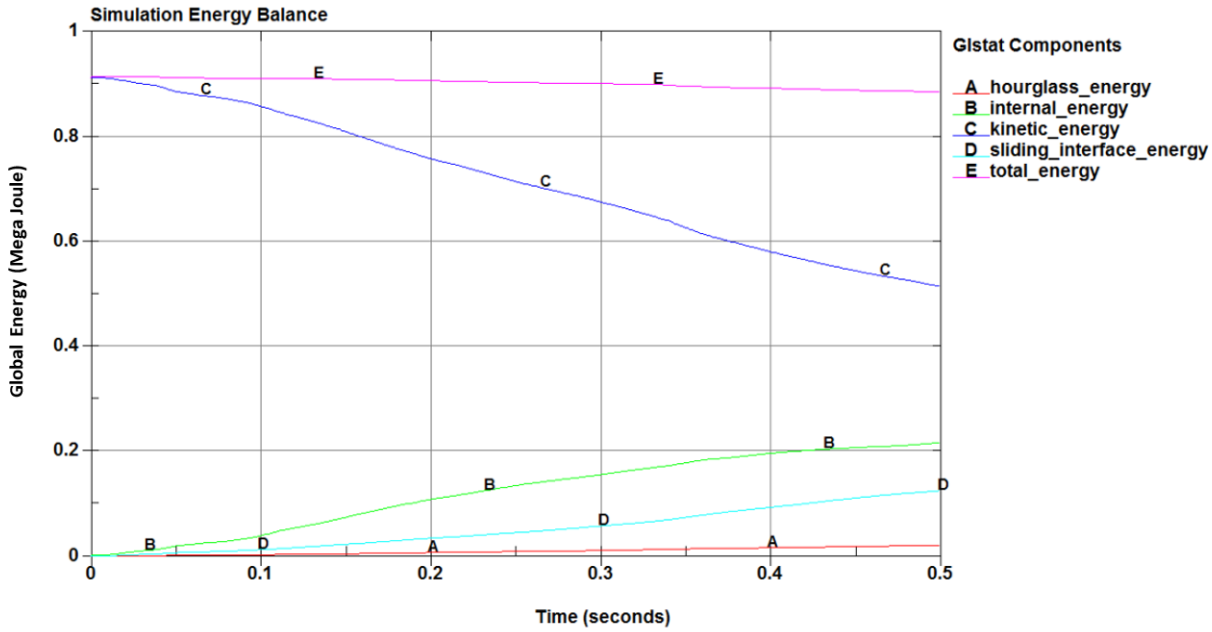

Figure 5.5: Energy Balance of Modified G2 Weak Post W-Beam Guardrail Simulation (Multiply by a factor of 737562 to convert to ft-lbf)

The simulation results were then uploaded into RSVVP and compared to signals measured in MASH Test 3-11 of the modified G2 weak post W-beam guardrail. The data was filtered according to the validation procedure shown in Figure 5.1. Figure 5.6 shows an image of the RSVVP results from the multi-channel analysis of the modified G2 weak post W-beam guardrail simulation. The comparison was acceptable based on both the MPC and ANOVA metrics.

Table 5.1 provides a summary of the RSVVP results. While most of the individual channels did not pass, the multi-channel analysis passed all of the metrics. The X acceleration, Y acceleration and yaw rate were weighted the most heavily by RSVVP. The simulation matched the crash test very closely on yaw rate, and also did quite well on the X acceleration and Y acceleration. The simulation did not match the crash test on the roll rate, pitch rate and Z acceleration very well, but these quantities are not a large portion of the truck's response with this guardrail system. When all of the channels are considered together, the simulation passes the RSVVP criteria.

The simulation data was then uploaded into TRAP. A Phenomena Importance Ranking Table (PIRT) was created to compare various aspects of the the modified G2 weak post W-Beam guardrail simulation to the crash test data. The results are presented in Table 5.2.

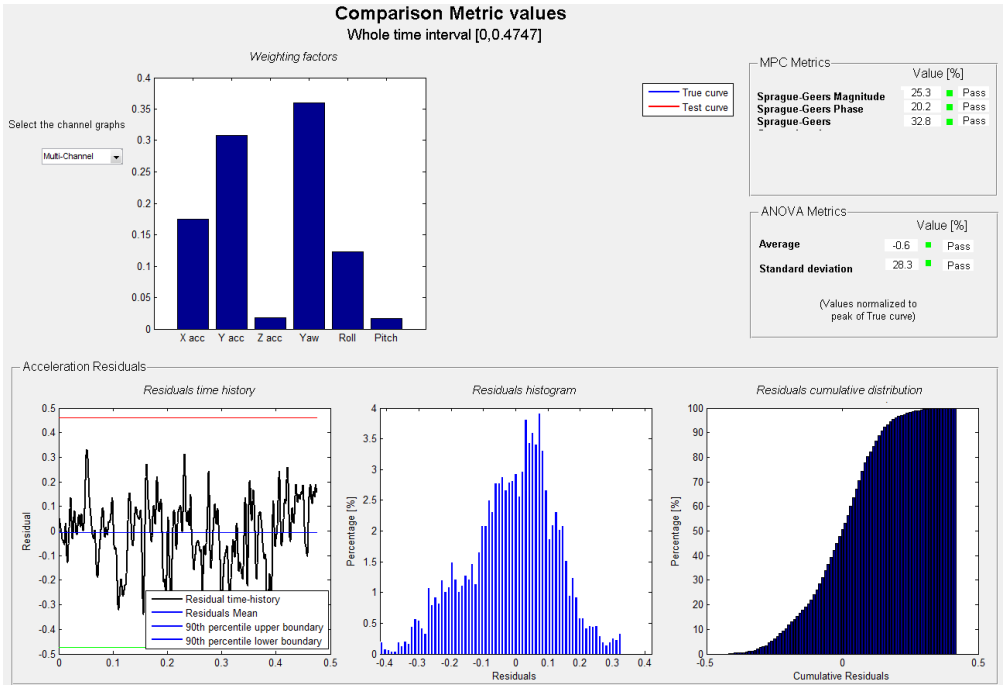

Figure 5.6: Multi-Channel RSVVP Results for MASH Test 3-11 on Modified G2

Table 5.1: RSVVP Results Summary for Modified G2

Channel Type	**Weighting factor (Area II) (45)**	**Spague-Geers Metrics**		**ANOVA Metrics**		**Pass**?
		M ≤ 40	**P ≤ 40**	**Mean Residual ≤ 0.05**	**Std. Deviation ≤ 0.35**	
X acceleration	0.17	44.1	29.5	0.08	0.44	N
Y acceleration	0.31	18.0	21.9	0.09	0.35	N
Z acceleration	0.02	137.9	45.0	0.03	0.70	N
Roll rate	0.12	46.6	41.8	0.18	0.33	N
Pitch rate	0.02	46.1	45.6	0.17	0.61	N
Yaw rate	0.36	8.6	4.4	0.04	0.10	Y
Multiple Channel	1.00	25.3	20.2	0.01	0.28	**Y**

Table 5.2: PIRT for Modified G2 Weak Post W-Beam Guardrail Simulation

Evaluation Criteria	Test	Simulation	Absolute Difference	Relative Difference ≤20%	Pass?
Maximum Roll (deg.)	-9.5	-3.6	5.9	>20%	N
Maximum Yaw (deg.)	30	28.1	1.9	<20%	Y
Maximum Pitch (deg.)	4.6	-1.9	6.5	>20%	N
Longitudinal direction: OIV ≤ 12 m/s (30 ft/s); RA ≤ 20 g	 9.51 (ft/s) -2.5 g	 11.2 (ft/s) -4.2 g	 1.69 (ft/s) 1.7 g	 <20% >20%	 Y Y
Lateral direction: OIV ≤ 12 m/s (30 ft/s); RA ≤ 20 g	 29.85 (ft/s) -4.4 g	 -9.51(ft/s) 5.4 g	 0.99 (ft/s) 1 g	 <20% >20%	 Y Y
Number of Broken or Significant Bent Posts	10 (9~18)	9 (10~18)	1	<20%	Y
Maximum Dynamic Deflection	8.60 ft	8.58	0.02 ft	<20%	Y

The maximum roll, yaw and pitch angles are considered acceptable if the relative difference between the simulation and crash test is less than 20% or the absolute difference is less than 5 degrees as recommended in NCHRP Project 22-24. The yaw passed these criteria, but the maximum roll and pitch did not. While the maximum roll and pitch did not pass the criteria, their magnitudes are both small and the difference was close to the preferred criteria.

The ridedown accelerations (RAs) are considered passing if the relative difference between the simulation and crash test is less than 20% or the absolute difference is less than 4 g as recommended in NCHRP Project 22-24. Both values also had to be below the maximum allowed value of 20.49 g as required by *MASH*. Both the longitudinal and lateral ridedown acceleration passed validation criteria.

The occupant impact velocities (OIVs) are considered passing if the relative difference between the simulation and crash test is less than 20% or the absolute difference is less than 6.56 ft/s (2 m/s) as recommended in NCHRP Project 22-24. Both values also had to be below the maximum allowed value of 40 ft/s as required by *MASH*. Both the lateral and longitudinal occupant impact velocities passed the validation criteria.

The number of broken or significantly bent posts and maximum dynamic deflection considered acceptable if the relative difference between the simulation and crash test is less than 20%. Both the number of broken or significantly bent posts and maximum dynamic deflection met this criteria. Note that the number of significantly bent posts corresponds to the selected simulation time of 0.5 s.

Based on the visual comparison, energy balance, RSVVP signal analysis, and TRAP occupant risk analysis, the modified G2 weak post W-beam guardrail finite element model was considered sufficiently validated against MASH Test 3-11 results.

5.3. MIDWEST GUARDRAIL SYSTEM (MGS)

The finite element model of the MGS was validated against MASH Test 3-11 with the 2270P pickup truck and MASH Test 3-10 with the 1100C passenger car. A description of the validation analyses for these tests is provided in the sections below.

5.3.1. MGS Validation with Pickup Truck

The MGS guardrail finite element model went through the previously described validation procedure for MASH Test 3-11 with the 2270P pickup truck. The validation procedure consisted of a graphical comparison, energy balance analysis, and analytical component using both RSVVP and TRAP.

The first step in the validation process was a qualitative visual comparison of the simulation results to the pickup truck crash test of the MGS guardrail. Figure 5.7 and Figure 5.8 show a sequential comparison of the impact event at selected times from frontal and overhead perspectives, respectively. The times used in the comparison correspond to those documented in the crash test report.

The comparison of the simulation and test results shows good agreement in terms of both yaw angle, vehicle redirection, and dynamic barrier deflection. Some of the blockouts in the impact region fractured, and those upstream and downsteam of the impact remained intact in both the simulation and crash test. The truck exited the barrier in the simulation and crash test at around 0.7 seconds at a similar exit angle.

A comparison of angular displacements between the pickup truck simulation and crash test are shown in Figure 5.9. The comparison is for a time period from 0 to 0.70 seconds, after which the pickup truck is no longer in contact with the barrier. The yaw angles reasonably agree. The magnitudes of both the roll and pitch angles are quite small. The roll angles follow the same trend until a deviation near the end of the time sequence. The difference in pitch angles is small because the magnitude of the pitch angles is very small.

The energy balance for the simulation is shown in Figure 5.10. The total energy for the simulation stayed relatively constant with a drop of about 4%. There is a small amount of hour glass energy that developed but it reached a maximum of only 3% of the total energy. The kinetic energy lowered as the truck decelerated and the internal energy increased as the barrier deflected and deformed. The energy balance shows that the simulation behaves as expected in terms of global energy characteristics.

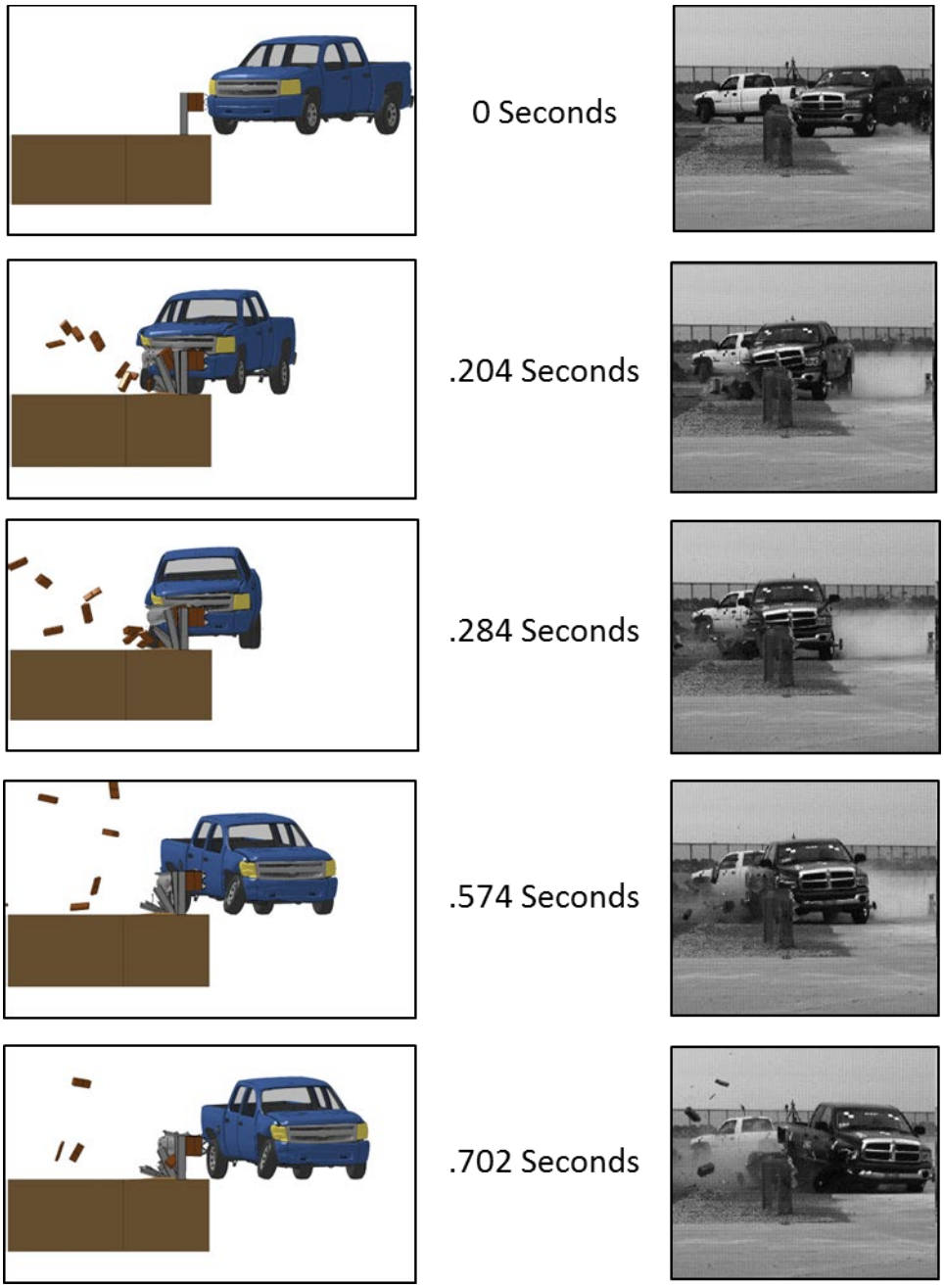

Figure 5.7: Comparison of Sequential Images for MASH Test 3-11 on MGS (Front View)

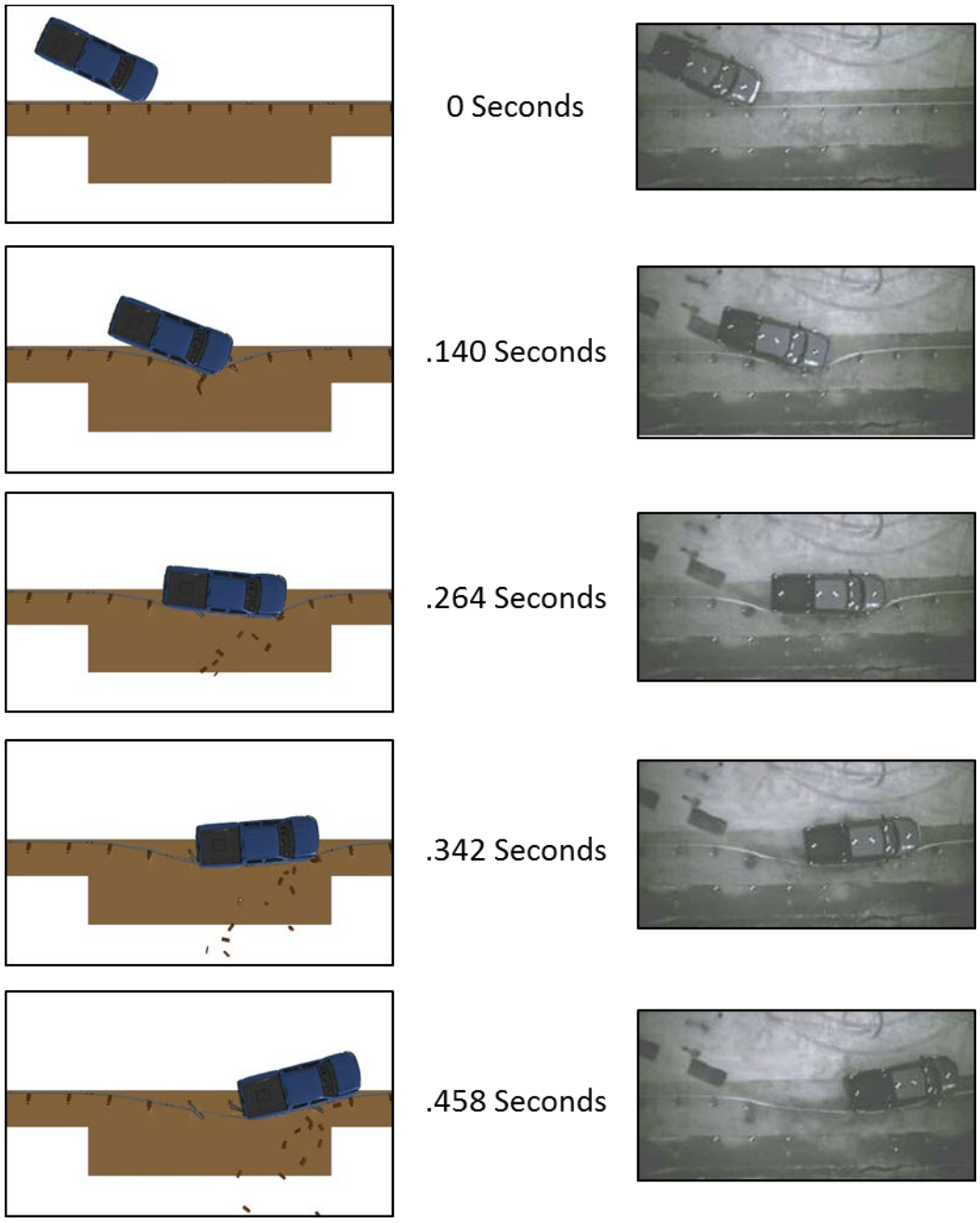

Figure 5.8: Comparison of Sequential Images for MASH Test 3-11 on MGS (Top View)

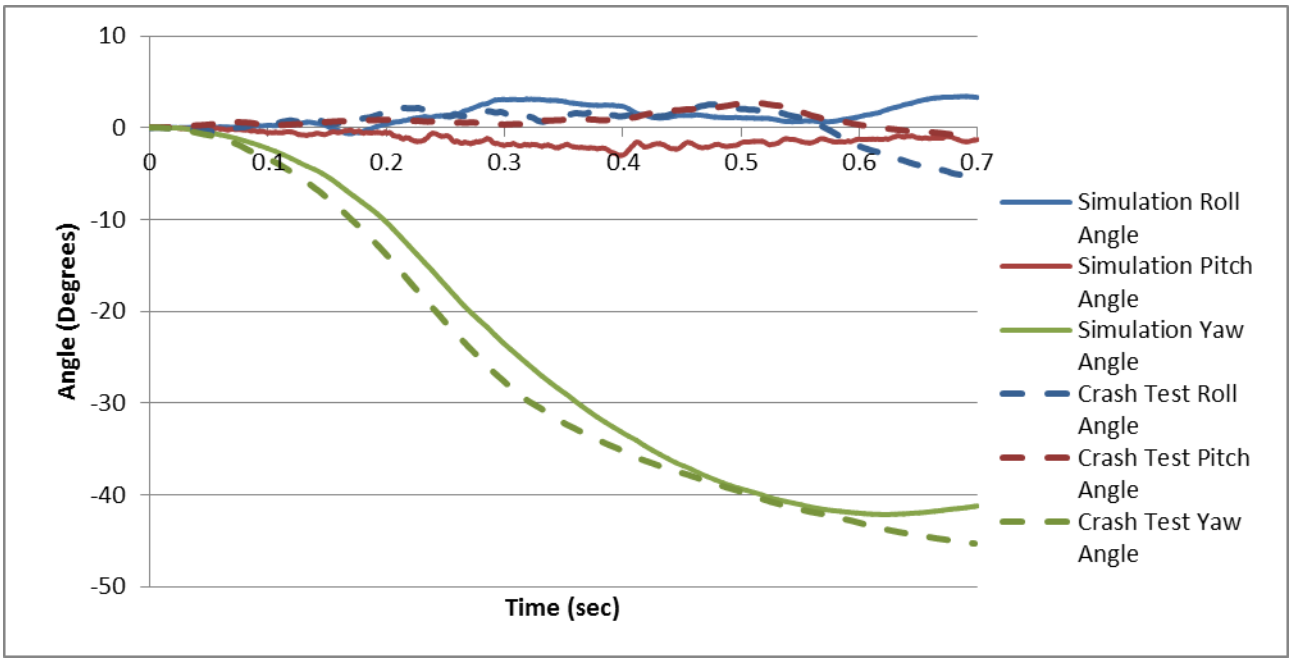

Figure 5.9: Comparison of Roll, Pitch and Yaw Angles for MASH Test 3-11 on MGS

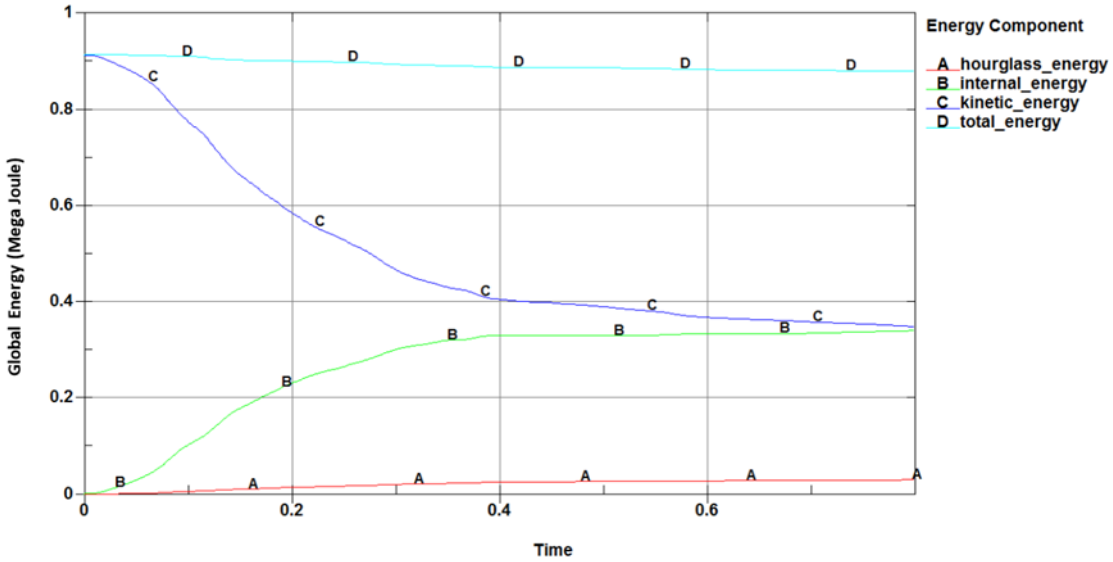

Figure 5.10: Energy Balance for MGS Pickup Truck Simulation
(Multiply by a factor of 737562 to convert to ft-lbf)

The simulation data was input into TRAP for calculation of occupant risk indices. The comparison of the occupant risk indices and other criteria between simulation and test is summarized in Table 5.3.

Table 5.3: PIRT for MGS Pickup Truck Simulation

Evaluation Criteria	Test	Simulation	Absolute Difference	Relative Difference ≤ 20%	Pass?
Maximum Roll (deg.)	-5	-3.4	1.8	> 20%	Y
Maximum Yaw (deg.)	-46	-42.1	3.9	< 20%	Y
Maximum Pitch (deg.)	3	-3.0	6.0	> 20%	N
Longitudinal direction: OIV ≤ 12 m/s (30 ft/s); RA ≤ 20 g	 15.32 (ft/s) -8.23 g	 17.7 ft/s -7.2 g	 2.39 (ft/s) 1.0 g	 < 20% < 20%	 Y Y
Lateral direction: OIV ≤ 12 m/s (30 ft/s); RA ≤ 20 g	 15.62 (ft/s) -6.93 g	 15.09 (ft/s) -8.3 g	 0.53 (ft/s) 1.37 g	 < 20% < 20%	 Y Y
Number of Broken or Significantly Bent Posts	4	4	0	< 20%	Y
Maximum Dynamic Deflection	1.114 m	1.275 m	.161 m	<20%	Y

The maximum roll, yaw and pitch angles are considered acceptable if the relative difference between the simulation and crash test is less than 20% or the absolute difference is less than 5 degrees. The roll and yaw both passed this criteria, but the maximum pitch did not. However, the magnitude of the pitch angle is very small and the difference was close to the preferred criteria.

The ridedown accelerations (RAs) are considered passing if the relative difference between the simulation and crash test is less than 20% or the absolute difference is less than 4 g. Both values also had to be below the maximum allowed value of 20.49 g as required by *MASH*. Both the longitudinal and lateral ridedown acceleration passed validation criteria.

The occupant impact velocities (OIVs) are considered passing if the relative difference between the simulation and crash test is less than 20% or the absolute difference is less than 6.56 ft/s (2 m/s). Both values also had to be below the maximum allowed value of 40 ft/s as required by *MASH*. Both the lateral and longitudinal occupant impact velocities passed the validation criteria.

The number of broken or significantly bent posts and maximum dynamic deflection considered acceptable if the relative difference between the simulation and crash test is less than

20%. Both the number of broken or significantly bent posts and maximum dynamic deflection met this criteria.

The simulation results were then uploaded into RSVVP and compared to signals measured in MASH Test 3-11 of the MGS. Table 5.1 provides a summary of the RSVVP results. While some of the individual channels did not pass, the multi-channel analysis passed all of the metrics. It should be noted that the simulation matched the crash test extremely closely on the channels whose behavior is the most critical to the truck's behavior. The X acceleration, Y acceleration and Yaw are the dominant behaviors and are given the highest weighting factors by RSVVP. The other quantities are very small in magnitude and not a large portion of the truck's response with this guardrail system. When all of the channels are considered together, the simulation passes the RSVVP criteria.

Table 5.4: Signal Analysis for MGS Pickup Truck Simulation

Channel Type	**Weighting Factor (Area II)**	**Spague-Geers Metrics**			**ANOVA Metrics**		**Pass?**
		M ≤ 40	**P ≤ 40**	**C ≤ 40**	**Mean Residual ≤ 0.05**	**Std. Deviation ≤ 0.35**	
X acceleration	0.21	11.5	32.4	34.4	0.010	0.248	Y
Y acceleration	0.28	4.30	23.8	24.2	0.020	0.295	Y
Z acceleration	0.01	86.2	48.8	99.1	0.015	0.544	N
Roll rate	0.04	28.6	53.1	60.3	0.106	0.484	N
Pitch rate	0.02	146.5	48.7	154.4	0.226	0.877	N
Yaw rate	0.44	3	7.4	8.0	0.037	0.113	Y
Multiple Channel	1.00	8.4	19.9	22.6	0.010	0.220	**Y**

Based on the visual comparison, energy balance, RSVVP signal analysis, and TRAP occupant risk analysis, the MGS guardrail finite element model was considered sufficiently validated against MASH Test 3-11 results.

5.3.2. MGS Validation with Small Car

The MGS guardrail finite element model went through the same validation procedure for MASH Test 3-10 with the 1100C passenger car. The validation procedure consisted of a graphical comparison, energy balance analysis, and analytical component using both RSVVP and TRAP.

Sequential images of the simulation and crash test are compared in Figure 5.11 and Figure 5.12 for frontal and overhead views, respectively. The comparison of the simulation and test results show significant agreement up to 0.4 seconds at which time the vehicle has redirected

and is beginning to exit the system. After this time, crash test vehicle rotates back into the barrier system while the simulated vehicle retains its exit angle and does not yaw back into the barrier. This may be due to suspension damage modes that are not fully captured in the small car finite element model. The research team concluded that the barrier model could move forward in the validation process since the vehicle containment and redirection reasonably matched the crash test and any vehicle underride behavior in the performance limit analysis would occur prior to this time.

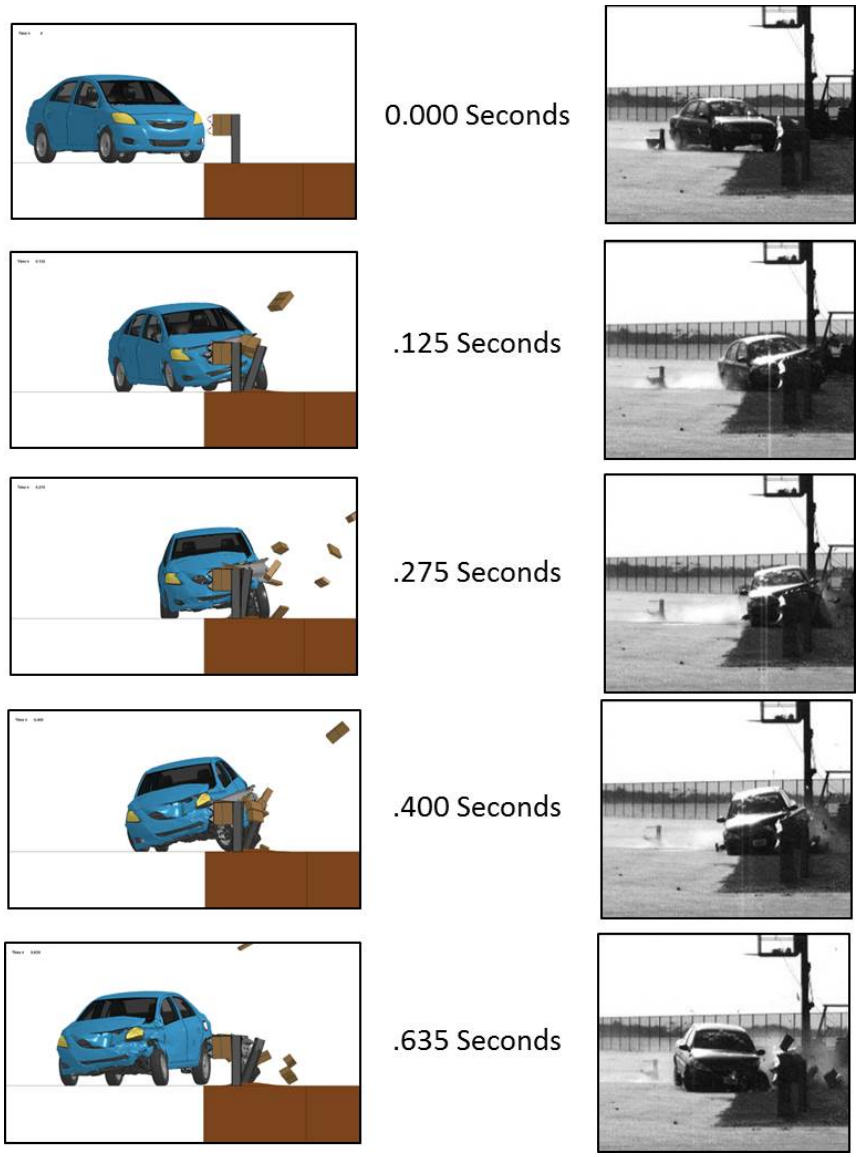

Figure 5.11: Comparison of Sequential Images for MASH Test 3-10 on MGS

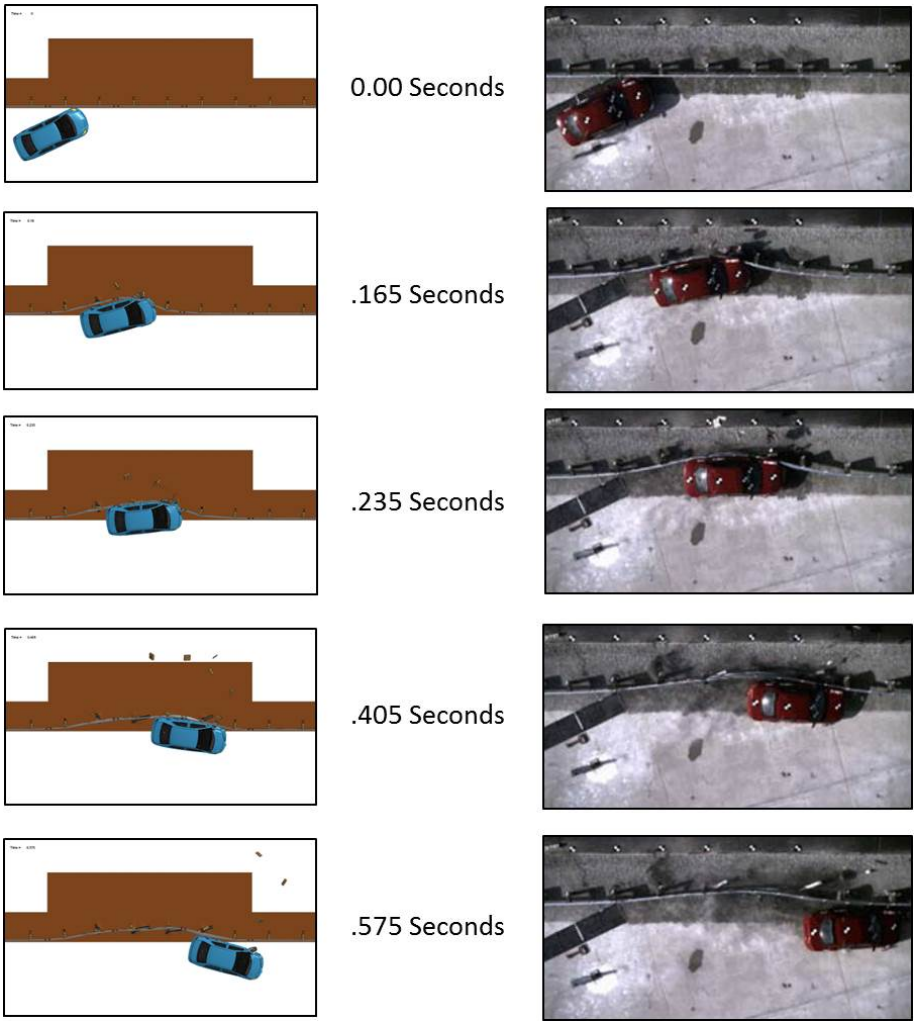

Figure 5.12: Comparison of Sequential Images for MASH Test 3-10 on MGS (Top View)

A comparison of angular displacements between the small car simulation and crash test are shown in Figure 5.13. The comparison is for a time period from 0 to 0.4 seconds, after which the small car has been redirected and is exiting the barrier. The roll, pitch, and yaw angles from the simulation follow the same trend as the crash test and compare reasonably. The magnitudes of both the roll and pitch angles are quite small. After the vehicle was redirected, a deviation in yaw angle occurs. This is likely due to the influence of various suspension damage modes that are not fully capture in the small car finite element model. However, it should not have a significant influence on the evaluation of performance limits of the barrier model.

Figure 5.14 shows the energy balance for the MGS small car simulation. The total energy stayed constant throughout the test. There was a small amount of hourglass energy that developed in the system, but it reached a maximum of less than 5.5% of the total energy. The kinetic energy decreased as the car decelerated, and the internal energy increased as the barrier and car deformed. The sliding interface energy increases due to frictional contact between the vehicle and barrier. The energy balance shows that the simulation behaves as expected in terms of global energy characteristics.

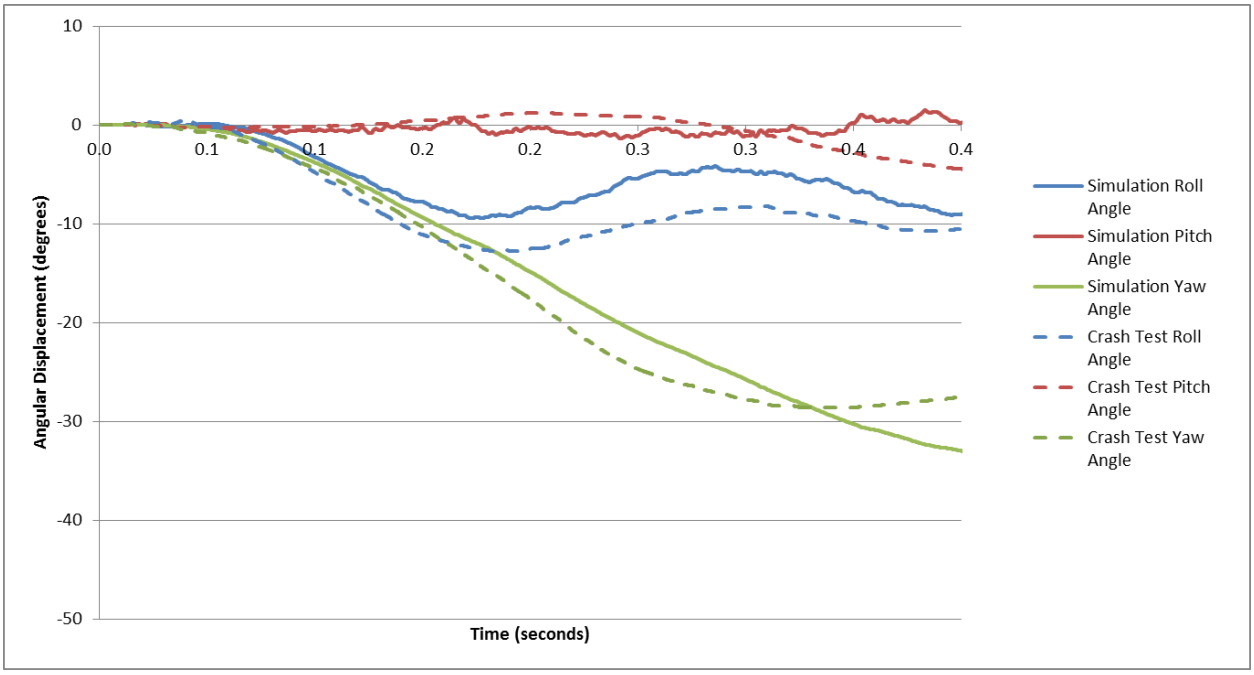

Figure 5.13: Comparison of Roll, Pitch and Yaw Angles for MASH Test 3-10 on MGS

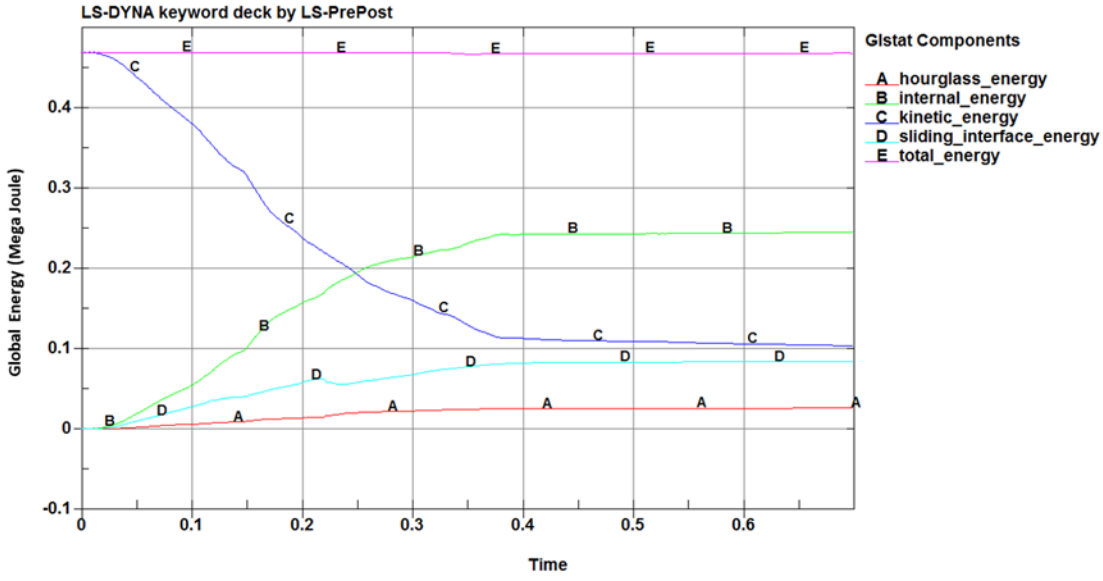

Figure 5.14: Energy Balance for MGS Small Car Simulation
(Multiply by a factor of 737562 to convert to ft-lbf)

The simulation data was input into TRAP for calculation of occupant risk indices. The comparison of the occupant risk indices and other criteria between simulation and test is summarized in the PIRT shown in Table 5.5. The maximum roll, yaw and pitch angles are considered acceptable if the relative difference between the simulation and crash test is less than 20% or the absolute difference is less than 5 degrees. The yaw, pitch, and roll angles all satisfied the criteria.

The ridedown accelerations (RAs) are considered passing if the relative difference between the simulation and crash test is less than 20% or the absolute difference is less than 4 g as recommended in NCHRP Project 22-24. Both values also had to be below the maximum allowed value of 20.49 g as required by *MASH*. Both the longitudinal and lateral ridedown acceleration were slightly above the preferred validation criteria.

The occupant impact velocities (OIVs) are considered passing if the relative difference between the simulation and crash test is less than 20% or the absolute difference is less than 2 m/s as recommended in NCHRP Project 22-24. Both values also had to be below the maximum allowed value of 40 ft/s as required by *MASH*. Both the lateral and longitudinal occupant impact velocities passed the validation criteria.

The number of broken or significantly bent posts and maximum dynamic deflection considered acceptable if the relative difference between the simulation and crash test is less than 20%. Both the number of broken or significantly bent posts and maximum dynamic deflection met this criteria.

Table 5.5: PIRT for MGS Small Car Simulation

Evaluation Criteria	**Test**	**Simulation**	**Absolute Difference**	**Relative Difference ≤ 20%**	**Pass?**
Maximum Roll (deg.)	-12.8	-9.6	3.2	> 20%	Y
Maximum Yaw (deg.)	-28.6	-32.8	4.2	< 20%	Y
Maximum Pitch (deg.)	-5.7	-1.9	3.8	> 20%	Y
Longitudinal direction: OIV ≤ 12 m/s (30 ft/s) RA ≤ 20 g	 14.4 -16	 17.7 -10.8	 3.3 5.2	 > 20% > 20%	 Y N
Lateral direction: OIV ≤ 12 m/s (30 ft/s) RA ≤ 20 g	 17.1 -8.2	 16.1 -12.4	 1.0 4.2	 < 20% > 20%	 Y N
Number of Broken or Significantly Bent Posts	4	4	0.0	< 20%	Y
Maximum Dynamic Deflection (m)	0.913	0.940	0.027	< 20%	Y

Table 5.6 provides a summary of the RSVVP signal analysis results. While some of the individual channels did not pass, the multi-channel analysis passed all of the metrics. The X and Y accelerations and yaw and roll rates were weighted the most heavily by RSVVP. When all of the channels are considered together, the simulation passes the RSVVP criteria.

Based on the visual comparison, energy balance, RSVVP signal analysis, and TRAP occupant risk analysis, the modified MGS finite element model was considered sufficiently validated against MASH Test 3-10 results.

Table 5.6: Signal Analysis for MGS Small Car Simulation

Channel Type	**Weighting factor (Area II)(45)**	**Spague-Geers Metrics**			**ANOVA Metrics**		**Pass?**
		M ≤ 40	**P ≤ 40**	**C ≤ 40**	**Mean Residual ≤ 5.0**	**Std. Deviation ≤ 35**	
X acceleration	0.23	10.8	26.6	28.7	-3.000	18.230	Y
Y acceleration	0.22	23.90	29	37.5	-0.050	31.460	Y
Z acceleration	0.05	24.6	41.4	48.2	2.750	26.250	N
Yaw rate	0.37	1.1	14.9	15	-6.470	21.010	N
Roll rate	0.13	0.9	24.8	24.8	0.310	29.950	Y
Pitch rate	0.00	221.1	47.8	226.2	4.550	108.040	N
Multiple Channel	1.00	9.6	23.4	26.2	-2.900	24.200	**Y**

5.4. MODIFIED STRONG STEEL-POST W-BEAM (MODIFIED G4(1S))

Researchers and the panel discussed adding the Modified Strong Steel-Post W-Beam Guardrail (modified G4(1S)) back into the matrix of barriers that are investigated in this project. Due to limited resources, rather than explicitly model the modified G4(1S), it was decided to apply the performance limits of the MGS with appropriate adjustments made for the lower mounting height of the modified G4(1S).

5.5. MODIFIED THRIE BEAM GUARDRAIL

Since there was not an existing *MASH* crash test of the modified thrie beam guardrail system during the time of this project, the finite element model of the modified thrie beam guardrail could not be validated against *MASH* crash test data. A simulation with the pickup truck was performed in accordance with MASH Test 3-11 impact conditions to debug the model and serve as a baseline on flat level ground based on which the perform performance limits of the system could be assessed. As shown in the sequential images provided in Figure 5.15, the pickup truck was successfully contained and redirected by the modified thrie beam guardrail.

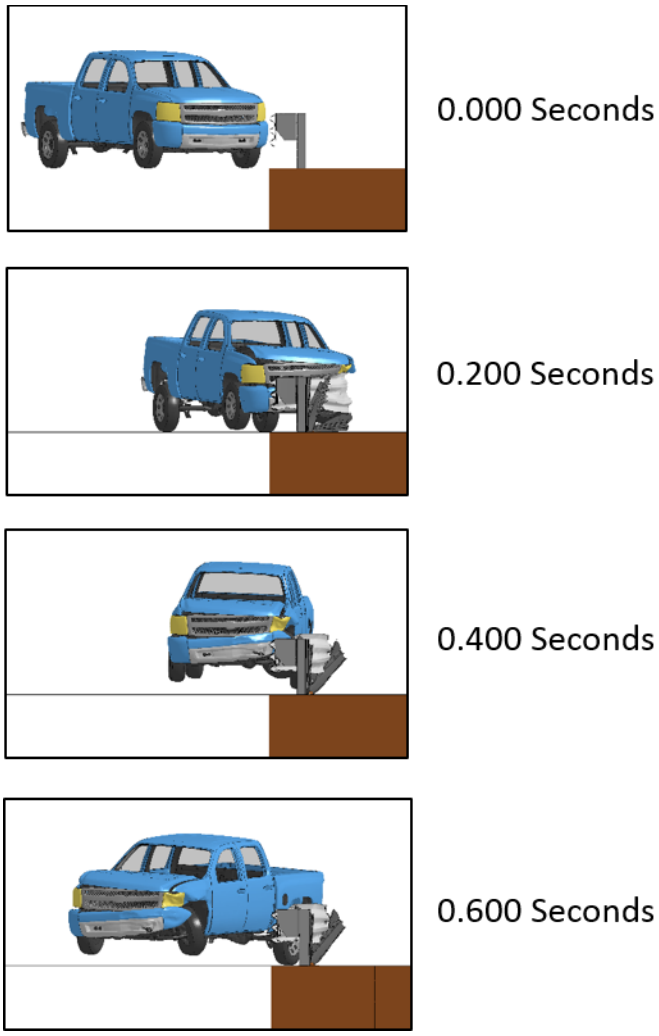

Figure 5.15: Sequential Images from Simulation of MASH Test 3-11 on Modified Thrie Beam Guardrail (Front View)

The simulation outputs were entered into TRAP to evaluate the occupant risk indices as a measure of MASH compliance prior to using the model to determine performance limits of the modified thrie beam guardrail. Table 5.7 presents the results of the simulation.

Table 5.1 of MASH contains the impact performance evaluation criteria for MASH Test 3-11. The maximum allowable occupant impact velocity is 40 ft/s and the preferred occupant impact velocity is 30 ft/s. As shown in Table 5.7, both the longitudinal (x) and lateral (y) occupant impact velocities are below the preferred limit.

The maximum and preferred ridedown accelerations in MASH are 20.49 g and 15 g, respectively. Both the longitudinal (x) and lateral (y) ridedown accelerations are below the preferred limit. Finally, the MASH limit on roll and pitch angles is 75 degrees, and the simulated angles are well below this value.

Table 5.7: Summary of Modified Thrie Beam Guardrail Simulation Results

Simulation TRAP Results:	
Impact Velocity, mph	62.2
Impact Angle (degrees)	25
Occupant Risk Factors	
Impact Velocity (ft/s)	
x-direction	29.5
y-direction	-12.8
Ridedown Accelerations (g)	
x-direction	-11.0
y-direction	8.5
Max Roll, Pitch, and Yaw Angles (degrees)	
Roll	-4.5
Pitch	-1.2
Yaw	51.8

The simulation of the modified thrie beam guardrail met all MASH requirements, and the model was considered acceptable to progress with the assessment of performance limits of the system.

5.6. WEAK POST W-BEAM (MB2)

Since there was not an existing MASH crash test with the weak post W-beam median barrier (MB2) during the time of this project, the finite element model of the weak post W-beam median barrier (MB2) could not be validated against MASH crash test data.

In evaluating NCHRP Report 350 Test 3-11 of the weak post W-beam median barrier (MB2), researchers observed a similar behavior of the median barrier its guardrail counterpart, the modified weak post W-beam guardrail (modified G2). Both the modified G2 and MB2 have a height to the top of the W-beam rail of 33 inches. The primary difference between the two systems is the addition of a second rail on the opposite face of the system in the MB2. Indeed, it is this feature that makes the MB2 a median barrier. Another difference between the two systems is the rail splice location. In the MB2, the splices are at post locations, while the rail splices in the modified G2 are located midspan between posts.

Sequential impact photos of NCHRP Report 350 Test 3-11 of the weak post W-beam median barrier (MB2) are shown in Figure 5.16. It was noted that the rail on the back side of the system disengaged from the posts early in the impact and provided little contribution in capturing and redirecting the vehicle. Furthermore, the rail on the backside released from the posts at more locations than the impact-side rail. Figure 5.17 shows the rail on the impact-side still connected to the first two posts at the bottom of the photo while the rail on the back-side of the barrier has separated from these posts.

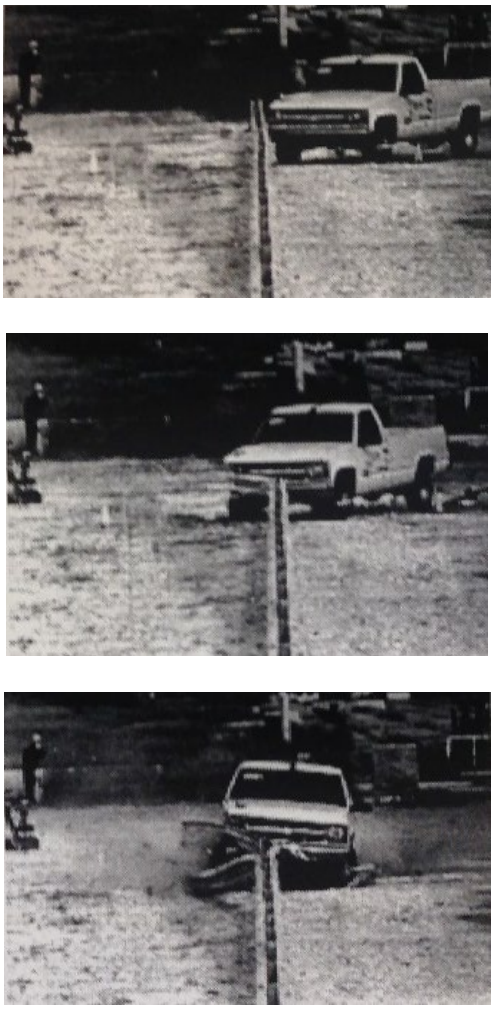

Figure 5.16: Sequential Photos of NCHRP Report 350 Test 3-11 on MB2 (Front View)

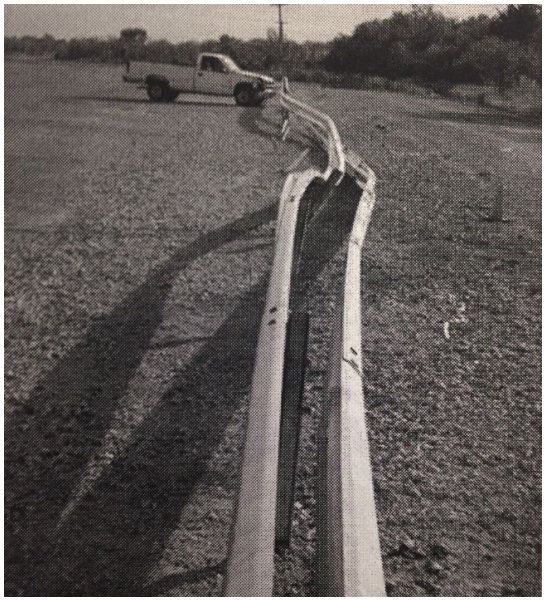

Figure 5.17: Separation of Rail on Back-Side of Barrier

Based on the analysis of this crash test, the research team concluded that the addition of a second rail does not significantly contribute to the stiffness of the MB2 system. Therefore, since the weak post W-beam median barrier (MB2) behaves in a similar manor to the modified G2 guardrail and they both have the same rail height, the research team concluded the performance limits of the roadside modified weak post W-beam guardrail (modified G2) would be applicable to the performance limits of the weak post W-beam median barrier (MB2).

5.7. MGS MEDIAN BARRIER

The finite element model of the MGS median barrier was validated against MASH Test 3-11 with the 2270P pickup truck and MASH Test 3-10 with the 1100C passenger car. In the testing, it was observed that some of the 8-inch wood blockouts fractured during interaction with the impacting vehicle. In absence of this failure mode, the simulations experienced snagging of the vehicle's suspension that led to a discrepancy in results compared to the crash tests. The blockout model was modified to have four prescribed fracture planes (see Figure 5.18) that permit fracture of the blockout to fracture through the plane that contains the post bolt hole. The four parts of the blockout are held together with a contact that has specified failure criteria. The values for the failure shear stress and failure tensile stress were initially determined by referencing Mark's Standard Handbook for Mechanical Engineers and calibrated to obtain good agreement between the simulations and crash tests. Once the shear and tensile failure stresses were determined they were held constant through all subsequent simulations. A description of the validation analyses against the MASH crash tests is provided in the sections below.

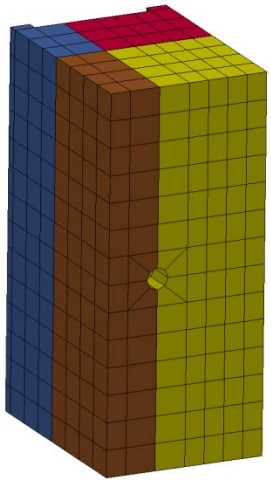

Figure 5.18: Finite Element Blockout Model with Failure Planes

5.7.1. MGS Median Barrier Validation with Pickup Truck

The MGS median barrier finite element model went through the previously described validation procedure for MASH Test 3-11 with the 2270P pickup truck. The validation

procedure consisted of a graphical comparison, energy balance analysis, and analytical component using both RSVVP and TRAP.

The first step in the validation process was a qualitative visual comparison of the simulation results to the pickup truck crash test of the MGS median barrier. Figure 5.19 shows a sequential comparison of the impact event at selected times. The times used in the comparison correspond to those documented in the crash test report. The comparison of the simulation and test results shows good agreement in terms of vehicle redirection and barrier performance.

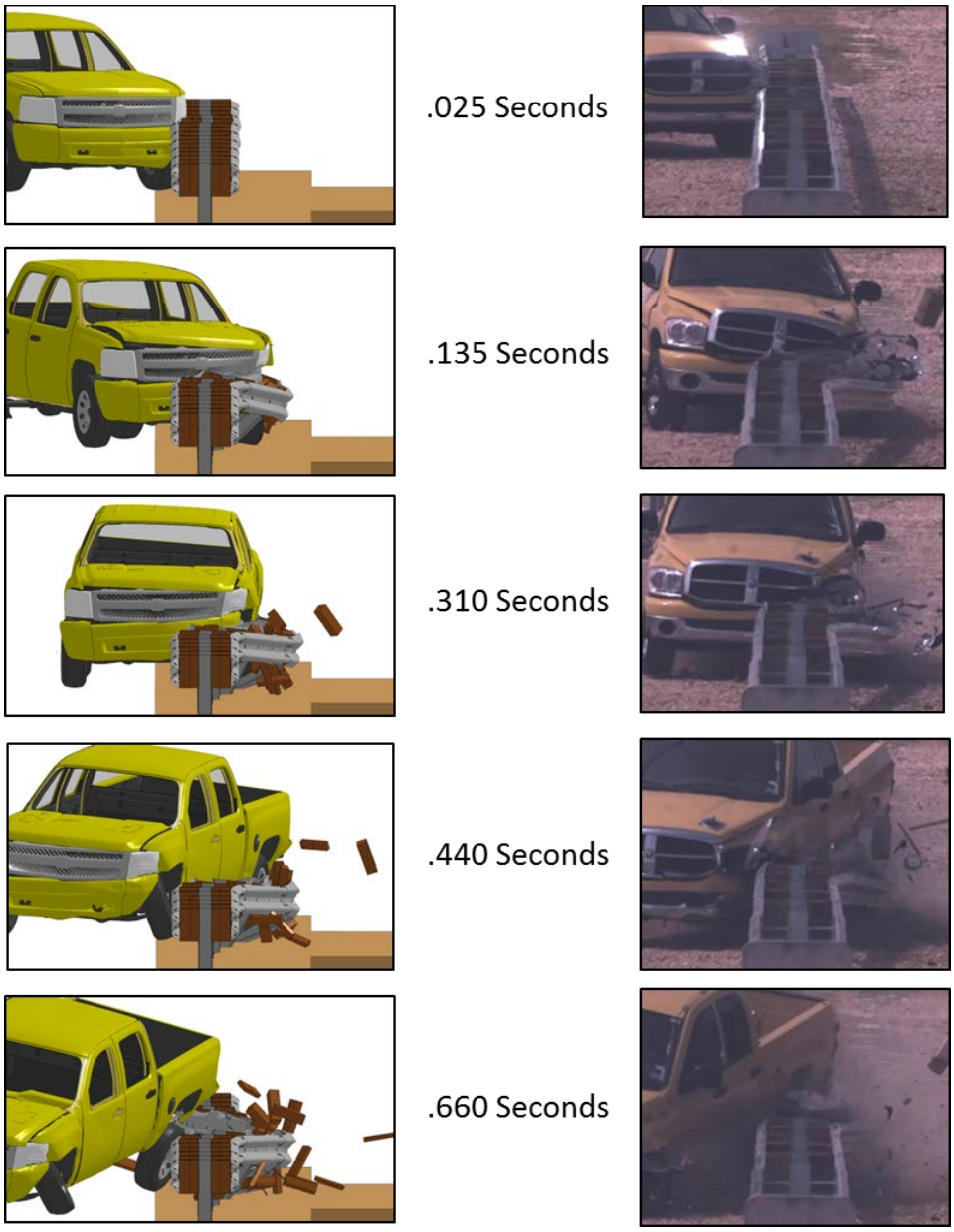

Figure 5.19: Comparison of Sequential Images for MASH Test 3-11 on MGS Median Barrier

A comparison of angular displacements between the pickup truck simulation and crash test are shown in Figure 5.20. The comparison is for a time period from 0 to 0.70 seconds, after which time the pickup truck has exited the barrier. The yaw and pitch angles reasonably agree. The magnitudes of both the roll and pitch angles are quite small. The roll angles follow the same trend until a small deviation occurs near the end of the time sequence after the vehicle was redirected. The simulation roll angle reaches a maximum of about -15 degrees while the crash test reaches a maximum of approximately -11 degrees. This may be due to increased snagging severity associated with the lack of various suspension damage modes in the pickup truck finite element model. However, this only represents a difference of 4 degrees and should not have a significant influence on the evaluation of override performance limits of the barrier system model.

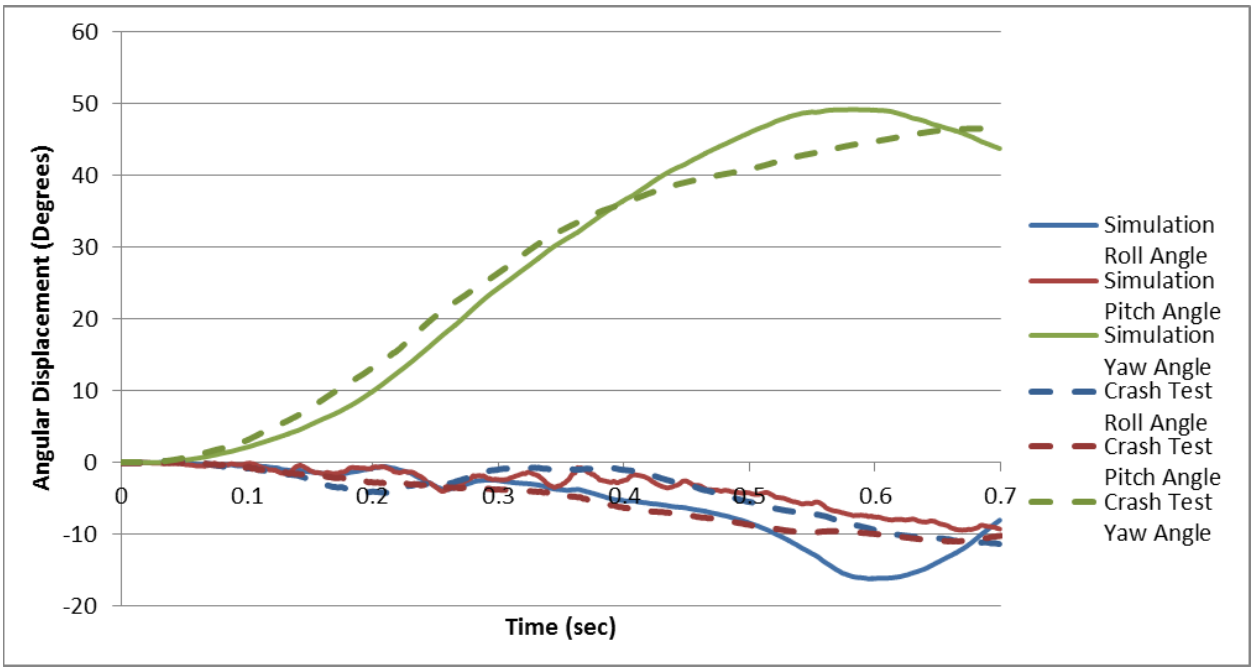

Figure 5.20: Comparison of Roll, Pitch and Yaw Angles for MASH Test 3-11 on MGS Median Barrier

The energy balance for the simulation is shown in Figure 5.21. The total energy for the simulation stayed relatively constant with a drop of about 6% during the simulation. There is a small amount of hour glass energy that developed but it reached a maximum of only 3% of the total energy. The kinetic energy decreased as the truck decelerated and the internal energy increased as the barrier and vehicle deformed. The sliding interface energy is related to frictional contact as the pickup truck slides along the barrier interface during the impact. The energy balance shows that the simulation behaves as expected in terms of global energy characteristics.

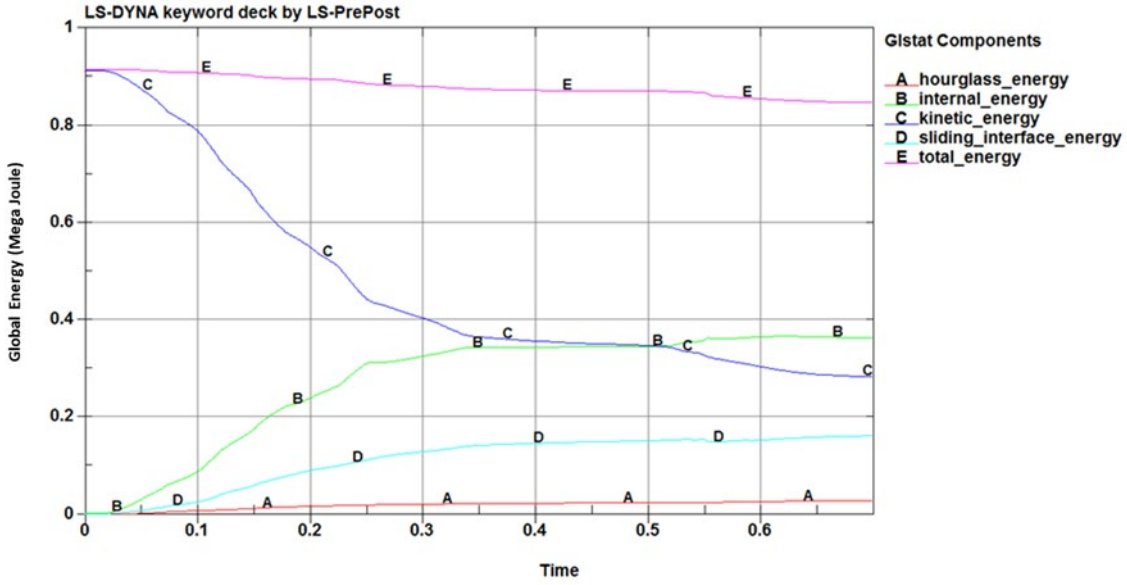

Figure 5.21: Energy Balance for MGS Median Barrier Pickup Truck Simulation
(Multiply by a factor of 737562 to convert to ft-lbf)

The simulation data was input into TRAP for calculation of occupant risk indices. The comparison of the occupant risk indices and other criteria between simulation and test is summarized in Table 5.8.

Table 5.8: PIRT for MGS Median Barrier Pickup Truck Simulation

Evaluation Criteria	TTI Test	Simulation	Absolute Difference	Relative Difference ≤ 20%	Pass?
Maximum Roll (deg.)	-11.5	-16.2	4.7	> 20%	Y
Maximum Yaw (deg.)	46.6	49.1	2.5	< 20%	Y
Maximum Pitch (deg.)	-11	-9.4	1.6	< 20%	Y
Longitudinal direction: OIV ≤ 12 m/s (30 ft/s) RA ≤ 20 g	19.0 ft/s -10.2 g's	19.68 ft/s -8.4 g's	.68 (ft/s) 1.8 g's	< 20% < 20%	Y Y
Lateral direction: OIV ≤ 12 m/s (30 ft/s) RA ≤ 20 g	15.1 ft/s -6.9 g's	14.76 ft/s -8.6 g's	.34 (ft/s) 1.6 g's	< 20% > 20%	Y
Number of Broken or Significantly Bent Posts	3 (12-14)	3 (12-14)	0	0	Y

The maximum roll, yaw and pitch angles are considered acceptable if the relative difference between the simulation and crash test is less than 20% or the absolute difference is less than 5 degrees. The roll, pitch, and yaw angles all passed this criteria.

The ridedown accelerations (RAs) are considered passing if the relative difference between the simulation and crash test is less than 20% or the absolute difference is less than 4 g as recommended in NCHRP Project 22-24. Both values also had to be below the maximum allowed value of 20.49 g as required by *MASH*. Both the longitudinal and lateral ridedown acceleration passed validation criteria.

The occupant impact velocities (OIVs) are considered passing if the relative difference between the simulation and crash test is less than 20% or the absolute difference is less than 2 m/s as recommended in NCHRP Project 22-24. Both values also had to be below the maximum allowed value of 40 ft/s as required by *MASH*. Both the lateral and longitudinal occupant impact velocities passed the validation criteria.

The number of broken or significantly bent posts and maximum dynamic deflection considered acceptable if the relative difference between the simulation and crash test is less than 20%. Both the number of broken or significantly bent posts and maximum dynamic deflection met this criteria.

The simulation results were then uploaded into RSVVP and compared to signals measured in MASH Test 3-11 of the MGS median barrier. Table 5.9 provides a summary of the RSVVP results. While several of the individual channels did not pass, the multi-channel analysis passed all of the metrics. The X acceleration, Y acceleration and yaw rate were weighted the most heavily by RSVVP. The simulation matched the crash test closely for these key data. The Roll rate and Pitch rate were both quite close to passing, but both channels had a standard deviation that was too high according to the ANOVA metrics. When all of the channels are considered together, the simulation passes the RSVVP criteria.

Table 5.9: Signal Analysis for MGS Median Barrier Pickup Truck Simulation

Channel Type	**Weighting Factor (Area II)**	**Spague-Geers Metrics**			**ANOVA Metrics**		**Pass?**
		M ≤ 40	**C ≤40**	**P ≤ 40**	**Mean Residual ≤ 0.05**	**Std. Deviation ≤ 0.35**	
X acceleration	0.23	2.4	31.6	31.5	0.01	0.22	Y
Y acceleration	0.24	5.10	24.90	24.3	0.00	0.29	Y
Z acceleration	0.03	62.2	74	40.2	0.02	0.31	N
Roll rate	0.08	25.1	44.6	36.9	0.01	0.40	N
Pitch rate	0.08	18.8	37.5	32.5	0.04	0.42	N
Yaw rate	0.34	12.4	18.7	13.9	0.03	0.23	Y
Multiple Channel	1.00	11.6	28.6	24.7	0.01	0.27	**Y**

Based on the visual comparison, energy balance, RSVVP signal analysis, and TRAP occupant risk analysis, the MGS Median barrier finite element model was considered sufficiently validated against MASH Test 3-11 results.

5.7.2. MGS Median Validation with Small Car

The MGS median barrier finite element model went through the same validation procedure for MASH Test 3-10 with the 1100C passenger car. The validation procedure consisted of a graphical comparison, energy balance analysis, and analytical component using both RSVVP and TRAP.

Sequential images of the simulation and crash test are compared in Figure 5.22 and Figure 5.23 for frontal and overhead views, respectively. The comparison of the simulation and test results show good correlation between the simulation and the crash test in terms of general vehicle kinematics and barrier response.

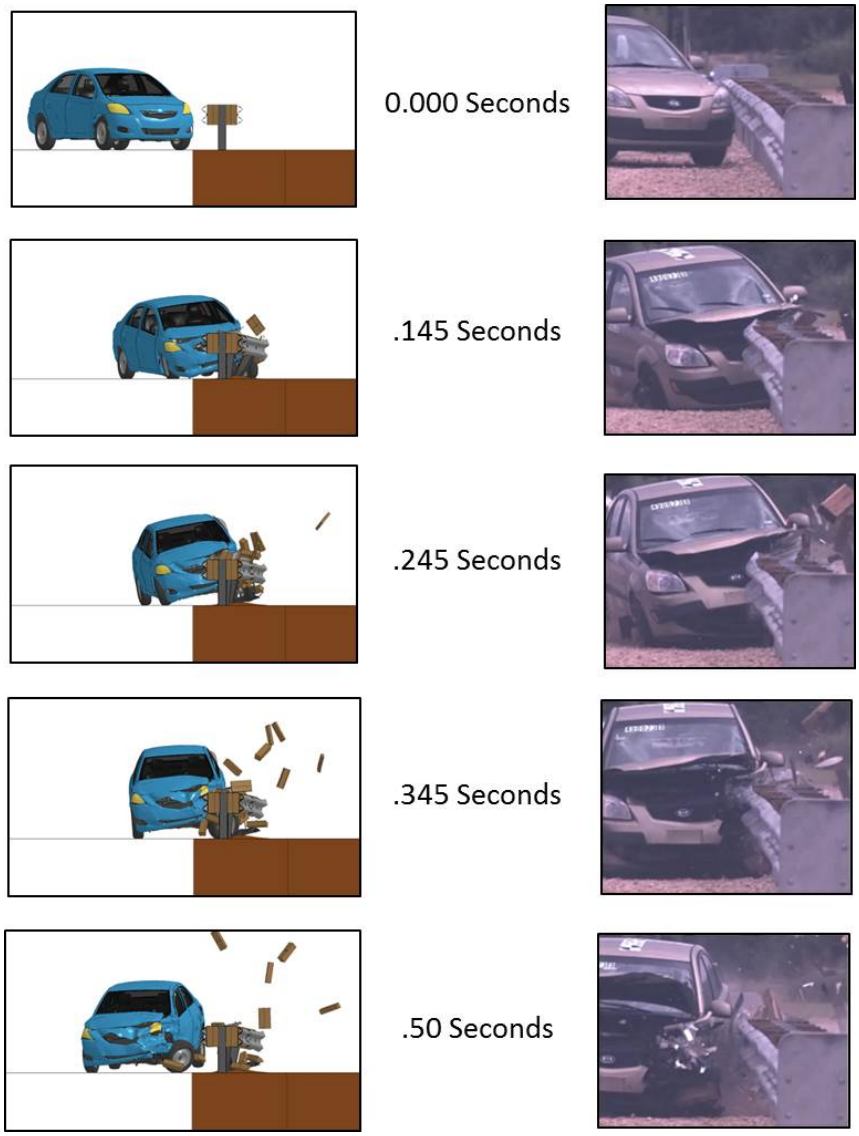

Figure 5.22: Comparison of Sequential Images for MASH Test 3-10 on MGS Median Barrier (Front View)

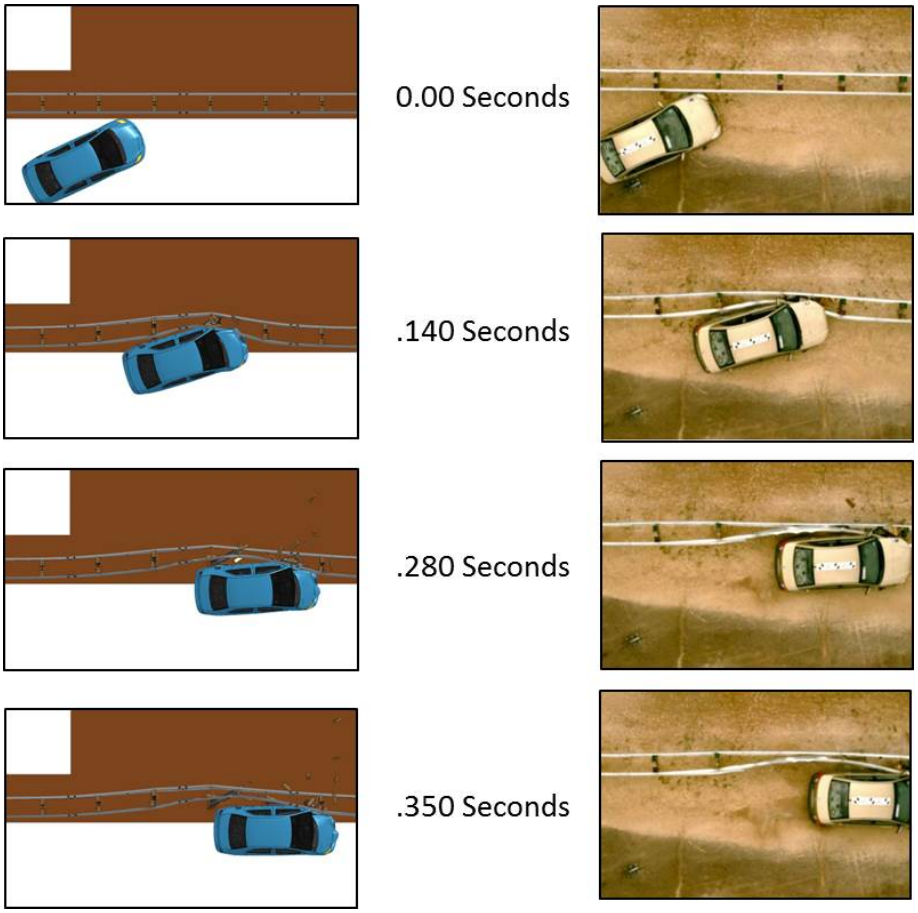

Figure 5.23: Comparison of Sequential Images for MASH Test 3-10 on MGS Median Barrier (Top View)

A comparison of angular displacements between the pickup truck simulation and crash test are shown in Figure 5.24. Overall, the plots show good correlation. Both the yaw and roll angles maintain the same general slope throughout the test. The pitch angles for both the crash test and the simulation stayed near 0 degrees until about 0.275 seconds, at which time the vehicle had been redirected. The pitch values remain small and the deviation occurs at a time that is unlikely to affect the outcome of the performance limits assessment.

The energy balance for the simulation is shown in Figure 5.25. The total energy stayed relatively constant throughout the test with a slight increase after 0.5 seconds, which corresponds to a time after which the vehicle had exited the system. There was a small amount of hourglass energy that developed in the system, but it reached a maximum around 6% of the total energy. The kinetic energy lowered as the truck decelerated and the internal energy increased as the barrier deflected and deformed. The energy balance shows that the simulation behaves as expected in terms of global energy characteristics.

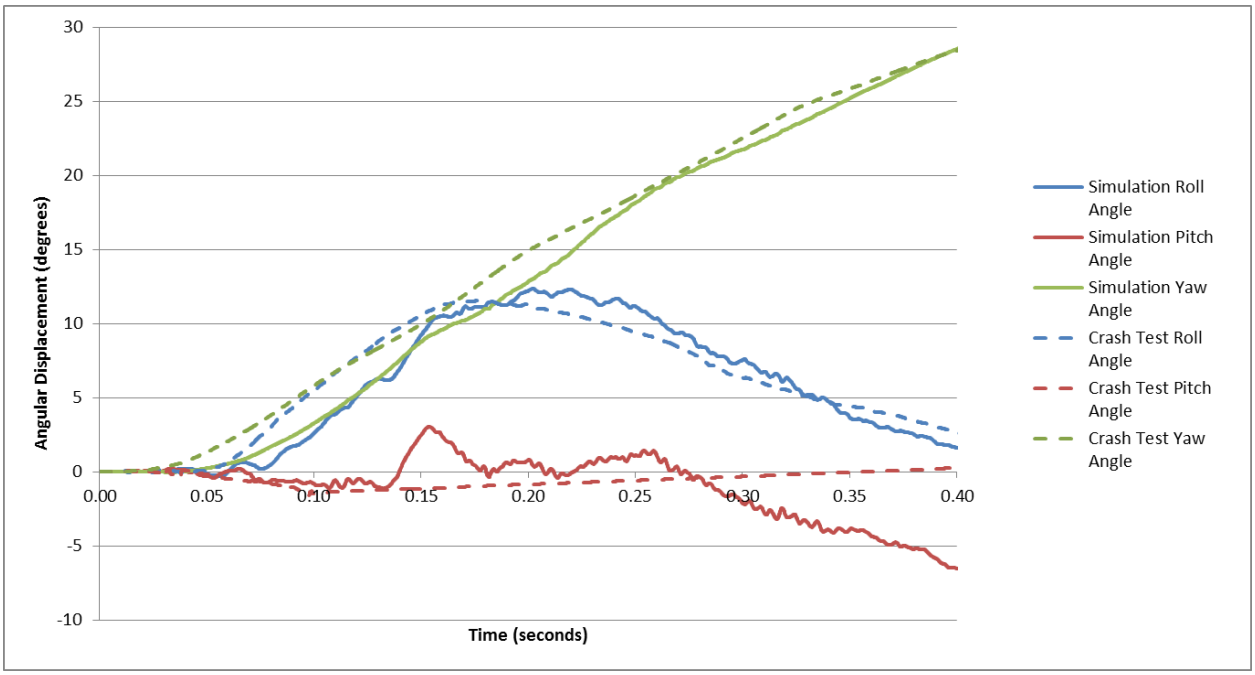

Figure 5.24: Comparison of Roll, Pitch and Yaw Angles for MASH Test 3-10 on MGS Median Barrier

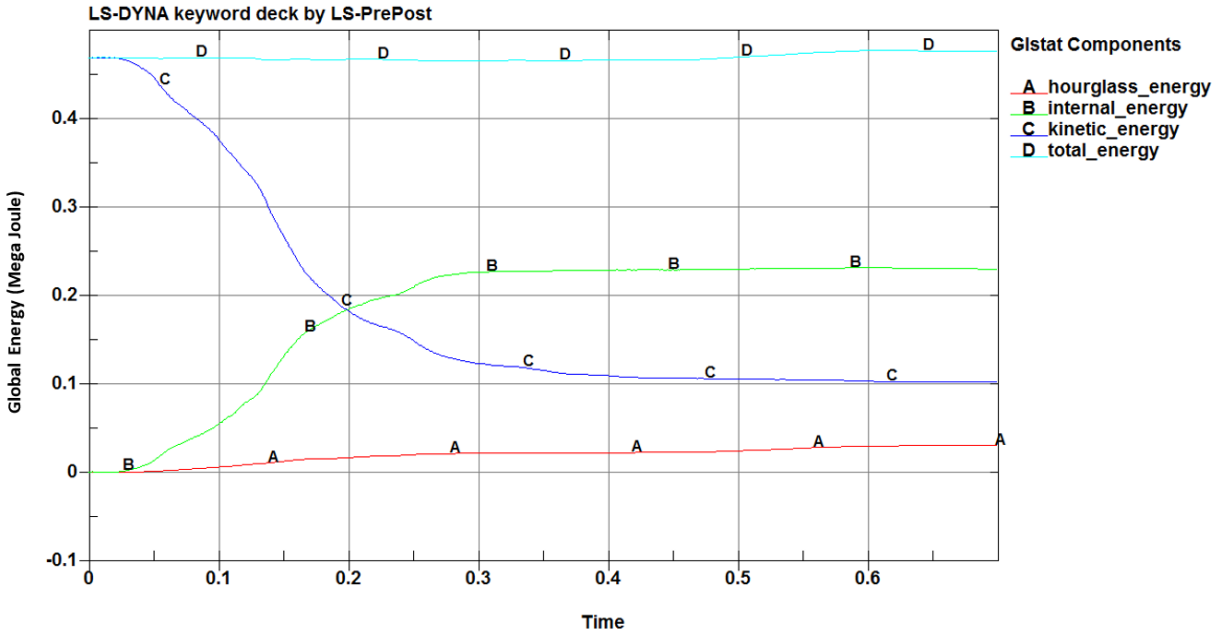

Figure 5.25: Energy Balance for MGS Median Barrier Small Car Simulation (Multiply by a factor of 737562 to convert to ft-lbf)

The simulation data was input into TRAP for calculation of occupant risk indices. The comparison of the occupant risk indices and other criteria between simulation and test is summarized in the PIRT shown in Table 5.10.

Table 5.10: PIRT for MGS Median Barrier Small Car Simulation

Evaluation Criteria	Test	Simulation	Absolute Difference	Relative Difference ≤ 20%	Pass?
Maximum Roll (deg.)	10.9	12.4	1.5	< 20%	Y
Maximum Yaw (deg.)	32.2	36.9	4.7	< 20%	Y
Maximum Pitch (deg.)	-6.1	-4.0	2.1	> 20%	Y
Longitudinal direction: Occupant Impact Velocity ≤ 12 m/s (30 ft/s)	20.0	24.3	4.3	> 20%	Y
Ridedown Acceleration ≤ 20 g's	-9.6	-11.5	1.9	< 20%	Y
Lateral direction: Occupant Impact Velocity ≤ 12 m/s (30 ft/s)	-17.4	-18.7	1.3	< 20%	Y
Ridedown Acceleration ≤ 20 g's	8.3	9.4	1.1	< 20%	Y
Number of Broken or Significantly Bent Posts	4	4	0.0	< 20%	Y
Maximum Dynamic Deflection (m)	0.645	0.750	0.105	< 20%	Y

The maximum roll, yaw and pitch angles are considered acceptable if the relative difference between the simulation and crash test is less than 20% or the absolute difference is less than 5 degrees. The roll, pitch, and yaw angles all passed this criteria..

The ridedown accelerations (RAs) are considered passing if the relative difference between the simulation and crash test is less than 20% or the absolute difference is less than 4 g as recommended in NCHRP Project 22-24. Both values also had to be below the maximum allowed value of 20.49 g as required by *MASH*. Both the longitudinal and lateral ridedown acceleration passed validation criteria.

The occupant impact velocities (OIVs) are considered passing if the relative difference between the simulation and crash test is less than 20% or the absolute difference is less than 2 m/s as recommended in NCHRP Project 22-24. Both values also had to be below the maximum allowed value of 40 ft/s as required by *MASH*. Both the lateral and longitudinal occupant impact velocities passed the validation criteria.

The number of broken or significantly bent posts and maximum dynamic deflection considered acceptable if the relative difference between the simulation and crash test is less than 20%. Both the number of broken or significantly bent posts and maximum dynamic deflection met this criteria.

The simulation results were then uploaded into RSVVP and compared to signals measured in MASH Test 3-10 of the MGS median barrier. Table 5.11 provides a summary of the RSVVP results.

Table 5.11: Signal Analysis for MGS Median Barrier Small Car Simulation

Channel Type	Weighting factor (Area II)(45)	Spague-Geers Metrics			ANOVA Metrics		Pass?
		M ≤ 40	P ≤ 40	C ≤ 40	Mean Residual ≤ 5.0	Std. Deviation ≤ 35	
X acceleration	0.27	34.8	33.5	48.3	-2.260	32.090	N
Y acceleration	0.20	25.70	29.9	39.4	0.720	21.390	Y
Z acceleration	0.02	38.5	44.6	58.9	0.330	25.600	N
Yaw rate	0.45	9.2	5.3	10.6	7.610	9.360	N
Roll rate	0.02	9.3	23	24.8	3.990	20.900	Y
Pitch rate	0.03	80.3	48.9	94.1	2.200	16.250	N
Multiple Channel	1.00	22.6	20.6	30.9	3.100	18.800	Y

While several of the individual channels did not pass, the multi-channel analysis passed all of the metrics. The X acceleration, Y acceleration and yaw rate are the dominant behaviors and are given the highest weighting factors when the multi-channel analysis is performed by RSVVP. The simulation matched the crash test very closely on these key data. When all of the channels are considered together, the simulation passes the RSVVP criteria.

Based on the visual comparison, energy balance, RSVVP signal analysis, and TRAP occupant risk analysis, the modified G2 weak post W-beam guardrail finite element model was considered sufficiently validated against MASH Test 3-10 results.

5.8. CONCRETE: SINGLE SLOPE (42-INCH)

5.8.1. Single Slope Simulation

The initial proposed validation procedure was to compare the results of MASH Test 3-11 on the TxDOT Single Slope Traffic Rail (Type SSTR) on pan-formed bridge to the simulation results of the single slope barrier model. A MASH Test 3-11 impact was simulated on a single slope finite element model. The results of the RSVVP signal analysis between simulation and crash test is presented in Figure 5.26. As shown in this figure, the multi-channel analysis passed all of the recommended metrics.

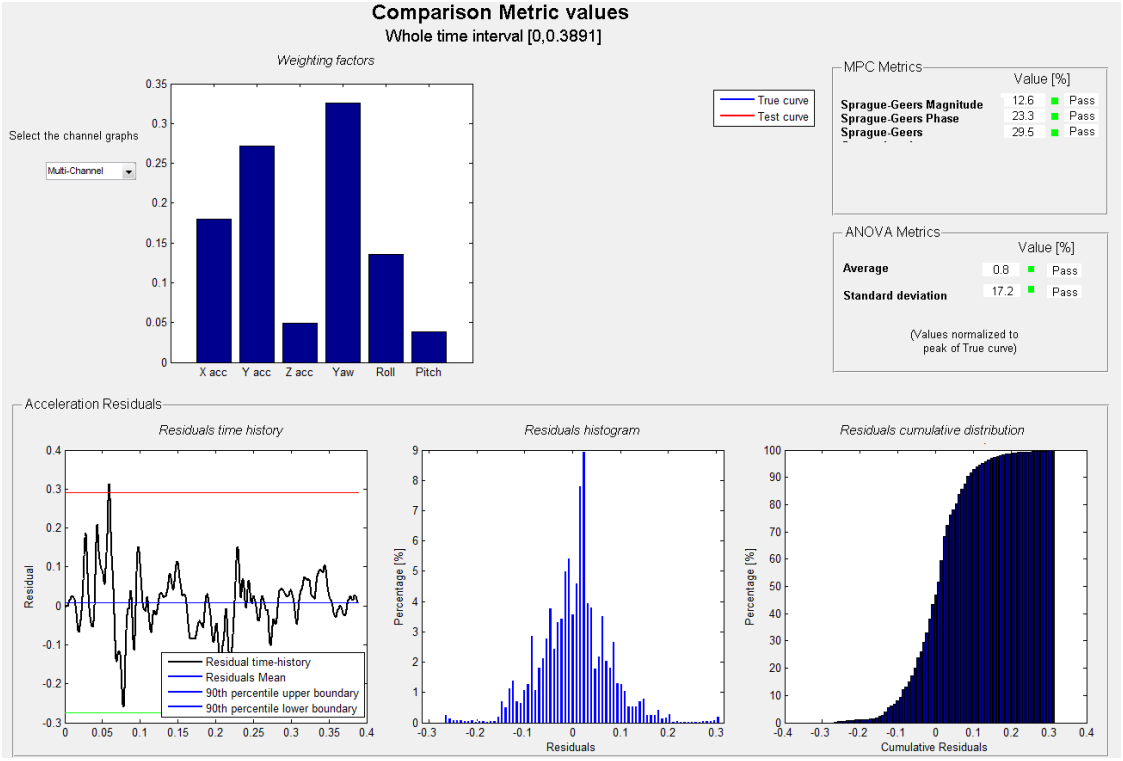

Figure 5.26: Signal Analysis Results for Single Slope Concrete Barrier Pickup Truck Simulation

The simulation data was input into TRAP for calculation of occupant risk indices. The comparison of the occupant risk indices and other criteria between simulation and test is summarized in Table 5.12.

Table 5.12: PIRT for Single Slope Concrete Barrier Pickup Truck Simulation

Evaluation Criteria	TTI Test	Simulation	Relative Difference	Pass ?
Maximum Roll (deg.)	-8.8	-9.8	< 20%	Y
Maximum Yaw (deg.)	-27.9	-29.7	< 20%	Y
Maximum Pitch (deg.)	5	-4.3	> 20%	N
Longitudinal direction: Occupant Impact Velocity ≤ 12 m/s (30 ft/s); Ridedown Acceleration ≤ 20 g's	36.7 (ft/s); -11.7 g's	32.8 (ft/s); -19.2 g's	< 20% >20%	N

As shown, the single slope concrete barrier simulation does not pass all of suggested validation metrics. The ridedown accelerations from the simulation are greater than the ridedown accelerations from MASH Test 3-11 on the TxDOT SSTR on pan-formed bridge. While the pitch angles are quite different, their importance is relatively minor due to their small magnitude. However, at this stage, the single slope concrete barrier finite element model could not be considered validated.

5.8.2. Geometric Differences between Simulated and Tested Single Slope Barriers

The researchers performed further analysis to explore possible reasons for the differences observed between the tested and simulated single slope barrier systems. One difference that could be a source of the difference in the ridedown accelerations between the simulated single slope concrete barrier system and the TxDOT Single Slope Traffic Rail (Type SSTR) on pan-formed bridge was the barrier connection to the bridge deck. Figure 5.28 shows that the SSTR had a bolted connection to a relatively thin pan-formed bridge deck. The single slope concrete barrier model (depicted in Figure 5.29) was modeled as a rigid barrier attached to a rigid foundation.

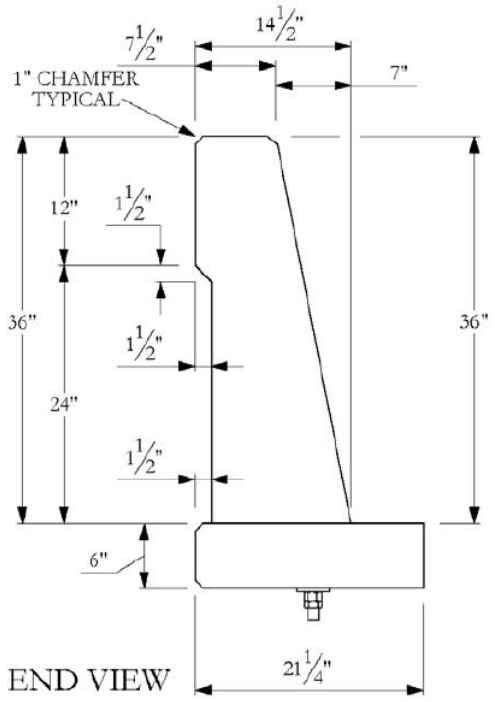

Figure 5.27: TxDOT Single Slope Traffic Rail (Type SSTR) on Pan-Formed Bridge Deck

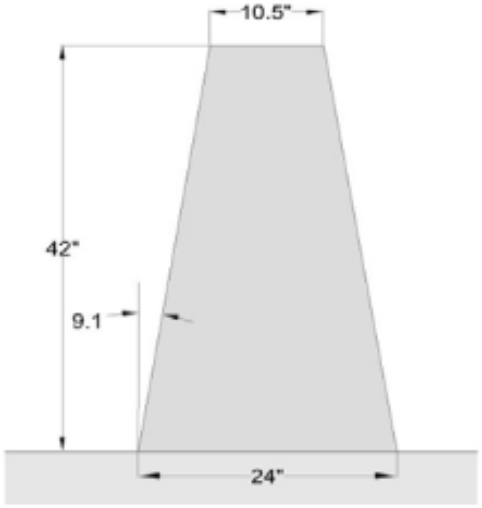

Figure 5.28: Single Slope Barrier Model Representation

To investigate the influence of these differences on occupant risk indices, an explicit finite element model of the TxDOT SSTR on pan-formed bridge deck was created. The plan developed by the research team was to validate the model of the TxDOT SSTR on pan-formed bridge deck for MASH Test 3-11, and then use the same material cards and contacts in the single slope barrier finite element model. Figure 5.30 describes this proxy validation process for the single slope concrete barrier system.

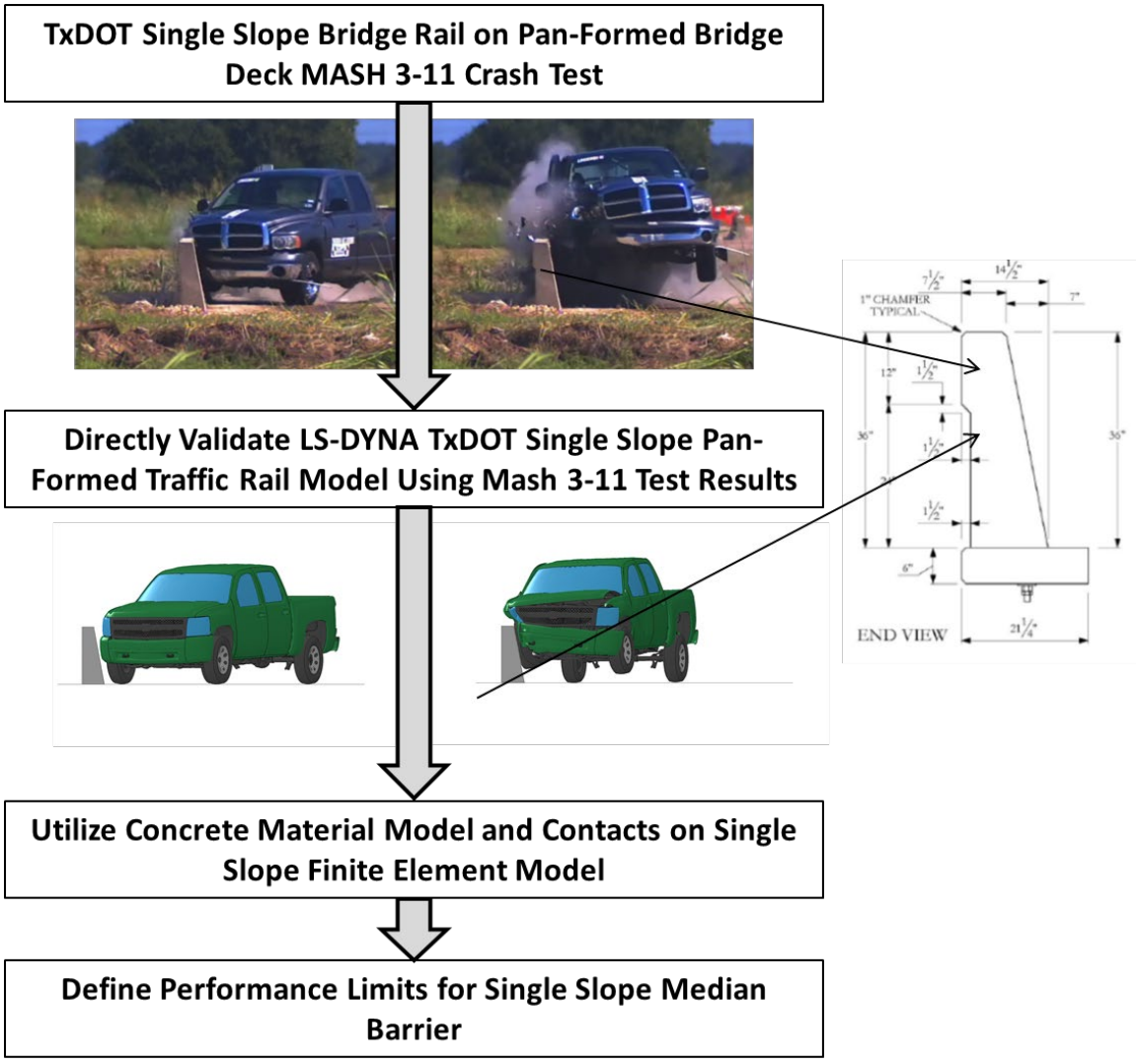

Figure 5.29: Proxy Validation Procedure for Single Slope Concrete Barrier Finite Element Model

5.8.3. Validation of SSTR on Pan-Formed Bridge Deck

The model of the SSTR on pan-formed bridge deck was comprised of solid elements assigned general properties of concrete. The material model chosen for this finite element model is a linear elastic material. The modulus of elasticity for the material was modeled after the American Concrete Institute's (ACI) common equation:

$$E = 57{,}000\sqrt{f'_c}$$

where f'c is the unconfined compressive strength of the concrete.

The variable f'c was taken to be equal to 3600 psi, which is the concrete strength specified in Research Report 9-1002-3 that documents MASH Test 3-11 of the TxDOT SSTR on pan-formed bridge deck. The only other parameters that had to be defined was Poison's Ratio and mass density of concrete, which were taken to be 0.15 and 2.400e-009 ton/mm^3 respectively.

Utilizing the linear elastic concrete material and connection and contact updates, a successful MASH Test 3-11 simulation was performed on the TxDOT SSTR on pan-formed bridge deck. Sequential images of the simulation and corresponding crash test are presented in Figure 5.31 and Figure 5.32 from the front and top views, respectively. The comparison shows good general agreement between the simulation and test results that permitted the validation procedure to progress.

The energy balance for the simulation is shown in Figure 5.33. There is a slight loss of total energy and a small amount of hourglass energy developing, but nothing too large to be of concern. The kinetic energy decreased as the pickup truck decelerated and the internal energy increased due to barrier and vehicle deformation. The energy balance shows that the simulation behaves as expected in terms of global energy characteristics.

Figure 5.30: Comparison of Sequential Images for MASH Test 3-11 on SSTR on Pan-Formed Bridge Deck (Front View)

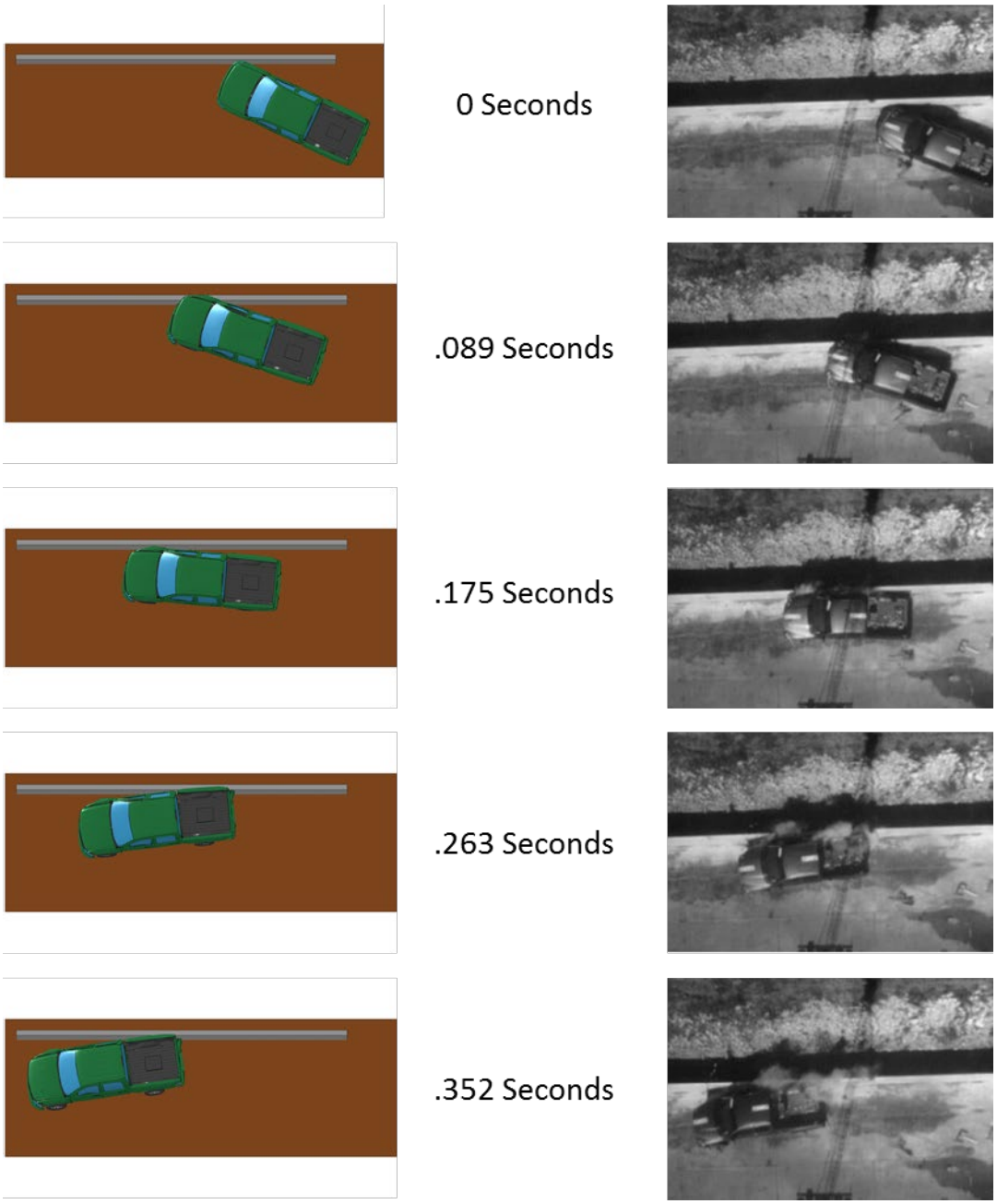

Figure 5.31: Comparison of Sequential Images for MASH Test 3-11 on SSTR on Pan-Formed Bridge Deck (Top View)

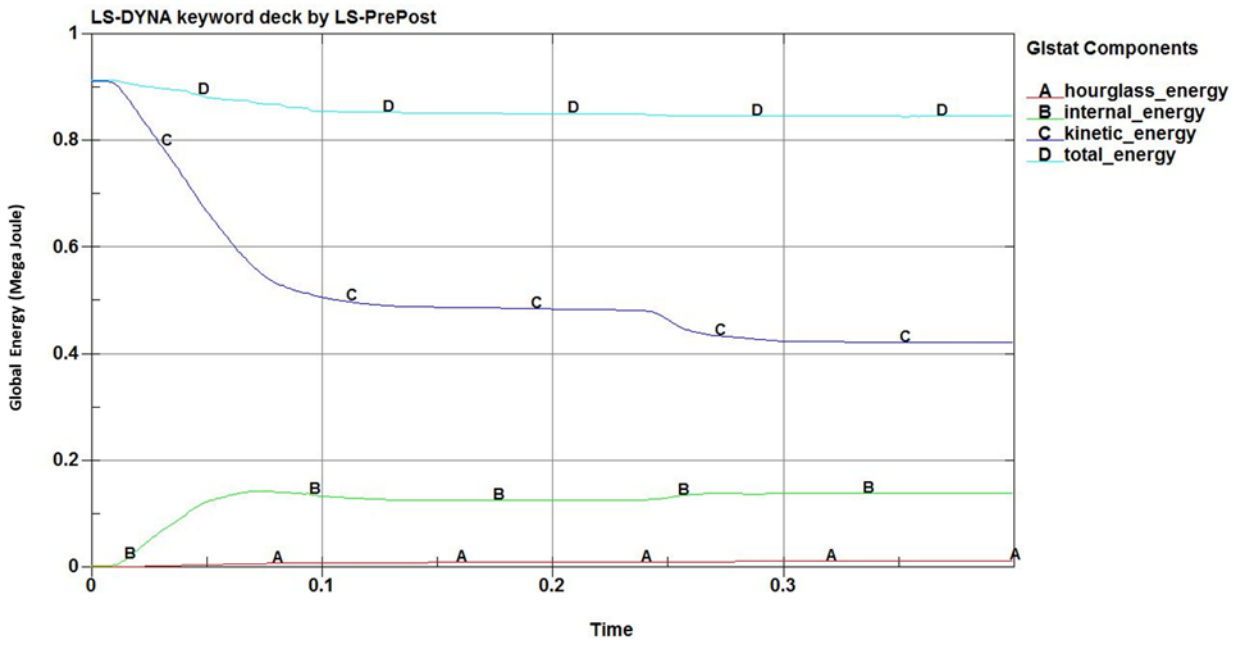

Figure 5.32: Energy Balance for SSTR on Pan-Formed Bridge Deck Pickup Truck Simulation (Multiply by a factor of 737562 to convert to ft-lbf)

The next step in the validation process was a comparison of the simulation results to the crash test results utilizing RSVVP with multiple channels. The simulation and crash test were compared from 0 to 0.33 seconds, which is the time from first contact to the time when the truck exited the barrier during the simulation. Figure 5.34 below shows a screenshot of the RSVVP validation results.

The simulation results were then uploaded into RSVVP and compared to signals measured in MASH Test 3-11 of the SSTR on pan-formed bridge deck. Figure 5.35 shows an image of the RSVVP results from the multi-channel analysis of the SSTR on pan-formed bridge deck simulation. The comparison was acceptable based on both the MPC and ANOVA metrics.

Table 5.13 provides a summary of the RSVVP results. While several of the individual channels did not pass, the multi-channel analysis passed all of the metrics. The X acceleration, Y acceleration and yaw rate, which dominated the response characteristics, were weighted the most heavily by RSVVP. Note that the simulation performed well with respect to these data and, when all of the channels are considered together, the simulation passes the RSVVP criteria.

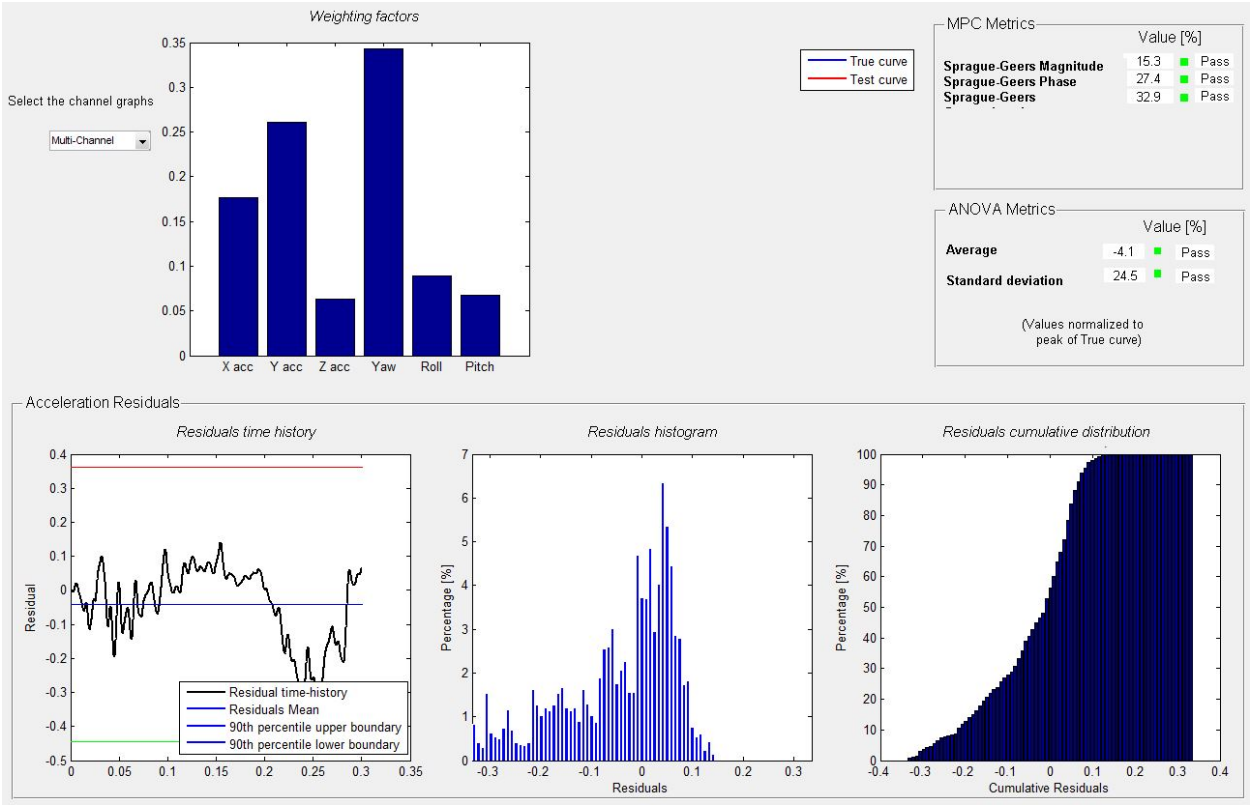

Figure 5.33: RSVVP Multi-Channel Comparison for SSTR on Pan-Formed Bridge Deck Pickup Truck Simulation

Table 5.13: Signal Analysis Summary for SSTR on Pan-Formed Bridge Deck Pickup Truck Simulation

Channel Type	**Weighting factor (Area II)(45)**	**Spauge-Geers Metrics**		**ANOVA Metrics**		**Pass?**
		M ≤ 40	**P ≤ 40**	**Mean Residual ≤ 0.05**	**Std. Deviation ≤ 0.35**	
X acceleration	0.18	21.5	27.3	-0.01	0.21	Y
Y acceleration	0.26	16.7	28.4	-0.02	0.21	Y
Z acceleration	0.06	11	41.8	-0.06	0.26	N
Roll rate	0.09	62.2	44.4	-0.12	0.23	N
Pitch rate	0.07	9.4	44.6	0.03	0.09	Y
Yaw rate	0.34	.7	16.1	-0.12	0.31	N
Multiple Channel	1.00	15.3	27.4	-0.04	0.25	Y

The simulation data was input into TRAP for calculation of occupant risk indices. The comparison of the occupant risk indices and other criteria between simulation and test is summarized in PIRT shown in Table 5.14.

Table 5.14: Phenomena Importance Ranking Table

Evaluation Criteria	Test	Simulation	Absolute Difference	Relative Difference ≤ 20%	Pass?
Maximum Roll (deg.)	-8.8	-9.3	0.5	< 20%	Y
Maximum Yaw (deg.)	-27.9	-32.8	4.9	< 20%	Y
Maximum Pitch (deg.)	5.0	-6.0	11.0	> 20%	N
Longitudinal direction: OIV ≤ 12 m/s (30 ft/s) RA ≤ 20 g	22.0 -5.2	28.2 -8.2	6.2 3.0	> 20% > 20%	Y Y
Lateral direction: OIV ≤ 12 m/s (30 ft/s) RA ≤ 20 g	29.9 -11.7	24.3 -12.4	5.6 0.7	< 20% < 20%	Y Y
The rail did not rupture or fail	Yes	Yes	-	-	Y

The maximum roll, yaw and pitch angles are considered acceptable if the relative difference between the simulation and crash test is less than 20% or the absolute difference is less than 5 degrees. The roll and yaw both passed these criteria, however the pitch did not. The magnitude of the maximum pitch angle is very small, and the difference is not believed to significantly alter the pickup truck's response.

The ridedown accelerations (RAs) are considered passing if the relative difference between the simulation and crash test is less than 20% or the absolute difference is less than 4 g as recommended in NCHRP Project 22-24. Both values also had to be below the maximum allowed value of 20.49 g as required by *MASH*. Both the longitudinal and lateral ridedown acceleration passed validation criteria.

The occupant impact velocities (OIVs) are considered passing if the relative difference between the simulation and crash test is less than 20% or the absolute difference is less than 2 m/s as recommended in NCHRP Project 22-24. Both values also had to be below the maximum allowed value of 40 ft/s as required by *MASH*. Both the lateral and longitudinal occupant impact velocities passed the validation criteria.

Based on the visual comparison, energy balance, RSVVP signal analysis, and TRAP occupant risk analysis, the SSTR on pan-formed bridge deck finite element model was considered sufficiently validated against MASH Test 3-11 results.

5.8.4. Single Slope Concrete Barrier Model

A single slope concrete barrier finite element model was created using the same concrete material model, element formulation, and contacts utilized in the validated SSTR on pan-formed bridge deck model. By validating the SSTR on pan-formed bridge deck finite element model and then using the same materials, elements and contacts, the single slope concrete barrier finite element model is considered proxy validated. The single slope concrete barrier finite element model is shown in Figure 5.36.

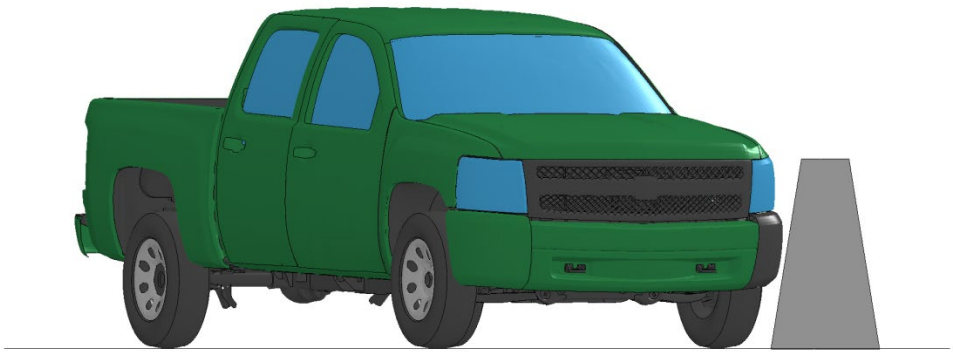

Figure 5.34: Single Slope Concrete Barrier Finite Element Model

A simulation with the pickup truck was performed in accordance with MASH Test 3-11 impact conditions to debug the model, confirm MASH compliance, and serve as a baseline on flat level ground based on which the perform performance limits of the system could be assessed. As shown in the sequential images provided in Figure 5.37, the pickup truck was successfully contained and redirected by the single slope concrete barrier.

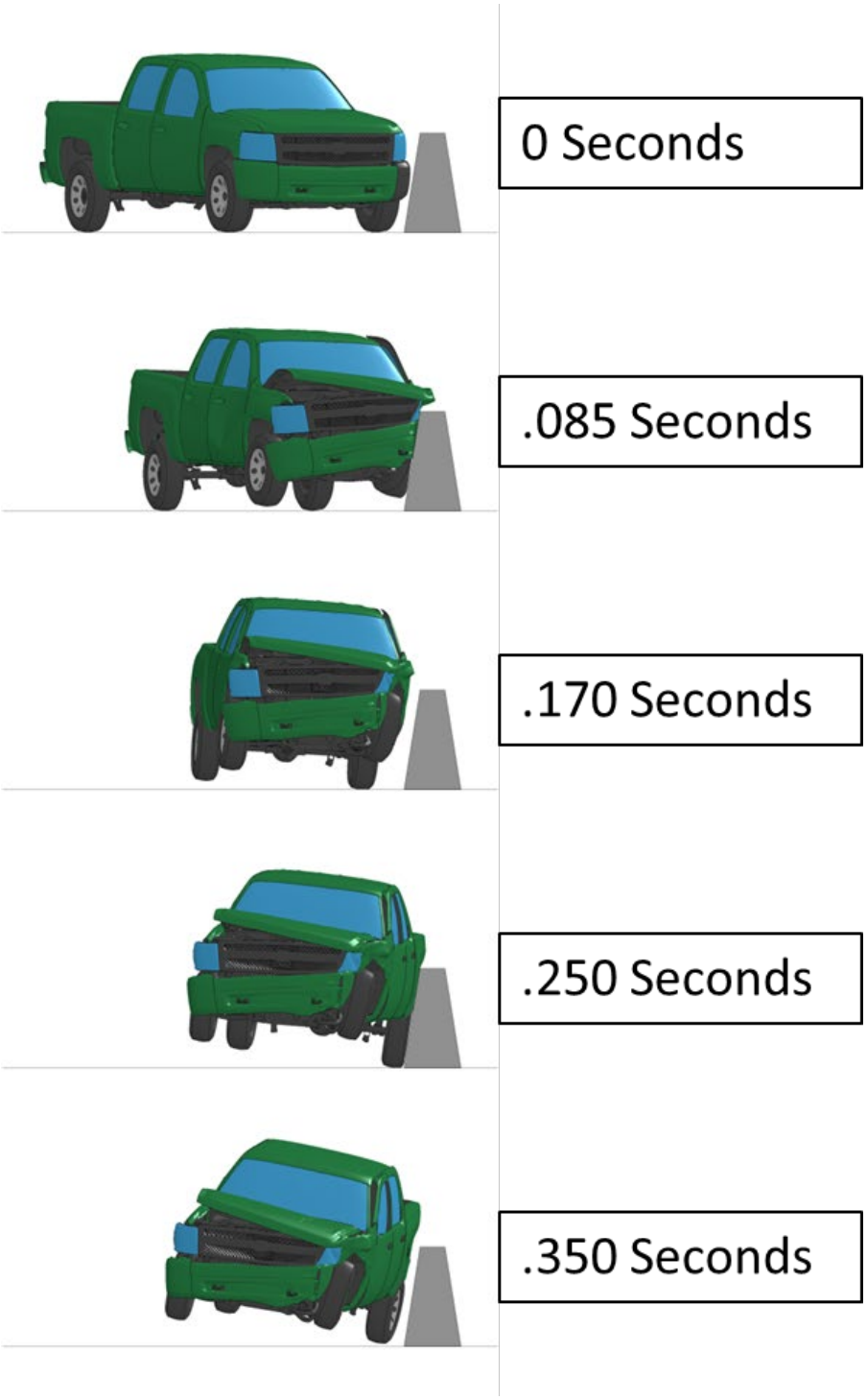

Figure 5.35: Sequential Images from Single Slope Concrete Barrier Pickup Truck Simulation

The energy balance for the simulation is shown in Figure 5.37. The total energy remains relatively constant with no large losses that could significantly affect the simulation. The hourglass energy stays relatively small as well which is the desired result. The kinetic energy lowered as the truck decelerated and the internal energy increased as the barrier and vehicle deform. The sliding interface energy, which is related to friction, increases as the pickup truck slides along the single slope concrete barrier. The energy balance shows that the simulation behaves as expected in terms of global energy characteristics.

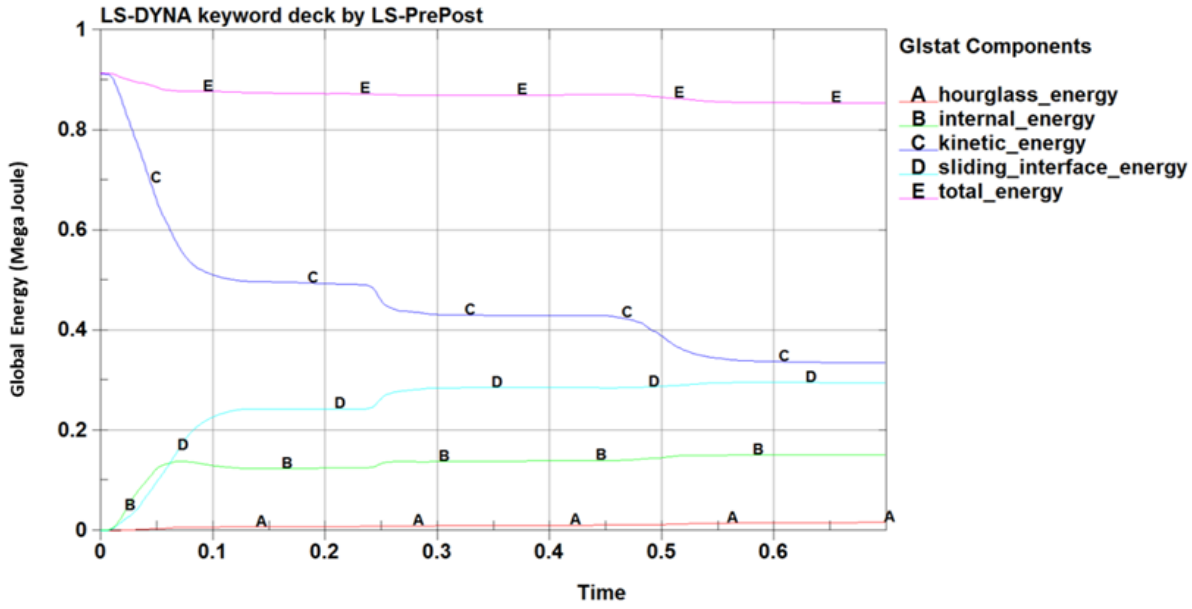

Figure 5.36: Energy Balance of Simulation of Single Slope (Multiply by a factor of 737562 to convert to ft-lbf)

With the single slope concrete barrier finite element model running as expected and validated using the model of the SSTR on pan-formed bridge deck, the model is considered satisfactory for use in a performance limits analysis for the barrier system.

6. BARRIER PERFORMANCE LIMITS

6.1. PERFORMANCE LIMITS PROCEDURE

The performance limits of the selected barrier systems were defined by performing impact simulations using the validated finite element barrier models described in Chapter 4. The performance limits are related to two distinct behaviors: barrier override and barrier underride.

When a barrier is impacted on flat, level ground, the impact occurs at a particular height defined by the characteristics of the impacting vehicle and the geometric profile and response of the barrier system. The impact forces applied by the taller pickup truck design vehicle will be at a greater height than the smaller passenger car. This is a function of vehicle characteristics such as wheel size, bumper height, hood height, and vertical center of gravity (C.G.). Hence, it will control the override limit of a barrier system. Conversely, the underride limit of a barrier will be dictated by the small passenger car due to its lower height, smaller wheels, and generally sloped front end.

When a vehicle traverses a slope or ditch, the elevation of its front end with respect to the local ground level can change. When initially encroaching onto a slope, the height of a vehicle relative to the local ground will increase compared to its equilibrium position. The degree of slope and encroachment conditions (i.e., encroachment speed and angle) will dictate the extent to which this occurs. Under some circumstances, the vehicle can become airborne and the suspension can fully extend. Such conditions cause the vehicle to interact with a barrier at a greater height, increasing the propensity for vehicle instability or override of the barrier. The pickup truck will be more prone to become unstable and/or override a barrier in this manner.

When a roadside encroachment continues, the vehicle will recontact the local terrain, causing the suspension to compress and the front end of the vehicle to lower with respect to the local terrain compared to its normal equilibrium position on flat, level ground. Such behavior can occur on a slope or at a ditch bottom when a vehicle encounters the ditch backslope. When the contact height of a vehicle with a barrier system decreases, the propensity for vehicle underride increases. The small passenger car will be more prone to underride at barrier as a result of such behavior.

The performance limit analyses were conducted using LS-DYNA. LS-DYNA is an explicit finite element code capable of simulating complex nonlinear dynamic impact problems. Simulations were performed at different impact heights to define a performance envelope for each guardrail and median barrier system of interest. These parametric analyses were conducted with the barrier system installed on flat, level terrain similar to how longitudinal barriers are crash tested and how the finite element models of the barrier systems were validated. This approach significantly reduced the time and complexity of the impact analyses by removing the need to simulate the traversal of terrain in advance of the barrier and permitting the simulation to be initiated with the vehicle in contact with the barrier. Current finite element models do not have fully validated tire and suspension models, therefore, the validity of the vehicle trajectory and response during slope and ditch encroachments is not fully known.

Defining the performance limits for a given barrier required multiple impact simulations. Each barrier model was placed on flat, level ground and impacted by the two different MASH design vehicles following the prescribed TL-3 impact conditions. They consist of the pickup truck and small passenger car impacting the barrier at a speed of 62 mph (100 km/h) and an angle of 25 degrees.

The initial simulation for each vehicle type involved the barrier being impacted at the conventional height defined by the vehicle's equilibrium condition on flat terrain. The results of these simulations were used to validate to barrier models against full-scale crash test data when available. The results of these simulations established the baseline performance of the barrier.

The height of impact was then parametrically varied to determine the performance limits of the barrier as defined by initiation of rollover or override for the pickup truck and high deceleration or underride for the small passenger car. Since underride is not a concern for continuous concrete barriers, only the override analyses was conducted.

6.1.1. Override Analysis Procedure

MASH Test 3-11 impact conditions with the 2270P pickup truck model were simulated to obtain the override limit for each barrier. The vehicle height was incrementally raised relative to the barrier from its equilibrium position established on flat, level ground, and the barrier performance was evaluated. The ground level remained the same to simulate the response of the barrier relative to what would be the local ground elevation. This is analogous to the vehicle being unweighted similar to if it were to encroach off a slope.

The top of the bumper was selected as the reference point on the pickup truck for defining the override limit of the barrier. The top of bumper height for a MASH pickup truck was measured at 29.1 inches (740 mm). If the vehicle overturned or overrode the barrier during a simulation, the override performance limit was defined as the last height increment for which satisfactory containment and redirection was achieved.

6.1.2. Underride Analysis Procedure

MASH Test 3-10 impact conditions with the 1100C passenger car model were simulated to obtain the underride limit for each barrier. The vehicle height was incrementally lowered relative to the barrier from its equilibrium position established on flat, level ground, and the barrier performance was evaluated. The ground contact surface was lowered with the vehicle, but the soil surrounding the barrier system remained at the same elevation to capture proper post-soil and vehicle-post interaction. Note that the soil volume was excluded from the vehicle contact. This approach is roughly analogous to a vehicle's suspension compressing and lowering the interaction height of the vehicle with the barrier relative to the local terrain.

Similar to the truck, the top of the bumper was selected as the reference point on the small car for defining the underride limit of the barrier. The top of bumper height for a MASH small car was measured at 21 inches (533 mm). This height was designated as the reference point for the underride performance limit analysis for all barrier systems. If the vehicle experienced unacceptable accelerations or occupant risk indices associated with underride or snagging, or if the small car underrode the rail to an extent that the rail element reached the elevation of the side window, the underride performance limit was defined as the last height increment for which satisfactory performance was achieved.

A description of the performance limit analyses for each barrier system is described in the sections below.

6.2. MODIFIED G2 WEAK POST W-BEAM

6.2.1. Override Analysis

Utilizing the validated modified G2 weak post W-beam guardrail finite element model, the override performance limit was determined. The impact height of the pickup truck with respect to the barrier was incrementally varied. Figure 6.1 through Figure 6.4 show sequential images corresponding to four impact simulations performed at bumper heights of 33.1 inches, 32.1 inches, 31.1 inches and 30.1 inches, respectively, These heights correlate to the height of the pickup truck interaction with the guardrail being raised by 4 inches, 3 inches, 2 inches and 1 inch, respectively.

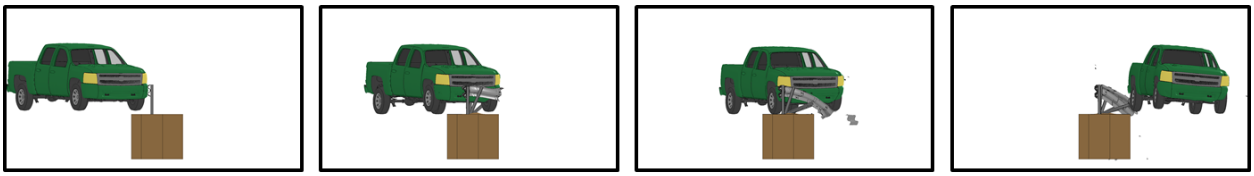

Figure 6.1: Modified G2 - Vehicle Raised 4 inches (Bumper Height 33.1” from Ground)

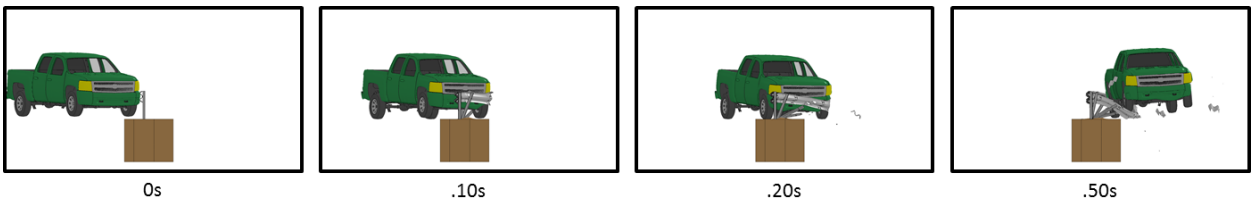

Figure 6.2: Modified G2 - Vehicle Raised 3 inches (Bumper Height 32.1” from Ground)

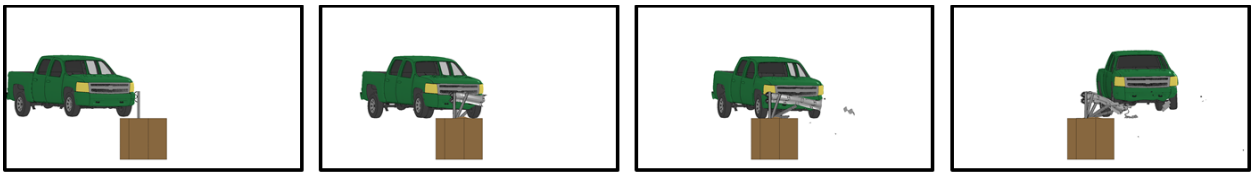

Figure 6.3: Modified G2 - Vehicle Raised 2 inches (Bumper Height 31.1" from Ground)

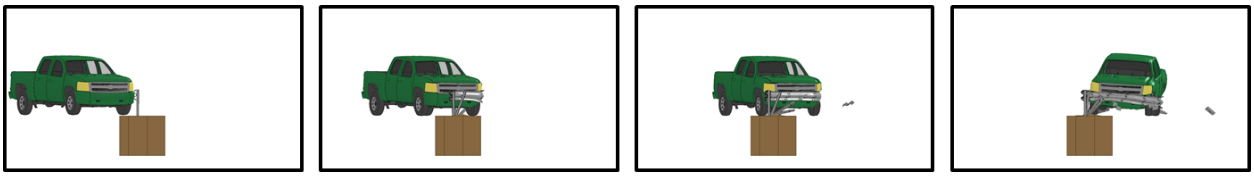

Figure 6.4: Modified G2 - Vehicle Raised 1 inches (Bumper Height 30.1" from Ground)

The truck overrode the barrier at an effective bumper height of 31.1 inches (see Figure 6.4). At a bumper height of 30.1 inches (see Figure 6.4), the vehicle was contained and redirected in a stable manner. Therefore, the designated override limit for the modified G2 weak post W-beam guardrail was determined to be a bumper height of 30.1 inches, which corresponds to an effective vehicle height that is 1 inch above the nominal ground elevation. Table 6.1 provides a summary of the override performance limit analysis for the modified G2 weak post W-beam guardrail.

Table 6.1: Modified G2 Weak Post W-Beam Guardrail Override Performance Limit Summary

Override Limit Analysis Results for Modified G2 Weak Post W-beam Guardrail					
Vehicle Type	**Height to Top of Rail**	**Raised Truck Height Off the Ground**	**Top of Bumper Height from Ground**	**Containment Result**	**Override/ Rollover Limit**
5000-lb Pickup Truck	33 in.	4 in.	33.1 in.	Override	Truck height 1 inch above nominal ground surface; Top of bumper height 30.1 inches above ground
		3 in.	32.1 in.	Override	
		2 in.	31.1 in.	Override	
		1 in.	30.1 in.	Contained	

6.2.2. Underride Analysis

Utilizing the validated modified G2 weak post W-beam guardrail finite element model, the underride performance limit was investigated. Simulations with the car being lowered 3 in and 2 in were performed. These correspond to a bumper height of 18 in and 19 in, respectively. Figure 6.5 shows the simulation with the small car lowered 3 in, and Figure 6.6 shows the simulation with the small car lowered 2 in.

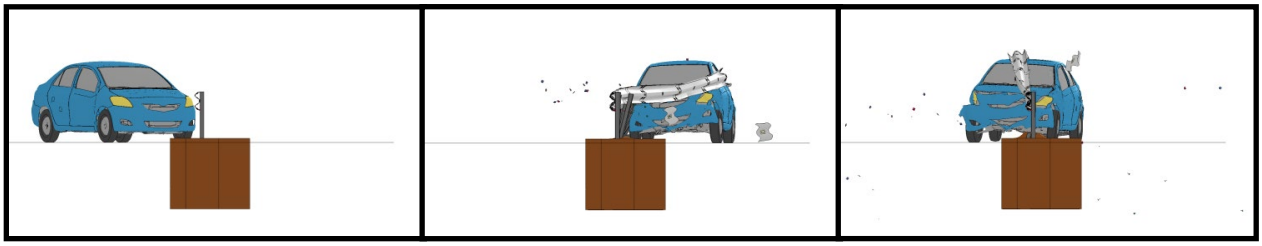

Figure 6.5: Modified G2 - Vehicle Lowered 3 inches (Bumper Height 18" from Ground)

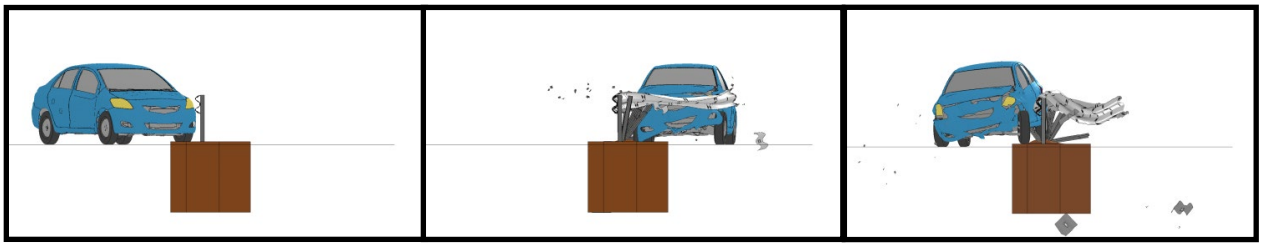

Figure 6.6: Modified G2 - Vehicle Lowered 2 inches (Bumper Height 19" from Ground)

The car was contained during the impact with a bumper height of 19 in. (see Figure 6.6). At a bumper height of 18 inches (see Figure 6.5), the rail rose above the passenger side window and over the roof of the car, and was considered unacceptable due to underride. Table 6.2 shows a summary of the underride limits.

Table 6.2: Modified G2 Weak Post W-Beam Guardrail Underride Performance Summary

Underride Limit Analysis Results for Modified G2 Weak Post W-beam Guardrail					
Vehicle Type	**Height to Top of Rail**	**Lowered Car Height Below the Ground**	**Top of Bumper Height from Ground**	**Containment Result**	**Underride Limit (in)**
2425-lb Small Car	32 in.	2 in.	19 in.	Contained	Car height 2 in below normal; Top of bumper 19 in. above ground
		3 in.	18 in.	Rail rose above window (fail)	

6.3. MIDWEST GUARDRAIL SYSTEM (MGS)

6.3.1. Override Analysis

Utilizing the validated MGS finite element model, the override performance limit was determined. Simulations were performed at three heights to determine the override limit. Figure 6.7 through Figure 6.9 show sequential images of three simulations with the vehicle at 3, 4, and 5 inches above nominal ground height, respectively. Note that these heights correspond to effective bumper heights of 32.1, 33.1, and 34.1 inches, respectively.

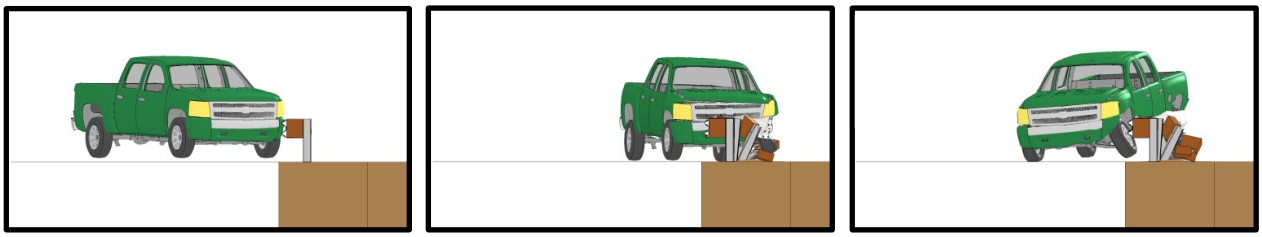

0.001 s 0.220 s 0.495 s

Figure 6.7: MGS Guardrail - Vehicle Raised 3 inches (Bumper Height 32.1" From Ground)

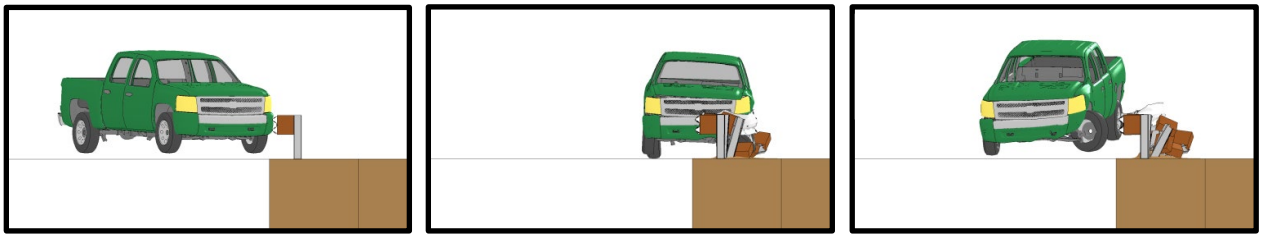

0.005 s 0.320 s 0.700 s

Figure 6.8: MGS Guardrail - Vehicle Raised 4 inches (Bumper Height 33.1" From Ground)

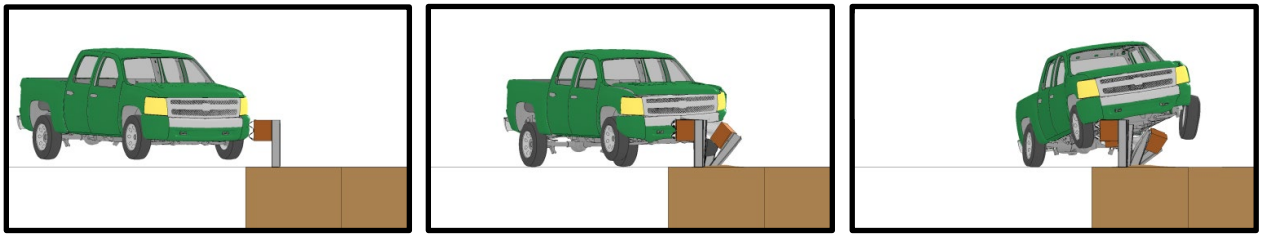

0.005 s 0.100 s 0.260 s

Figure 6.9: MGS Guardrail - Vehicle Raised 5 inches (Bumper Height 34.1" From Ground)

The truck was contained at effective bumper heights of 32.1 and 33.1 inches. However, at a bumper height of 34.1 inches, the vehicle overrode the barrier. Therefore, the designated override limit for the MGS W-beam guardrail was determined to be a bumper height of 33.1 inches, which corresponds to an effective vehicle height that is 4 inches above the nominal ground elevation. Table 6.3 provides a summary of the performance limit analysis for the MGS W-beam Guardrail.

Table 6.3: MGS Guardrail Override Performance Limit Summary

Override Limit Analysis Results for Midwest Guardrail System W-beam					
Vehicle Type	**Height to Top of Rail**	**Raised Truck Height Off the Ground**	**Top of Bumper Height from Ground**	**Result**	**Override/Roll Over Limit (in)**
5,000-lb Pickup Truck	31 in.	3 in.	32.1 in.	Contained	Truck height 4 inches above nominal ground surface; Top of bumper height 33.1 inches above ground
		4 in.	33.1 in.	Contained	
		5 in.	34.1 in.	Overrode barrier	

6.3.2. Underride Analysis

Utilizing the validated MGS W-beam guardrail finite element model, the underride performance limit was investigated. With the validation of the MGS complete, the underride analysis of the Midwest Guardrail System could be performed. The limiting factor on the underride limit of the MGS was based on the geometry of the Toyota Yaris finite element vehicle model. When the Yaris is lowered 6 inches, the bottom of the Yaris contacts the ground and cannot be lowered any further. For this reason, the underride analysis began by lowering the vehicle 6 inches. Figure 6.10 shows sequential images of the simulation. At this height, the vehicle was successfully contained and redirected. It was concluded that the underride limit of the MGS is be at a bumper height of 15 inches with the car lowered 6 inches. The results of the performance simulation are summarized in Table 6.4.

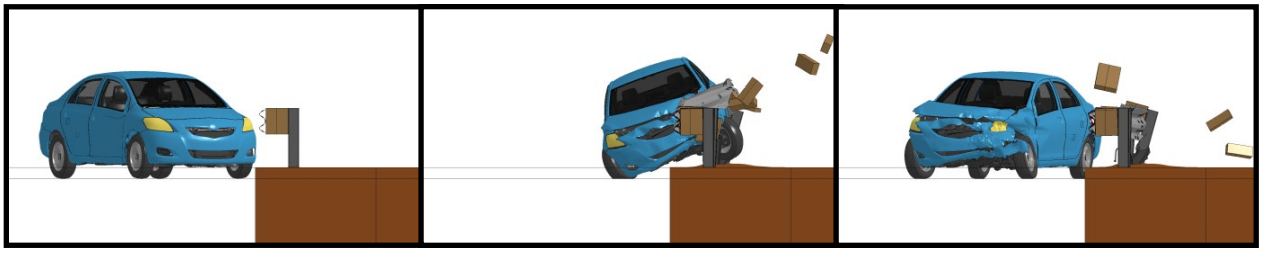

Figure 6.10: MGS Guardrail - Vehicle Lowered 6 inches (Bumper Height 15" From Ground)

Table 6.4: MGS Guardrail Underride Performance Limit Summary

Underride Limit Analysis Results for Midwest Guardrail System					
Vehicle Type	**Height to Top of Rail**	**Lowered Car Height Below the Ground**	**Top of Bumper Height from Ground**	**Containment Result**	**Underride Limit (in)**
2425-lb Small Car	31 in.	6 in.	15 in.	Contained	Car Height Lowered 6 in.

6.4. MODIFIED STRONG STEEL-POST W-BEAM (G4 (1S))

The Modified Strong Steel-Post W-Beam guardrail was initially excluded from the barrier matrix considered under the project. After further deliberation by the panel, the researchers were directed to add the Modified Strong Steel-Post W-Beam guardrail back into the matrix. The similarities between the Modified Strong Steel-Post W-Beam guardrail and the MGS Guardrail were used to establish the performance limits for the system. This was accomplished by offsetting the performance limits of the MGS guardrail to account for the difference in barrier height.

6.4.1. Override Analysis

The barrier height of the MGS guardrail is 31 inches and the barrier height of the Modified Strong Steel-Post W-Beam guardrail is 27 inches. The override limit for the MGS guardrail corresponds to a bumper height of 33.1 inches, which is 2 inches above the top of the W-beam. The nominal bumper height for the MASH pickup truck is 29.1 inches above ground, which is 2 inches above the top of the W-beam in the Modified Strong Steel-Post W-Beam guardrail. Therefore, the pickup truck is at its override performance limit for this system with no additional increase permitted. The override limit is summarized in Table 6.5.

Table 6.5. Modified Strong Steel-Post W-Beam Override Limit Summary

Override Limit for the Modified Strong Steel-Post W-Beam					
Vehicle Type	**Height to Top of Rail**	**Raised Truck Height Above the Ground**	**Top of Bumper Height from Ground**	**Result**	**Override/Roll Over Limit (in)**
5,000-lb Pickup Truck	27 in.	0 in.	29.1 in.	Contained	Truck height at equilibrium position (0 inch increase above nominal ground surface; Top of bumper height 29.1 inches above ground

6.4.2. Underride Analysis

The barrier height of the MGS guardrail is 31 inches and the barrier height of the Modified Strong Steel-Post W-Beam guardrail is 27 inches. The underride for the car with the MGS guardrail is 6 inches below the equilibrium position corresponding the undercarriage of the vehicle. Since this represents a physical limitation of the vehicle, the Modified Strong Steel-Post W-Beam guardrail has the same underride limit despite the W-beam rail having a lower mounting height. The underride limit for the Modified Strong Steel-Post W-Beam guardrail is summarized in Table 6.6 below.

Table 6.6. Modified Strong Steel-Post W-Beam Guardrail Underride Limit Summary

Underride Limit for the Modified Strong Steel-Post W-Beam					
Vehicle Type	**Height to Top of Rail**	**Lowered Car Height Below the Ground**	**Top of Bumper Height from Ground**	**Containment Result**	**Underride Limit (in)**
2425-lb Small Car	27 in.	6 in.	15 in.	Contained	Car Height Lowered 6 in.

6.5. MODIFIED THRIE BEAM GUARDRAIL

6.5.1. Override Analysis

Utilizing the validated modified thrie beam guardrail finite element model, the override performance limit was determined. Simulations were performed at height increases of 2 and 3 inches. Figure 6.11 and Figure 6.12 show sequential images of the performance limit simulations with the vehicle raised 2 and 3 inches, respectively. Note that these heights correspond to effective bumper heights of 31.1 and 32.1 inches, respectively.

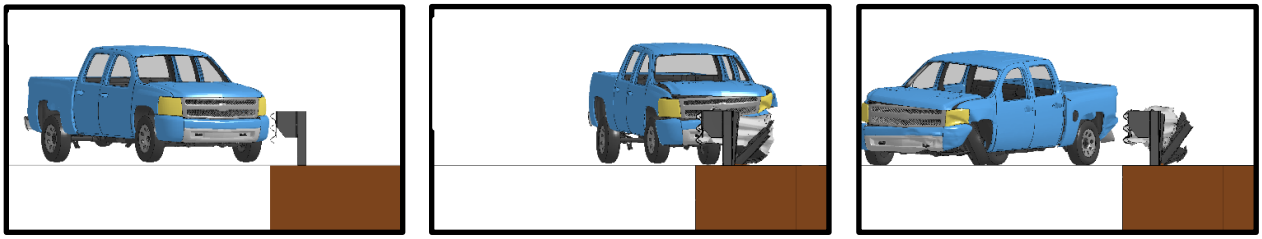

0.000 s 0.245 s 0.845 s

Figure 6.11: Modified Thrie Beam Guardrail - Vehicle Raised 2 inches (Bumper Height 31.1" From Ground)

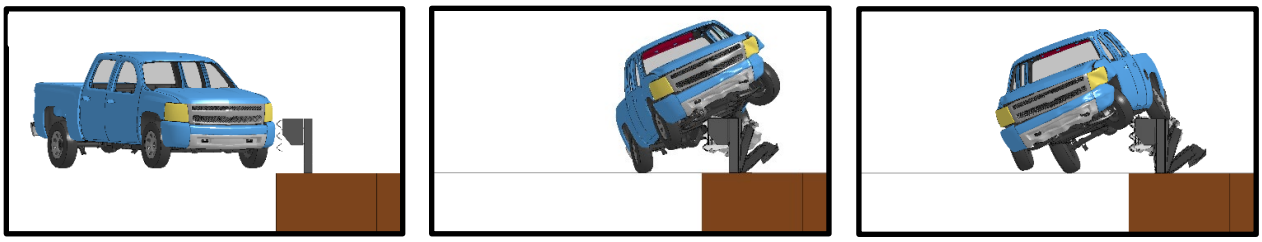

0.000 s 0.395 s 1.095 s

Figure 6.12: Modified Thrie Beam Guardrail - Vehicle Raised 3 inches (Bumper Height 32.1" From Ground)

When raised was raised 3 inches, giving an effective bumper height of 32.1 inches, the truck overrode the barrier. When the truck was raised 2 inches, giving an effective bumper height of 31.1 inches, the barrier successfully contained and redirected the vehicle. From these results, the override limit for the Modified Thrie Beam Guardrail was determined to be a bumper height of 31.1 inches, which corresponds to an effective vehicle height that is 2 inches above the nominal ground elevation. Table 6.7 provides a summary of the override performance limit analysis for the Modified Thrie Beam Guardrail.

Table 6.7: Modified Thrie Beam Guardrail Override Performance Limit Summary

Override Limit Analysis Results for Modified Thrie Beam Guardrail					
Vehicle Type	**Height to Top of Rail**	**Raised Truck Height Off the Ground**	**Top of Bumper Height from Ground**	**Result**	**Override/Roll Over Limit (in)**
5,000-lb Pickup Truck	34 in.	3 in.	32.1 in.	Overrode barrier	Truck height 2 inches above nominal ground surface; Top of bumper height 31.1 inches above ground
		2 in.	31.1 in.	Contained	

6.5.2. Underride Analysis

Utilizing the validated modified thrie beam guardrail finite element model, the underride performance limit was determined. Simulations were performed with the car lowered in 1 inch increments up to 3 inches. Figure 6.13 through Figure 6.15 show sequential images of the vehicle lowered 1, 2, and 3 inches, respectively.

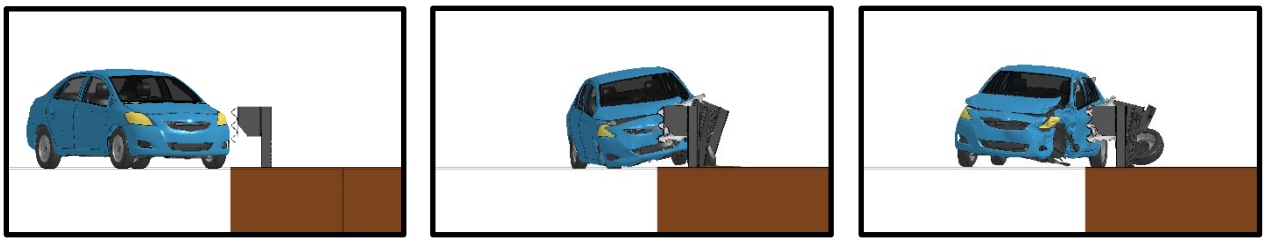

Figure 6.13: Modified Thrie Beam Guardrail - Vehicle Lowered 1 inch (Bumper Height 20 inches from Ground)

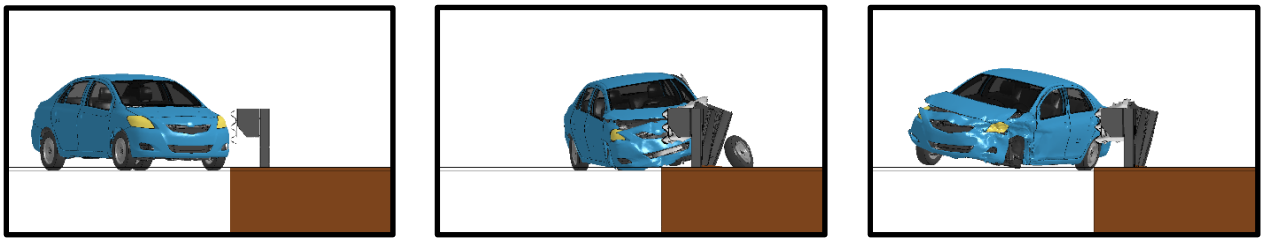

Figure 6.14: Modified Thrie Beam Guardrail - Vehicle Lowered 2 inches (Bumper Height 19 inches from Ground)

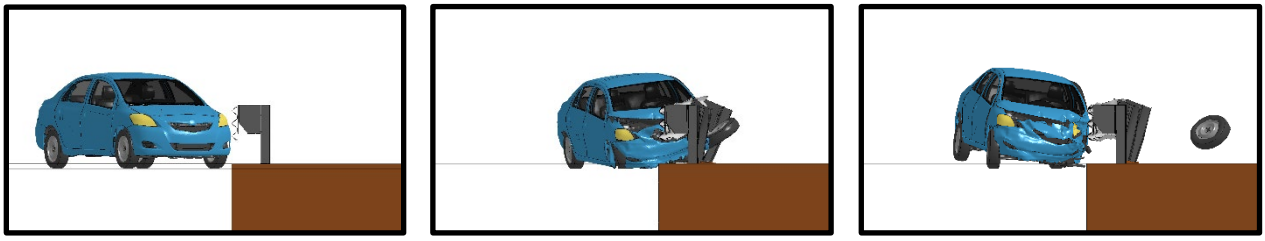

Figure 6.15: Modified Thrie Beam Guardrail - Vehicle Lowered 3 inches (Bumper Height 18 inches from Ground)

As shown in Figure 6.14, when the vehicle was lowered 2 inches, the barrier redirects the vehicle. At a height decrease of 3 inches (see Figure 6.15), the vehicle wedges under the rail and snags on a post. This interaction causes the X-direction ridedown acceleration to exceed the allowable MASH limit of 20.49 g. Based on this behavior, the underride limit was determined to be 2 inches below the equilibrium position of the small car. Table 6.8 provides a summary of the underride performance limit analysis for the Modified Thrie Beam Guardrail.

Table 6.8: Modified Thrie Beam Guardrail Underride Performance Limit Summary

Underride Limit Analysis Results for Modified Thrie Beam Guardrail					
Vehicle Type	**Height to Top of Rail**	**Lowered Car Height Below the Ground**	**Top of Bumper Height from Ground**	**Containment Result**	**Underride Limit (in)**
2425-lb Small Car	34 in.	1 in.	20 in.	Contained	Car Height Lowered 2 in.
		2 in.	19 in.	Contained	
		3 in.	18 in.	Failed	

6.6. WEAK POST W-BEAM MEDIAN BARRIER (MB2)

For the Weak Post W-beam median barrier (MB2), the performance limits were taken as the same limits as the Modified G2 Weak Post W-Beam guardrail based on the analysis and discussion presented in Chapter 5. The back side W-beam releases quickly from the posts and provides little to no additional stiffness to the Weak Post W-beam median barrier (MB2). Thus, the behavior and performance limits are similar to the Modified G2 Weak Post W-beam guardrail.

6.6.1. Override Analysis

The override limit for the Weak Post W-beam median barrier (MB2) is taken from the override limit of the Modified G2 Weak Post W-Beam guardrail. Table 6.9 provides a summary of the override performance limit analysis for the Weak Post W-beam median barrier (MB2).

Table 6.9: Weak Post W-Beam (MB2) Override Performance Limit Summary

Override Limit Analysis Results for Modified G2 Weak Post W-beam Guardrail					
Vehicle Type	**Height to Top of Rail**	**Raised Truck Height Off the Ground**	**Top of Bumper Height from Ground**	**Containment Result**	**Override/ Rollover Limit**
5000-lb Pickup Truck	33 in.	1 in.	30.1 in.	Contained	Truck height 1 inch above nominal ground surface; Top of bumper height 30.1 inches above ground

6.6.2. Underride Analysis

The underride limit for the Weak Post W-beam median barrier (MB2) is taken from the underride limit of the Modified G2 Weak Post W-Beam guardrail. Table 6.10 provides a summary of the override performance limit analysis for the Weak Post W-beam median barrier (MB2).

Table 6.10: Weak Post W-Beam (MB2) Underride Performance Limit Summary

Underride Limit Analysis Results for Modified G2 Weak Post W-beam Guardrail					
Vehicle Type	**Height to Top of Rail**	**Lowered Car Height Below the Ground**	**Top of Bumper Height from Ground**	**Containment Result**	**Underride Limit**
2425-lb Small Car	32 in.	2 in.	19 in.	Contained	Car Height Lowered 2 in.; Top of Bumper Height 19 in. above Ground

6.7. MIDWEST GUARDRAIL MEDIAN BARRIER

6.7.1. Override Analysis

Utilizing the validated MGS median barrier finite element model, the override performance limit was determined. The impact height of the pickup truck with respect to the barrier was incrementally varied. Figure 6.16 through Figure 6.19 show sequential images of four impact simulations performed at height ranging from 2 inches to 5 inches above the ground surface, respectively.

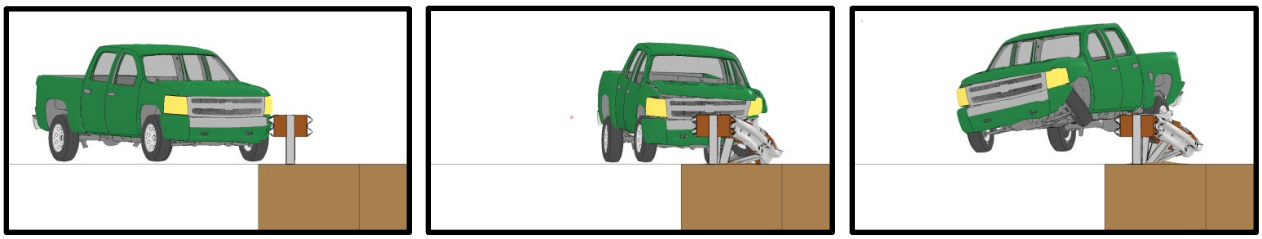

0.020s 0.245s 0.520s

Figure 6.16: MGS Median Barrier - Vehicle Raised 2 inches (Bumper Height 31.1" From Ground)

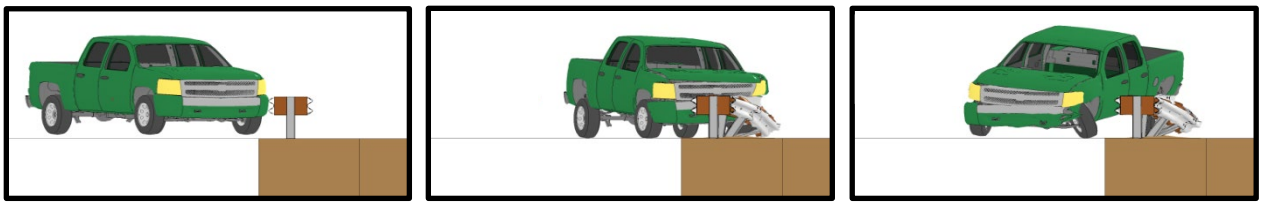

0.010s 0.185s 0.510s

Figure 6.17: MGS Median Barrier -Vehicle Raised 3 inches (Bumper Height 32.1" From Ground)

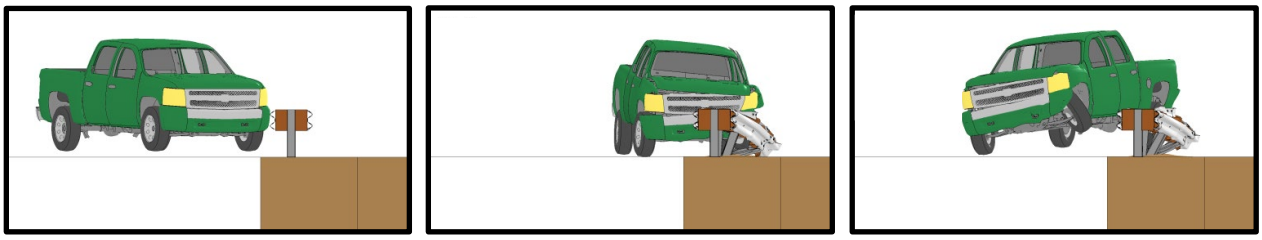

0.010s 0.270s 0.520s

Figure 6.18: MGS Median Barrier -Vehicle Raised 4 inches (Bumper Height 33.1" From Ground)

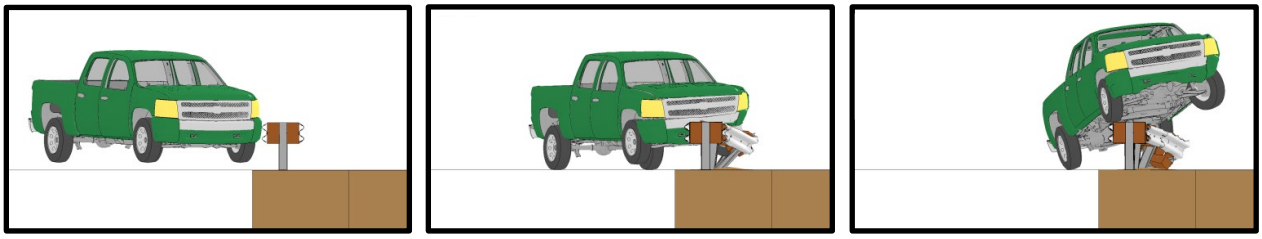

0.010s 0.130s 0.360s

Figure 6.19: MGS Median Barrier -Vehicle Raised 5 inches (Bumper Height 34.1" From Ground)

The MGS median barrier failed to contain the truck after it was raised 5 inches above nominal ground position (top of bumper at 34.1 inches). Therefore, the override performance limit for the MGS W-beam Median barrier was defined as is 33.1 inches measured from the top of the bumper to the ground, which is 4 inches above the nominal interaction height with the 31-inch tall barrier system. Note that this is consistent with the override performance limit established for the MGS guardrail system. Table 6.11 presents a summary of the override performance limit analysis for the MGS W-beam Median barrier.

Table 6.11: Performance Limit Summary Table for MGS Median

Override Limit Analysis Results for Midwest Guardrail System Median					
Vehicle Type	**Height to Top of Rail**	**Height of Truck Above Nominal Ground Surface**	**Top of Bumper Height from Ground**	**Result**	**Override/Roll Over Limit**
5,000-lb Pickup Truck	31 inches	2 in.	31.1 in.	contained	Truck height 4 inch above nominal ground surface; Top of bumper height 33.1 inches above ground
		3 in.	32.1 in.	contained	
		4 in.	33.1 in.	contained	
		5 in.	34.1 in.	overrode barrier	

6.7.2. Underride Analysis

Utilizing the validated MGS median barrier finite element model, the underride performance limit was determined. The limiting factor on the underride limit of the MGS Median Barrier was ground clearance of the Toyota Yaris finite element vehicle model. When the Yaris is lowered 6 inches, the bottom of the Yaris hits the ground and cannot be lowered any further. Figure 6.20 shows sequential images of the performance simulation with the vehicle lowered 6 inches. At this height, the vehicle was successfully contained and redirected. It was concluded that the underride limit of the MGS Median Barrier is at a bumper height of 15 inches with the car lowered 6 inches from its equilibrium position. The results of the underride performance simulation are summarized in Table 6.12.

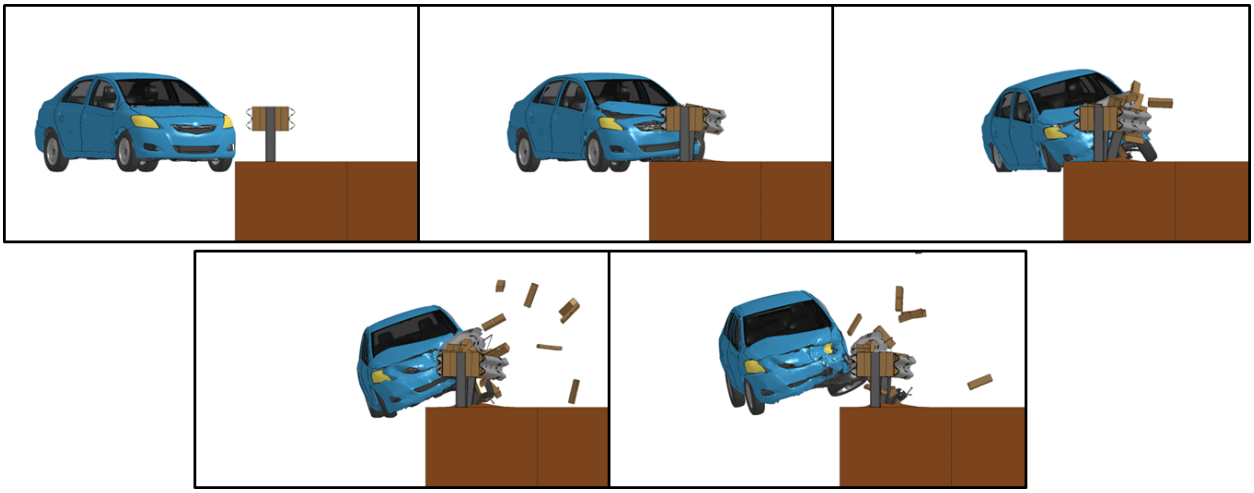

Figure 6.20: MGS Median Barrier - Vehicle Lowered 6 inches (Bumper Height 15" From Ground)

Table 6.12: MGS Median Barrier Underride Performance Limit Summary

Underride Limit Analysis Results for Midwest Guardrail System					
Vehicle Type	**Height to Top of Rail**	**Lowered Car Height Below the Ground**	**Top of Bumper Height from Ground**	**Containment Result**	**Underride Limit (in)**
2425-lb Small Car	31 in.	6 in.	15 in.	Contained	Car Height Lowered 6 in.

6.8. CONCRETE: SINGLE SLOPE (42-INCH)

6.8.1. Override Analysis

Utilizing the validated single slope concrete barrier finite element model, the override performance limit was determined. The truck was raised 22 inches off the ground and then 25 inches off the ground to determine the override limits. Raising the truck 22 inches off the ground corresponded to a top of bumper height of 51.1 inches from ground. Raising the truck 25 inches off the ground corresponded to a top of bumper height of 54.1 inches from ground. Selected sequential images from these two LS-DYNA simulations are shown in Figure 6.21 and Figure 6.22, respectively.

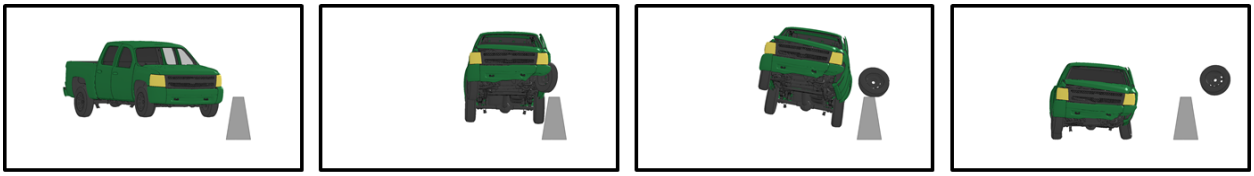

Figure 6.21: Single Slope Concrete Barrier - Vehicle Raised 22 inches (Bumper Height 51.1" From Ground)

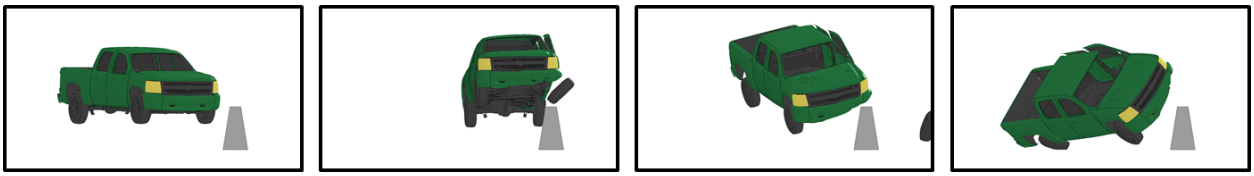

Figure 6.22: Single Slope Concrete Barrier - Vehicle Raised 25 inches (Bumper Height 54.1" From Ground)

The truck was contained and redirected when raised 22 inches off the ground and did not roll. This was considered an acceptable result. At the 25 inch interaction height, the truck was contained, but rolled over on the traffic side of the barrier. This analysis established the override limit of the truck to be 22 inches off the ground.

The performance limit of the truck being raised 22 inches off the ground is quite high and the project team wanted to perform a sanity check of this result. In the performance limit simulations, the ground was kept at the bottom of the barrier. This models an airborne truck impacting a barrier, with gravity acting on the truck as it interacts with the barrier.

An LS-DYNA run was performed where both the truck and the ground level were raised the same 22 inches. This simulation models the truck impacting the top 20 inches of the 42 inch single slope barrier. The expected result was that the truck would either override or be unstable. Figure 6.23 displays the sequential images from the simulation of the truck and ground raised 22 inches.

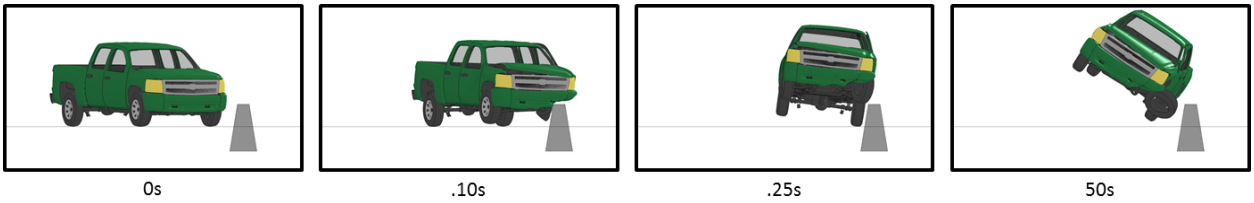

Figure 6.23: Single Slope Concrete Barrier - Truck and Ground Raised 22 inches

As expected, the truck became unstable and rolled. In Figure 6.21, the rear of the truck drops down during the barrier interaction (see times 0.25 s and 0.75 s), and this helps stabilize the truck by better aligning the backslap impact forces with the vehicle center of gravity. In Figure 6.23, the back end lifts off the ground and the impact forces associated with the back slap are below the center of gravity and impart a roll moment. This causes the vehicle to become unstable as it exits the barrier.

It was concluded that since the vehicle will be airborne at the height of 22 inches off the ground, gravity acts on the vehicle and causes the back end to drop during the impact event. This drop helps stabilize the truck's tendency to roll as it impacts the barrier. For this reason, it was concluded that the override limit for the Single Slope concrete barrier is 22 inches. Table 6.13 gives a summary for the Single Slope Concrete Barrier override performance analysis.

Table 6.13: Single Slope Concrete Barrier Override Performance Limit Summary

Vehicle Type	Height to top of Barrier	Height of Truck Above Nominal Ground Surface	Top of Bumper Height from Ground	Result	Override/Roll Over Limit
5,000-lb Pickup Truck	42 in.	25 in.	54.1 in.	Rolled	Truck height 22 inches above nominal ground surface; Top of bumper height 51.1 inches above ground
		22 in.	51.1 in.	Contained	

Due to the solid nature of the single slope concrete barrier, no underride analysis was performed.

7. VEHICLE TRAJECTORY ANALYSIS

Vehicle dynamic simulations were conducted to evaluate vehicle trajectory as the selected design vehicles traversed various median ditch configurations at prescribed encroachment conditions. A commercially available analysis package from Mechanical Simulation Corporation (MSC) called CarSim was used for the analysis. Details of the vehicle model development and validation, the simulation matrix, and the vehicle trajectory results are described below.

7.1. VEHICLE MODELING AND VALIDATION

7.1.1. Vehicle Model Development

The research team developed vehicle models to represent the MASH design test vehicles in CarSim. Researchers performed a thorough investigation of the "pre-set" vehicle models included with CarSim to select the base model that most closely resembles the MASH design test vehicles and then modified them to meet MASH vehicle specifications. This evaluation was based on key factors including mass, dimensions (e.g., wheelbase, track width, wheel center height, and vehicle length), center of gravity (CG) location, and various suspension and engine specifications. Researchers determined that the Class-B car model was the closest CarSim model available to the MASH 1100C test vehicle; therefore, the Class-B model was selected as the base model for further development and validation of an 1100C passenger car model.

Modifications were made to properties of the base model to specifically model a Kia Rio, which is the vehicle make and model used by most test laboratories. This work included modifying the sprung mass, unsprung mass, suspension properties, and dimensions of the base Class-B model. TTI researchers previously developed a model for the MASH 2270P pickup truck that was used in this study[5]. Table 7.1 includes the MASH specific design specifications to which these test vehicles conform.

Table 7.1: 2009 MASH Recommended Properties for 1100C and 2270 Test Vehicles [7]

Property	1100C (Small Car)	2270P (Pickup Truck)
Mass, lb (kg)	2420 ±55 (1100±25)	5000 ± 110 (2270 ± 50)
Dimensions, in. (mm)		
Wheelbase	98 ± 5 (2500 ± 125)	148 ± 12 (3760 ± 300)
Front Overhang	35 ± 4 (900 ± 100)	39 ± 3 (1000 ± 75)
Overall Length	169 ± 8 (4300 ± 200)	237 ± 13 (6020 ± 325)
Overall Width	24 ± 4 (600 ± 100)	78 ± 2 (1950 ± 50)
Track Width*	56 ± 2 (1425 ± 50)	67 ± 1.5 (1700 ±38)
Center of Mass Location, in. (mm)		
Aft of Front Axle	39 ± 4 (990 ± 100)	63 ±4 (1575 ± 100)
Above Ground (minimum)	N/A	28.0 (710)
Location of Engine	Front	Front
Location of Drive Axle	Front	Rear
Type of Transmission	Manual or Automatic	Manual or Automatic

Table 7.2 shows the CarSim vehicle models that have been modified to reflect MASH design standards. In order to model the small car in CarSim as accurately as possible, a Kia Rio was suspended from a lift to determine the exact center of gravity (CG) of the vehicle as shown in Figure 7.1 and Figure 7.2. Additionally, the mass distribution on each tire was determined, as well as other dimensional properties of the Kia Rio as shown in Figure 7.3. Critical suspension properties were also determined during this process, and various suspension elements were documented with photographs and measured as shown in Figure 7.4 to Figure 7.8.

Table 7.2: Vehicle Models from CarSim

2420-lb (1100-kg) Small Car	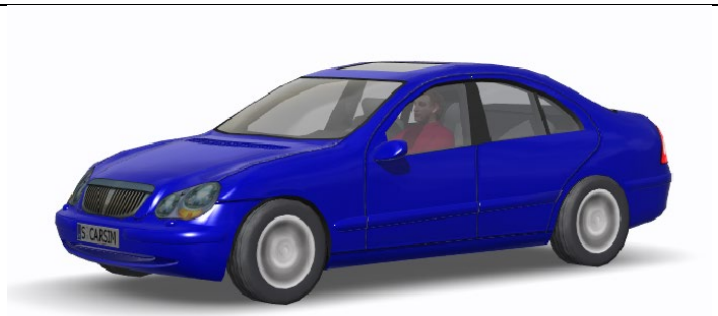
5000-lb (2270-kg) Pickup Truck	

Figure 7.1: 2008 Kia Rio Suspended to Determine Vehicle's Center of Gravity (CG)

Figure 7.2: Determination of the CG of a 2008 Kia Rio

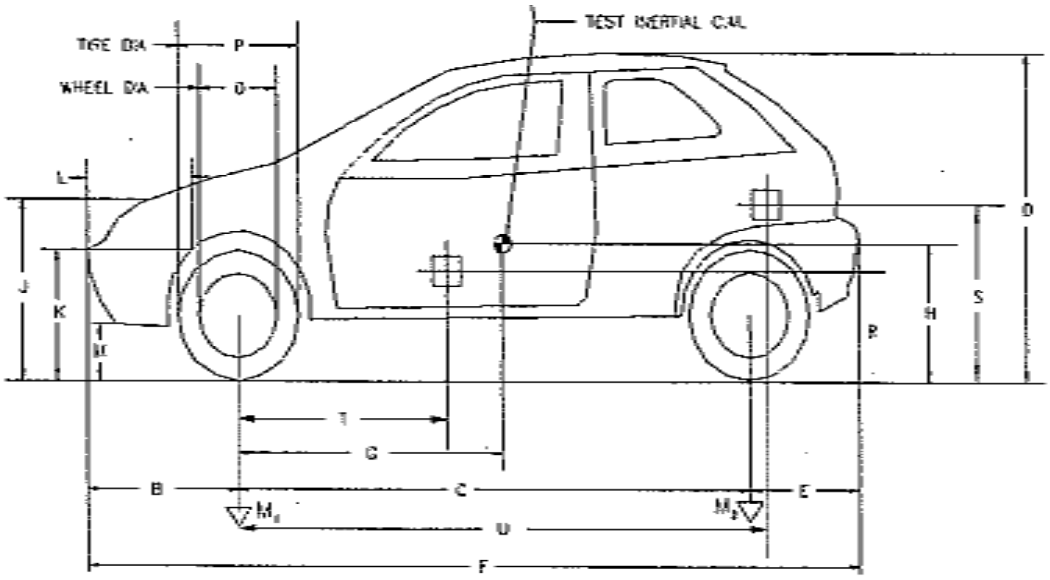

Figure 7.3: Dimensional Parameters Measured from 2008 Kia Rio

Figure 7.4: 2008 Kia Rio Front Suspension

Figure 7.5: 2008 Kia Rio Front Suspension

Figure 7.6: 2008 Kia Rio Rear Suspension

Figure 7.7: 2008 Kia Rio Rear Suspension

Figure 7.8: 2008 Kia Rio Rear Suspension

For properties which could not be directly measured, researchers estimated values for the Kia Rio model by maintaining relevant ratios from the base model, and scaling the values accordingly for the Kia Rio model. For example, the "roll-center height" of the Kia Rio was determined by maintaining the ratio of the roll-center height and rear wheel center height of the B-Class base model. Using a measured rear wheel center height of the Kia Rio, researchers were able to approximate a roll-center height for the Kia Rio (Table 7.3). This process was also used to determine appropriate sprung and unsprung masses for a Kia Rio.

Table 7.3: Approximating the Roll-Center Height with Ratios

	Rear Wheel Center Height (mm)	**Roll-Center (mm)**	**Ratio**
Class B-Base Model (Original)	310.00	165	0.532
Kia Rio	279.40	148.713	
Difference	30.60	16.29	

After the modification to the 1100C model was complete, researchers began focusing their efforts on simulations. First, the location of seven critical "hard-points" or structurally solid locations were identified on the Kia Rio (Table 7.4). In the event that one of these "hard-points" contacts the ground, the motion of the vehicle will be affected. CarSim does not have capabilities to model body to ground contact during a simulation. Consequently, in CarSim, the trajectory of a "hard-point" on the car may appear to penetrate the ground surface as seen in Figure 7.10. Therefore it is important for researchers to monitor the location of these hard points relative to the ground during simulations to identify and flag any ground contact cases. Those cases which are flagged as having "ground contact," such as the case shown in Figure 7.10, will later be reanalyzed with a CarSim subroutine code developed by TTI researchers. This subroutine accounts for ground contact when determining the dynamic motion of the vehicle.

Table 7.4: Kia Rio "Hard-Point" and CG Locations

22-22(2) Kia Rio Points			
Description	**X**	**Y**	**Z**
Driver Side Bottom of Front Bumper	838.20	508	262.5
Passenger Side Bottom of Front Bumper	838.20	-508	262.5
Driver Side Middle of Vehicle	-1480	682.5	200
Passenger Side Middle of Vehicle	-1480	-682.5	200
Driver Side Bottom of Rear Bumper	-3252.45	619	400
Passenger Side Bottom of Rear Bumper	-3252.45	-619	400
CG of Vehicle	-870.458	0	519.1125

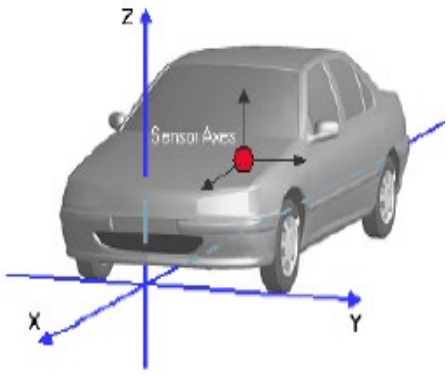

Figure 7.9: Coordinate System

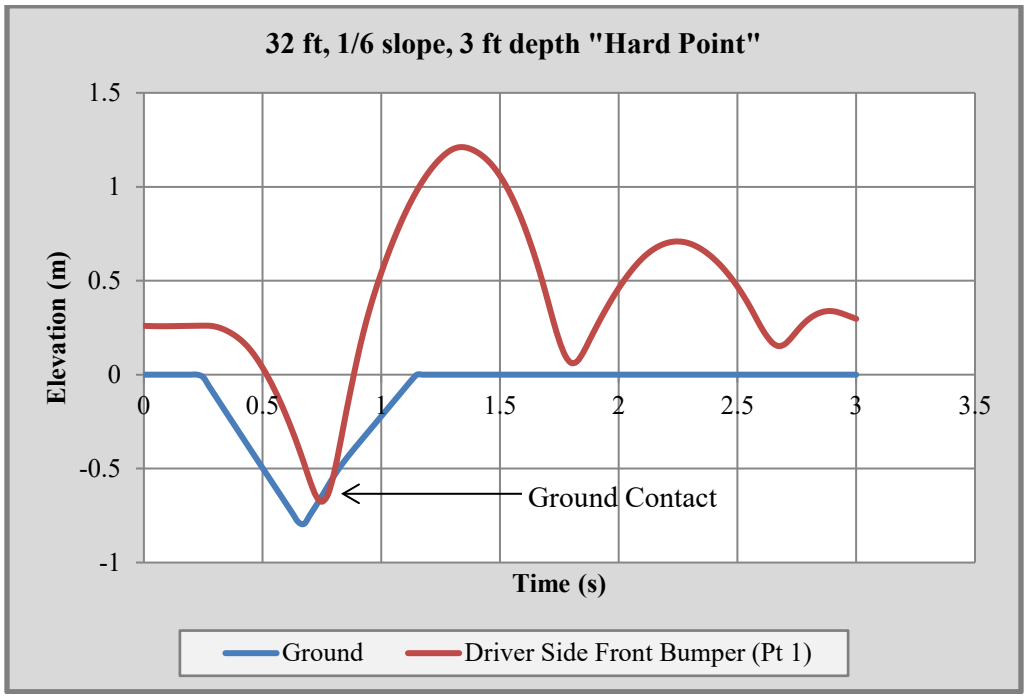

Figure 7.10: CarSim Ground "Penetration" Plot

7.1.2. Vehicle Model Validation

To perform validation of the small car and pickup vehicle models developed by TTI, the researchers obtained data for encroachment tests conducted at the Federal Outdoor Impact Laboratory (FOIL) under FHWA sponsorship. Tests were performed with different vehicles entering a 32-ft wide symmetric V ditch with 1V:6H slopes at encroachment angle of 25 degrees and varying speeds. As the vehicles traversed through the ditch, their C.G. accelerations and roll, pitch and yaw angles were measured. The FOIL testing included a Kia Rio small passenger car and Dodge Ram pickup truck, which the researchers planned to use for validation of the CarSim models.

However, the researchers identified some errors in the crash test data, which limited the scope of the validation exercise. In some of the tests, the vehicle acceleration data, which is integrated to obtain the vehicle's velocity, exhibited an erroneous gain as it traversed the ditch and came to a stop. This can be seen in Figure 7.11 for a 100 km/h encroachment. The vehicle enters the ditch at 0 seconds and exits the ditch at approximately 1 second. The test video shows the vehicle coming to a complete stop afterwards. However, the velocity-time graph in Figure 7.11 shows the vehicle decelerating to a speed of 50 km/h and then accelerating to 70 km/h and maintaining that final speed. The researchers communicated the error to the FOIL, who confirmed this observation and initiated an investigation of the reasons for the errors.

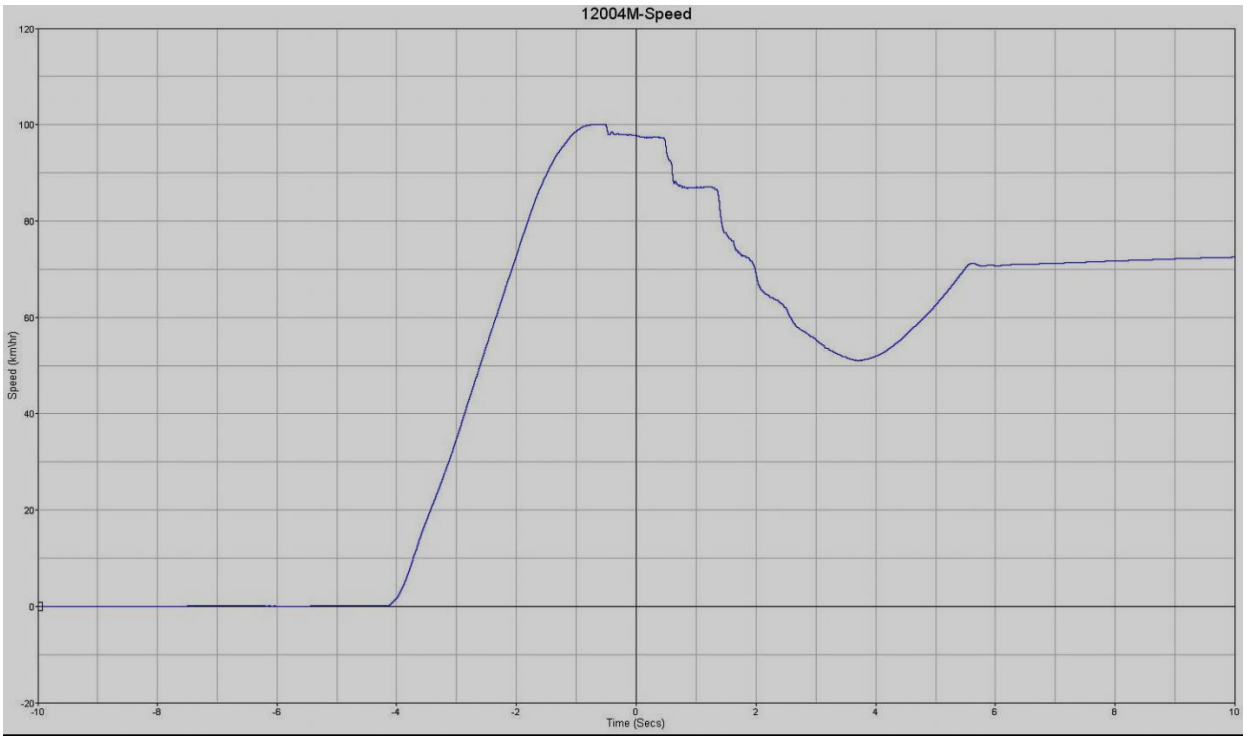

Figure 7.11 Velocity History for a FOIL ditch test with a 70 km/h end speed

7.1.2.1. Imagery Comparison

A sequential comparison of the NCAC Dodge Ram and CarSim Pickup model traversing a 1V:6H V-shaped ditch and a speed of 70 km/h and an encroachment angle was 25° is shown in Figure 7.12.

Figure 7.12 Case 1 - Sequential Comparison of Pickup Truck Encroachment (70 km/h)

An encroachment with the pickup truck at a higher initial speed of 100 km/h and encroachment angle of 25° was performed in the same ditch. Figure 7.13 provides a sequential comparison of the Dodge Ram and CarSim Pickup model traversing the 1V:6H V-shaped ditch at the prescribed encroachment conditions.

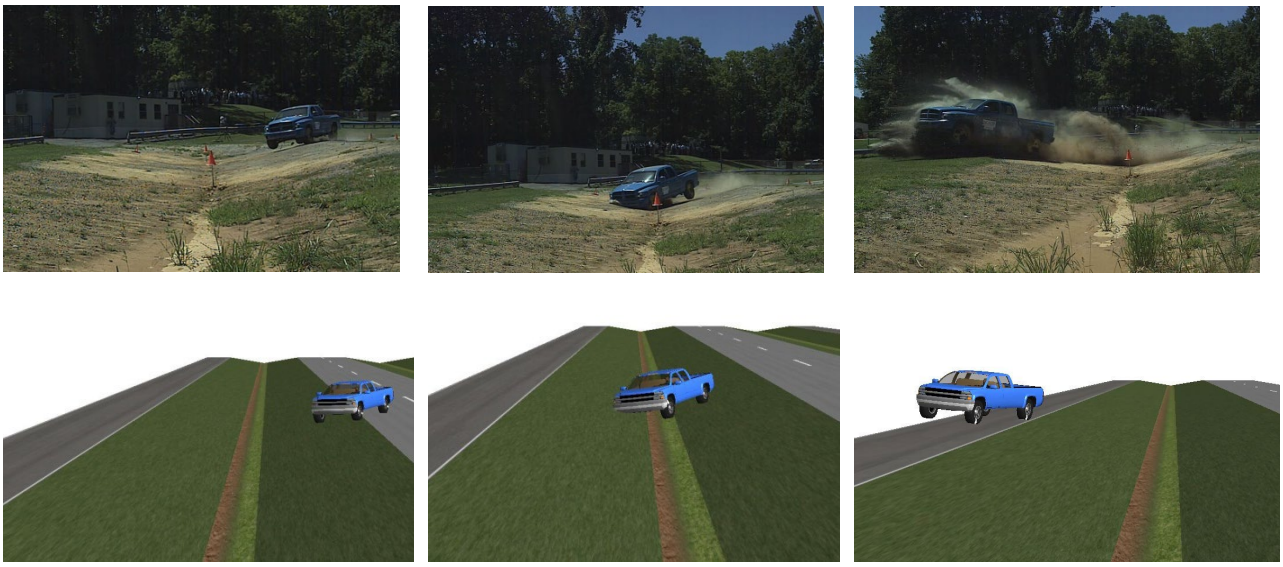

Figure 7.13 Case 2- Sequential Comparison Pickup Truck Encroachment (100 km/h)

As for the small passenger car, Figure 7.14 shows a sequential comparison of the Kia Rio and CarSim "Kia Rio" model traversing a 1V:6H V-shaped ditch at an initial speed of 70 km/h and an encroachment angle of 25°.

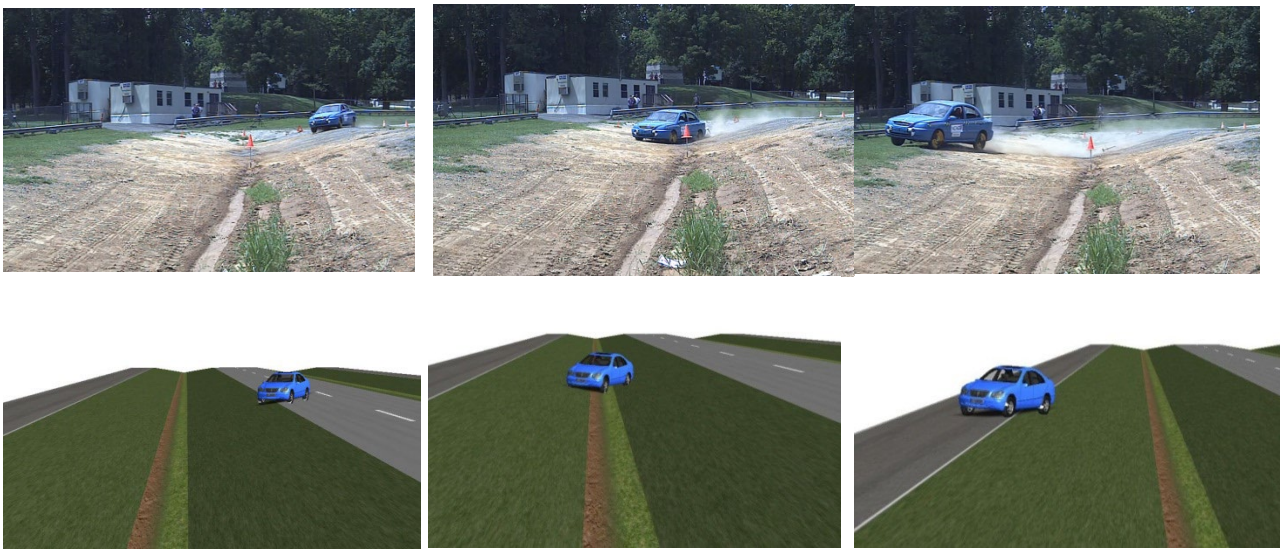

Figure 7.14 Case 3- Sequential Comparison Small Car (70 km/h)

Another test was conducted for the small car with a higher initial speed of 100 km/h. Figure 7.16 shows a sequential comparison of the NCAC Kia Rio and CarSim "Kia Rio" model traversing a 1V:6H V-shaped ditch with an initial speed of 100 km/h and an encroachment angle of 25°.

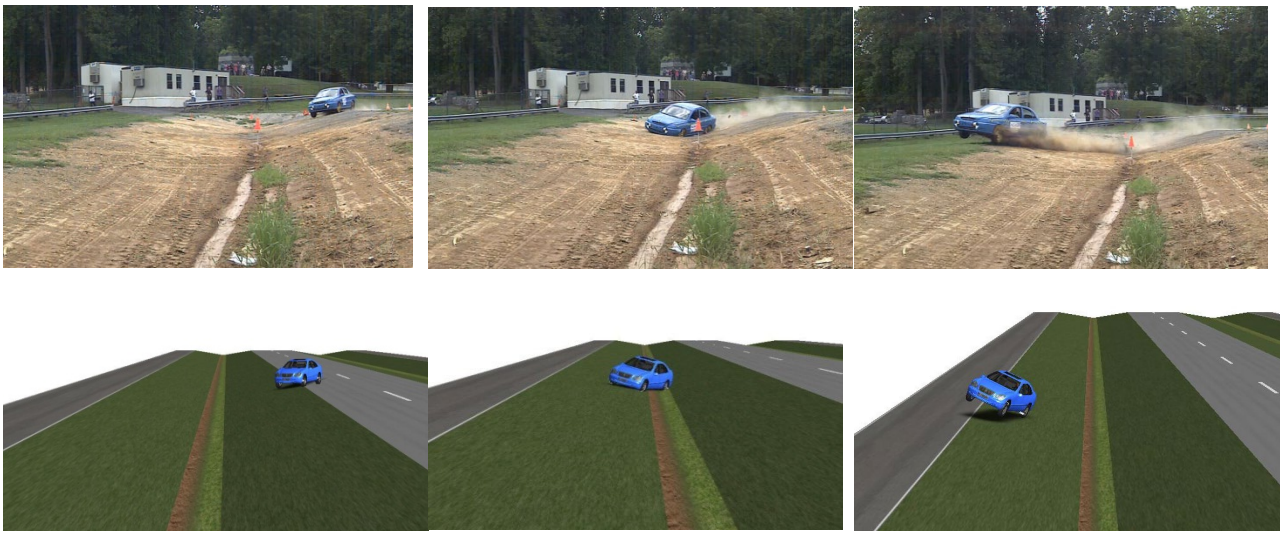

Figure 7.15 Case 4- Sequential Comparison Small Car (100 km/h)

Based on the imagery analysis of the aforementioned tests and simulation, a reasonable overall correlation is observed in vehicular orientation and position between the tests and the simulations.

7.1.2.2. Signal Comparison

The following series of graphs compare the longitudinal, lateral, and vertical acceleration as well as the roll pitch and yaw angles of the four encroachment cases previously described. The longitudinal acceleration (Figure 7.17) and lateral acceleration (Figure 7.18) of the test data and CarSim simulation appear to correlate reasonably well for the 70 km/h encroachment with the pickup truck. Note that the test data is filtered and sampled differently and contains more noise than the CarSim simulation data. The lateral acceleration does deviate at approximately 0.8 seconds.

There appears to be good correlation between the test data and simulation data of the vertical acceleration (Figure 7.19) and roll angle (Figure 7.20). The vertical acceleration simulation data appears to follow the trend of the test data. Similarly, the simulation roll angle data appears to match the measured test data.

The pitch angle simulation data and measured test data appear to correlate well too as shown in Figure 7.21. Some deviation exists after 1 second, however this is after the vehicle has exited the ditch. The yaw angle data exhibits deviation after approximately 0.5 seconds as depicted in Figure 7.22.

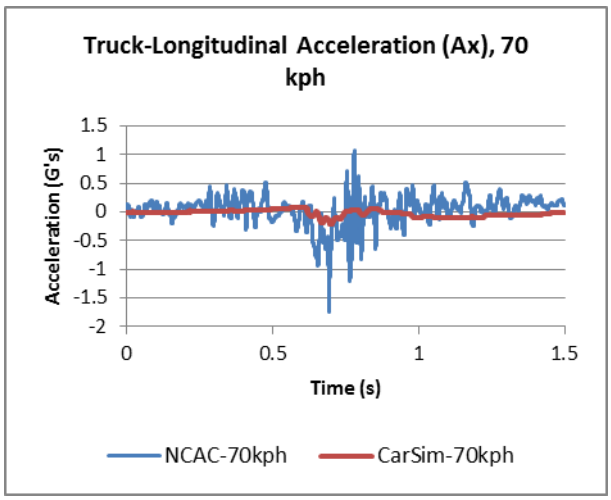

Figure 7.16: Truck Longitudinal Acceleration (Ax), 70 km/h

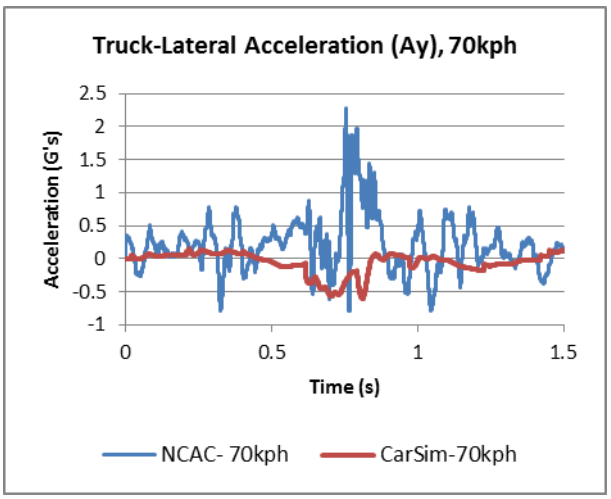

Figure 7.17: Truck Lateral Acceleration (Ay), 70 km/h

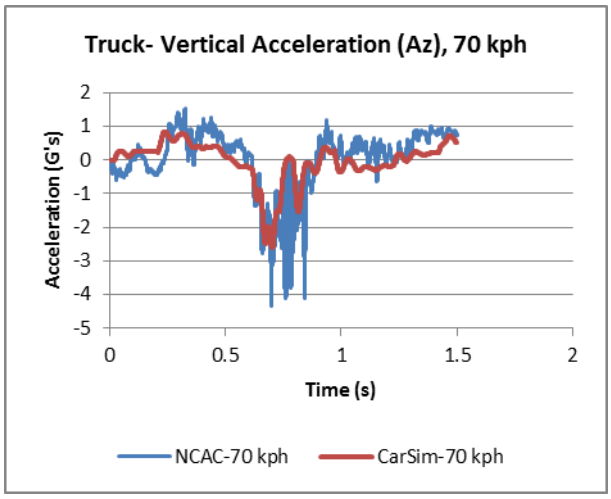

Figure 7.18: Truck Vertical Acceleration (Az), 70 km/h

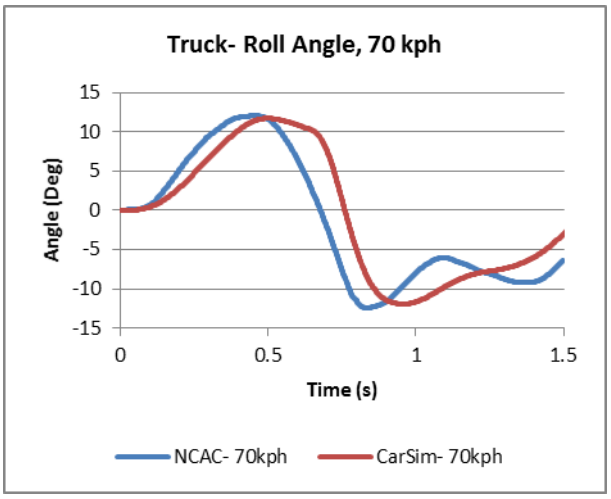

Figure 7.19: Truck Roll Angle, 70 km/h

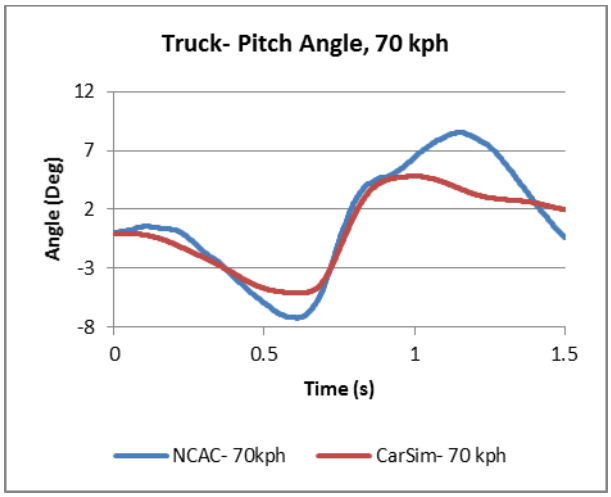

Figure 7.20: Truck Pitch Angle, 70 km/h

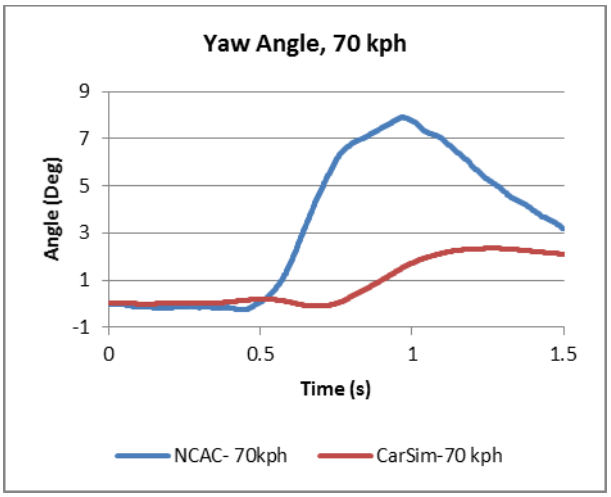

Figure 7.21: Truck Yaw Angle, 70 km/h

A similar comparison was performed for the 100 km/h encroachment of the pickup truck. The longitudinal accelerations shown in Figure 7.23 have significant deviation (approximately 12 G's) at 0.6 seconds. This was attributed to "body-to-ground" contact as the truck traversed the ditch. This behavior was confirmed using the available video footage of the truck traversing the ditch. The data from the test reflects a significant deceleration experienced by the vehicle during the contact. CarSim lacks the capability to account for body-to-ground contact. Therefore, this simulation does not reflect the actual decelerations. The lateral accelerations in Figure 7.24 appear to correlate fairly reasonably, as do the vertical accelerations (Figure 7.25) and roll angles (Figure 7.26).

Case 2- Pickup Truck (100 kph) CarSim Correlation Graphs

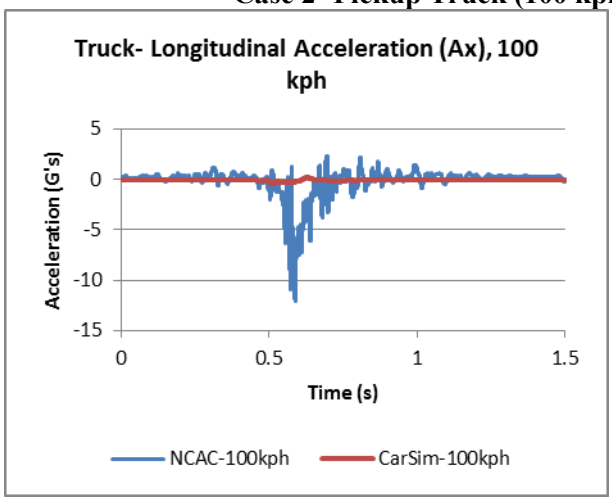

Figure 7.22: Truck Longitudinal Acceleration (Ax)d, 100 km/h

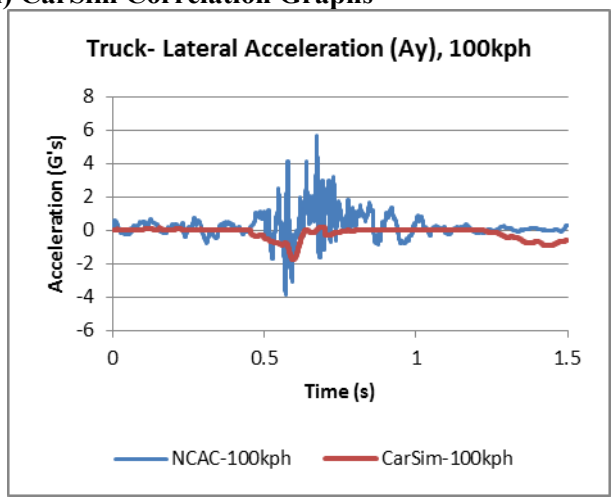

Figure 7.23: Truck Lateral Acceleration (Ay), 100 km/h

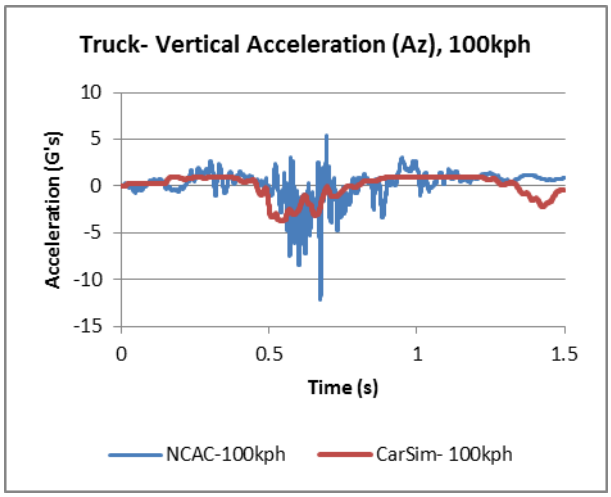

Figure 7.24: Truck Vertical Acceleration (Az), 100 km/h

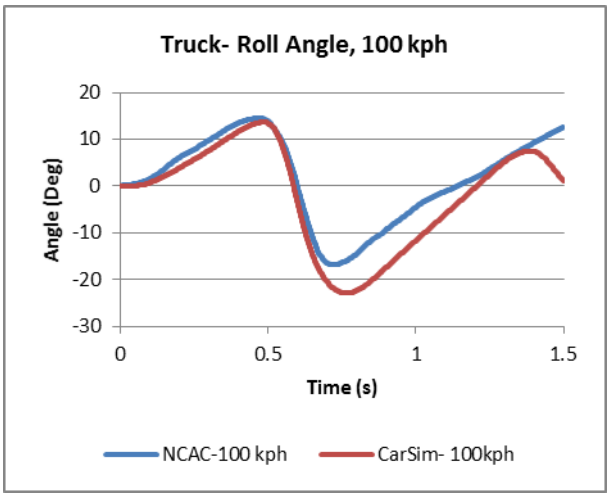

Figure 7.25: Truck Roll Angle, 100 km/h

The pitch angles shown in Figure 7.27 appear to correlate well between the simulation and the measured test data up to 0.6 seconds. Deviation begins at 0.6 seconds; however the overall trend of the data still appears to be similar. The yaw angles exhibit a large deviation starting at 0.5 seconds as shown in Figure 7.28. Again, these discrepancies occur at the same time and appear related to the body-to-ground contact that occurred during the test.

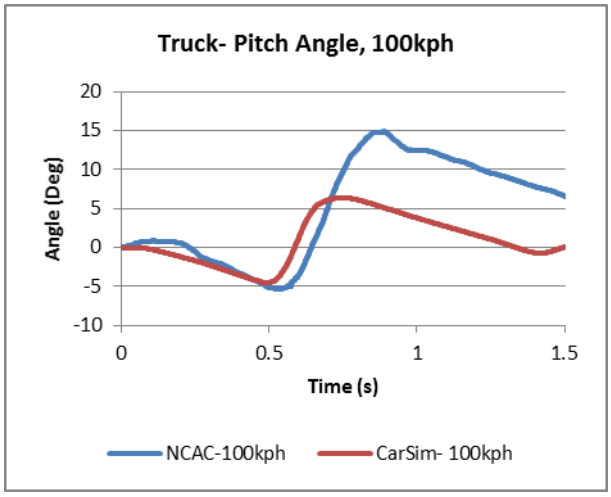

Figure 7.26: Truck Pitch Angle, 100 km/h

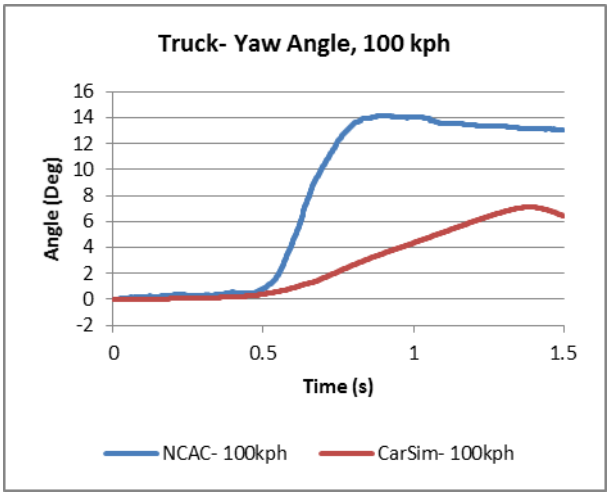

Figure 7.27: Truck Yaw Angle, 100 km/h

For the case of the small car encroachment at 70 km/h, the trends of the longitudinal accelerations shown in Figure 7.29 of the simulation data and test data appear to be comparable. There does appear to be a vertical shift between the two data sets. TTI researchers believe that the measured test data (blue) may have been flawed due to the fact that the data begins at 0.2 G's and tends to oscillate around 0.2 rather than 0 G's, and this would explain the apparent shift. The lateral accelerations shown in Figure 7.30 appear to correlate fairly well. The vertical accelerations shown in Figure 7.31, and the roll angles shown in Figure 7.32 also appear to correlate well.

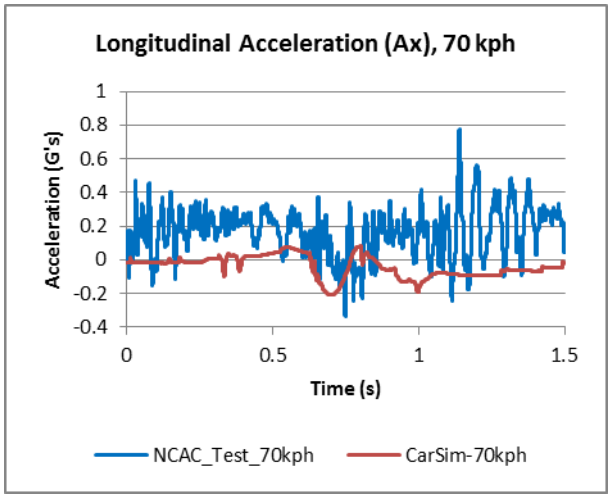

Figure 7.28: Car Longitudinal Acceleration (Ax), 70 km/h

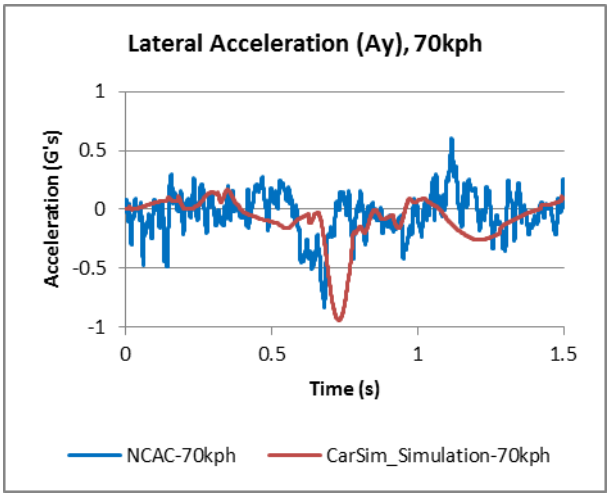

Figure 7.29: Car Lateral Acceleration (Ay), 70 km/h

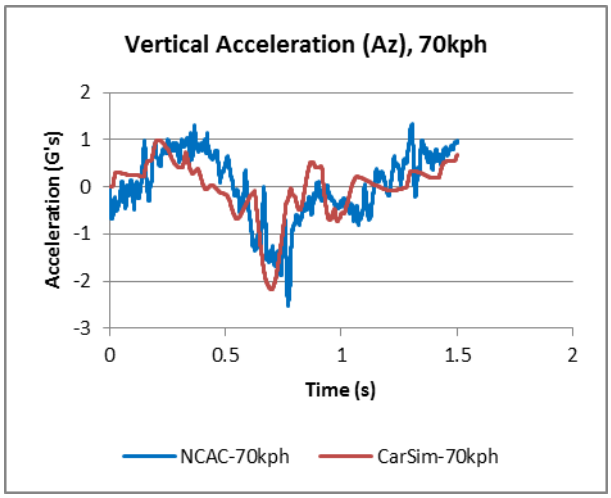

Figure 7.30: Car Vertical Acceleration (Az), 70 km/h

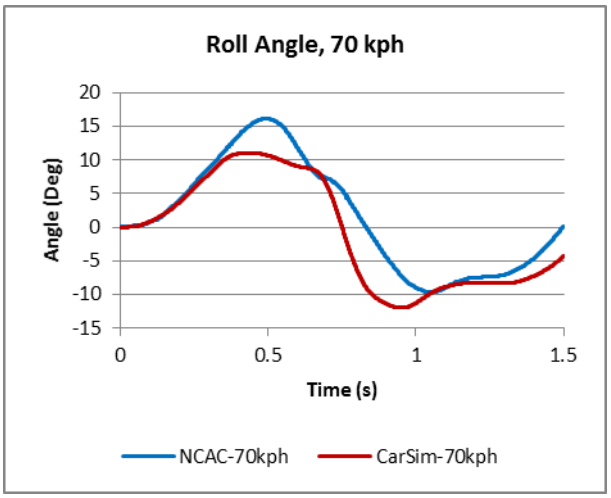

Figure 7.31: Car Roll Angle, 70 km/h

The pitch angles shown in Figure 7.33 appear to correlate reasonably well. However, the yaw angles shwon in Figure 7.34 do not seem to correlate well. TTI researchers believe an instrument malfunction occurred during the test due to the vertical line in the test data at 0.75 seconds. The vertical shift suggests the vehicle is 2.1° and also 3.9° at the same time, which is physically impossible. If the discontinuity had not occurred, TTI researchers believe the data would have better correlation.

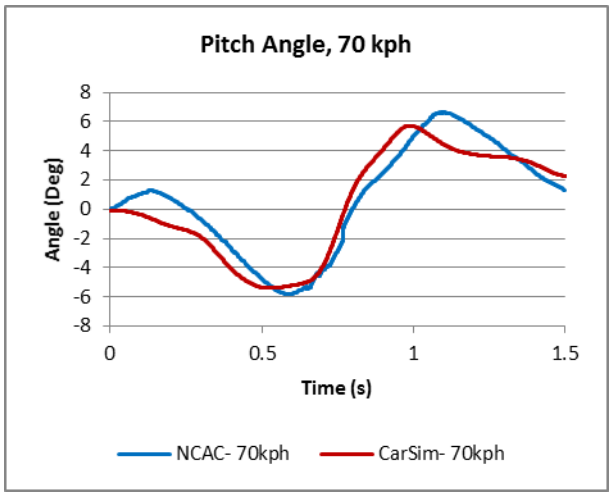

Figure 7.32: Car Pitch Angle, 70 km/h

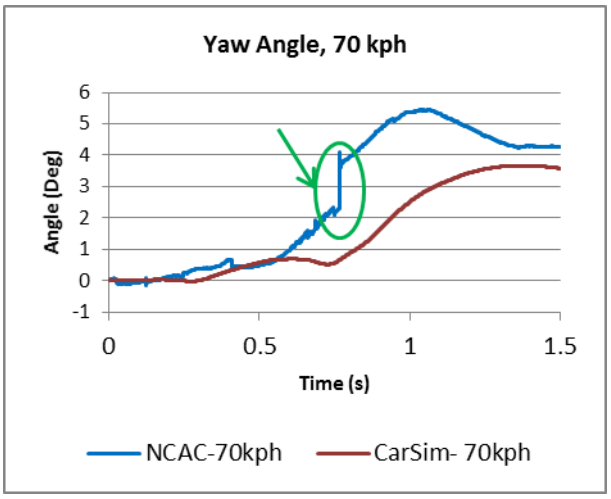

Figure 7.33: Car Yaw Angle, 70 km/h

Finally for case of the small car encroachment at 100 km/h, the longitudinal accelerations shown in Figure 7.35 deviate at 0.5 seconds by approximately 5 g. TTI researchers believe this deviation is once again due to contact between the vehicle body and the ground during the high speed test. This contact would explain the deceleration present in the test data and absent from the CarSim simulation data. As previously mentioned, CarSim does not have the capacity to account for "body to ground" contact. Subsequent simulations of this nature during the vehicle trajectory analyses will be analyzed using a subroutine that detects and approximates the forces associated with the body-to-ground contact. The lateral accelerations shown in Figure 7.36 appear to correlate relatively well, as do the vertical accelerations presented in Figure 7.37. The roll angles (Figure 7.38) display some deviation at 0.7 seconds. Overall, the trends are similar for both data sets.

As for the pitch angles shown in Figure 7.39, they appear to correlate well until 0.75 seconds. At 0.75 seconds, the data sets begin to deviate. Again, this deviation is likely due to the body-to-ground contact that occurs during the test. The yaw angles shown in Figure 7.40 appear to correlate relatively well although some deviation is present at about 1.3 seconds after the vehicle has exited the ditch.

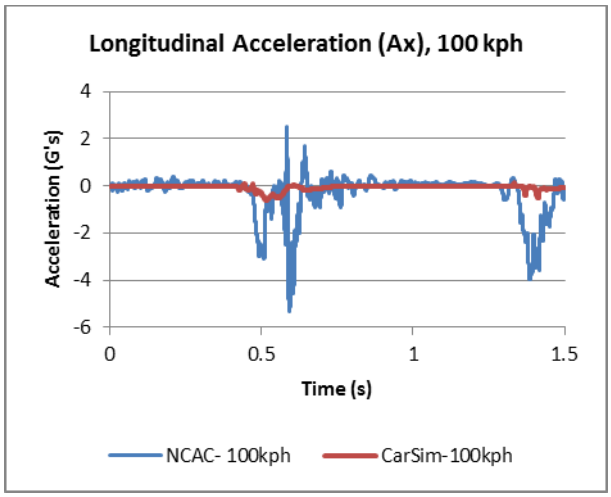

Figure 7.34: Car Longitudinal Acceleration (Ax), 100 kph

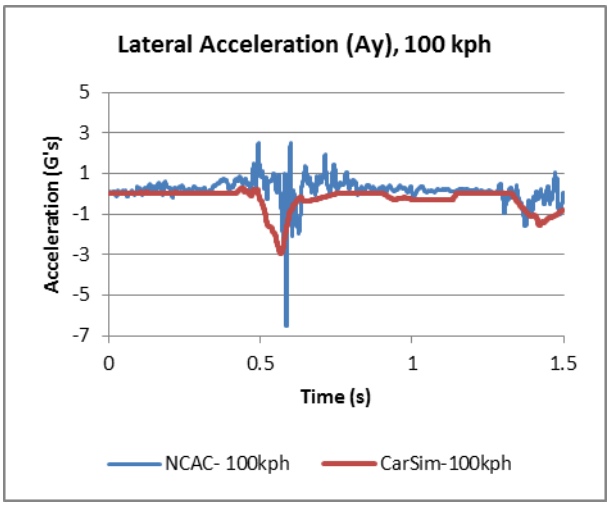

Figure 7.35: Car Lateral Acceleration (Ay), 100 kph

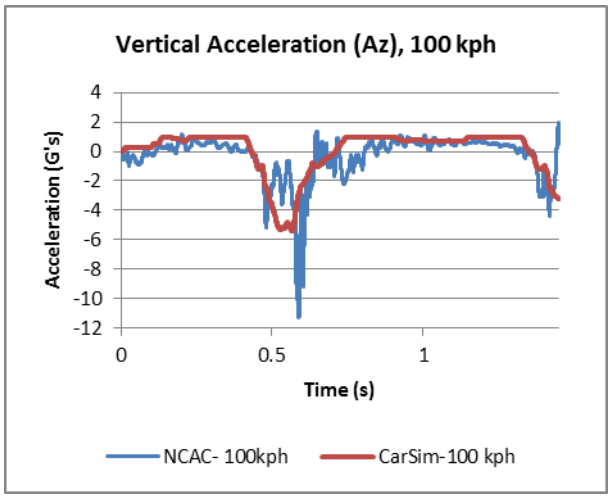

Figure 7.36: Car Vertical Acceleration (Az), 100 kph

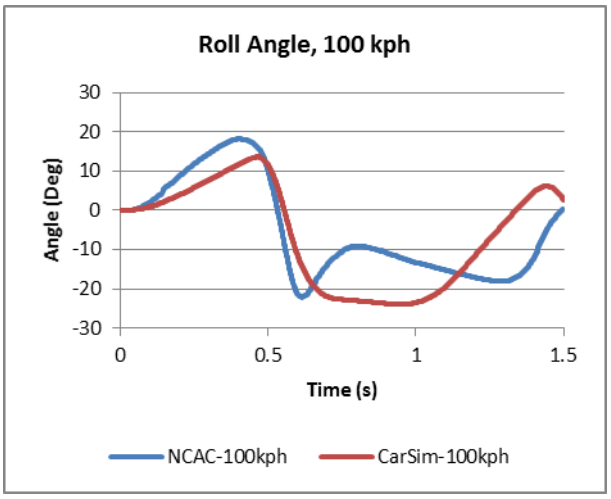

Figure 7.37: Car Roll Angle, 100 kph

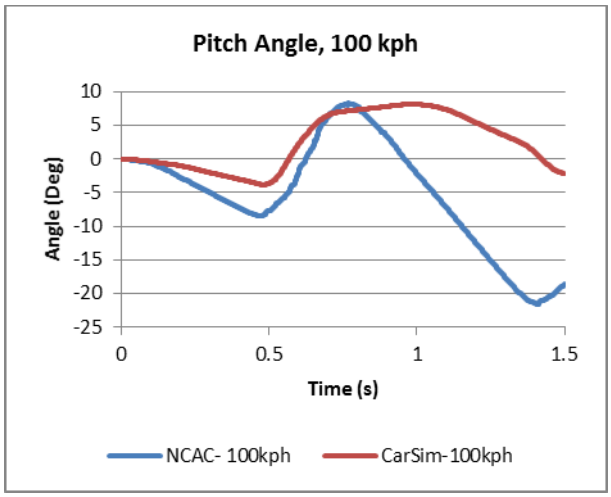

Figure 7.38: Car Pitch Angle, 100kph

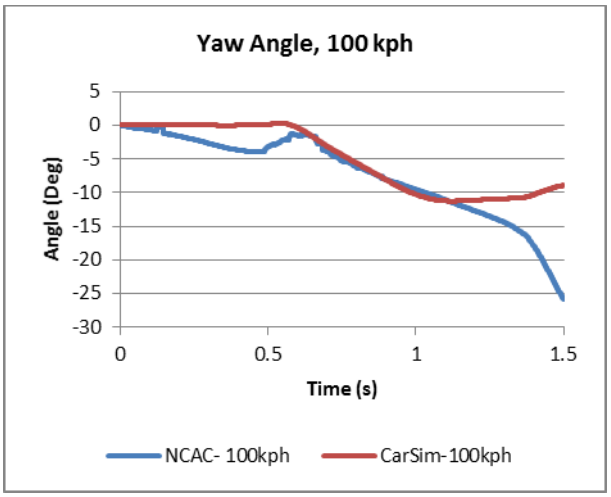

Figure 7.39: Car Yaw Angle, 100 kph

Overall, based on the review of the signal and image comparisons, there appears to be reasonable general agreement between the encroachment tests and vehicle dynamics simulations. Some of the test data had identified errors, and some discrepancies between test and simulation were attributed to body-to-ground contact that was confirmed during video review of the tests. Further, some discrepancies occurred outside the boundaries of the ditch, which is beyond the range of interest for this project.

7.1.3. Validation with Contact Code

In an effort to further validate the CarSim models, the research team used a code developed by TTI under a different project to account for the body-to-ground contact that occurs in some encroachment cases. The contact code tracks the user defined vehicle reference points over a terrain profile. The code then calculates the ground penetration of the reference points and uses the penetration of the ground to apply a force on the vehicle at the reference point. TTI researchers applied the contact code to the two high-speed encroachments described above to determine if better correlation can be achieved for these cases, particularly in regard to the longitudinal vehicle accelerations.

Figure 7.41 and Figure 7.42 show a comparison of the longitudinal accelerations for the pickup truck encroachment test at 100 km/h with and without use of the ground contact algorithm, respectively. Recall that these encroachments involved a MASH pickup truck encroaching across a 6H:1V symmetric ditch at an initial speed of 100 km/h and an angle of 25 degrees. Figure 7.43 and Figure 7.44 show a comparison for a similar encroachment with the MASH passenger car.

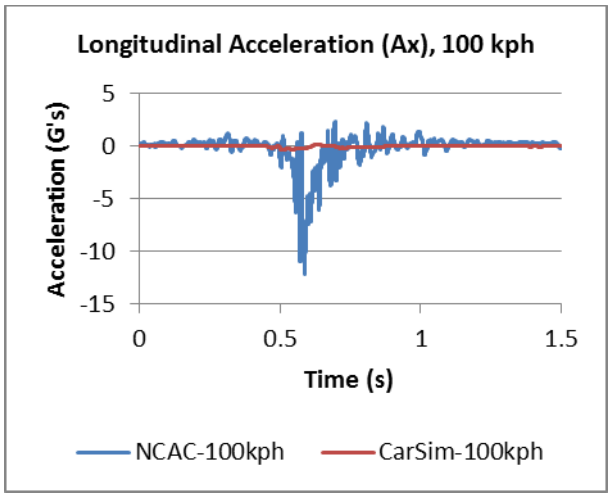

Figure 7.40: Case 2 Without Contact Code

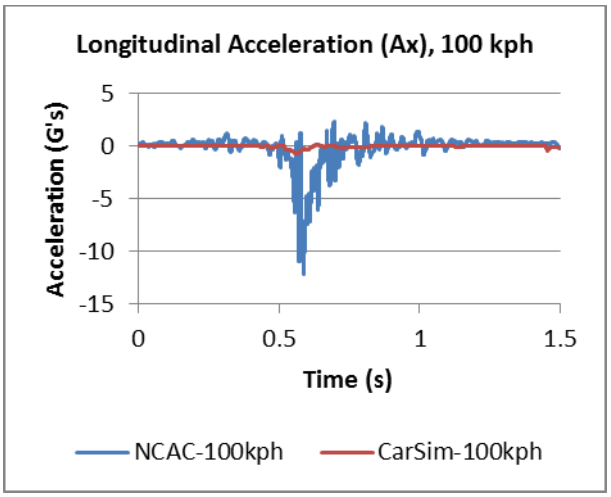

Figure 7.41: Case 2 With Contact Code

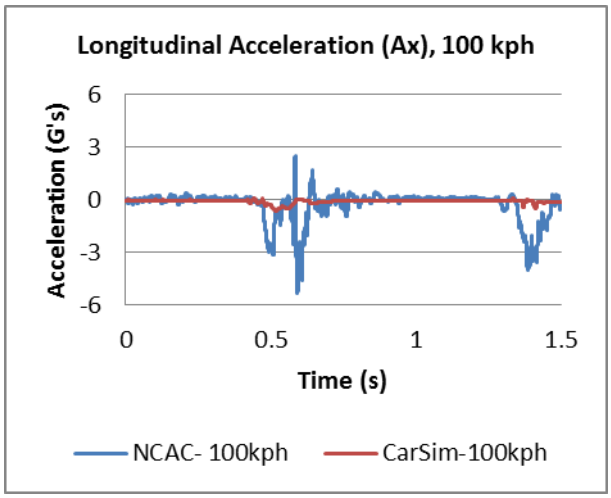

Figure 7.42: Case 4 Without Contact Code

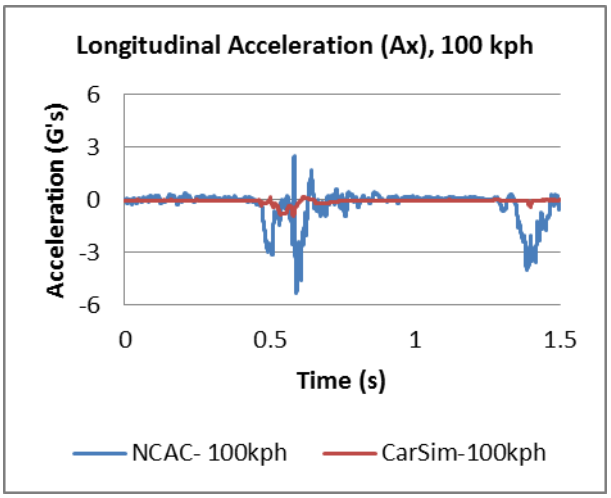

Figure 7.43: Case 4 With Contact Code

Application of the contact algorithm did not have much effect on the longitudinal acceleration of either vehicle. Researchers believe that this is in part due to the fact that CarSim reference points are limited and cannot be used to fully define all points on the vehicle bumper and chassis that might interact with the terrain. However, researchers do believe that the chosen reference points should be adequate for capturing ground contact and improving vehicle trajectory behavior in many instances. Researchers also believe that the test data has errors (some of which have been discussed) that can affect correlation.

It was noted that the contact algorithm does exert forces on selected vehicle reference points, and those forces do have an effect on the overall vehicle response. Bumper trajectory profiles for the 100 km/h encroachment simulations with and without the contact algorithm are shown in Figure 7.45 and Figure 7.46 for the pickup truck and small car, respectively.

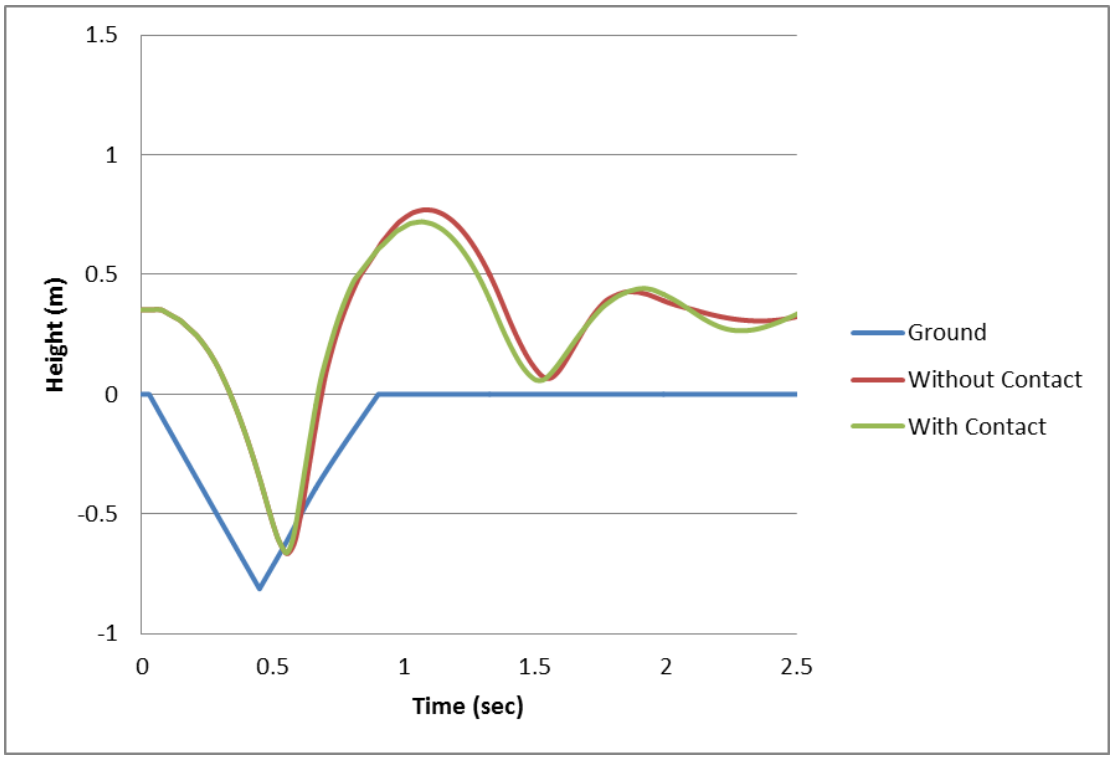

Figure 7.44: Vehicle Trajectories of Pickup Truck Without and With the Contact Code

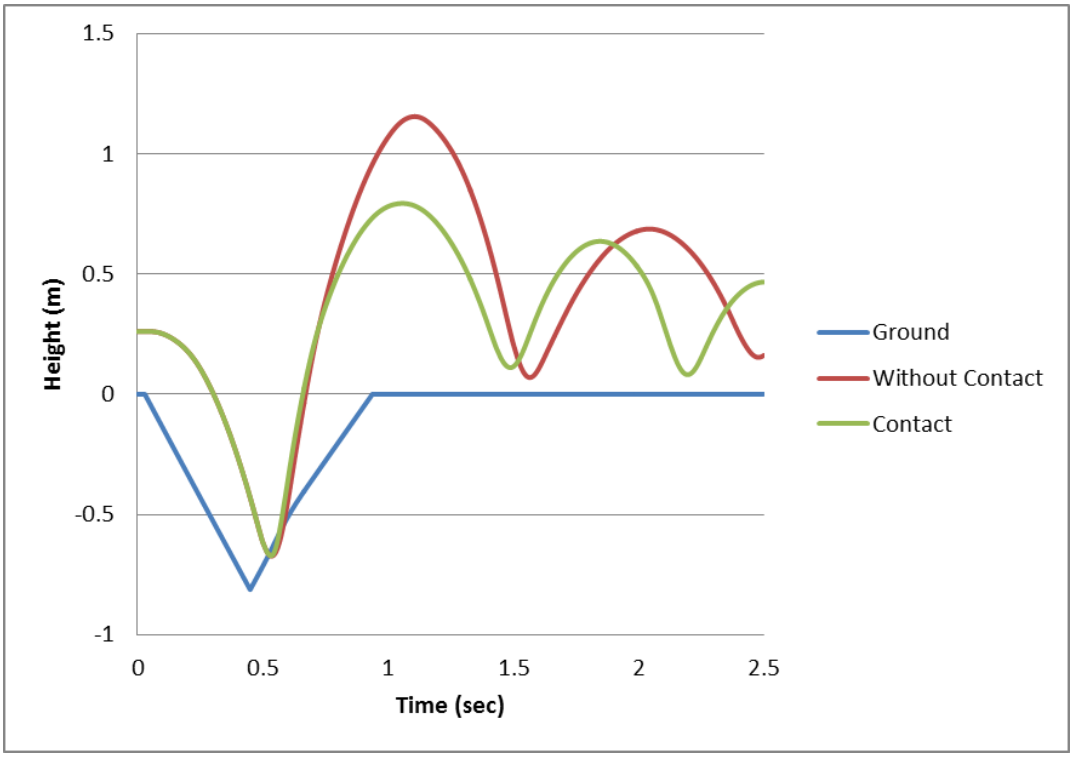

Figure 7.45: Vehicle Trajectories of Small Car without and With the Contact Code

In the pickup truck encroachment, the terrain contact results in a slight deceleration of the vehicle. This deceleration results in a slight reduction in bumper height after the pickup truck rebounds off the ditch backslope.

The small car experiences a larger deceleration from the body-to-ground contact. A reduction in both bumper height and vehicle velocity is evident from the bumper profiles shown in Figure 7.46.

Based on the above analyses and observations, the researchers believe that the CarSim vehicle models are reasonably validated and the use of the contact algorithm is necessary and sufficient for the purposes of the vehicle trajectory analysis simulations. The vehicle trajectory analyses are intended to be used for developing preliminary barrier placement guidelines, which will then be more accurately validated using finite element simulations.

7.2. VEHICLE DYNAMICS RUNS

Vehicle dynamics simulations were performed as part of the guideline development process. The median profiles that were modeled are listed in Table 7.5.

Table 7.5: Actual Median Profiles Used in the Trajectory Analysis

Ditch Slope	1/6									1/8					
Ditch Width (ft)	32	42		52			62			32	42	52		62	
Actual Ditch Depth (ft)	2.67	3	3.5	3	4	4.33	3	4	5.17	2	2.63	3	3.25	3	3.88
Ditch Profile	V	T	V	T	T	V	T	T	V	V	V	T	V	T	V

The simulation matrix consisted of two vehicles, two encroachment speeds, and two encroachment angles as follows:

- Vehicles
  - 2270P (5000 lb) pickup truck
  - 1100C (2420 lb) passenger car
- Encroachment Conditions
  - Speed: 50 and 62 mph (80 and 100 km/h)
  - Angle: 15 and 25 deg

This results in 8 simulations per ditch terrain profile and a total of 120 simulations.

The tracking point on the vehicle was taken as the top corner of the bumper. This would typically be the location of first contact of a vehicle with a longitudinal barrier system. A code was written to track and extract the position and elevation of the corner of the bumper as the vehicle traversed across the ditch. This process involved analysis of six CarSim output vectors: 3-sprung mass origin vectors ({Xo},{Yo},{Zo}), and 3-angular displacement vectors ({Yaw}, {Roll}, {Pitch}) of the vehicle C.G. The origin of the sprung mass in CarSim is defined by the

center of the front axle (Xo, Yo) and initial tire-ground contact level (Zo). In order to obtain the location of the vehicle bumper along the ditch cross section, following steps were performed:

Step 1: The initial trace point vector, {Vtr}, and vehicle C.G. vector, {Vcg}, (shown in Figure 7.33) were rotated following a prescribed {Yaw}-{Roll}-{Pitch} sequence. These were then added to the 3-sprung mass origin vectors ({Xo},{Yo},{Zo}) to obtain the coordinate vectors ({Xtr},{Ytr},{Ztr}) of the bumper point along the direction of vehicle travel.

Step 2: The adjustment of {Ztr} for ditch offset ({dz}) was then calculated.

Step 3: The bumper point coordinate vectors ({Xtr},{Ytr},{Ztr}) were then rotated about the Z axis towards the ditch cross section to obtain a bumper trace profile along the ditch cross-section (X_{ditch}).

Step 4: The bumper profile was then normalized by adding the adjustment {dZ} to the bumper tracking point heights {Ztr} to obtain the bumper point profile trace { $Ztr_{adjusted}$} with respect to the ditch cross-section.

Figure 7.47 shows a resulting output plot from this routine. Both the actual and normalized bumper height profiles are shown with respect to the ditch profile. The actual plot begins at the equilibrium height of the vehicle bumper with reference to level ground (height = 0). Note that this curve follows the terrain and may be positive or negative depending on the location in the ditch and the ditch depth. This plot is more difficult to analyze in this form, because it requires the ditch elevation to be subtracted from the absolute bumper elevation. When this calculation is performed along the cross-section of the ditch, the normalized bumper profile is obtained. The reference for the normalized bumper elevation profile is the horizontal axis. The height of the bumper above the local ditch terrain is readily define for any lateral offset. When the barrier performance limits are incorporated, this normalized curve permits acceptable and unacceptable lateral barrier placement ranges to be readily identified along the ditch section.

Note that the plots shown in Figure 7.47 are for the vehicles traversing across the median from left to right side (i.e., increasing direction of lateral offset). This data is sufficient for evaluating a scenario in which a guardrail is placed on a roadside or on both sides of a median ditch.

For median configurations with a single median barrier placed in the ditch, consideration needs to be given to vehicles encroaching into the median from either side of the divided roadway. This is accomplished by mirroring the traces plotted in Figure 7.35 along the centerline of the ditch and retaining the maximum (or minimum) elevation value associated with the left and right side encroachment plots.

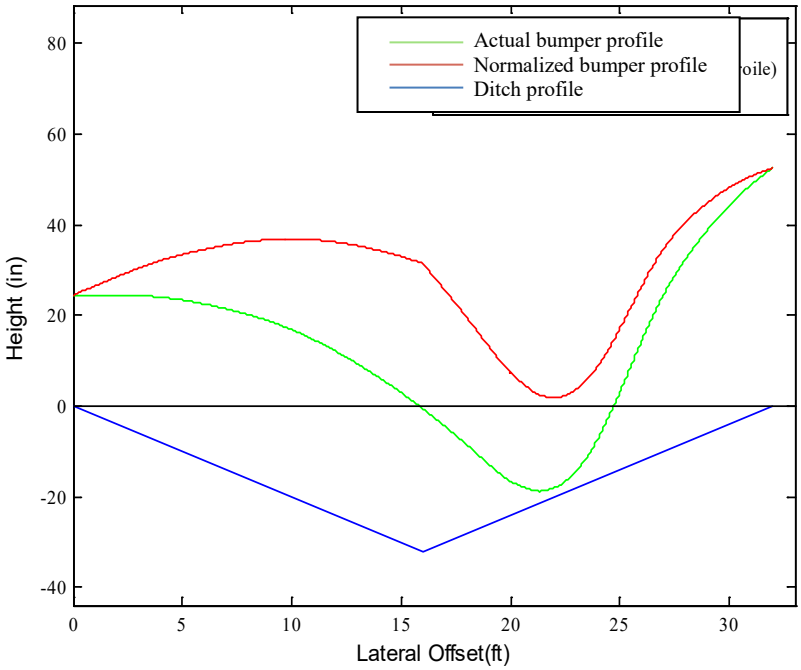

Figure 7.47. Bumper profile curves obtained from CarSim

This analysis was performed to obtain normalized plots for all 120 encroachment simulations. Figure 7.48 through Figure 7.56 present the bumper trajectories obtained for the various ditch profiles that were modeled with 1V:6H sideslopes. The ditch profile is described for each case in terms of slope, width, height, and shape (i.e., V-shape or trapezoidal). Each of these figures provides overlays of the bumper profiles from the four small car encroachment simulations and four pickup truck encroachment simulations. The legend for these figures is as follows:

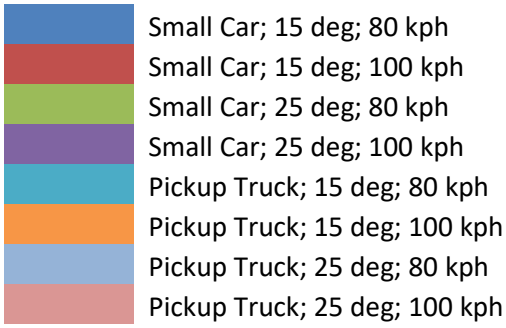

The bumper trajectory profiles corresponding to the ditch profiles with 1V:8H slopes are similarly presented in Figure 7.57 through Figure 7.62.

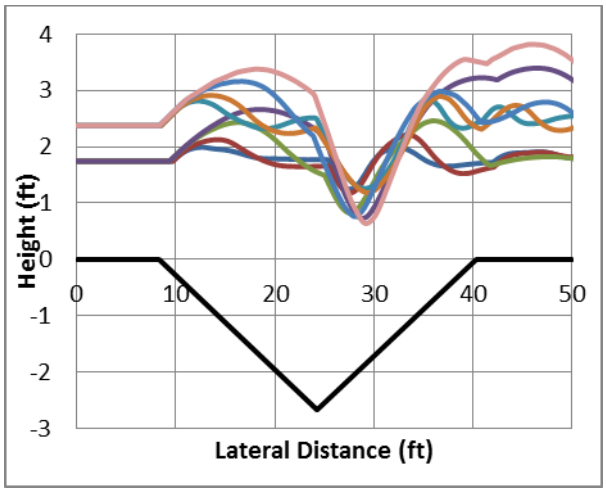

Figure 7.46: 1V:6H, 32 ft, 2.67 ft V

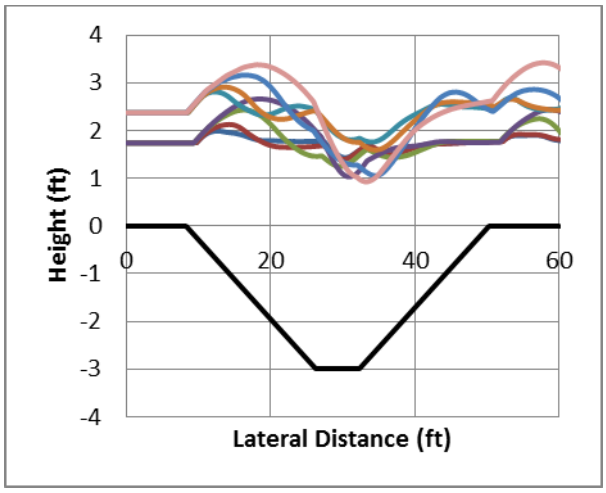

Figure 7.47: 1V:6H, 42 ft, 3 ft T

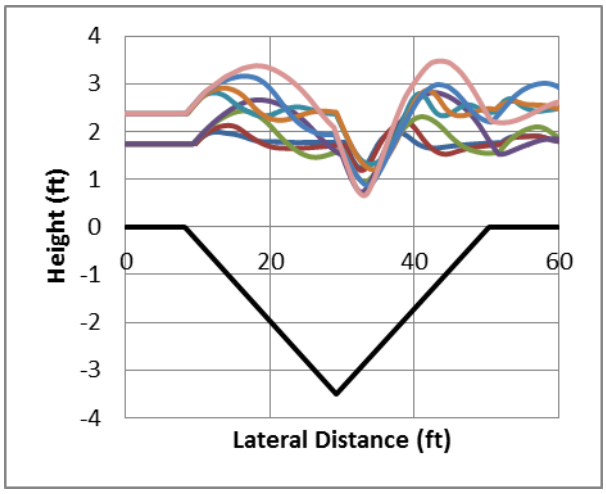

Figure 7.48: 1V:6H, 42 ft, 3.5 ft V

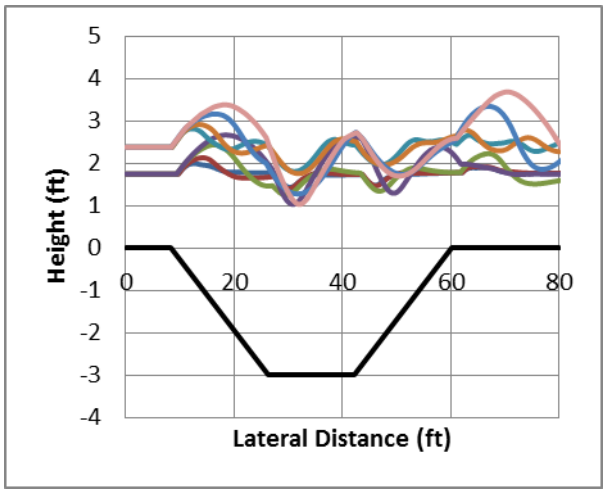

Figure 7.49: 1V:6H, 52 ft, 3 ft T

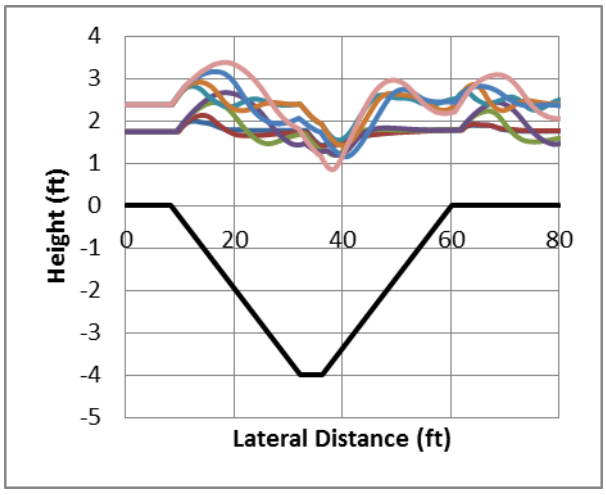

Figure 7.50: 1V:6H, 52 ft, 4 ft T

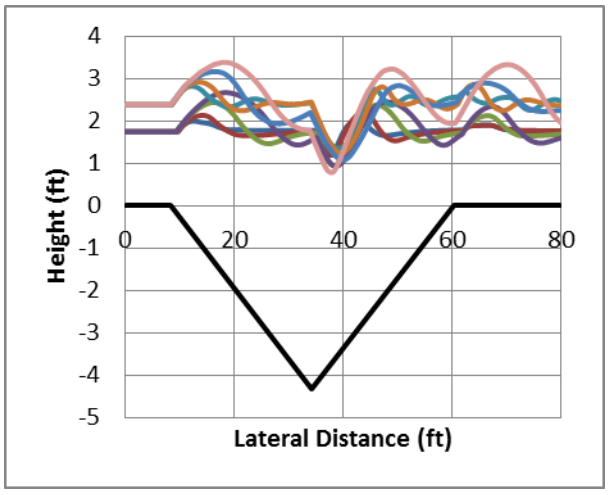

Figure 7.51: 1V:6H, 52 ft, 4.33 ft V

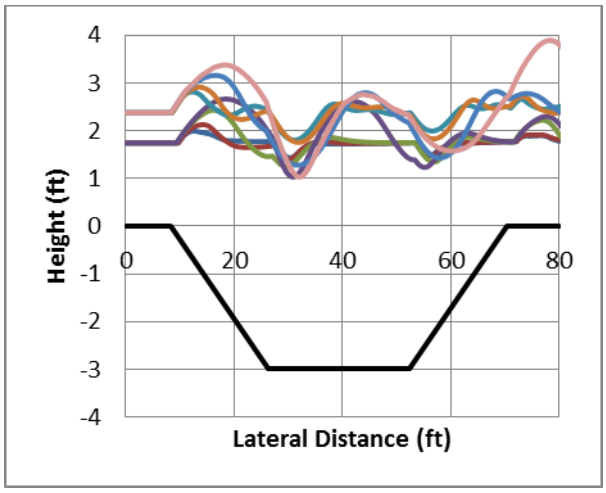

Figure 7.52: 1V:6H, 62 ft, 3 ft T

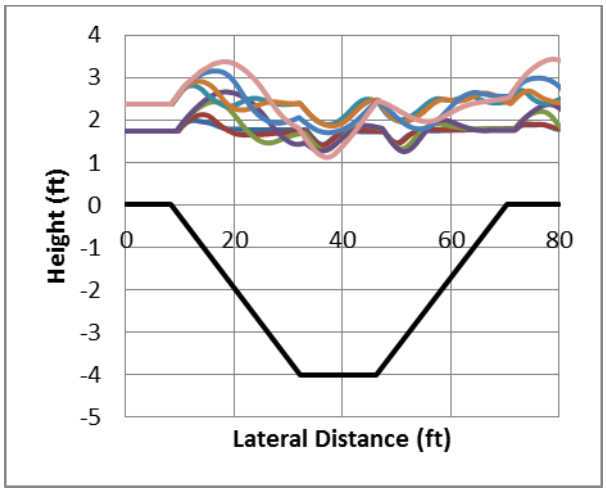

Figure 7.53: 1V:6H, 62 ft, 4ft T

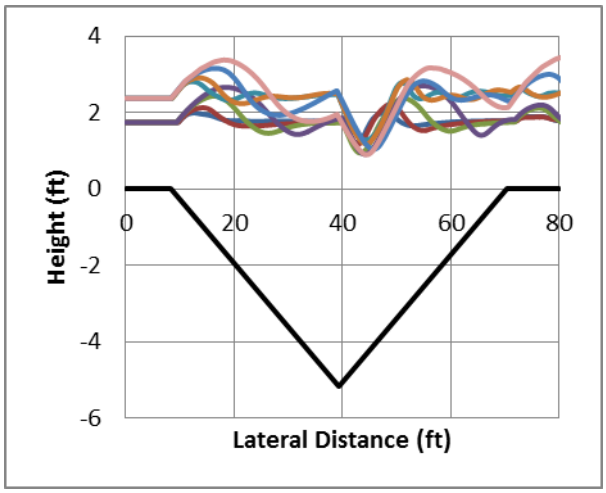

Figure 7.54: 1V:6H, 62 ft, 5.17 ft V

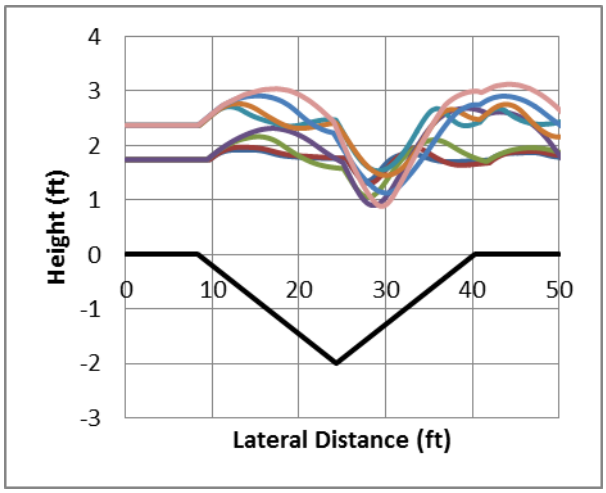

Figure 7.55: 1V:8H, 32 ft, 2 ft V

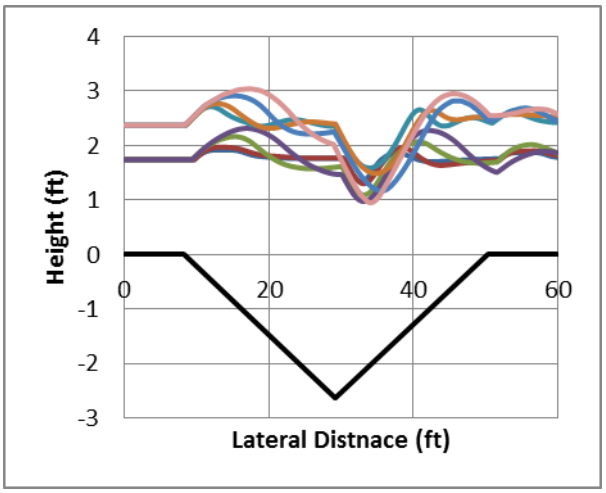

Figure 7.56: 1V:8H, 42 ft, 2.63 ft V

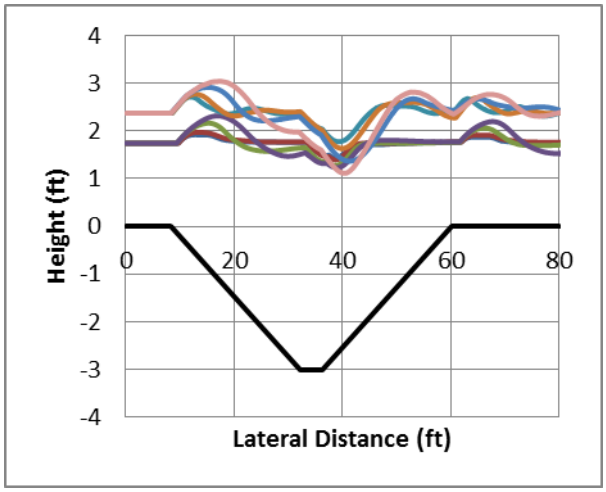

Figure 7.57: 1V:8H, 52 ft, 3 ft T

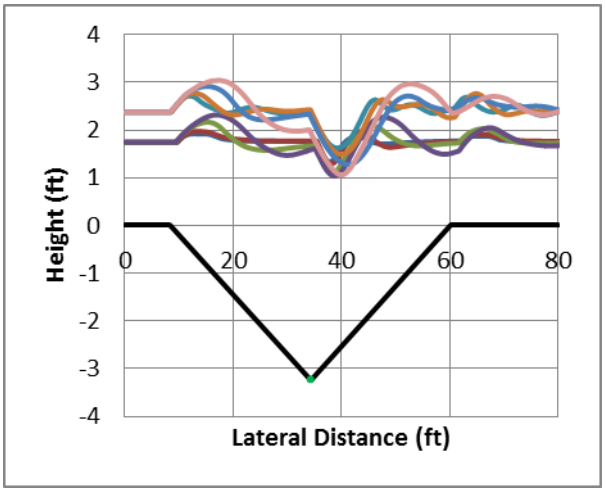

Figure 7.58: 1V:8H, 52 ft, 3.25 ft V

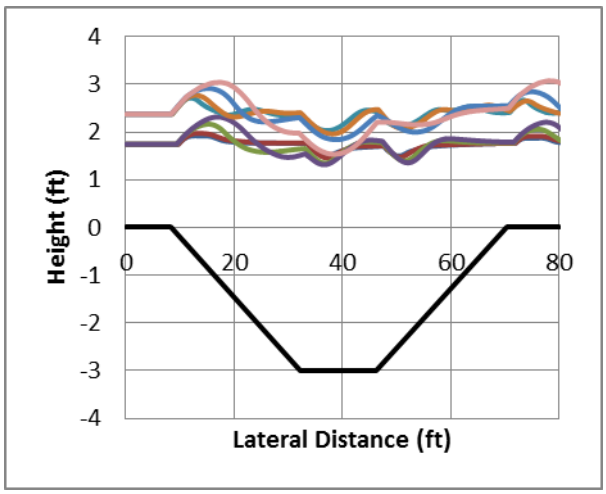

Figure 7.59: 1V:8H, 62 ft, 3 ft T

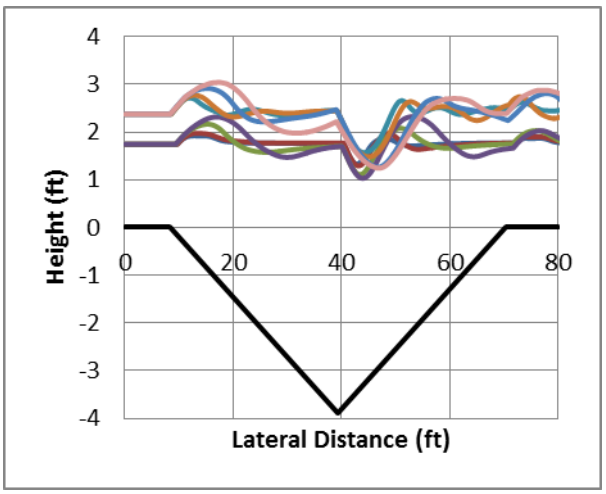

Figure 7.60: 1V:8H, 62 ft, 3.88 ft V

When considering placement of a barrier on a roadside slope, some of the bumper trajectory profiles may be truncated by the presence of the ditch bottom or back slope. Therefore, additional encroachment simulations were performed with the two design vehicles traversing infinite 1V:6H and 1V:8H slopes following the prescribed set of encroachment conditions. The overlaid bumper trajectory plots for these simulations are shown in Figure 7.63 and Figure 7.64 for the 1V:6H and 1V:8H slopes, respectively. The normalized bumper height relative to the local sloped terrain is plotted versus the lateral offset on the slope. The sloped ground is not plotted, but the break point of the sloped terrain is at x = 0. This is the legend for these two figures is as follows:

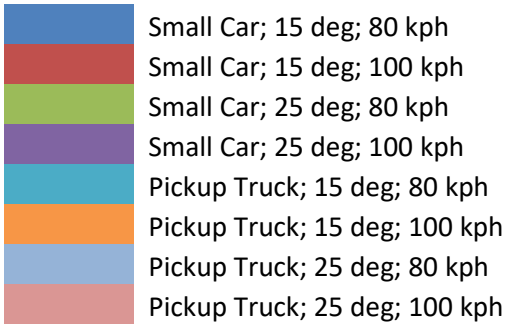

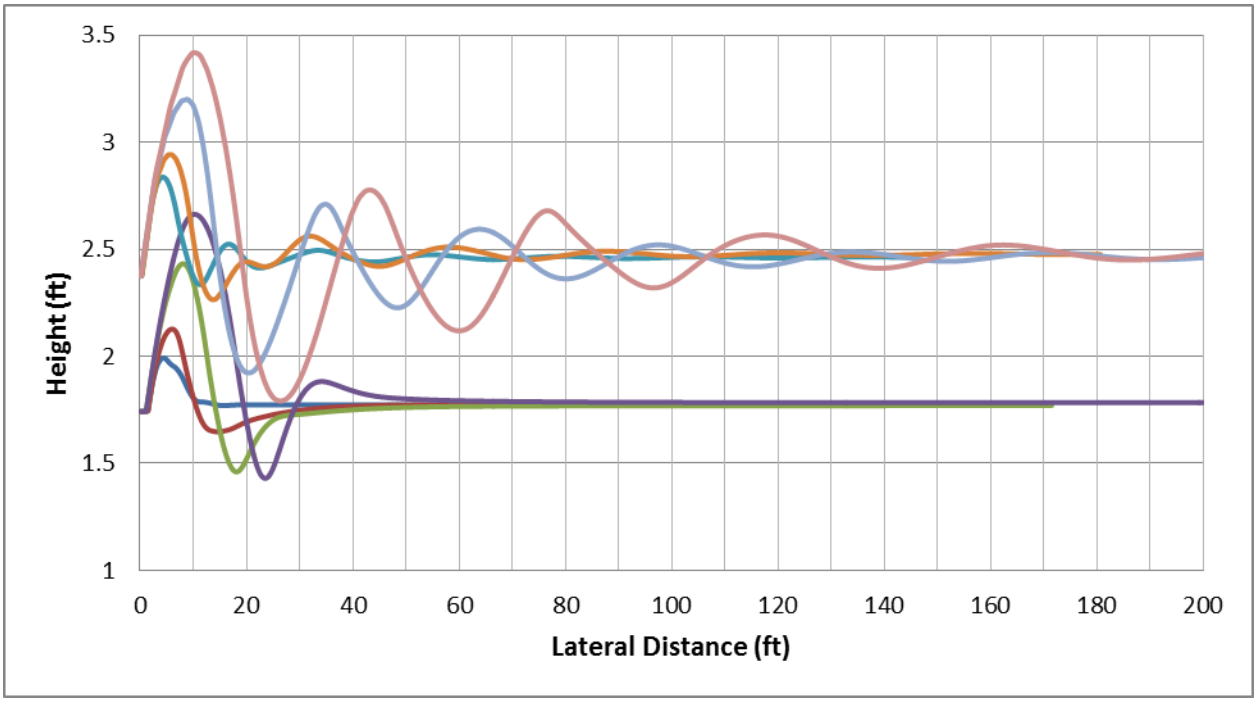

Figure 7.61: Vehicle Trajectory on 1V:6H Slope

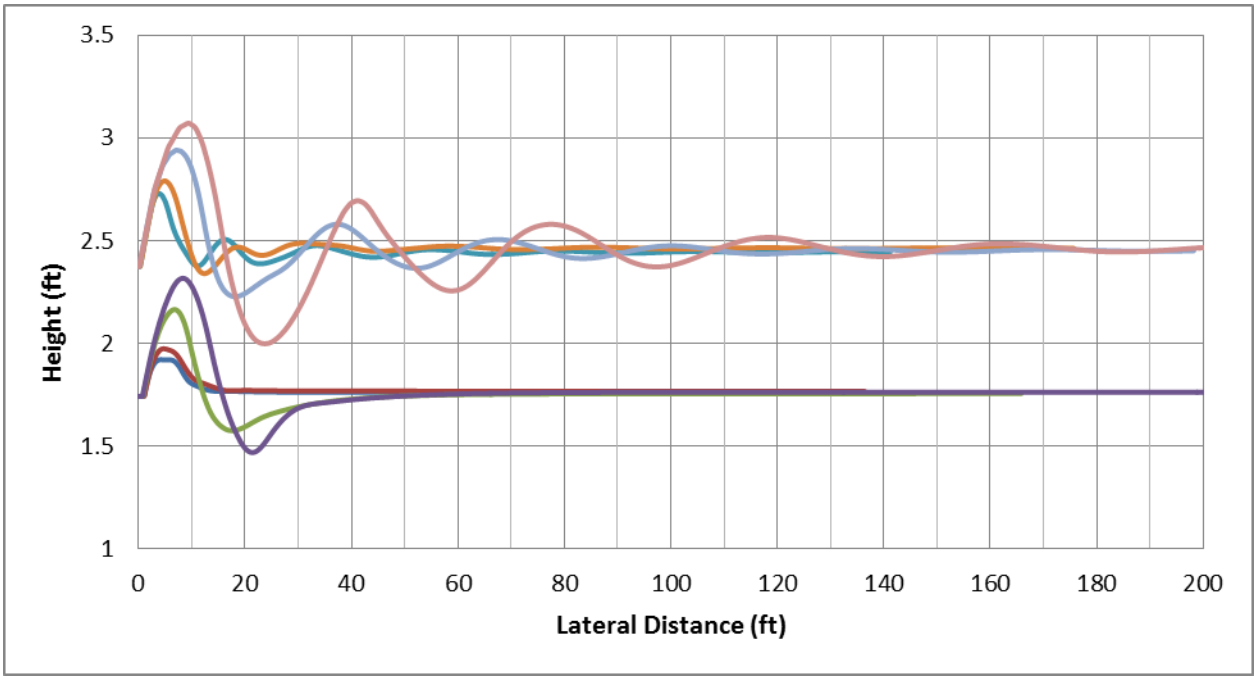

Figure 7.62: Vehicle Trajectory on 1V:8H Slope

8. BARRIER PLACEMENT GUIDELINE DEVELOPMENT

8.1. PRELIMINARY PLACEMENT GUIDELINE DEVELOPMENT

Based on the performance limits of each barrier system obtained from LS-DYNA and the vehicle trajectory data obtained from CarSim, preliminary placement guidelines for each barrier system of interest were established.

The override/rollover limit and underride limits were superimposed on the normalized bumper trajectory envelopes for each terrain configuration. The pickup truck bumper trajectories were analyzed against the override/rollover limit, and the bumper trajectories associated with the small passenger car encroachments were analyzed against the underride limit.

The override/rollover and underride limits plot as horizontal lines on the normalized bumper trajectory profiles. If, at a given lateral offset, one or more of the bumper trajectory profiles for the pickup truck exceed the override/rollover limit, rollover of the pickup truck or override of the barrier is probable (depending on the encroachment conditions), and the barrier is not recommended for placement at that location on the ditch or roadside slope. If, on the other hand, the bumper trajectory profiles all fall below the override/rollover limit defined for the barrier system, the containment of the pickup truck is likely and that offset location on the ditch or slope would be further considered through evaluation of the underride limit.

If, at a given lateral offset, one or more of the bumper trajectory profiles for the small car fall below the underride limit, it is probable that the small care will underride the barrier system (depending on the specific encroachment conditions), resulting in severe vehicle snagging, excessive decelerations, and/or penetration under the barrier system, and the barrier is not recommended for placement at that location on the ditch or roadside slope. If, on the other hand, the bumper trajectory profiles are all above the underride limit defined for the barrier system, containment of the small car is likely and that offset location on the ditch or slope would be included in the placement guidelines as an acceptable location for placement of that barrier system.

In this manner, the encroachment data for each ditch profile was analyzed for each barrier system and filtered to exclude all ranges where the bumper height of the small car was less than the corresponding underride limit and/or the bumper height for the pickup truck exceeded the corresponding override/rollover limit.

For roadside barriers, only the fore slope was considered for barrier placement. Figure 8.1 shows an example of the vehicle bumper trajectory analysis on a 1V:6H slope for the MGS guardrail system. The short dashed line represents the override limit of the MGS guardrail, and the long dash line represents the underride limit of the MGS guardrail. The normalized bumper trajectory profiles for the eight encroachment conditions are superimposed over the performance limits.

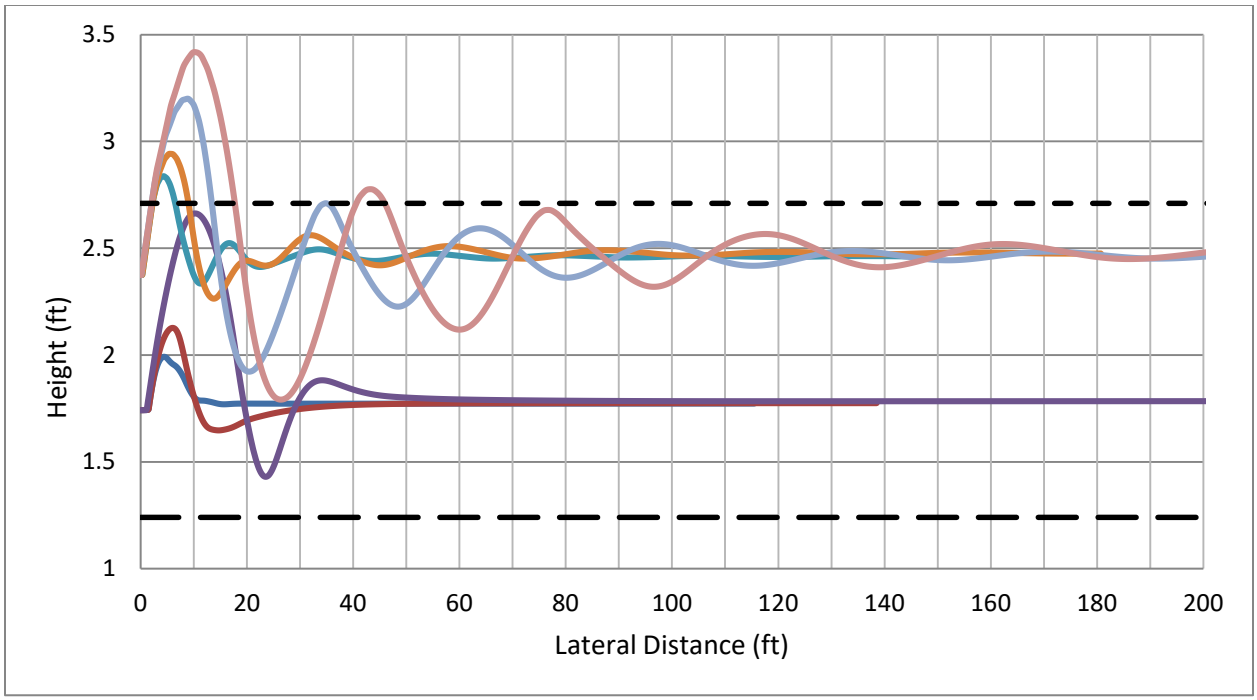

Figure 8.1: Vehicle Trajectory Plot on 1V:6H Slope with Performance Limits for MGS

As can be seen in Figure 8.1, none of the small car bumper trajectories extend below the underride limit. However, at several offsets, the bumper trajectories for the pickup truck exceed the override/rollover limit. Consequently, the placement of the MGS would not be recommended on a 1V:6H slope at these offsets. Unacceptable offset ranges include 2 ft – 17 ft and 40 ft – 45 ft. Offsets other than these would be considered acceptable placement locations in the guidelines.

For the median barriers, a two-way encroachment analysis was performed. This two-way encroachment analysis accounts impact of the barrier from both directions of travel on a divided highway. For example, if a median barrier is placed in a median ditch at a location other than the ditch centerline, it requires satisfactory impact performance on the ditch foreslope from one direction and on the ditch backslope from the other direction.

Consider the example of an MGS median barrier in the 1V:6H median ditch presented in Figure 8.2. The normalized bumper trajectory plots shown in this figure are for an encroachment traveling across the ditch from left to right. The short dashed line represents the override/rollover limit of the MGS median barrier, and the long dashed line represents the underride limit of the MGS median barrier. In Figure 8.2, the green highlighted area on the slope indicates the acceptable placement range of the MGS median barrier on the ditch foreslope for an encroachment from the left. In this limited range of 0 – 2 ft from the slope break point, the pickup truck bumper trajectories are below the override/rollover limit and the small car bumper trajectories are above the underride limit, constituting an acceptable placement range.

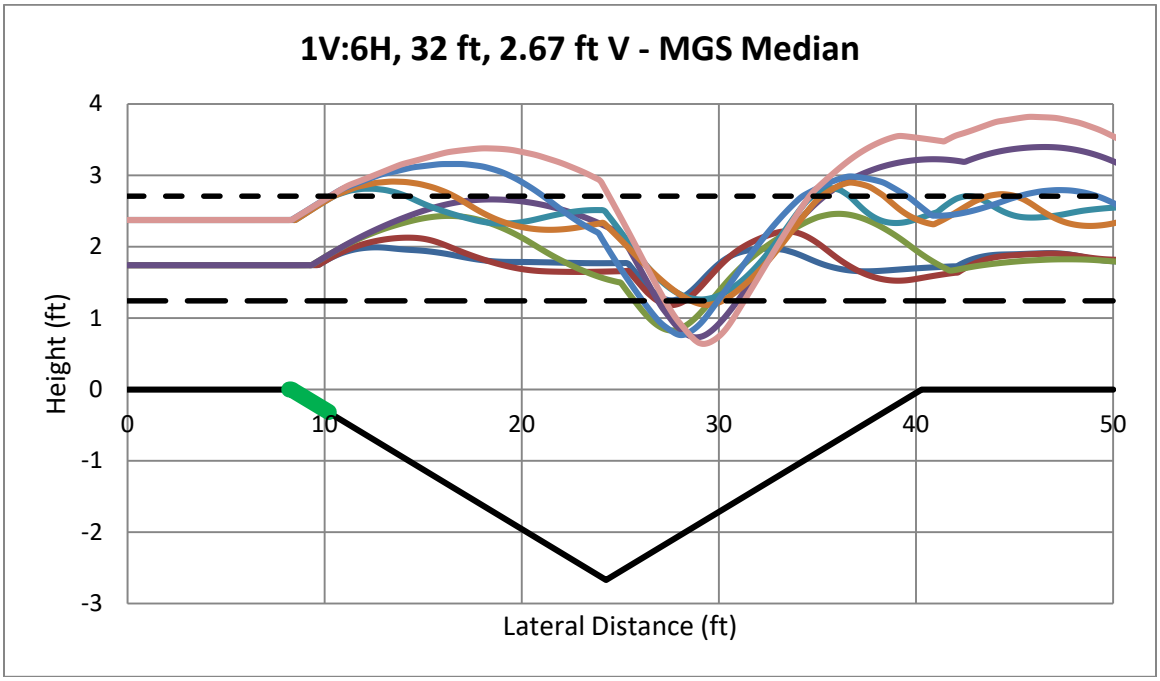

Figure 8.2: Preliminary Placement Range of One-Way Encroachment of MGS Median Barrier on 1V:6H Slope, 32 feet wide, 2.67 feet Deep Ditch Profile

However, to properly consider the median barrier application, encroachments from both directions must be analyzed. This is accomplished by mirroring the bumper trajectory profiles about the ditch centerline and reanalyzing the data to account for both encroachment directions. When this is done for the current example, the placement range that was acceptable for the single direction encroachment is no longer acceptable. This can be visualized by looking at that same offset on the other side of the ditch. It can clearly be seen that in the range from 0 – 2 ft from the slope break point, there are pickup truck bumper trajectories that exceed the override/rollover threshold. This indicates that a pickup truck encroaching across the 32-ft wide 1V:6H ditch would likely vault over the MGS median barrier in this placement range as it traverses the backslope. Thus, it is concluded that for this ditch configuration, there is not acceptable placement range for the MGS median barrier.

Such an analysis was performed for each barrier system for each median ditch configuration. The preliminary placement guidelines resulting from these analyses are presented below by barrier type.

8.1.1. Midwest Guardrail System (MGS)

A preliminary placement matrix was created for the Midwest Guardrail System (MGS) using the override and underride limits from LS-DYNA and the vehicle trajectory from CarSim. The results are shown in Table 8.1. Note that the ditch configurations are abbreviate in the table using the nomenclature <ditch width-slope-ditch height>. As shown in Table 8.1 below, apart from the two, 32-foot wide ditch configurations, all ditch configurations on the 1:6 slope had a starting placement range at 17 feet from the slope breakpoint, and all ditch configurations on the 1:8 slope had a starting placement range at 14 feet from the slope break point.

Table 8.1: Preliminary Placement Guideline for Midwest Guardrail System across Ditch Profiles

Guardrail	Possible Ditch Configuration	Placement Boundary (upper) (ft)	Placement Boundary (lower) (ft)	Range of Placement > 2 ft
MGS	32-6-3	0	2	2*
	42-6-3	17	21	4
	42-6-4	17	21	4
	52-6-3	17	26	9
	52-6-4	17	26	9
	52-6-6	17	26	9
	62-6-3	17	31	14
	62-6-4	17	31	14
	62-6-6	17	31	14
	32-8-3	14	16	2*
	42-8-3	14	21	7
	52-8-3	14	26	12
	52-8-4	14	26	12
	62-8-3	14	31	17
	62-8-4	14	31	17

*Not recommended due to narrow width of range

It is generally recommended that a barrier not be placed at a location that is associated with a very narrow range of placement. For example, the MGS guardrail system has a narrow 2-ft wide range of placement indicated from 0 – 2 ft from the slope break point. Due to inherent limitations in both the finite element and vehicle trajectory simulations upon which the guidance is based, placement at such a location has a higher probability of undesired impact performance. A wider placement range provides a greater probability of acceptable barrier impact performance if the barrier is placed inside the range (e.g., center of range) away from the outer fringes. While the impact performance at the outer edges of the range may be uncertain, the interior of such a range provides a much higher confidence level related to barrier performance.

8.1.2. Modified Weak Post W-Beam Guardrail (G2)

Using the performance limits determined for the Modified Weak Post W-beam (G2) guardrail and the vehicle trajectory bumper profiles, preliminary guidelines for the placement of the barrier on the ditch configurations of interest were established. These guidelines compared the bumper height of both the small car and the pickup truck with their corresponding limits, and used this data to create acceptable ranges for barrier placement across all 15 ditch configurations.

Most of the ditch configurations had no acceptable placement range for the Modified Weak Post W-beam (G2) guardrail, or had an acceptable placement range of 1 foot or less. The research team concluded that these placement ranges were too small to realistically place a barrier, so they were not considered when creating the preliminary guidelines.

Only one ditch configuration had an acceptable range greater than 1 foot. The 62 feet wide ditch with 1V:8H slopes has an acceptable range of placement from 26 feet to 30 feet measured from the slope break.

8.1.3. Modified Strong Steel-Post W-Beam (G4(1S))

A preliminary matrix was created for the modified G4(1S) guardrail by using the appropriate override and underride performance limits and the vehicle trajectory from CarSim. Table 8.2 presents the preliminary placement ranges across the various ditch profiles. The barrier was acceptable on all but two ditch profiles (the 32 foot wide ditches with both 1V:6H and 1V:8H slopes).

8.1.4. Single Slope Concrete Barrier

A preliminary matrix was created for the single slope concrete barrier by using the override performance limit determine through LS-DYNA simulation and the vehicle trajectory bumper profiles obtained from CarSim. There was no underride analysis for the single slope concrete barrier since it is not feasible for a car to underride this barrier. The analysis indicated the single slope concrete barrier could be placed anywhere along any of the 15 ditch configurations analyzed.

8.1.5. Weak Post W-Beam Median Barrier (MB2)

Recall that the weak post W-beam median barrier (MB2) had the same height and performance limits as the modified weak post W-beam guardrail (G2). Only one ditch configuration had an acceptable placement range greater than 1 foot. The 62 feet wide ditch with 1V:8H slopes has an acceptable range of placement from 26 feet to 30 feet measured from the slope break, giving a total range of 4 feet on each side of the ditch.

Table 8.2: Preliminary Placement Guidelines for Modified G4(1S)

Guardrail	Possible Ditch Configuration	Placement Boundary (upper) (ft)	Placement Boundary (lower) (ft)	Range of Placement > 2 ft
Modified G4(1S)	32-6-3	0	0.5	0.5*
	42-6-3	18	21	3
	42-6-4	18.5	21	2.5
	52-6-3	18.5	26	7.5
	52-6-4	18.5	26	7.5
	52-6-6	18.5	26	7.5
	62-6-3	18	28.5	10.5
	62-6-4	18.5	30.5	12
	62-6-6	18.5	26.5	8
	32-8-3	15.5	16	0.5*
	42-8-3	15.5	21	5.5
	52-8-3	15.5	26	10.5
	52-8-4	16.5	26	9.5
	62-8-3	16.5	31	14.5
	62-8-4	16.5	31	14.5

*Not recommended due to narrow width of range

8.2. REFINED GUIDELINE DEVELOPMENT

The purpose of this stage of the project was to verify or refine as needed the preliminary placement ranges derived from combining the barrier performance limits and vehicle bumper trajectory data. This was accomplished by performing selected explicit finite element impact simulations of the barrier systems installed in the actual ditch configurations using LS-DYNA. The validated barrier models were placed at the edge of the selected placement range and moved in 1 foot increments in either direction depending on the outcome of the simulation at that location. The vehicle selected for a particular simulation was based on the nature of the placement violation that occurred immediately outside the boundary of the acceptable placement range. For example, if a placement range was limited or controlled by override of the pickup at the edge of the range, the pickup truck model was used in the simulation.

If the outcome of the impact simulation was acceptable containment and redirection, the range was incrementally expanded and another simulation was performed. This repeated until an unacceptable outcome was obtained. If the outcome of the impact simulation was unacceptable according to MASH evaluation criteria, the allowable placement range was contracted and another simulation was performed. This process repeated until an acceptable outcome was achieved. The results were then used to revise/update the placement guidance for each barrier system.

8.2.1. Midwest Guardrail System

In order to further refine the preliminary placement guidance for the MGS guardrail system, full scale simulations were run with the traffic face of the W-beam aligned at the upper edge of placement range.

A 42-foot wide ditch with 1V:6H slopes and a depth of 4 feet was chosen to refine the barrier placement on the 1V:6H slopes. This ditch profile was chosen arbitrarily as the vehicles are airborne at the beginning of the placement range and the geometry of the ditch does not affect the truck's interaction with the barrier. The barrier was placed on the slope such that the traffic face of the W-beam was initially 17 feet from the slope break point. As presented in Table 8.1, this distance represents the beginning of the acceptable barrier placement range for any ditch with 1V:6H slopes. The impact conditions conformed to MASH Test 3-11, which is the most critical encroachment condition evaluated from the perspective of barrier override.

The barrier successfully contained and redirected the pickup truck when placed 17, 16, and 15 feet from the slope break point. Figure 8.4 shows sequential images from the simulation with the barrier placed 17 feet from the slope break point. Figure 8.5 shows images from the simulation with the barrier placed at 15 feet from the slope break point. The increase in the placement range compared to the initial performance limits shows that the trajectory of the vehicle prior to impacting the barrier plays an important role in the interaction between the vehicle and barrier. Since the MGS was able to successfully contain the vehicle up to 15 feet, the range of placement of the MGS on 1V:6H slopes was expanded to begin at 15 feet from the slope break point, giving an extra 2 feet of placement compared to the preliminary placement guidelines.

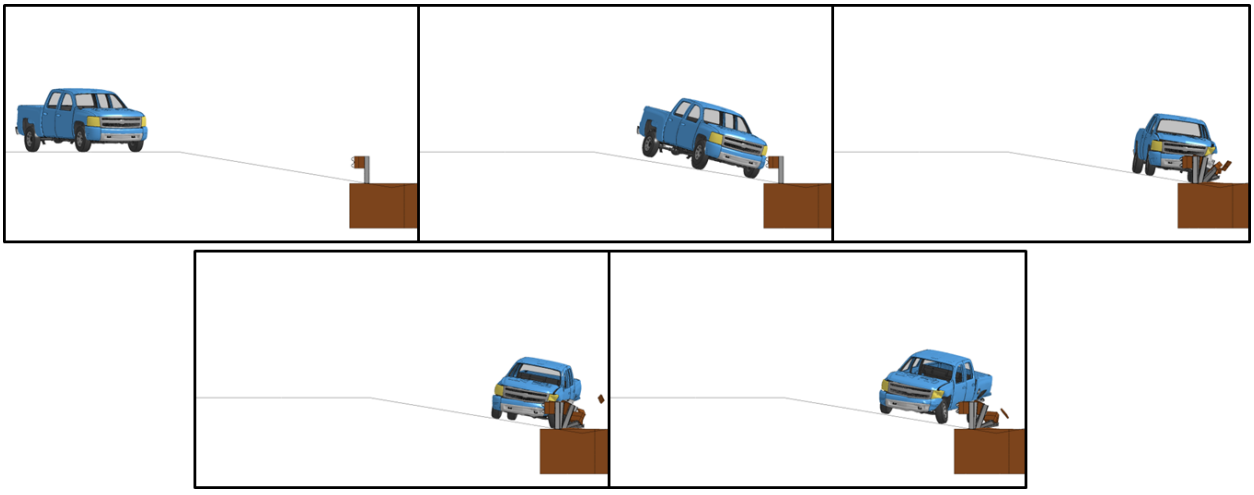

Figure 8.3: MGS on 42-6-4 Ditch Placed 17 ft from Slope Break Point

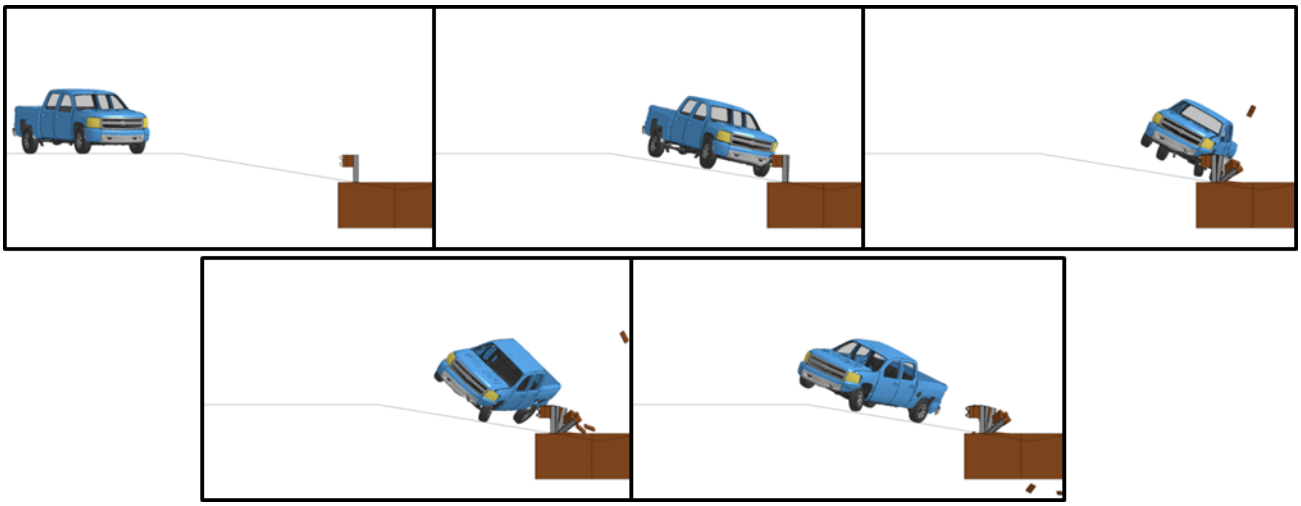

Figure 8.4: MGS on 42-6-4 Ditch placed 15 ft from Slope Break Point

The next step in refining the placement guidance for the MGS guardrail system due to override was to run simulations with the pickup truck on a ditch profile with 1V:8H slopes. This ditch profile was chosen arbitrarily as the vehicles are airborne at the beginning of the placement range and the geometry of the ditch does not affect the truck's interaction with the barrier. The barrier was placed on the slope such that the traffic face of the W-beam was initially 14 feet from the slope break point. As presented in Table 8.1, this distance represents the beginning of the acceptable barrier placement range for any ditch with 1V:8H slopes. The impact conditions conformed to MASH Test 3-11, which is the most critical encroachment condition evaluated from the perspective of barrier override.

The barrier was successful in redirecting the pickup truck when placed at 14, 13, 12, and 11 feet from the slope break point. Figure 8.6 shows the results of the simulation with the barrier placed at 11 feet from the slope break point. When the barrier was placed at 10 feet from the slope break point, the truck overrode the barrier. Figure 8.7 shows this override behavior. The increase in the placement range compared to the initial performance limits shows that the trajectory of the vehicle prior to impacting the barrier plays an important role in the interaction between the vehicle and barrier. Since the MGS was able to successfully contain the vehicle up to 11 feet, the range of placement of the MGS on 1V:8H slopes was expanded to begin at 11 feet from the slope break point, giving an extra 3 feet of placement compared to the preliminary placement guidelines.

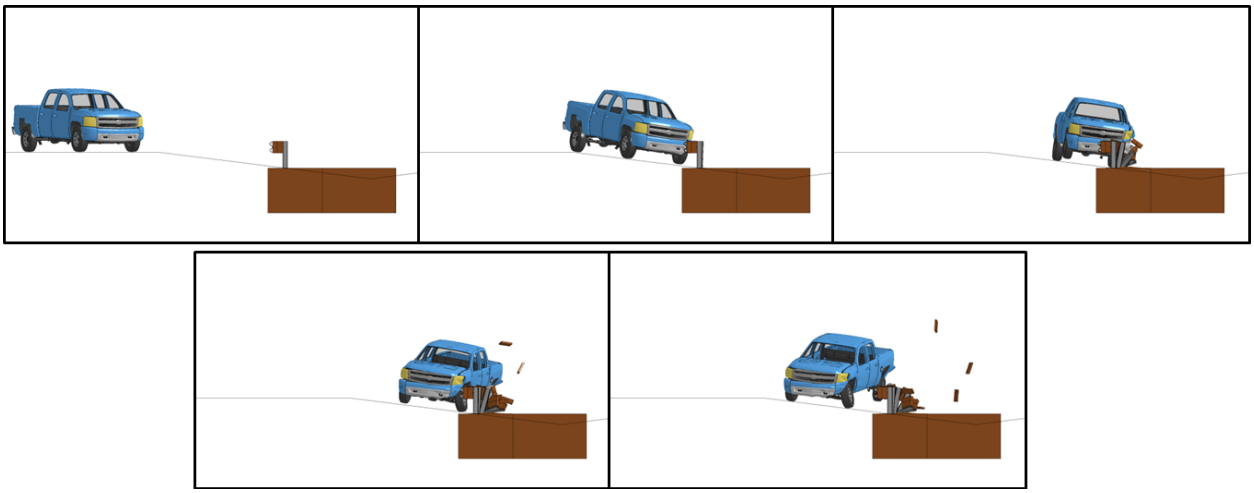

Figure 8.5: MGS on 42-8-3 Slope 11 ft from Slope Break Point

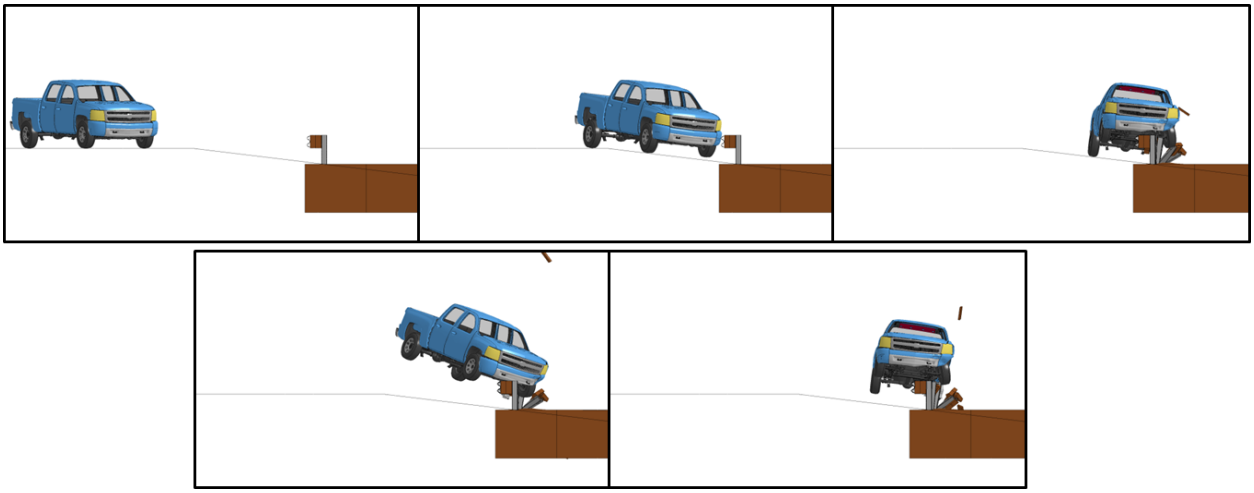

Figure 8.6: MGS on 42-8-3 Slope 10 ft from Slope Break Point

With the placement guidelines refined with respect to the override criteria, the next step investigate the underride limit. Recall that the 6-inch underride limit of the small car was limited by the height of the undercarriage of the vehicle rather than the vehicle's interaction with the barrier. This corresponds to a bumper height of 15 inches. This result led the researchers to believe that the MGS could be placed at any location along the ditch profiles to successfully contain the small car. However, the data from CarSim showed that the bumper height fell slightly below the 15 inch limit in some of the ditch encroachment. This lower height was attributed to the vehicle pitching downward and allowing the bumper to move closer to the ground before bottoming out.

To confirm that the MGS could still contain the small car at a bumper height lower than underride limit, researches selected the ditch configuration that had the lowest bumper height

relative to the local terrain. The 62-6-3 ditch profile had a minimum relative bumper height of 1.03 feet (12.4 inches) for the small car entering the ditch at 100 km/h and at an angle of 25 degrees. Figure 8.8 below shows the vehicle bumper trajectory plots for the 62-6-3 ditch profile and it can be seen that the minimum relative bumper height occurs 22.5 feet from the slope break point.

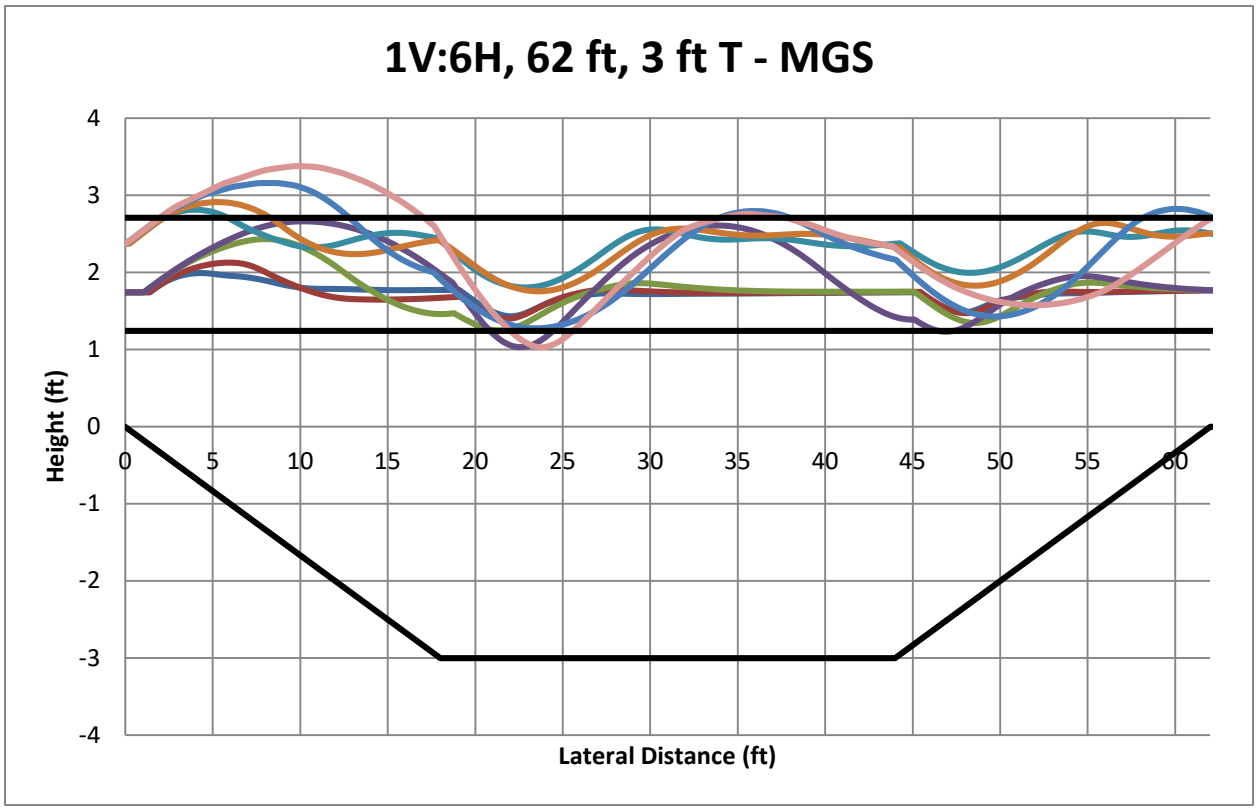

Figure 8.7: MGS Performance Limits on 62-6-3 Ditch Profile

The barrier was placed on the 1V:6H slope such that traffic face of the W-beam was 22.5 feet from the slope break point. The results of the simulation are shown in Figure 8.9. As shown, the MGS was successful in containing and redirecting the small car at this location. Since the barrier was able to contain the most critical location along the ditch profile, the MGS placement guidelines ddid not need any further refinement from underride limits. The refined placement guidelines for the MGS are shown in Table 8.3 below.

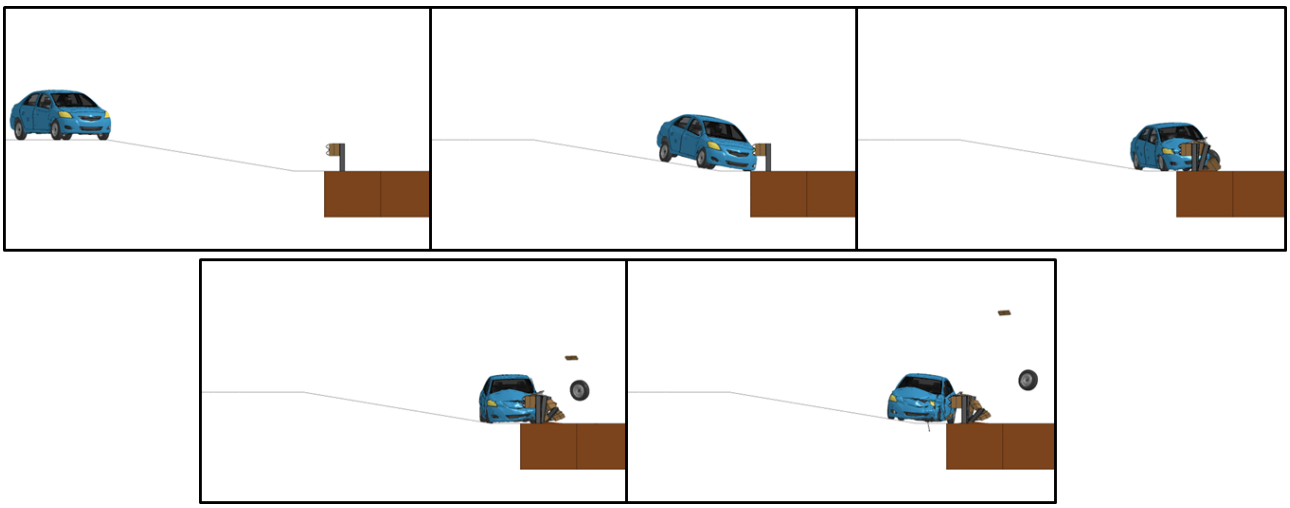

Figure 8.8: MGS on 62-6-3 Slope at 22.5 Feet from Slope Break Point

Table 8.3: Refined Placement Guidelines for MGS

Barrier Type	Ditch Width	Slope	Ditch Depth	Boundaries of Placement (upper) (ft)	Boundaries of Placement (lower) (ft)
Encroachment:					
MGS	62	8	3.88	11	31
			3	11	31
		6	5.17	15	31
			4	15	31
			3	15	31
	52	8	3.25	11	26
			3	11	26
		6	4.33	15	26
			4	15	26
			3	15	26
	42	8	2.63	11	21
		6	3.5	15	21
			3	15	21
	32	8	2	11	16
		6	2.67	Not Recommended	

8.2.2. Modified Weak Post W-Beam (G2)

To further refine the preliminary placement guidelines for the modified weak post W-beam guardrail, full-scale finite element simulations with the barrier placed on a 62 ft wide ditch with a 1V:8H slopes were performed. This corresponded to the only ditch configuration for which an acceptable placement range was identified. The barrier was placed in the center of this placement range, 28 ft from the slope break point. A simulation was performed with the small car encroaching onto the ditch at a speed of 100 km/h and an angle of 25 degrees. The results of this simulation are shown in Figure 8.10.

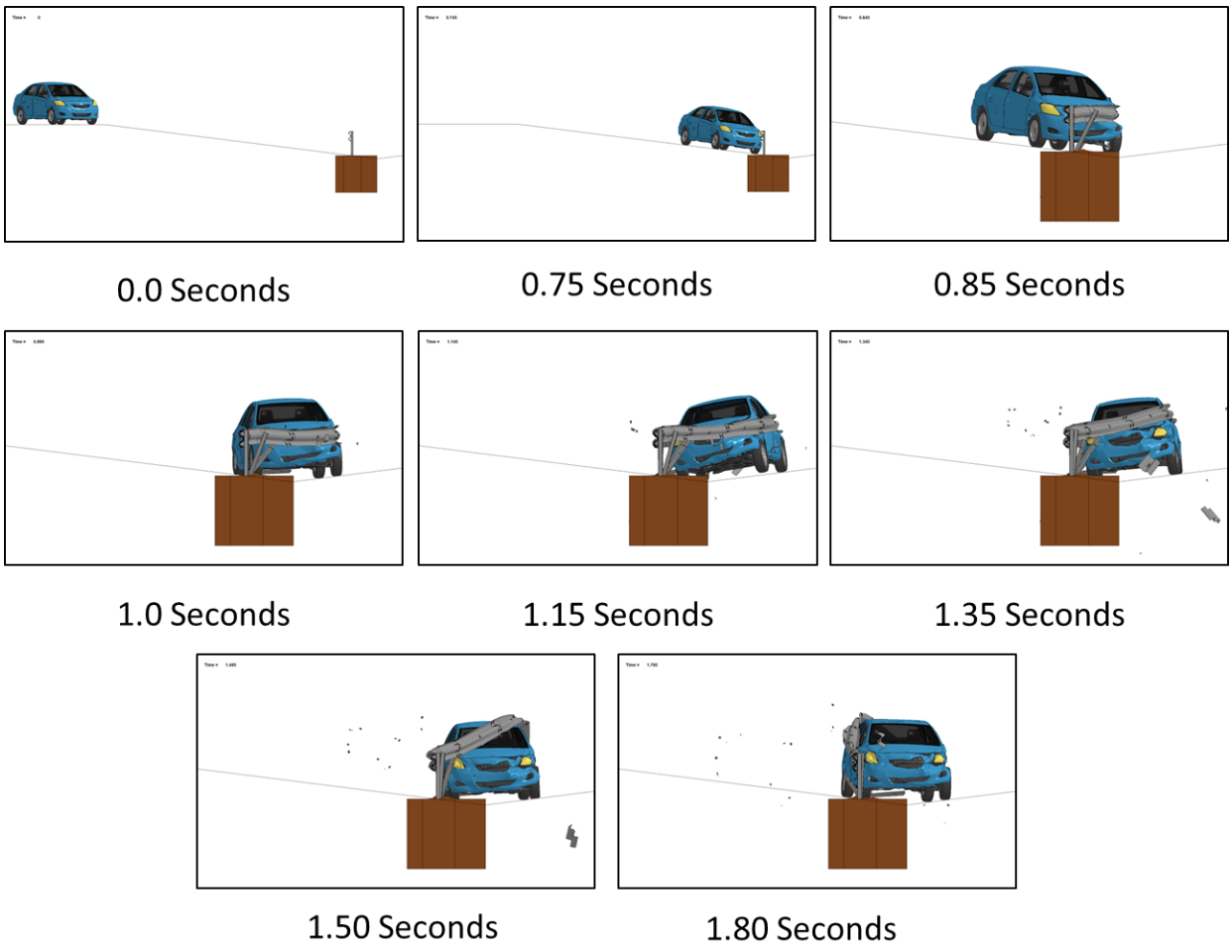

Figure 8.9: Front View of Small Car and Weak Post (G2) on 1V:8H, 62 ft, 3.88 ft V

The vehicle was contained by the barrier up to 1.35 seconds. After this time, the rail began to rise up and over the left side of car and window causing the vehicle to underride the barrier. The underride of the vehicle caused the barrier to fail at this location. Since the barrier was placed well within the acceptable range as defined by the preliminary placement guidelines

and failed due to an underride, the research team has concluded that this placement range is unacceptable for the Weak Post (G2).

After refining the placement guidelines, it is determined that the Modified Weak Post W-beam (G2) is unacceptable for placement on any of the terrain profiles analyzed as summarized in Table 8.4.

Table 8.4: Refined Placement Guidelines for Weak Post (G2)

Barrier Type	Ditch Width	Slope	Ditch Depth	Boundaries of Placement (upper) (ft)	Boundaries of Placement (lower) (ft)
Encroachment:					
Weak Post (G2)	62	8	3.88	No acceptable location on slope	
			3		
		6	5.17		
			4		
			3		
	52	8	3.25		
			3		
		6	4.33		
			4		
			3		
	42	8	2.63		
		6	3.5		
			3		
	32	8	2		
		6	2.67		

8.2.3. Modified Strong Steel-Post W-Beam (G4(1S)) Guardrail

When refining the MGS guardrail placement guidelines, the detailed simulation analysis resulted in a larger placement region being prescribed on both 1V:6H and 1V:8H slopes. The placement range was expanded on both 1V:6H and 1V:8H slopes by 2 ft and 3 ft, respectively.

Since the Modified Strong Steel-Post W-Beam G4(1S) guardrail was not modeled, the refined placement guidelines are based on the data for the MGS guardrail adjusted for the difference in barrier height. The resulting placement guidelines for the Modified Strong Steel-Post W-Beam G4(1S) guardrail are presented in Table 8.5. It should be noted that the preliminary placement guidelines showed that the barrier was not recommended for placement on the 32 foot-wide ditch with 1V:8H slopes. However, after expanding the placement range by an extra 3 ft, the overall placement range was 3.5 ft and was considered sufficient to be considered for barrier placement.

Table 8.5: Refined Placement Guidelines for Modified G4 (1S)

Barrier Type	Ditch Width	Slope	Ditch Depth	Boundaries of Placement (upper) (ft)	Boundaries of Placement (lower) (ft)
Encroachment:					
Modified G4 (1S)	62	8	3.88	13.5	31
			3	13.5	31
		6	5.17	16.5	8
			4	16.5	12
			3	16	10.5
	52	8	3.25	13.5	9.5
			3	12.5	10.5
		6	4.33	16.5	26
			4	16.5	26
			3	16.5	26
	42	8	2.63	12.5	21
		6	3.5	16.5	21
			3	16	21
	32	8	2	12.5	16
		6	2.67	Not Recommended	

8.2.4. Single Slope Concrete Barrier

The override analysis of the single slope concrete barrier concluded that the barrier could be placed anywhere along any section of the ditch configurations analyzed. To confirm the preliminary placement range, the encroachment that gave the highest bumper height for the pickup truck was analyzed in a full-scale finite element simulation. The ditch configuration selected for this full-scale simulation was 32 ft wide with 1V:6H slopes and a depth of 2.67 ft. The barrier was placed at a lateral offset of 9.6 ft from the slope break point. This location corresponds to the point on the slope where the vehicle had the highest bumper height relative to the local terrain. The pickup truck encroachment into the ditch was at a speed of 100 km/h and an angle of 25 degrees. Figure 8.11 and Figure 8.12 show the results of the pickup truck impact with the single slope concrete barrier on the slope. At this location, the barrier successfully contained and redirected the vehicle.

The vehicle accelerations and angular rates obtained from the simulation were input into the Test Risk Assessment Program (TRAP) to assess occupant risk factors prescribed by MASH. Table 8.6 compares the occupant risk values from the simulation with the preferred and maximum values recommended in MASH. The occupant impact velocities are below the maximum allowed value, and the ridedown accelerations are below the preferred value. The roll and pitch angles were also acceptable based on MASH criteria.

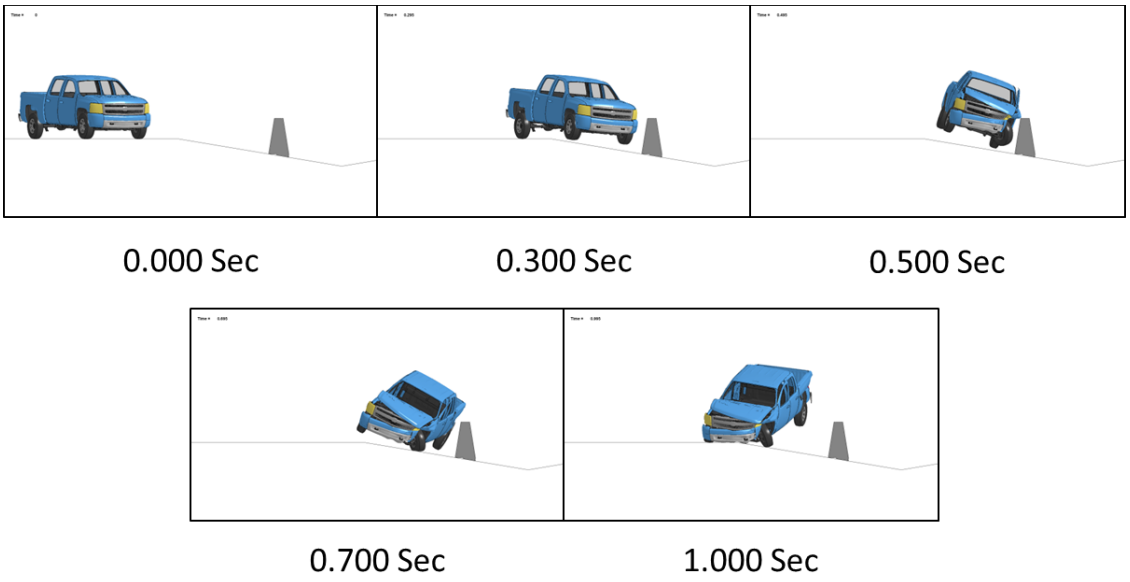

Figure 8.10: Front View of Simulation of Pickup Truck into Single Slope Concrete Barrier on 1V:6H slope

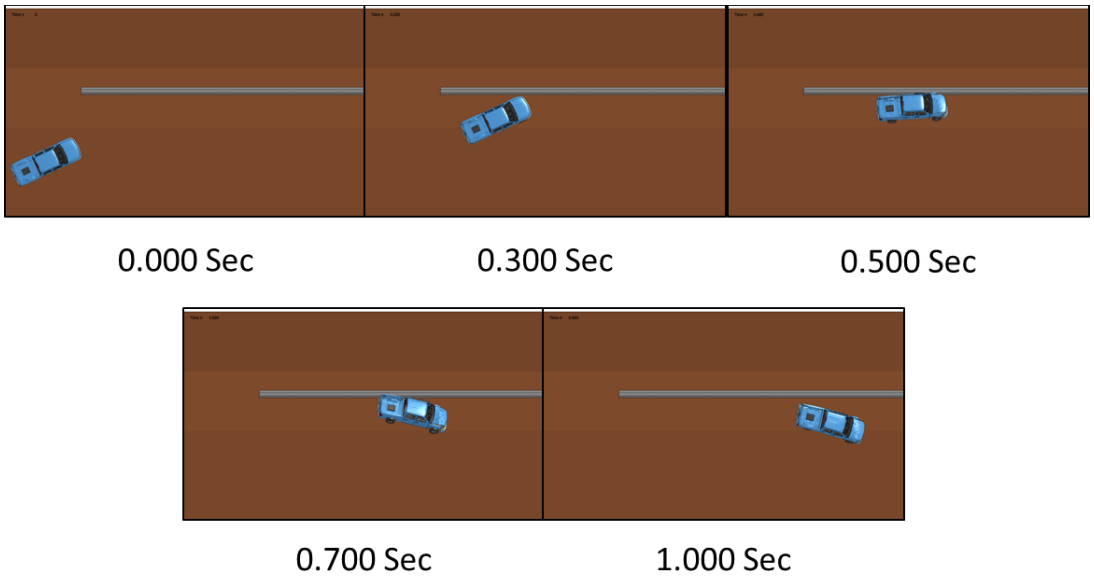

Figure 8.11: Top View of Simulation of Pickup Truck into Single Slope Concrete Barrier on 1V:6H slope

Table 8.6: Occupant Risk Assessment for Single Slope Concrete Barrier on 1V:6H Slope

Occupant Risk Factors		Preferred	Maximum
Impact Velocity (ft/s)			
x-direction	38.1	30	40
y-direction	19.7	30	40
Ridedown Accelerations (Gs)			
x-direction	-8.2	15	20
y-direction	12.6	15	20
Max Roll, Pitch, and Yaw Angles (degrees)			
Roll	-20.7		75
Pitch	42.4		75
Yaw	28.7		75

Based on the results from this full-scale simulation, the research team concluded that the preliminary guidelines were acceptable and the 42-inch single slope concrete barrier can be placed anywhere along the ditch configurations analyzed under the project. This is summarized in Table 8.7.

Table 8.7: Refined Placement Guidelines for Single Slope

Barrier Type	Ditch Width	Slope	Ditch Depth	Boundaries of Placement (upper) (ft)	Boundaries of Placement (lower) (ft)
Encroachment:					
Single Slope	62	8	3.88	Acceptable at all locations on slope	
			3		
		6	5.17		
			4		
			3		
	52	8	3.25		
			3		
		6	4.33		
			4		
			3		
	42	8	2.63		
		6	3.5		
			3		
	32	8	2		
		6	2.67		

9. FINAL BARRIER PLACEMENT GUIDELINES

This chapter presents the recommended barrier placement guidelines. After developing and refining the placement guidance for the selected barrier systems, the information was further analyzed and formatted in both tabulated and graphical formats that can be considered for inclusion in the AASHTO Roadside Design Guide (RDG) or other guidance documents. The guidelines present recommended placement ranges for roadside barriers on 1V:6H and 1V:8H slopes as well as median barriers on various ditch profiles having 1V:6H and 1V:8H slopes and widths ranging from 32 to 62 ft. The barriers considered include Modified Weak Post W-Beam Guardrail (G2), Midwest Guardrail System (MGS), Modified Strong Steel-Post W-Beam Guardrail (modified G4(1S)), Weak Post W-Beam Median Barrier (MB2), MGS Median Barrier, and Single Slope Concrete Barrier (42-inch).

9.1. GUARDRAIL SYSTEMS

The acceptable placement ranges for each barrier type are shown graphical in the following sections. The graphs show the normalized composite bumper trajectory profiles for both the pickup truck and small car superimposed over the barriers override/rollover and underride limits. The normalized composite bumper trajectories are developed by taking the maximum (or minimum) of the bumper trajectory profiles for the different encroachment conditions at each lateral offset distance. The maximum composite bumper trajectory plot is derived from the pickup truck encroachments and is evaluated against the override/rollover limit. The minimum composite bumper trajectory plot is derived from the small car encroachments and is evaluated against the underride limit. The acceptable barrier placement ranges are denoted by a green bar along the horizontal axis with the lateral offset distance referenced from the slope break point.

9.1.1. Modified Weak Post W-Beam Guardrail (G2)

The acceptable placement ranges identified for the modified weak post w-beam guardrail (modified G2) are shown in Figure 9.1 and Figure 9.2 for 1V:6H and 1V:8H slopes, respectively. The modified weak post w-beam guardrail (modified G2) has a small range of acceptable performance beyond 20 ft on each slope.

9.1.2. Midwest Guardrail System (MGS)

The acceptable placement ranges identified for the MGS guardrail are shown in Figure 9.3 and Figure 9.4 for 1V:6H and 1V:8H slopes, respectively. The MGS guardrail has an initial placement range near the breakpoint and an extensive placement range beyond 10 ft for each slope.

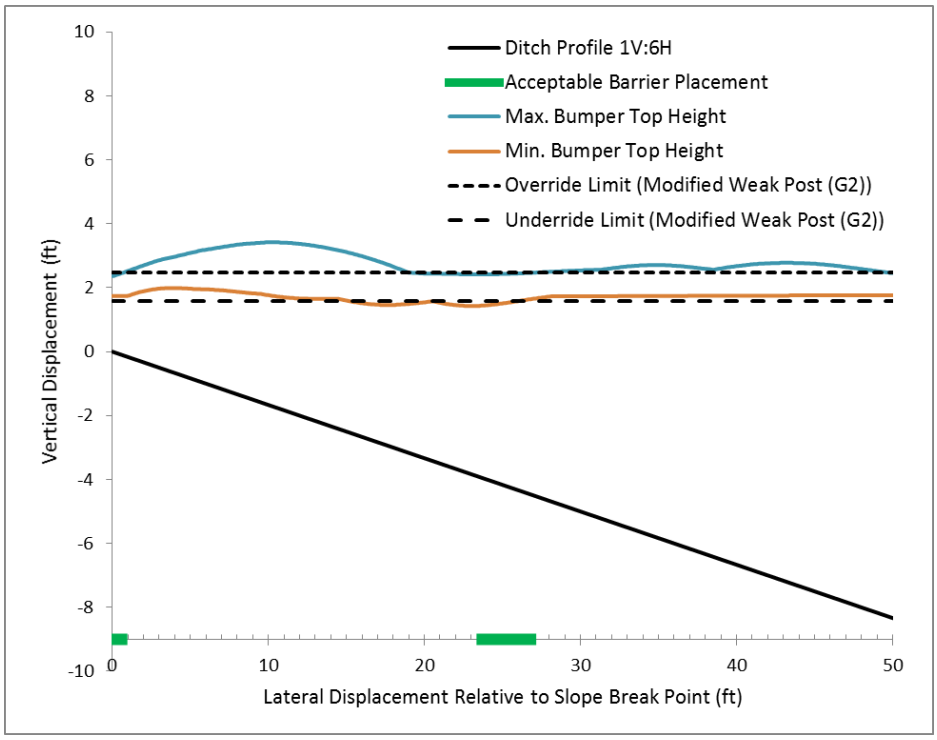

Figure 9.1: Acceptable Barrier Placement of Modified Weak Post (G2) on 1V:6H Slope

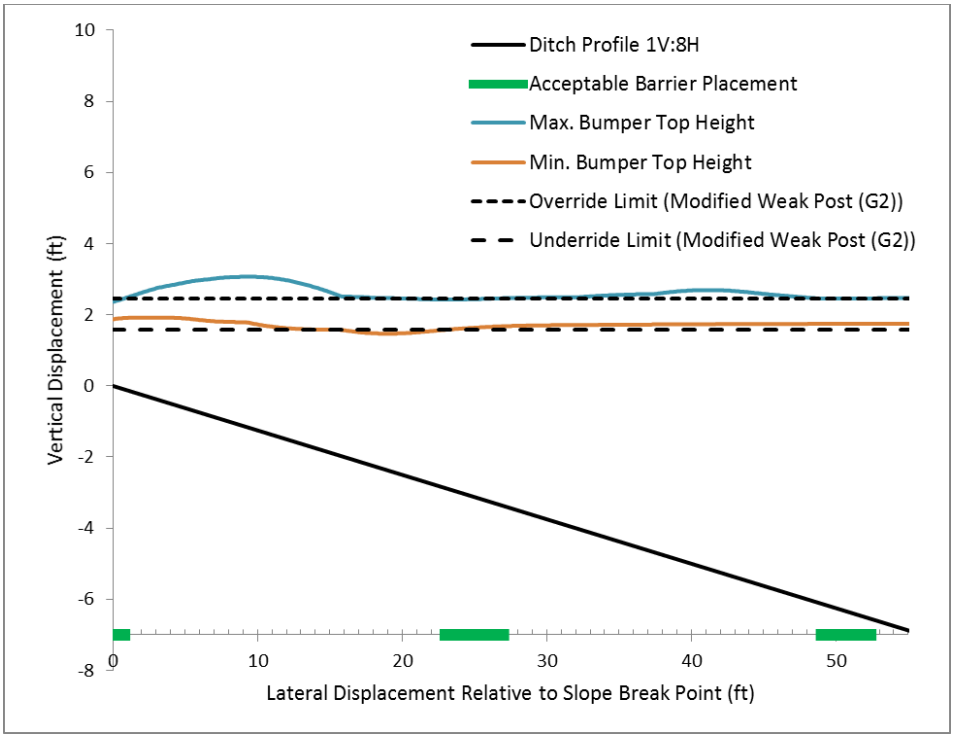

Figure 9.2: Acceptable Barrier Placement of Modified Weak Post (G2) on 1V:8H Slope

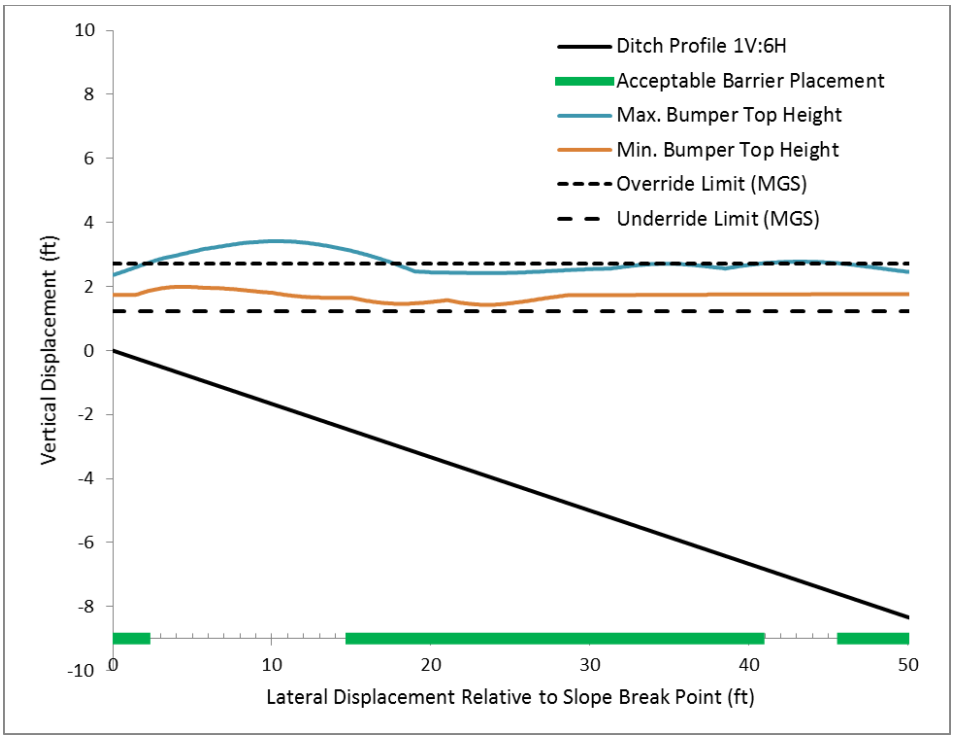

Figure 9.3: Acceptable Barrier Placement of MGS on 1V:6H Slope

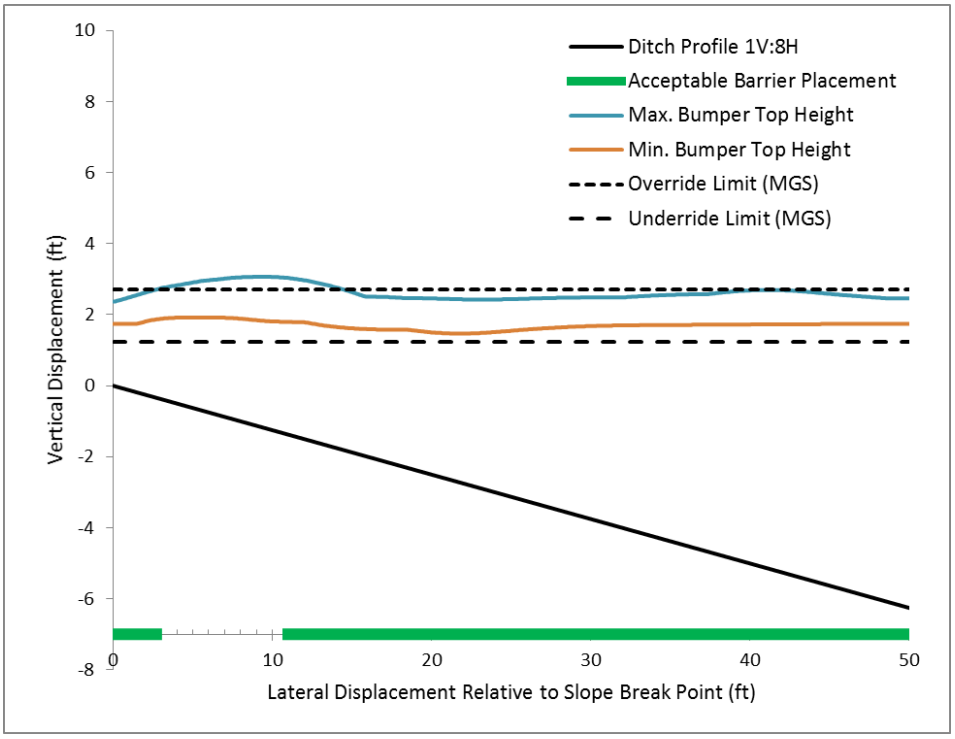

Figure 9.4: Acceptable Barrier Placement of MGS on 1V:8H Slope

9.1.3. Modified Strong Steel-Post W-Beam Guardrail (Modified G4(1S))

The acceptable placement ranges identified for the modified strong steel-post W-beam guardrail (modified G4(1S)) are shown in Figure 9.5 and Figure 9.6 for 1V:6H and 1V:8H slopes, respectively. Due to its lower mounting height, the acceptable placement ranges for the modified strong steel-post W-beam guardrail (modified G4(1S)) are smaller than the taller MGS guardrail.

9.1.4. Modified Thrie Beam Guardrail

The acceptable placement ranges identified for the modified strong steel-post W-beam guardrail (modified G4(1S)) are shown in Figure 9.5 and Figure 9.6 for 1V:6H and 1V:8H slopes, respectively. Due to its lower mounting height, the acceptable placement ranges for the modified strong steel-post W-beam guardrail (modified G4(1S)) are smaller than the taller MGS guardrail.

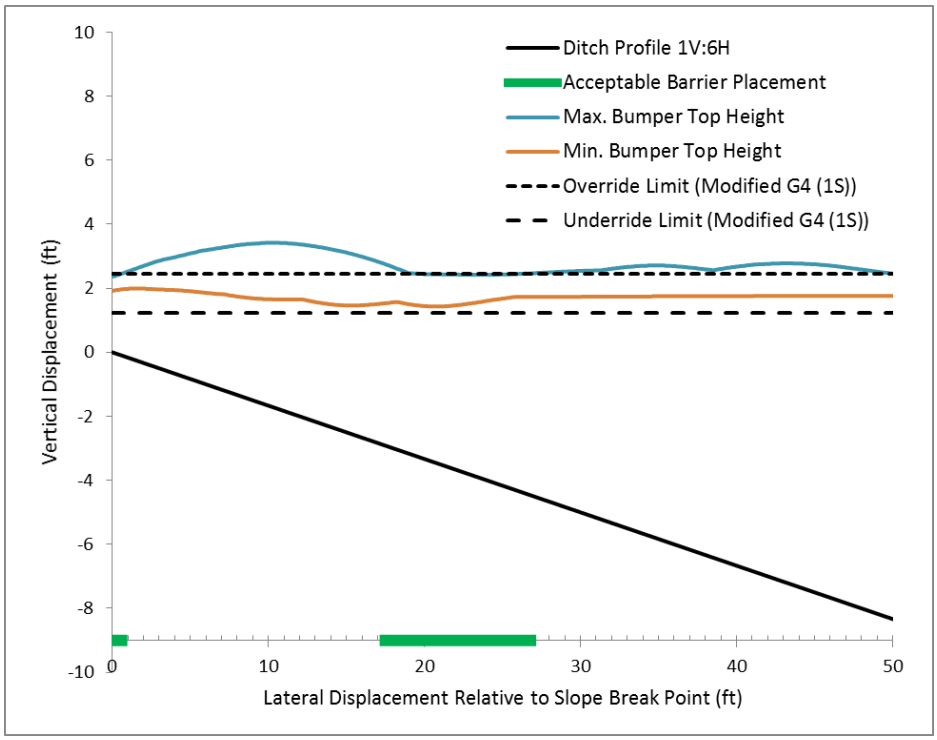

Figure 9.5: Acceptable Barrier Placement of G4 (1S) on 1V:6H Slope

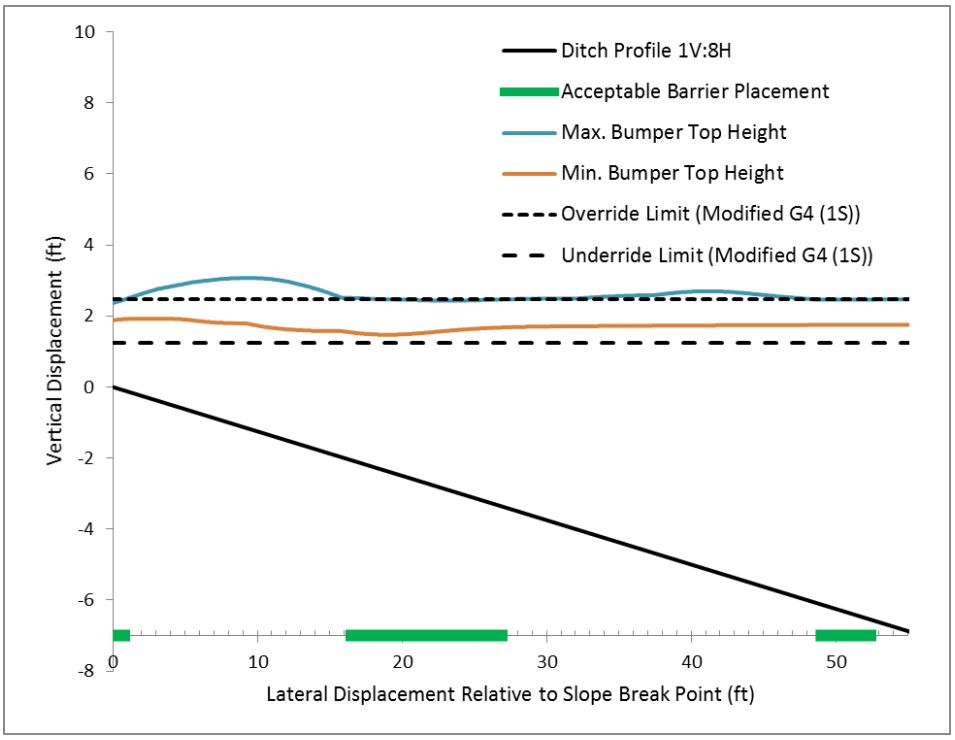

Figure 9.6: Acceptable Barrier Placement of G4 (1S) on 1V:8H Slope

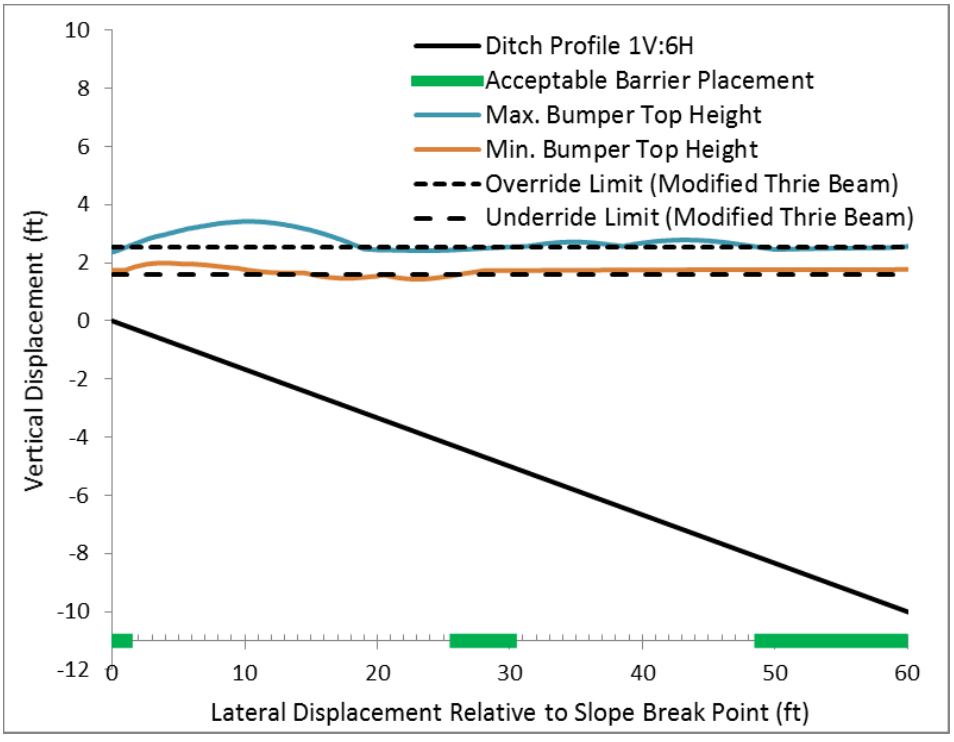

Figure 9.7: Acceptable Placement Region for Modified Thrie Beam on 1V:6H Slope

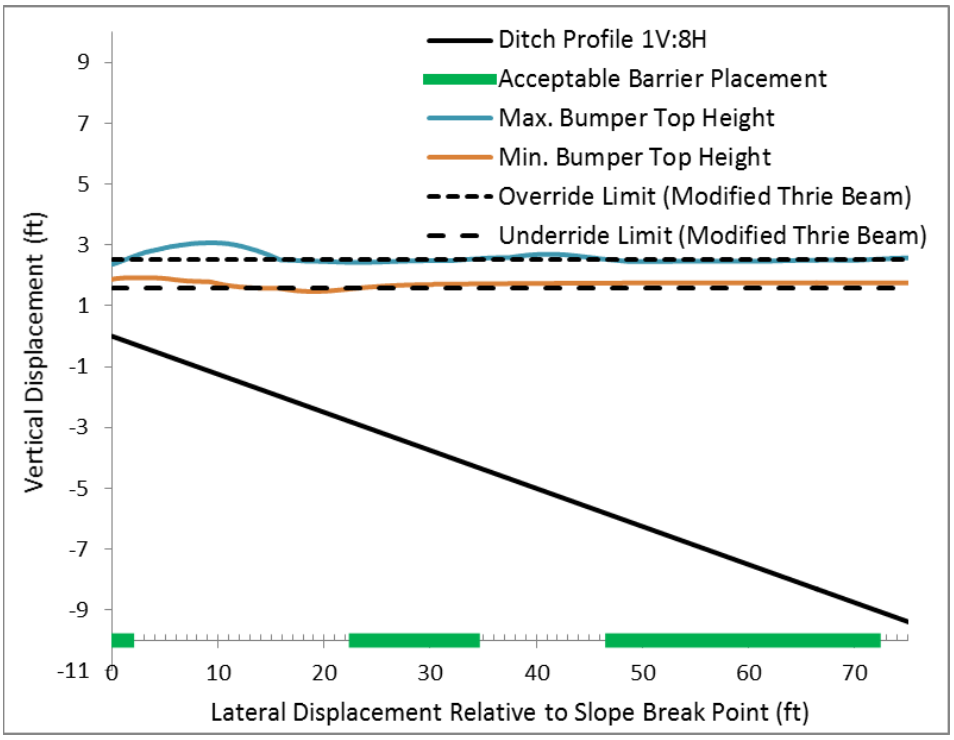

Figure 9.8: Acceptable Placement Region for Modified Thrie Beam on 1V:8H Slope

9.1.5. Recommended Guardrail Placement Guidance

The acceptable placement ranges for the selected guardrail systems on 1V:6H and 1V:8H roadside slopes is summarized in Table 9.1. Placement ranges that were less than 2 ft in width were excluded. Although a long infinite slope was considered in the analysis, this placement guidance is based on a practical limit of 50 ft. Note that this guidance is applicable to roadside slopes or installation of barrier on both slopes of a median ditch.

9.2. MEDIAN BARRIER SYSTEMS

The acceptable placement ranges for the selected median barrier systems on ditches with 1V:6H and 1V:8H slopes is summarized in Table 9.2. It is applicable to symmetric V-shape and trapezoidal ditches within the range of ditch widths analyzed. Placement ranges that were less than 2 ft in width were excluded. This guidance considers impact of the median barrier system from both directions in the median ditch. Note that the placement guidance presented in Table 9.2 is in reference to the ditch bottom centerline rather than the slope break point. However, it can be translated to any other reference point that is desired.

As shown in the table, there is no recommended placement range for weak post W-beam median barrier (MB2) on any of the analyzed ditch configurations. Conversely, the 42-inch single slope concrete median barrier has acceptable placement anywhere on the ditch configurations that were analyzed. The MGS median barrier has an acceptable placement range on most of the ditch profiles analyzed that extends upslope from the ditch bottom on both sides of the ditch centerline.

Table 9.1: Acceptable Placement of Barriers on Roadside

Roadside Barrier Placement*		
Cross-Slope	**Barrier Type**	**Acceptable Barrier Location (ft)****
1V:6H	MGS	0-2, 18-40.5, 46-50
	Modified Weak Post (G2)	24-26.5
	G4 (1S)	19.5-26.5
	Modified Thrie Beam	26-30
1V:8H	MGS	0-2.5, 14.5-50
	Modified Weak Post (G2)	23-27
	G4 (1S)	19.5-26.5
	Modified Thrie Beam	23-34, 46.5-50

* Barrier Placement is relative to the traffic face of the barrier

** Lateral offset is measured from the slope break point

Table 9.2: Acceptable Placement of Barriers on Median Ditch Profiles

Median Barrier Placement on V and T Shape Ditches				
Barrier Type	**Ditch Width (ft)**	**Slope**	**Acceptable Barrier Location (ft)***	
			V-Shape Ditch	**Trapezoidal Ditch**
MGS Median	32	1V:6H	None	n/a***
		1V:8H	0-4	n/a***
	42	1V:6H	0-4	0-4
		1V:8H	0-7	n/a***
	52	1V:6H	0-9	0-9
		1V:8H	0-12	n/a***
	62	1V:6H	0-12.5	0-3, 7-14
		1V:8H	0-17, 28.5-31	0-17, 28.5-31
Weak Post W-beam (MB2)	32	1V:6H	Not Recommended	Not Recommended
		1V:8H		
	42	1V:6H		
		1V:8H		
	52	1V:6H		
		1V:8H		
	62	1V:6H		
		1V:8H		
Concrete: Single Slope (42 inch)	32	1V:6H	Acceptable anywhere along the ditch	Acceptable anywhere along the ditch
		1V:8H		
	42	1V:6H		
		1V:8H		
	52	1V:6H		
		1V:8H		
	62	1V:6H		
		1V:8H		

* Lateral offset is measured from the Center Line of the ditch.
** Barrier Placement is relative to the traffic face of the barrier.
*** Ditch depths of 3, 4 and 6 feet were evaluated in this project. Trapezoidal ditches do not exist for some of these depths as dictated by the ditch width and slope.

9.2.1. MGS Median Barrier

As noted in Table 9.2, the placement regions for the MGS median barrier differ with ditch slope and ditch width. While use of the tabulated data should be relatively straightforward, the researcher explored other ways for presenting the placement ranges for this barrier system.

Figure 9.9 provides a graphical guideline for the acceptable placement ranges for the MGS median barrier for a 1V:6H ditch slope. As can be seen, it is symmetrical about the ditch centerline and pertains to V-shaped ditch configurations. This chart can be used to determine an acceptable placement location for any ditch width between 42 ft and 62 ft. This is more obvious in the graphical format than in the tabular format of Table 9.2. The chart also shows the narrow ranges that are acceptable adjacent to the break point of the ditch. While these placement ranges should be acceptable, the researchers express caution with their use merely due to some of the limitations of the modeling and simulation upon which they are based.

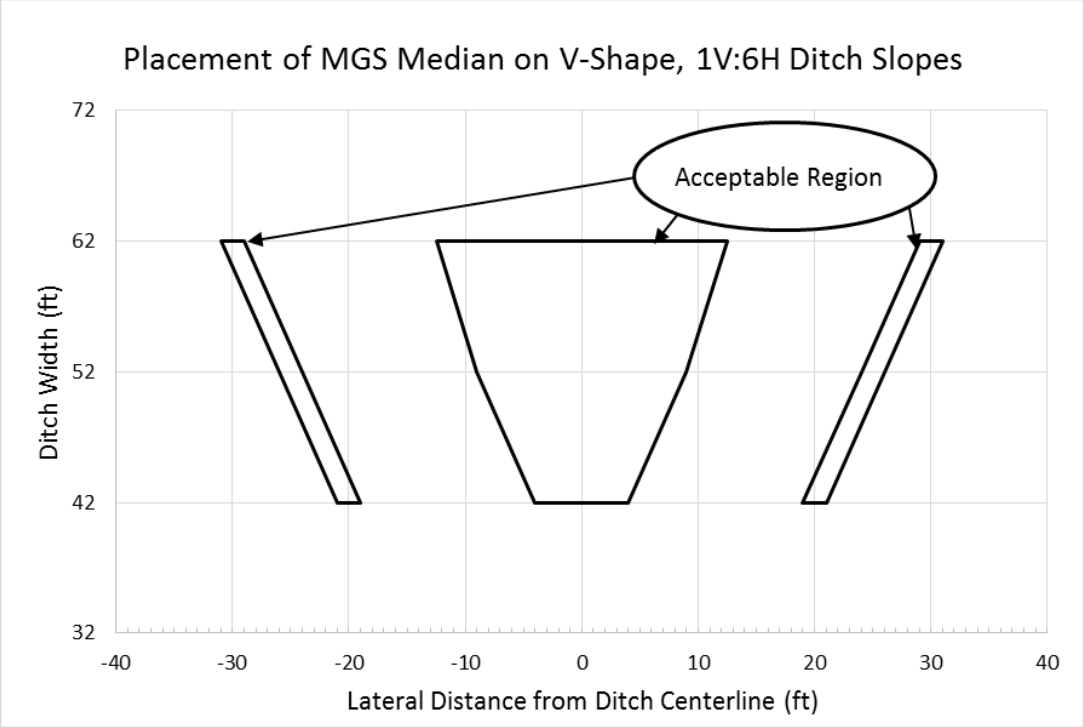

Figure 9.9: Acceptable Placement Region for MGS Median on V-Shape, 1V:6H Ditch Slope

Figure 9.10 provides a similar graphical guideline for the acceptable placement ranges for the MGS median barrier for trapezoidal ditches with a 1V:6H ditch slope. While the ranges are very similar to those shown in Figure 9.9 for V-shaped ditches, there are some regions associated with the wider ditch configurations that are excluded for placement of the MGS median barrier when the ditch is trapezoidal.

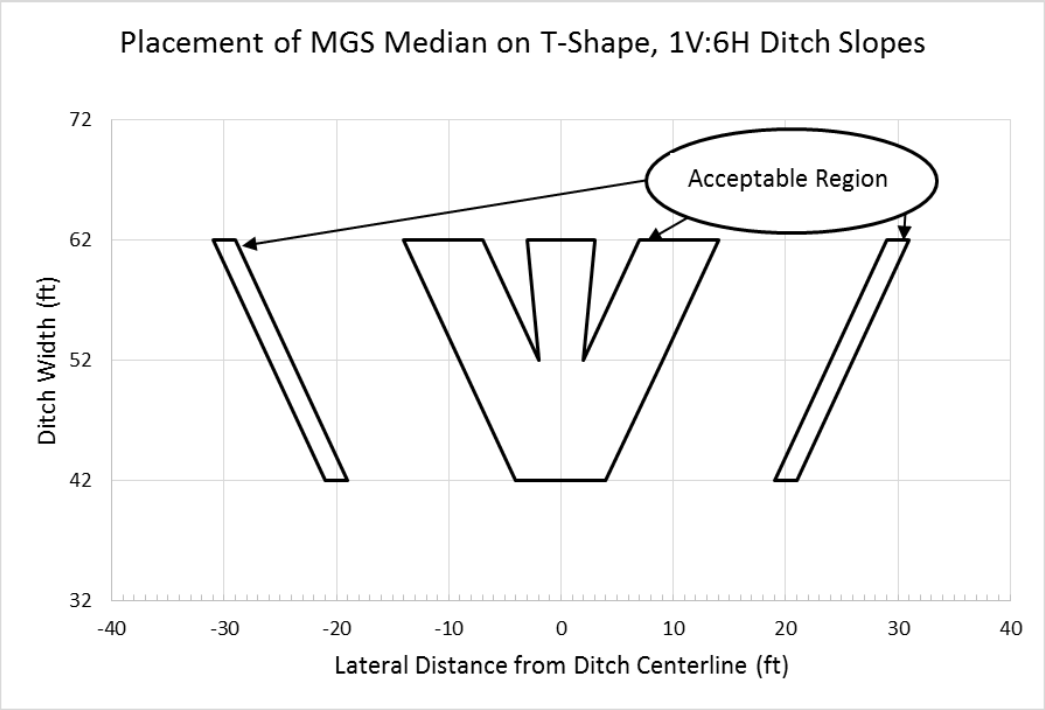

Figure 9.10: Acceptable Placement Region for MGS Median on T-Shape, 1V:6H Ditch Slope

Figure 9.11 provides a graphical guideline for the acceptable placement ranges for the MGS median barrier for V-shaped ditch configurations with a 1V:8H ditch slope. As expected, the acceptable placement ranges expand on the shallower 1V:8H slopes. This chart can be used to determine an acceptable placement location for any ditch width between 32 ft and 62 ft.

Figure 9.12 provides a similar graphical guideline for the acceptable placement ranges for the MGS median barrier for trapezoidal ditches with a 1V:8H ditch slope. Note that the seemingly limited placement guidance is merely attributed to the fact that a trapezoidal ditch shape does not exist for the narrower ditch depths with a 1V:8H ditch slope. Since the guidance is only applicable to a ditch width of 62 ft (ditch widths between 52 and 62 ft were not explicility analyzed), the result is merely a set of horizontal lines.

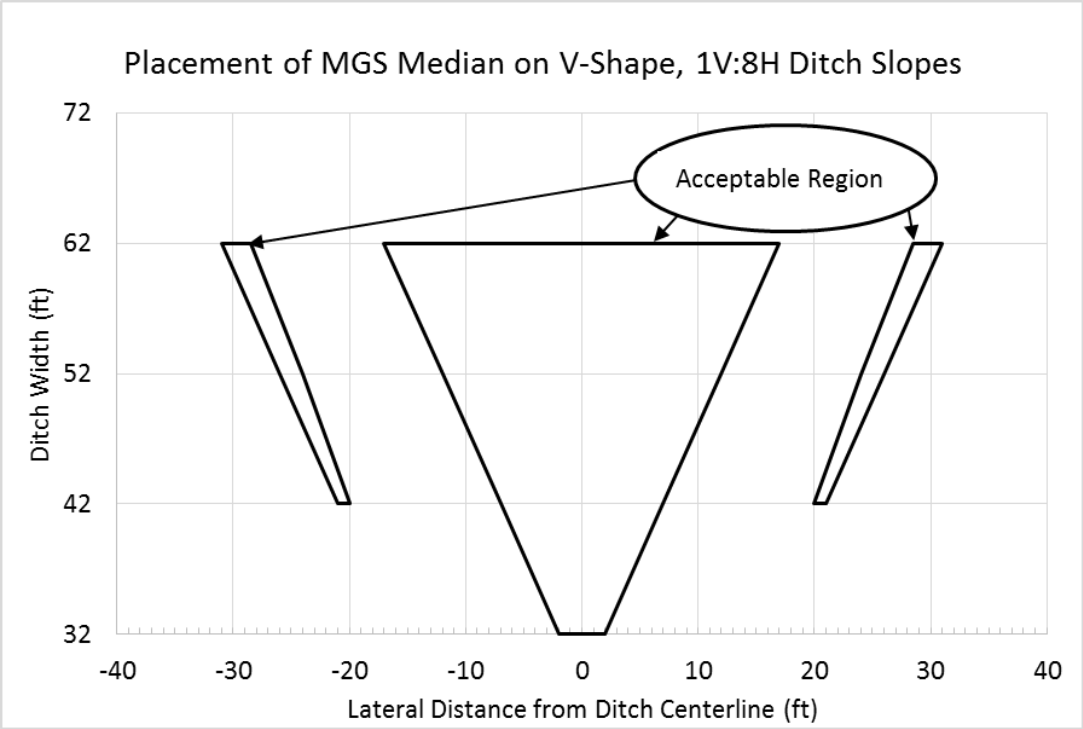

Figure 9.11: Acceptable Placement Region for MGS Median on V-Shape, 1V:8H Ditch Slope

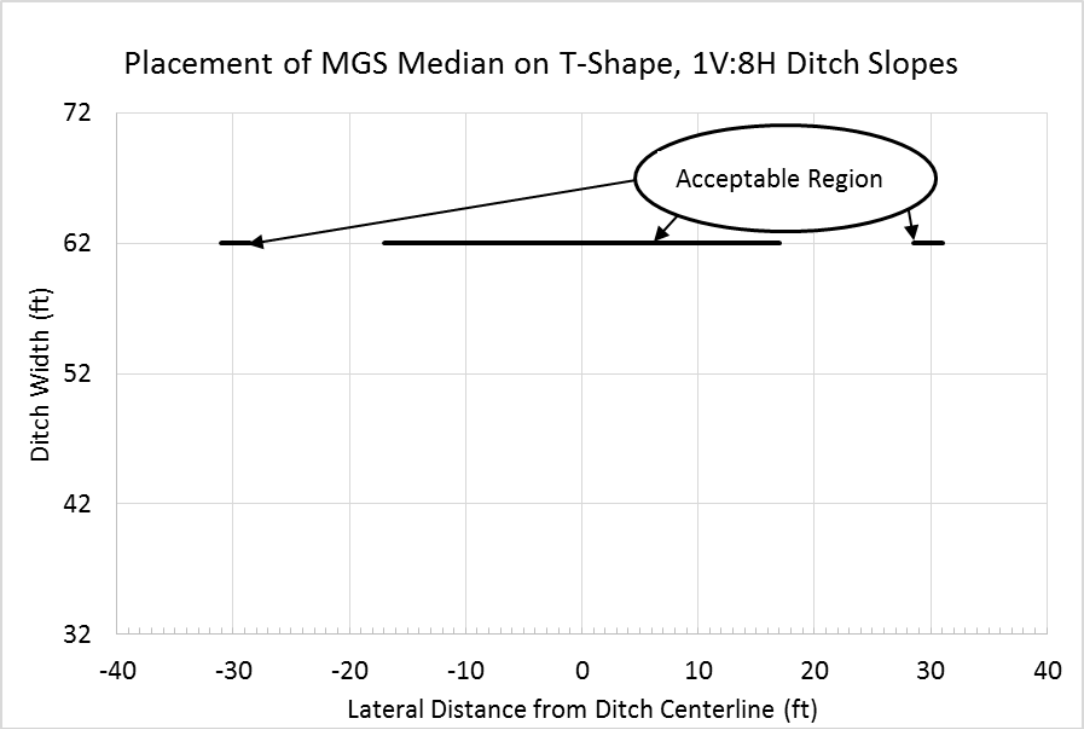

Figure 9.12: Acceptable Placement Region for MGS Median on T-Shape, 1V:8H Ditch Slope

10. CONCLUSIONS AND RECOMMENDATIONS

Placement guidelines for implementation of selected guardrail and median barrier systems on slopes and ditches were developed using barrier impact performance limits derived from LS-DYNA finite element impact simulations and CarSim vehicle trajectory encroachment data. The finite element barrier models were validated against available MASH crash test data, and the CarSim vehicle models were validated against available ditch encroachment tests. The barrier performance limits were defined in terms of interaction heights that resulted in vehicle override and underride. The vehicle trajectory data was defined in terms of vehicle bumper trajectory profiles as the vehicles encroached across selected ditch configurations.

The barrier systems that were included in the evaluation included the following:

- Guardrails
  - Modified Weak Post W-beam (G2)
  - Midwest Guardrail System (MGS)
  - Modified Strong Steel-Post W-beam (modified G4(1S))
  - Modified Thrie Beam Guardrail
- Median Barriers
  - Weak-Post W-beam (MB2)
  - Midwest Guardrail System Median Barrier
  - Concrete Single Slope Barrier (42-inch)

The ditch configurations included in the analyses included ditches with 1V:6H and 1V:8H slopes and widths ranging from 32 ft to 62 ft. Some of the ditches were V-shaped while others were trapezoidal, depending on the depth.

The placement guideline development process involved identifying locations (lateral offsets) along the ditch profile where the bumper heights associated with vehicle encroachments of the same ditch profile were contained within the override and underride limits for the barrier system. Placement guidelines for the median barrier systems considered impact from both directions in the ditch.

Explicit finite element impact simulations of the barrier placed in the ditch were performed to further validate the placement guidelines and revise them as warranted. These impact simulations were limited to evaluation of barrier performance on the ditch foreslope. Such impact simulations were not performed for placement ranges on the backslope because the suspension systems of the available finite element vehicle models were not validated for such conditions and inaccurate suspension response could deliver the vehicle to the barrier at inaccurate heights, which would have a profound effect on barrier performance outcomes and the resulting placement guidelines.

There was one barrier system (weak post W-beam median barrier (MB2)) for which no acceptable placement ranges were identified. Conversely, it was determined that the 42-inch single slope concrete median barrier could be placed anywhere along any of the ditch

configurations analyzed. Other barriers such as the MGS guardrail and median barrier had extensive ranges for which placement on both 1V:6H and 1V:8H slopes and ditches were found to be acceptable.

The resulting placement guidelines were presented in both tabulated and graphical form. The tubular format provides a very concise presentation, which the graphical format can be more readily visualized and applied to a range of ditch widths.

Although the placement guidelines are considered to be sound, crash testing could be conducted to verify some of the placement ranges. Verification of the placement ranges on ditch backslopes would be particular useful. However, delivering test vehicles to a barrier installed on the backslope of a relatively wide ditch is challenging.

11. REFERENCES

Abu-Odeh, Akram Y., Menges, Wanda L., and Haug, Rebecca R., *NCHRP Report 350 Test 3-11 of the New York DOT W-Beam on Light Post Median Barrier,* Contract No. DTFH61-02-P-00403, Report No. 400611-1. Texas Transportation Institute, Texas A&M University System, College Station, TX, February 2003.

American Association of State Highway and Transportation Officials (AASHTO). "A Guide to Standardized Highway Barrier Hardware." *Rep. No. Task force 13 Report*, 2002.

AASHTO. *Roadside Design Guide*. 2002

AASHTO. *Roadside Design Guide*. 2006

AASHTO. *Roadside Design Guide*. 2009

Baxter, J. R., Director, Office of Safety Design, Federal Highway Administration (FHWA), Hardware Acceptance Letter Reference for Brifen Wire Ropes Safety Fence on a 4H:1V slope (HAS-10/B82-B1), May 9, 2006.

Baxter, J. R., Director, Office of Safety Design, Federal Highway Administration (FHWA), Hardware Acceptance Letter Reference for Gibraltar cable barrier on 4H:1V slope (HAS-10/B137C), July 12, 2006.

Beason, W. L., Ross, Jr., H. E., Perera, H. S., Campise, W. L., and Bullard, Jr., D. L., *Development of a Single-Slope Concrete Median Barrier*, Research Report 9429CDK-1, Texas Transportation Institute, College Station, TX, June 1989.

Bligh, R. P., unpublished data from HVOSM simulations, Texas Transportation Institute, Texas A&M University System, College Station, TX, 2004.

Bullard, D. Lance., Jr., Menges, Wanda L., and Alberson, Dean C., *NCHRP Report 350 Compliance Test 3-11 of the Modified G4(1S) Guardrail with Timber Blockout*, Contract No. DTFH61-95-C-00090, Research Project No. 405421-1. Texas Transportation Institute, Texas A&M University System, College Station, TX, January 1996.

Buth, C. E. , Campise, W. L., Griffin III, L.I, Love, M. L. and Sicking, D. L. "Performance Limits of Longitudinal Barrier Systems, Volumes I,II, III, IV and V, Federal Highway Administration, U. S. Department of Transportation Contract DTFH61-82-C-00051, Texas Transportation Institute, 1986.

Buth, C. E., Menges, W. L., and Schoeneman, S. K., *NCHRP Report 350 Assessment of Existing Roadside Safety Hardware*, Research Report 404211-F, Texas Transportation Institute, College Station, TX, November 2000.

California Department of Transportation (Caltrans). *Traffic Manual: Chapter 7 Traffic Safety Systems*. California Department of Transportation, May 1998.

Cansiz, O. F., and Atahan, A. O., "Crash Test Simulation of a Modified thrie-beam High Containment Level Guardrail under NCHRP 350 TL4-12 Conditions." *International Journal of Heavy Vehicle System*, 13(1), 2-18, 2006.

Faller, R. K., Polivka, K. A., Kuipers, B. D., Bielenberg, B. W., Reid, J. D., Rohde, J. R., and Sicking, D. L.. *Midwest Guardrail System for Standard and Special Applications*, *Transportation Research Board, 83rd Annual Meeting,* 2003.

Federal Highway Administration. Acceptance Letter B64. Washington, D.C., February 14, 2000.

Hallquist, J.O., "LS_DYNA Theory Manual." Livemore Software Technology Corporation, California, 2006.

H. E. Ross, D. L. Sicking, R. A. Zimmer, and J. D. Michie, *Recommended Procedures for the Safety Performance Evaluation of Highway Features*, National Cooperative Highway Research Program Report 350, Transportation Research Board, National Research Council, Washington, D.C., 1993.

Ivey, D. L., Robertson, R., and Buth, C. E., *Test and Evaluation of W-Beam and Thrie-Beam Guardrails*, Research Report 4098, Texas Transportation Institute, College Station, TX, March 1982.

Livermore Software Technology Corporation, " LS-DYNA Keyword User's Manual (Version 971). Vol. 1 & II", 2007.

Mak, K. K. and Menges, W. L., *NCHRP Report 350 Compliance Test of the New Jersey Safety Shaped Barrier*, Report No. FHWA-RD-96-201, Federal Highway Administration, Washington, D.C., November 1996.

Mak, K. K. and Menges, W. L., NCHRP Report 350 Evaluation of the Wyoming Box-Beam End Terminal (WYBET-350), Contract EsE9743 and SPR-RS10(197), Project RF473160-01, Texas Transportation Institute, Texas A&M University System, College Station, TX, September 1999.

Mak, King K., Bligh, Roger P., and Menges, Wanda L., *Testing of State roadside Safety Systems: Volume I: Technical Report,* Contract No. DTFH61-89-C-00089, Research Project No. RF 471470. Texas Transportation Institute, Texas A&M University System, College Station, TX, February 1998a.

Mak, King K., Bligh, Roger P., and Menges, Wanda L., *Testing of State roadside Safety Systems: Volume XI: Appendix J- Crash Testing and Evaluation of Existing Guardrail Systems*, Contract No. DTFH61-89-C-00089, Research Project No. RF 471470. Texas

Transportation Institute, Texas A&M University System, College Station, TX, February 1998b.

Marzougui, Dhafer, Mohan, Pradeep, Mahadeviah, Umashankar and Kan, Steve, *Performance Evaluation of Low-Tension, Three Strand Cable Median Barriers on Slopped Terrains,* National Crash Analysis Center, The George Washington University, Washington, D.C., April 2007.

Marzougui, Dhafer, Mohan, Pradeep, Kan, Steve and Opiela Kenneth., *Evaluation of Rail Height Effects on the Safety Performance of W-Beam Barriers*. (6th European ls-dyna conference)

Mechanical Simulation Corporation, CarSim Version 8, 1996.

Mechanical Simulation Corporation (MSC), *CarSim Reference Manual*, 2008.

National Crash Analysis Center, "Development of a Finite element Model for W-beam Guardrails." *http://www. ncac. gwu. edu/research/infrastructure.html*, 2007.

National Crash Analysis Center, *Development of Guidance for the Selection, Use, and Maintanance of Cable barrier Systems*, National Cooperative Highway Research Program Project 22-25, Transportation Research Board, Washington, D. C., 2009.

Orengo, F., Ray, M. H., and Plaxico, C. A., *Modeling Tire Blow-out in Roadside Hardware Simulations using LS-DYNA,* pages 71-80, 2003.

Polivka, K. A., Faller, R. K., Sicking, D. L., Reid, J. D., Rohde, J. R., Holloway, J. C., Bielenberg, B. W., and Kuipers, B. D., *Development of the Midwest Guardrail system (MGS) for Standard and reduced Post Spacing and in Combination with Curbs*, *Rep. No. TRP-03-139-04*, Midwest Roadside Safety Facility, 2004.

Polivka, K. A., Faller, R. K., Sicking, D.L., Rohde, J. R., Bielenberg, B. W., and Reid, J. D., *Performance Evaluation of the Midwest Guardrail System – Update to NCHRP 350 Test No. 3-11 with 28" C.G. Height (2214MG-2)*, Research Report TRP-03-171-06, Midwest Roadside Safety Facility, Lincoln, NE, October 2006.

Ray, M. H. and McGinnis, R. G.*"Guardrail and Median Barrier Crashworthiness,"* NCHRP Synthesis 244, Transportation Research Board, National Research Council, Washington, D.C., 1997

Ray, M. H., Engstrand, K., Plaxico, C. A., and McGinnis, R. G., "Improvements to the Weak-Post W-Beam Guardrail," *Transportation Research Record 1743,* Transportation Research Board, Washington, D.C., 88-96, 2001.

Ray, M. H., Plaxico, C. A., and Anghileri, M., *Recommended Procedures for Verification and Validation of Computer Simulations used for Roadside Safety Applications*, National

Cooperative Highway Research Program Project 22-24, Draft Final Report, Transportation Research Board, Washington, D.C., 2009.

Reid, J. D., Bielenberg, B. W., " Using LS-DYNA Simulation to Solve a design Problem: A Bullnose Guardrail Example" *78th Annual Meeting*, Transportation Research Board, Washington, DC, 1999.

Reid, J. D., Boesch, D. A., and Bielenberg, R. W., "Detailed Tire Modeling for Crash Applications," *International Journal of Crashworthiness*, 12(5), 521-529, 2007.

Ross, H. E., Jr., Bligh, R. P., and Liu, J. C., *Evaluating the Benefits of Slope Rounding,* Research Report 0468F-1F, *Minnesota DOT Research Study No. 0468F,* Texas Transportation Institute, College Station, TX, June 1993.

Ross, Hayes E., Jr., Sicking, Dean L., *Development of Guidelines for Placement of Longitudinal Barriers on Slopes: Volume I Executive Summary,* Contract No. DOT-FH-11-9343, Report No. 3659-1. Texas Transportation Institute, Texas A&M University System, College Station, TX, 1983.

Ross, Hayes E., Jr., Sicking, Dean L., *Development of Guidelines for Placement of Longitudinal Barriers on Slopes: Volume III Guidelines*, Contract No. DOT-FH-11-9343, Report No. 3659-3. Texas Transportation Institute, Texas A&M University System, College Station, TX, 1983.

Ross, Hayes E., Jr., Smith, Darrel G., Sicking, Dean L., Hall, Patricia R., *Development of Guidelines for Placement of Longitudinal Barriers on Slopes: Volume II Full-Scale Crash Tests*, Contract No. DOT-FH-11-9343, Report No. 3659-2. Texas Transportation Institute, Texas A&M University System, College Station, TX, 1983.

Segal, D. J., *Highway-Vehicle-Object Simulation Model (HVOSM) User's Manual*, FHWA report FHA-RD-89-178, 1976.

Sheikh, N. M., Bligh, R. P. *Analysis of the Impact Performance of Concrete Median Barrier Placed on or Adjacent to Slopes*. Technical Report. 0-5210-1. Texas Transportation Institute, College Station, TX. May 2006.

Sheikh, N. M., Bligh, R. P., and Menges, W. L., *Crash Testing and Evaluation of F-Shape Barriers on Slopes*. Research Report. 0-5210-3. Texas Transportation Institute, College Station, TX. March 2008.

Stine, J. S., *Analyzing Highway Median Safety through Vehicle Dynamic Simulations*, Master of Science Thesis, Department of Mechanical and Nuclear Engineering, The Pennsylvania State University, 2009.

Uddin, W., "Crashworthiness Analysis and Simulation of Vehicles Impacting a Roadside Guardrail." *Computer Modeling in Engineering and Science*, 5(3), 269-278, 2004.

Weaver, G. D. and Marquis, E. L., Olsen, R. M., *The Relation of Side Slope Design to Highway Safety*, Highway Research Board NCHRP Project 20-7, Texas Transportation Institute, September 1974.